Universitat Autònoma de Barcelona

Metabolic engineering of Pichia pastoris for 3-hydroxypropionic acid production from glycerol

Albert Fina Romero

Universitat Autònoma de Barcelona

ESCOLA D'ENGINYERIA

Departament d'Enginyeria Química, Biològica i Ambiental

Metabolic engineering of *Pichia pastoris* for 3-hydroxypropionic acid production from glycerol

Memòria per optar al grau de Doctor

per la Universitat Autònoma de Barcelona

dins del Programa de Doctorat en Biotecnologia

sota la direcció dels doctors

Joan Albiol Sala i Pau Ferrer Alegre

per

Albert Fina Romero

Bellaterra, Setembre 2022

El Dr. Joan Albiol Sala i el Dr. Pau Ferrer Alegre, ambdós Professors Agregats del Departament d'Enginyeria Química, Biològica i Ambiental de la Universitat Autònoma de Barcelona,

Certifiquem:

Que Albert Fina Romero ha dut a terme sota la nostra direcció al Departament d'Enginyeria Química, Biològica i Ambiental de la Universitat Autònoma de Barcelona la tesi doctoral titulada "Metabolic engineering of *Pichia pastoris* for 3-hydroxypropionic acid production from glycerol". La mateixa, es presenta en aquesta memòria i constitueix el manuscrit per optar al Grau de Doctor en Biotecnologia per la Universitat Autònoma de Barcelona.

I per tal que se'n prengui coneixement i consti als efectes oportuns, signem la present declaració a Bellaterra, a 14 de setembre de 2022.

Dr. Joan Albiol Sala	Dr. Pau Ferrer Alegre	Albert Fina Romero
(Co-director)	(Co-director)	(Autor)

Agraïments – Agradecimientos – Acknowledgements

Vull començar agraint a en Pau i en Joan, supervisors d'aquesta tesi, l'oportunitat que m'han donat de treballar en aquest projecte. Conjuntament, hem tingut un procés d'aprenentatge fructífer que ha fet que tots plegats entenguem una mica millor com funciona "la *Pichia*" i que siguem conscients del potencial que té. Gràcies també per les hores dedicades a millorar el text que conforma aquesta tesi i els articles que se'n deriven.

També vull agrair a la resta de professors del grup d'Enginyeria de Bioprocessos del Departament d'Enginyeria Química, Biològica i Ambiental de la Universitat Autònoma de Barcelona (Paco, José Luis i Dolors) les seves aportacions i discussions sobre el meu projecte durant els seminaris i les reunions de grup.

Vull agrair també a tots els meus companys i amics del departament haver fet que aquets 4 anys i mig hagin sigut inoblidables. Començant pels antics (per no dir vells) companys: Sergi, Jordi, Javi, Miguel Ángel, Juanjo, Miquel i Josu. Ens ho hem passat bé... Molt bé! En especial vull agrair a en Josu tot el que hem compartit aquets 4 anys: molts bons moments i riures, però també paraules de suport i empatia. També agrair a en Sergi i en Juanjo que m'hagin ajudat amb la Biologia Molecular quan ho he necessitat. Agrair a l'Arnau i la Fela haver-me ajudat amb les fermentacions. Tots fem molt bon equip i mai falten voluntaris per donar un cop de mà en el que faci falta quan algú ho demana. Moltes gràcies.

Per mi, del més rellevant en aquest procés d'aprenentatge, ha sigut poder aprendre conjuntament amb els estudiants que he tutoritzat: la Sílvia, en Kike i l'Èric. Amb la Sílvia podríem dir que estàvem els 2 en pràctiques: ella aprenia biologia molecular i jo aprenia a ensenyar i a tenir paciència. Crec que al final tots dos ens n'hem sortit molt bé. Els resultats ho demostren! I puc dir el mateix per en Kike i l'Èric. Gràcies als tres per la feina feta i us desitjo el millor.

No em vull deixar d'agrair a cap de la resta de companys i amics del departament els bons moments viscuts: Núria, Aina, Jesi, Xènia, Albert C, Albert S, Arnau B i Mario.

També vull agrair als tècnics (Pili, Rosi i Manuel), a totes les *secres* i al personal de neteja tota la seva feina. I sempre feta amb alegria! Tots junts feu que el DEQBA sigui un lloc on ve de gust anar a treballar. On les coses són fàcils i amenes. Això fa que tots ens emportem un molt bon record del nostre pas pel DEQBA.

I also want to acknowledge Stéphanie Heux and her team for welcoming me at the MetaSys research group at the Toulouse Biotechnology Institute. During my research stay, I felt I was getting personalized masterclasses of fluxomics every day. Thank you for that and thank you for making my time in Toulouse a memorable experience. Merci!

Aunque no haya estado involucrado en mi formación doctoral y durante estos años nos hayamos visto poco, quiero agradecer al Dr. Karel Olavarria todo lo que me ha enseñado y transmitido. Los 9 meses de mi Master's Thesis en Delft fueron una formación intensiva. Te esforzaste en no solo enseñarme lo que sabías, sino también en trasmitirme tu pasión por la ciencia y por la vida. Gracias.

Acabant, vull agrair als meus pares tot el que han fet per mi. Per l'educació que m'han donat i per la llibertat i el suport que he rebut per part seva en totes les eleccions que he anat prenent al llarg de la vida. Als meus germans, per fer-me aterrar de peus a terra, per fer-me riure, per fer-me sentir estimat.

Per últim, a tu Lorena, res del que escrigui podria descriure com d'agraït estic i com d'afortunat em sento. Gràcies per tot.

Table of contents

Abstract

3-hydroxypropionic acid (3-HP), a platform chemical, has been identified as one of the top value-added products to be produced from biomass by the US Energy Department. Consequently, 3-HP bioproduction has gained remarkable attention in recent years. So far, production of 3-HP for revalorization of multiple carbon sources has been reported using a variety of microorganisms. In this thesis, the yeast *P. pastoris* (*Komagataella phaffii*) has been metabolically engineered to produce 3-HP using glycerol as substrate. This methylotrophic yeast is able to grow on crude glycerol from the biodiesel industry and can grow at a low pH, facilitating the downstream processing of 3-HP.

Expression of the malonyl-CoA to 3-HP pathway, encoded in the malonyl-CoA reductase gene (*mcr*) from *Chloroflexus aurantiacus* in *P. pastoris* resulted in 3-HP production at low yields on glycerol (0.01 Cmol $Cmol^{-1}$, strain PpHP1). Further enzyme and metabolic engineering approaches aimed at increasing the cofactor and metabolic precursors availability allowed for a 14-fold increase in the production of 3-HP compared to the starting strain (0.14 Cmol $Cmol^{-1}$, strain PpHP6). Notably, this yield was slightly higher to those previously reported using other yeasts with the same heterologous pathway, such as *Saccharomyces cerevisiae* or *Schyzosaccharomyces pombe* (0.12 Cmol $Cmol^{-1}$ in both yeasts). This suggests that the Crabtree negative profile of *P. pastoris* allows a better conservation of carbon and a lower energy waste through fermentative pathways. In addition, the strength of the constitutive pGAP promoter in *P. pastoris* led to a remarkably higher MCR specific activity compared to pTEF1 in *S. cerevisiae* (0.30 U $mg_{protein}^{-1}$ and 0.008 U $mg_{protein}^{-1}$, respectively).

A second metabolic engineering cycle was performed, aiming at increasing the malonyl-CoA supply. To this end, a second copy of the gene encoding the C-terminal domain of MCR was added (strain PpHP8). In addition, the overexpression of the endogenous cytosolic acetyl-CoA production pathway and the deletion of the reaction producing the by-product D-arabitol in strain PpHP8 yielded the strain PpHP18. While the second copy of the C-terminal domain of MCR (PpHP8) yielded the highest producing strain (0.18 Cmol $Cmol^{-1}$), strain PpHP18 showed a lower production yield (0.15 Cmol $Cmol^{-1}$), while its maximal growth rate (μ_{max}) was higher (0.17 h^{-1} compared to 0.13 h^{-1}) in small-scale cultivations.

To further characterize this series of strains, ^{13}C-based Metabolic Flux Analysis (^{13}C-MFA) was performed using a high throughput fluxomics robotic platform. The results point at the tight control of the glycolytic flux in Crabtree negative yeast *P. pastoris* causing depletion of acetyl-CoA, resulting in reduced resources for cell growth of strain PpHP8, but higher 3-HP yields. ^{13}C-MFA also shows how the upper glycolysis and pentose phosphate pathway fluxes in strain PpHP18 were highly increased, pointing at a considerable waste of ATP, which might explain the lower 3-HP yield observed in strain PpHP18 at maximal growth rate.

Fed-batch cultures of strains PpHP8 and PpHP18 were performed at a pre-programmed constant growth rate of 0.075 h^{-1}. In contrast to the strain rankings observed in small scale cultures, final 3-HP titer obtained for the strain PpHP18 was higher (37.05 g L^{-1}, 0.20 Cmol $Cmol^{-1}$) than in PpHP8 (35.4 g L^{-1}, 0.18 Cmol $Cmol^{-1}$). Moreover, productivity of strain PpHP18 was remarkably higher than productivity of strain PpHP8 (0.71 g L^{-1} h^{-1} compared to 0.62 g L^{-1} h^{-1}), due to the higher growth rate of PpHP18, which led to a shorter batch phase.

The volumetric productivity and the final 3-HP concentration achieved herein are the highest values reported in yeast to date, showing the great potential of *P. pastoris* to produce 3-HP.

Resum

L'àcid 3-hidroxipropiònic (3-HP), un producte plataforma, ha estat identificada com un dels productes de valor afegit més prometedors per ser obtinguts a partir de biomassa pel Departament d'Energia dels Estats Units. En conseqüència, en els darrers anys, els estudis centrats en la bioproducció de 3-HP han guanyat una atenció notable. Fins ara, s'ha informat de la producció de 3-HP per a la revalorització de múltiples fonts de carboni utilitzant diversos microorganismes. Aquesta tesi s'emmarca en un projecte per aconseguir produir 3-HP a partir de glicerol en *P. pastoris* (*Komagataella phaffii*). Aquest llevat metilotròfic és capaç de créixer consumint el glicerol cru provinent de la indústria del biodièsel i pot créixer a un pH baix, facilitant la posterior purificació del 3-HP.

L'expressió de la via del malonil-CoA al 3-HP, codificada pel gen de la malonil-CoA reductasa (*mcr*) de *Chloroflexus aurantiacus*, en *P. pastoris* va donar lloc a la producció de 3-HP amb rendiments baixos (0.01 Cmol Cmol^{-1}, soca PpHP1). Posteriorment, estretègies d'enginyeria enzimàtica i metabòlica dirigides a augmentar la disponibilitat de cofactors i precursors metabòlics van permetre augmentar 14 vegades el rendiment de producció de 3-HP en comparació amb la soca inicial (0.14 Cmol Cmol^{-1}, soca PpHP6). En particular, aquest rendiment va ser lleugerament superior als que s'han descrit anteriorment utilitzant altres llevats que expressaven la mateixa via heteròloga, com *Saccharomyces cerevisiae* o *Schyzosaccharomyces pombe* (0.12 Cmol Cmol^{-1} en ambdós llevats). Això suggereix que el perfil Crabtree negatiu de *P. pastoris* permet una millor conservació del carboni i un menor malbaratament energètic a través de vies fermentatives. A més, la força del promotor constitutiu pGAP en *P. pastoris* va provocar que l'activitat específica de MCR fos notablement més alta en comparació amb el promotor pTEF1 en *S. cerevisiae* (0.30 U $mg_{proteïna}^{-1}$ i 0.008 U $mg_{proteïna}^{-1}$, respectivament).

Es va realitzar un segon cicle d'enginyeria metabòlica amb l'objectiu d'augmentar el subministrament de malonil-CoA. Amb aquesta finalitat, es va afegir una segona còpia del gen que codifica el domini C-terminal de MCR (soca PpHP8). La sobreexpressió de la via endògena de producció d'acetil-CoA citosòlic i la supressió de la reacció que produeix el subproducte D-arabitol a la soca PpHP8 va donar lloc a la soca PpHP18. Mentre que la segona còpia del domini C-terminal de MCR (PpHP8) va produir la soca amb un rendiment més alt (0.18 Cmol Cmol^{-1}), la soca PpHP18 va mostrar un rendiment

de producció inferior (0.15 Cmol $Cmol^{-1}$), mentre que la seva taxa de creixement màxim (μ_{max}) va ser més alta (0.17 h^{-1} enfront de 0.13 h^{-1}) en cultius a petita escala.

Per caracteritzar encara més aquesta sèrie de soques, es va portar a terme una anàlisi dels fluxos metabòlic basada en ^{13}C (^{13}C-MFA) utilitzant una plataforma robotitzada d'alt rendiment (High Throughput) per experiments de fluxòmica. Els resultats apunten que el control estricte del flux glicolític en el llevat Crabtree negatiu *P. pastoris* provoca l'esgotament d'acetil-CoA, donant lloc a limitacions en els recursos per al creixement cel·lular de la soca PpHP8, però rendiments més elevats de 3-HP. Els resultats de ^{13}C-MFA també mostren com els fluxos de la via de la glicòlisi superior i de la via de les pentoses fosfat a la soca PpHP18 es van incrementar molt, cosa que apunta a un malbaratament considerable d'ATP. Això podria explicar el menor rendiment en la producció de 3-HP observat a la soca PpHP18 a la velocitat màxima de creixement.

Els cultius en discontinu alimentat (*fed-batch*) de les soques PpHP8 i PpHP18 es van realitzar a una taxa de creixement preprogramada i constant de 0.075 h^{-1}. En contra de les classificacions de les soques obtingudes en cultius a petita escala, la concentració final de 3-HP obtinguda per a la soca PpHP18 va ser superior (37.05 g L^{-1}, 0.20 Cmol $Cmol^{-1}$) que en PpHP8 (35.4 g L^{-1}, 0.18 Cmol $Cmol^{-1}$). A més, la productivitat de la soca PpHP18 va ser notablement superior a la productivitat de la soca PpHP8 (0.71 g L^{-1} h^{-1} en comparació amb 0.62 g L^{-1} h^{-1}), ja que el fet que la taxa de creixement de PpHP18 fos més alta va comportar que la fase *batch* del cultiu fos més curta.

La productivitat volumètrica i la concentració final de 3-HP aconseguides en aquest estudi són els valors més alts descrits en llevats fins ara, mostrant el gran potencial de *P. pastoris* per a la producció de 3-HP.

1

INTRODUCTION

Table of contents

1.1. Metabolic engineering

Biotechnology is the use of living systems (or parts from them) to achieve the production of goods or the delivery of services. Industrial biotechnological processes result in the production of a number of different products, including proteins, biopharmaceuticals, platform chemicals, biofuels, and other desired products.

Metabolic engineering is a research field within the field of biotechnology consisting in the manipulation of the metabolism of living systems. Such modifications are made to achieve various objectives: to achieve the production of a non-natural product to that organism; to increase the performance (i.e., yield or growth rate) of the cells, so that a product is obtained more efficiently; or to make the cells able to consume a substrate they do not typically use.

Nowadays, metabolic engineering research adopts the Design-Build-Test-Learn (DBTL) cycle framework (Figure 1). First, the desired outcomes are conceived and the DNA constructs and the strains that will be generated are designed. Afterwards, such strains are built and tested. Finally, all the information which was learned from the previous steps is used for the design of the next DBTL cycle. The use of the DBTL framework contributes to efficiently guide the strain optimization process.

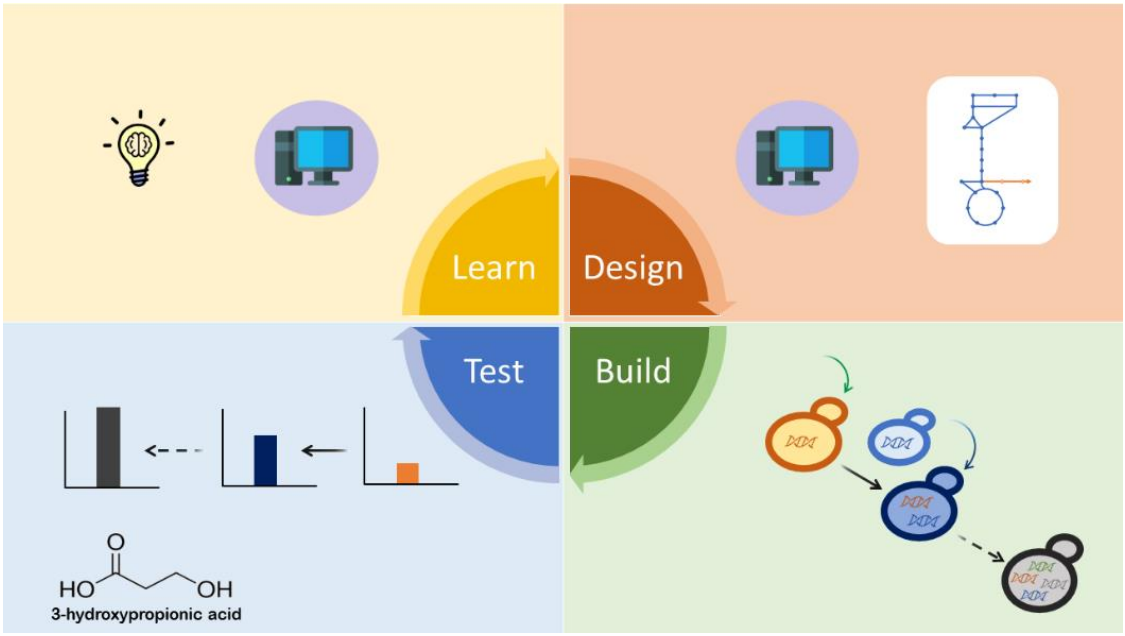

Figure 1. The DBTL cycle is the current workflow framework that guides strain optimization in metabolic engineering.

In the recent years, metabolic engineering has been placed as a central role-player to achieve a greener global economic system. It is well known the use of fossil fuels has led to an increase in the atmospheric amount of carbon dioxide, which is causing an increase in the global temperature resulting in climate change. Therefore, it is key to find new processes to produce fuels and chemicals which are not obtained from fossil carbon, but from renewable organic sources. Among these substrates, the most available ones include carbon dioxide, lignocellulosic feedstocks, and waste organic products (from industrial or urban origin). To convert such substrates to products of interest, metabolic engineering is often the key to obtain economically feasible processes. To do so, metabolic engineering researchers can benefit of all the advances of the recent years in the fields of systems biology and synthetic biology.

1.2. 3-Hydroxypropionic acid

In the year 2004, the US Energy Department published a report listing the Top Value-Added Chemicals from Biomass [1]. Later, in 2010, the list was updated [2]. The two lists considered the feasibility of the processes (considering current available knowledge), their market competitiveness, and their contribution towards a greener economy. In both cases, 3-hydroxypropionic acid (3-HP) was included into the list. From Figure 2, it can be deduced that research interest on the bioproduction of 3-HP boosted after the publication of both reports.

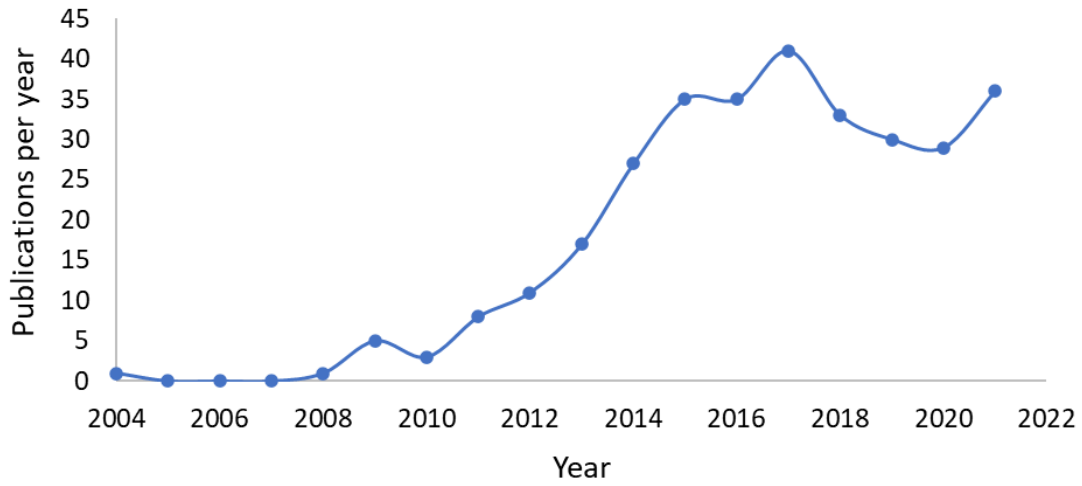

Figure 2. Number of yearly publications found on the Web of Science using "3-hydroxypropionic acid production" as a query search.

3-HP is a platform chemical, which means that it can be converted into several chemicals of industrial interest. It is a three carbon non-chiral molecule, containing a carboxyl group at C1 and a hydroxyl group at C3. Thus, it is a structural isomer of lactic acid, whose UPAC name is 2-hydroxypropionic acid, and it has the hydroxyl group at C2.

The fact 3-HP can be converted to several molecules leads to its use in multiple applications. Among them, the largest 3-HP application is the conversion of 3-HP into acrylic acid, which is typically derived from petroleum. The main use of acrylic acid is the production of superabsorbent plastics, but it is also used to produce paints and textiles. Another 3-HP application is its polymerization to make homo and heterobiopolymers, with applications in the biomedical, personal care, and adhesive sectors. Finally, 3-HP can be converted to other compounds, such as acrylamide, malonic acid, or 1,3-propanediol (PDO), among others [3].

1.3. Bioproduction of 3-HP

Bioproduction of 3-HP has been extensively reviewed in the recent years [4–8]. Metabolic engineering of natural and non-natural 3-HP producing microorganisms has been investigated. Natural production of 3-HP takes place through different pathways. In the following pages, the biological relevance of each natural pathway will be briefly described. Furthermore, metabolic engineering of natural and non-natural 3-HP producers will be reviewed.

1.2.1. Glycerol to 3-HP pathways

The first known report of 3-HP production as an end product was in *Lactobacillus* species at resting conditions [8,9]. Glycerol is first converted to 3-hydroxypropionaldehyde (3-HPA) using a coenzyme B12 dependent glycerol dehydratase. The glycerol dehydratase mechanism results in enzyme inactivation. Thus, re-activation of the enzyme is required at every cycle, which requires the consumption of 1 ATP. Afterwards, the 3-HPA is oxidized to 3-HP producing NADH. The 3-HPA is also reduced to PDO consuming NADH. Such system is used to achieve redox balance. Therefore, 3-HP and PDO are produced in almost equimolar amounts. It was later found that the conversion of 3-HPA to 3-HP is not performed in one single step, but in the three consecutive steps shown in Figure 3 [10]. The three genes coding for the enzymes catalysing each reaction are encoded in the same operon, which is named the *pdu*

operon. First, 3-HPA is converted to 3-hydroxypropionyl-CoA (3-HP-CoA), producing one NADH. In the next step, 3-HP-CoA is converted into 3-hydroxypropionyl-phosphate (3-HP-P) using inorganic phosphate. Finally, 3-HP is produced from 3-HP-P in an ATP producing reaction. As the coenzyme A (CoA) is involved in this pathway, this pathway is usually named the “Glycerol to 3-HP CoA-dependent pathway”.

The lactic acid bacterium *Lactobacillus reuteri* has been used for 3-HP production through this pathway, resulting in high product yields. However, *L. reuteri* produces 3-HP only under resting conditions. Thus, the total yield of the process (i.e., considering the growth and the production phase) is lower. Moreover, the fact that the cells need to be harvested and resuspended in a new medium, to shift from growth to resting conditions, lowers the process overall productivity [11].

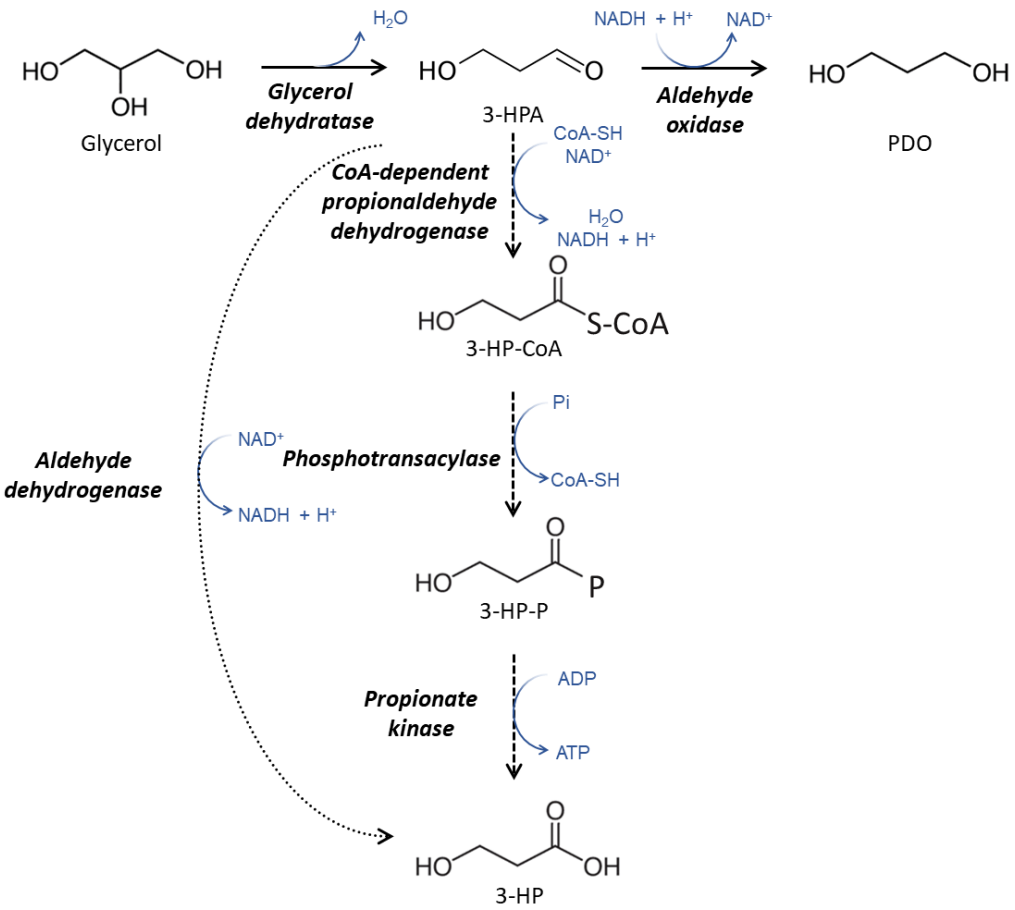

Figure 3. Glycerol to 3-HP CoA-dependent pathway (dashed line) and CoA-independent pathway (dotted line). Abbreviations: 3-HPA: 3-hydroxypropanaldehyde; 3-HP-CoA: 3-hydroxypropionyl-CoA; 3-HP-P: 3-hydroxypropionyl-phosphate; 3-HP: 3-hydroxypropionic acid; PDO: 1,3-propanediol.

The gram-negative bacteria *Klebsiella pneumoniae* can also produces 3-HPA from glycerol using a coenzyme B12 dependent glycerol dehydratase and the previously described CoA-dependent 3-HP producing route. However, in *K. pneumoniae*, glycerol dehydratase is also active under growth conditions (compared to *Lactobacillus* sp. resting cells) and PDO is produced as an electron acceptor under fermentative conditions, while glycerol is oxidized to pyruvate through lower glycolysis. Therefore, production of PDO is used to regenerate the NADH produced in the oxidative glycerol metabolism [12].

Further studies in *K. pneumoniase* identified an endogenous aldehyde dehydrogenase gene catalysing the conversion 3-HPA to 3-HP in *K. pneumoniae* in one single step [13]. However, this route produces really low amounts of 3-HP in the native microorganism, as the activity of the aldehyde dehydrogenase under physiological conditions is low [14]. Overexpression of such aldehyde dehydrogenase in *K. pneumoniae* resulted in the production of 3-HP [15].

The oxidation of 3-HPA to 3-HP catalysed by the aldehyde dehydrogenase takes place in one single step which produces NAD(P)H, while no ATP is produced (Figure 3). As CoA is not involved in this route, it is usually referred as the “glycerol to 3-HP CoA-independent pathway”. Metabolic engineering of *K. pneumoniae* for production of 3-HP through this pathway has mainly focused on increasing the activity of the aldehyde dehydrogenase. Promoter engineering of an endogenous *K. pneumoniae* aldehyde dehydrogenase gene (*puuC*) led to the highest titer of 3-HP reported to date, which was 102.6 g L^{-1} [16]. A possible issue while using *K. pneumoniae* is the production of by-products. Several studies have focused on the deletion of the pathways producing PDO, lactic acid, and acetic acid in *K. pneumoniae*. However, none of the by-products could be fully depleted [15,17].

The CoA-independent glycerol to 3-HP pathway has been largely employed in the heterologous host *Escherichia coli*. Overexpression of the B12-dependent glycerol dehydratase of *K. pneumoniae* DSM 2026 (*dhaB*) and an aldehyde dehydrogenase gene (*aldH*) from *E. coli* K-12 in *E. coli* BL21 led to 3-HP production [18,19]. In contrast to the natural producers *Lactobacillus* sp. and *K. pneumoniae*, which can produce the coenzyme B12 naturally, this vitamin was supplemented to the reactor medium to ensure the activity of the glycerol dehydratase. The results showed that PDO was also produced, pointing to the existence of non-specific enzymes that can catalyse the reduction of

3-HPA to PDO. In latter studies, genetic engineering of *E. coli* K-12 W3110 and bioprocess optimization allowed to increase the production of 3-HP while decreasing the production of by-products, leading to the recombinant microorganism with the highest productivity reported to date, which was 1.89 $g \cdot L^{-1} \cdot h^{-1}$ [20]. In the same study, the use of a *ΔlacI* strain with promoters *trc* and *tac* allowed constitutive strong expression of the genes of the glycerol to 3-HP pathway. The use of IPTG to induce gene expression is undesired as it might render the production of 3-HP economically unviable.

Interestingly, the less energy efficient CoA-independent pathway has been more studied than the CoA-dependent pathway. Only a few studies using the CoA-dependent pathway in heterologous organisms have been reported. The *pdu* operon from *K. pneumoniae* and *L. reuteri* have been expressed in *E. coli* [21,22]. Results showed that the heterologous expression of the CoA-dependent pathway resulted in lower amounts of 3-HP than the CoA-independent pathway. Nevertheless, the bioconversion of 3-HPA to 3-HP using the CoA-dependent pathway in *E. coli* yielded promising results, as the conversion yield of 3-HPA to 3-HP was close to 1 mol mol^{-1} [22]. Nevertheless, industrial implementation of such approach would be challenging, as it requires two bioprocesses and two downstream processes: production and purification of 3-HPA and 3-HP, respectively.

One of the limiting factors for the implementation of the glycerol pathway to produce 3-HP is its dependence on the use of a vitamin B12-dependent glycerol dehydratase. For the non-natural B12 producers, such as *E. coli*, vitamin B12 needs to be added to the medium. Recently, *E. coli* was made capable to produce coenzyme B12 *de novo*. To do so, 28 heterologous genes were simultaneously expressed [23].

Dependence on B12 poses an inconvenient even in the natural producers *K. pneumoniae* and *Lactobacillus* sp., as B12 is not produced in fully aerobic conditions. For this reason, in the most recent years, metabolic engineering of B12 producing microorganisms such as *Pseudomonas denitrificans* and *Pseudomonas asiatica* has been investigated [24,25]. *Pseudomonas* sp. can produce vitamin B12 under aerobic conditions. Thus, oxygen can be used as electron acceptor for the oxidation of the NAD(P)H produced in the 3-HPA to 3-HP route, while the glycerol dehydratase can remain active due to the production of B12. In this case, *P. asiatica* was cultured using glucose as a C-source for cell growth, while glycerol was used as a C-source to produce 3-HP. With this approach, 5.4 g L^{-1} of 3-HP were obtained when no vitamin B12 was

added to the medium, while 67.1 g L^{-1} of 3-HP were achieved when the medium was supplemented with vitamin B12. Therefore, further studies to reduce the vitamin B12 requirements or to increase B12 production in *P. asiatica* are required [25].

Finally, an alternative coenzyme B12-independent glycerol dehydratase was identified in the gram positive bacteria *Clostridium butyricum* [26]. However, its use has not been widely implemented, as it requires strict anaerobic conditions. The production of 3-HP from glycerol produces NADH. Therefore, oxygen is required for NADH reoxidation if no fermentation by-products such as PDO or lactic acid are desired, hampering the implementation of such strict anaerobic coenzyme B12-independent glycerol dehydratase.

The reports cited so far used glycerol as a sole C-source. Glycerol was both the substrate for growth and the 3-HP production pathway. However, the use of glucose and xylose as substrates is of high interest, as they are among the most abundant sustainable C-sources. To this end, *E. coli* was metabolically engineered to achieve accumulation of glycerol from glucose and xylose. Afterwards, the expression of the glycerol to 3-HP CoA-independent pathway led to the production of 53.7 g L^{-1} of 3-HP at a productivity of 0.63 g L^{-1} h^{-1} [27]. The same approach was reported in *Corynebacterium glutamicum*, a gram-positive bacterium widely used in the biotechnological industry to produce amino acids. Metabolically engineered *C. glutamicum* produced 62.6 g L^{-1} of 3-HP through the CoA-independent pathway using glucose as a sole C-source [28]. The same strain produced 54.8 g L^{-1} of 3-HP at a yield of 0.49 g g^{-1} using a mixture of 50% glucose and 50% xylose.

Some of the 3-HP titers and productivities found in the literature reported above are summarized in Table 1.

Table 1. Reported results on the production of 3-HP through the glycerol CoA-dependent and CoA-independent routes.

Microorganism	C-source	Culture conditions	Final titer (g L^{-1})	Yield (g g^{-1})	Productivity (g L^{-1} h^{-1})	Reference
Glycerol CoA-dependent pathway						
L. reuteri	Glycerol	Fed-batch culture with *L. reuteri* resting cells.	14	0.48	0.35*[1]	[11]
L. reuteri / *E. coli*	Glycerol	Production of 3-HPA in a fed-batch culture with *L. reuteri* / Shake flask bioconversion of 3-HPA to 3-HP in *E. coli*, B12 suppelementation.	1.1	0.67	0.06	[22]
Glycerol CoA-independent pathway						
K. pneumoniae	Glycerol	Fed-batch culture, IPTG induction, yeast extract supplementation.	102.6	0.86*[2]	1.07	[16]
E. coli	Glycerol	Fed-batch culture, B12 supplementation, IPTG induction.	31.0	0.34	0.43	[19]
E. coli	Glycerol	Fed-batch culture, B12 supplementation, IPTG induction.	76.2	0.46	1.89	[20]
E. coli	Glucose + Xylose	Fed-batch culture, B12 supplementation, IPTG induction.	53.7	0.26	0.63	[27]
C. glutamicum	Glucose + Xylose	Fed-batch culture, B12 supplementation, IPTG induction.	54.8	0.49	0.76	[28]
P. asiatica	Glucose + Glycerol	Fed-batch culture.	5.4	0.98*[3]	0.18	[25]
P. asiatica	Glucose + Glycerol	Fed-batch culture, B12 supplementation.	67.1	0.98*[3]	1.40	[25]

*[1]Excluding the batch growth phase.

*[2]Calculated during the fed-batch N-limited phase (no cell growth).

*[3]Based on glycerol consumption only (excluding the glucose used).

1.2.2. Malonyl-CoA to 3-HP pathway

3-HP is also involved as an intermediary metabolite in the fixation of carbon dioxide through several pathways, such as the 3-hydroxypropionate/malyl-CoA cycle (or 3-hydroxypropionate bi-cycle) [10,29], shown in Figure 4, or the 3-hydroxypropionate/ 4-hydroxybutyrate cycle [30], shown in Figure 5. The 3-hydroxypropionate/malyl-CoA cycle has been described in the phototrophic bacterium *Chloroflexus aurantiacus*, and it fixates CO_2 through two converging cycles (a bi-cycle). At every bi-cycle, 3 molecules of CO_2, 6 of NADPH, and 7 ATP equivalents are used to generate 1 molecule of pyruvate. The 3-hydroxypropionate/4-hydroxybutyrate cycle is a variant of the 3-hydroxypropionate/malyl-CoA cycle, and it is present in several archaeal species (*Metallosphaera* and *Sulfolobus* sp.). In this case, 3 molecules of CO_2, 5 of NADPH, 2 reduced ferredoxins, and 6 ATP equivalents are used to generate 1 molecule of pyruvate and 1 of NADH.

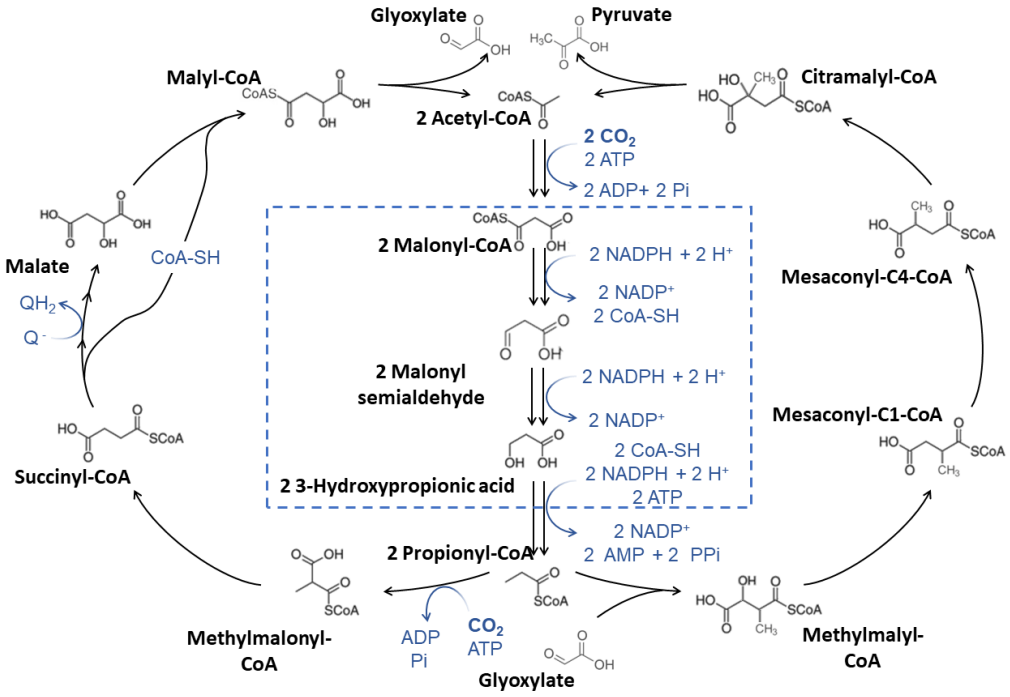

Figure 4. 3-Hydroxypropionic/malyl-CoA cycle. The malonyl-CoA to 3-HP pathway is highlighted in a dashed blue rectangle.

Compared to the Calvin-Benson-Bassham cycle, which is the most widespread autotrophic cycle, the 3-hydroxypropionate/malyl-CoA bi-cycle is present in microorganisms growing on slightly alkali media. At high pH, most inorganic C is found

as hydrogencarbonate, while the enzymes of the Calvin cycle have a higher affinity for dissolved CO_2. The enzymes of the 3-hydroxypropionate/malyl-CoA cycle have a higher affinity for hydrogencarbonate than for dissolved CO_2, which explains the positive selection pressure towards this autotrophic cycle [31].

The 3-hydroxypropionate/4-hydroxybutyrate cycle has only been described in thermophilic archaea (>70ºC). At such temperatures, Ribulose-1,5-bisphosphate carboxylase/oxigenase (Rubisco) activase is not active [32]. Therefore, autotrophy through the Calvin cycle is not possible.

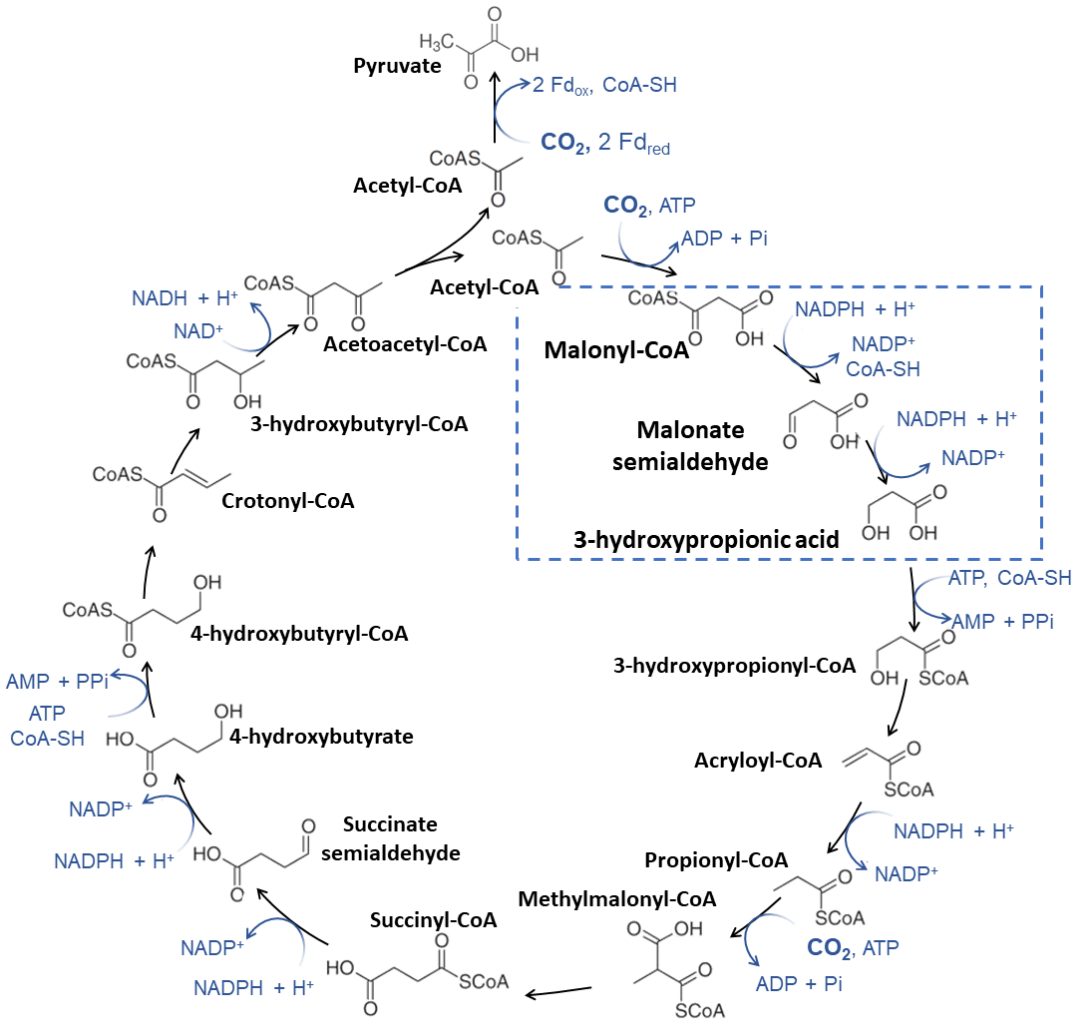

Figure 5. 3-hydroxypropionate/4-hydroxybutyrate cycle. The malonyl-CoA to 3-HP pathway is highlighted in a dashed blue rectangle.

In both pathways, 3-HP is produced from malonyl-CoA through two sequential reactions converting malonyl-CoA into malonyl semialdehyde (MSA), which is then

converted into 3-HP. Each step of the pathway consumes one NADPH, which is oxidized to $NADP^+$. While 3-HP is involved in the process, it is not an end-product, meaning that microorganisms naturally expressing the malonyl-CoA to 3-HP pathway do not accumulate 3-HP in significant amounts. For this reason, production of 3-HP through this route has focused on the use of recombinant microorganisms.

The heterologous use of the enzymes from hyperthermophilic archaea is inadequate because they are naturally adapted for high temperatures (>70ºC), which are unfeasible temperatures for most recombinant hosts. Therefore, genes of the mild thermophilic bacterium *C. aurantiacus* are usually the preferred option for the recombinant expression of the pathway. Moreover, the two consecutive reducing steps producing 3-HP from malonyl-CoA are encoded in one single gene in *C. aurantiacus*, the malonyl-CoA reductase (mcr_{Ca}). The optimal growth temperature of this bacterium is 55ºC [33], and the maximum activity of the bi-functional enzyme is achieved at 50ºC [34].

The two substrates of MCR are malonyl-CoA and NADPH. Malonyl-CoA is a key central metabolite which is present in all organisms, as it is a substrate for the synthesis of fatty acids. The pathway producing 3-HP from malonyl-CoA has been heterologously expressed in several microorganisms. In all cases, the sole expression of mcr_{Ca} led to the production of 3-HP. Some of the tested microorganisms are *E. coli* [34], *Saccharomyces cerevisiae* (Chen 2014), *Schizosaccharomyces pombe* [35], *C. glutamicum* [36], *Methylosinus trichosporium* [37], and *Methylobacterium extorquen* [38]. In addition to a large number of microorganisms, different substrates have been used to produce 3-HP through the malonyl-CoA pathway: glucose, xylose, fatty acids, methanol, methane, and CO_2.

The first reports on the use of the malonyl-CoA pathway to produce 3-HP used *E. coli* as a host microorganism and glucose as a C-source. The bi-functional enzyme MCR from *C. aurantiacus* was expressed. Moreover, the recombinant *accADBCb* operon was also expressed, which contains the genes encoding the endogenous acetyl-CoA carboxylase (ACC) complex and the biotin ligase gene (*birA*). The biotin ligase attaches biotin to the ACC complex, which catalyses the conversion of acetyl-CoA and CO_2 into malonyl-CoA (Figure 6). Finally, the *E. coli* strain was further modified to express the nicotinamide nucleotide transhydrogenase gene (*pntAB*), which catalyses the reduction of $NADP^+$ to NADPH coupled to the reaction oxidizing NADH to NAD^+. The transhydrogenase action increases the NADPH/$NADP^+$ ratio. In addition to the increased

precursors availability (malonyl-CoA and NADPH), genes related to the production of competing by-products such as lactic acid and acetate were deleted [34]. Using a similar metabolic engineering approach and an optimized bioprocess set up, an *E. coli* strain produced up to 48.4 g L^{-1} of 3-HP, at a yield of 0.53 g g^{-1} [39].

Later studies in *E. coli* have focused on increasing the activity of MCR. To do so, the dissection of the bi-functional MCR into the two independent subunits catalysing each of the two reactions led to a substantial increase in 3-HP production [40]. Further insight into the protein structure of MCR from *Porphyrobacter dokdonensis* show that the bi-functional enzyme is structured as a homodimer. Such structure leads to a rapid consumption of MSA to produce 3-HP by the N-terminal domain of the enzyme, minimizing the accumulation of toxic MSA [41]. However, such structure may hinder the interaction of the malonyl-CoA and/or the NADPH with the C-terminal domain of the enzyme. Indeed, separate expression of the two subunits of MCR from *C. aurantiacus* in *E. coli* led to a 4-fold increase of the K_m/k_{cat} of malonyl-CoA with the C-subunit of MCR [40], which was further increased to 14-fold by laboratory evolution of the MCR C-terminal fragment [42]. The latter strain produced 3-HP at a volumetric productivity of 0.56 g L^{-1} h^{-1}, which is the highest volumetric productivity reported through the malonyl-CoA pathway.

Similarly, *E. coli* was also engineered to produce 3-HP from fatty acids, which can be obtained from abundant sustainable sources. The evolved version of the mcr_{Ca}-C-terminal gene, the mcr_{Ca}-N-terminal gene, and the operons *pntAB* and *accADBC* were expressed in an *E. coli* strain capable of consuming fatty acids. The resulting strain produced 52 g L^{-1} of 3-HP in a fed-batch culture [43].

The use of the industrial workhorse *S. cerevisiae* to produce 3-HP through the malonyl-CoA pathway has also been investigated. First, the expression of mcr_{Ca} led to the production of 3-HP. The strain's product yield was further increased by increasing the availability of the two pathway precursors, i.e. malonyl-CoA and NADPH.

To increase malonyl-CoA availability, overexpression of the endogenous acetyl-CoA carboxylase gene (*ACC1*) led to a higher yield [44]. As malonyl-CoA is mostly derived from carboxylation of acetyl-CoA, to further foster the malonyl-CoA availability, several strategies have been reported aiming at increasing the acetyl-CoA delivery.

Acetyl-CoA production in the cytosol of yeast differs from its production in bacteria, as shown in Figure 6. The conversion of pyruvate to cytosolic acetyl-CoA in bacteria is performed through one single reaction (consisting of several elementary steps) producing NADH. The reaction is catalysed by the pyruvate dehydrogenase complex (PDHC). In eukaryotes, production of mitochondrial acetyl-CoA follows the same stoichiometry. However, cytosolic acetyl-CoA follow a different route, which consists of 3 steps producing 1 NADH and consuming 2 ATP equivalents. First approaches to increase 3-HP production in yeast focused on overexpressing the endogenous cytosolic acetyl-CoA production pathway, which includes the pyruvate decarboxylase (*PDC1*), the major aldehyde dehydrogenase (*ALD6*), and the acetyl-CoA synthase (*ACS*) [44,45]. For ACS, an unregulated and more active variant enzyme from *Salmonella enterica* was used [46], while the other two native genes were overexpressed.

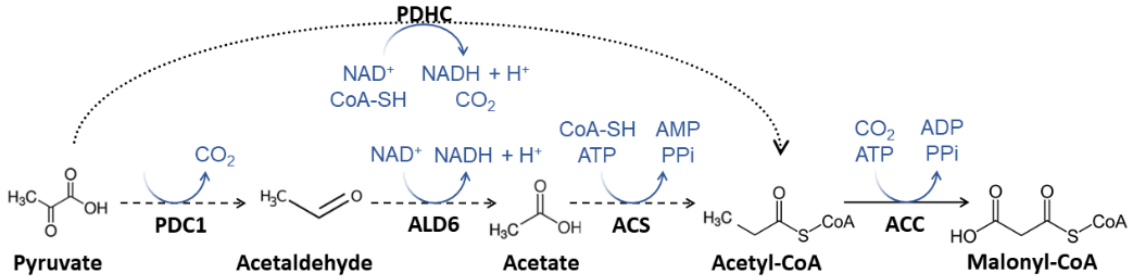

Figure 6. Cytosolic acetyl-CoA production pathway in *E. coli* (dotted arrows) and yeast (dashed arrows). The reaction producing malonyl-CoA from acetyl-CoA, catalysed by the acetyl-CoA carboxylase (ACC) is also showed. The stoichiometry of ACC is equal for both *E. coli* and yeast. PDHC: Pyruvate dehydrogenase complex; PDC1: major pyruvate decarboxylase; ALD6: aldehyde dehydrogenase; ACS: acetyl-CoA synthase.

In a different study, a variant of the phosphoketolase pathway was used to increase the availability of acetyl-CoA. The reported pathway produces 3 acetyl-CoA from fructose-6-phosphate. This strategy allows to maximize the C-yield, as there are no de-carboxylation reactions involved. The resulting strain showed a 109% increase in the product yield [47]. Other successful strategies to increase cytosolic acetyl-CoA in yeast have been extensively reviewed [48,49], but they have not been implemented to produce 3-HP.

Increasing the delivery of NAPDH, which is the other substrate of the malonyl-CoA to 3-HP pathway, was also addressed in *S. cerevisiae*. Expression of a non-phosphorylating NADP-dependant glyceraldehyde-3-phosphate dehydrogenase

(*GAPN*) [44] or a phosphorylating NADP-dependant glyceraldehyde-3-phosphate dehydrogenase (*NADP-GAPDH*), and the simultaneous downregulation or depletion of endogenous GAPDH encoding genes (*TDH1, TDH2,* and *TDH3)* resulted in increases in 3-HP production [45].

The best *S. cerevisiae* producing 3-HP from malonyl-CoA harbours multiple integrated copies of mcr_{Ca} and *ACC1*, it has an increased acetyl-CoA delivery due to the overexpression of the cytosolic acetyl-CoA pathway, it contains the deletion of relevant genes responsible for the formation of by-products, and it has an increased NADPH delivery due to the replacement of *TDH3* with a NADP-dependent glyceraldehyde-3-phosphate dehydrogenase. On a fed-batch process, this strain achieved the production of 9.8 g L^{-1} of 3-HP at a yield of 0. 13 g g^{-1} from glucose [45].

A similar approach was used in the fission non-conventional yeast *S. pombe*. Multiple copies of an evolved version of the mcr_{Ca}-C-terminal gene were expressed together with a single copy of the mcr_{Ca}-N-terminal gene. The strain was further engineered by overexpressing ACC and the cytosolic acetyl-CoA producing pathway. Some of the genes responsible for ethanol production, which is the main by-product of this Crabtree positive yeast, were deleted. This strain was grown on glucose achieving a similar 3-HP production than in *S.cerevisiae* (9.2 g L^{-1}). Interestingly, *S. pombe* was modified to display beta-glucosidase enzymes anchored to the yeast cell surface. The resulting yeast was able to metabolize cellobiose to produce 11.4 g L^{-1} 3-HP [35].

Other recent studies have addressed the use of *E. coli* to produce 3-HP from other C-sources, such as acetate [50,51], which, in turn, can be sustainably produced from syngas containing H_2, CO, and CO_2 [52]. Production of 3-HP from one-carbon sustainable sources, such as methanol and methane, has also been investigated. Production of 3-HP from methanol has been achieved in *M. extorquens* [38], while the production from methane was reported in *M. trichosporium* [37]. In both cases, the malonyl-CoA pathway was used.

Actual implementation of bioprocesses using small C molecules such as methanol, methane, and acetate is still challenging, as most microorganisms growing on these substrates do so at a low growth rate, which hampers their industrial implementation. Thus, further research to increase the volumetric productivity is necessary. To this end, the simultaneous use of acetate and glucose has been studied in *C. glutamicum*. Glucose was used as a carbon and energy source, while acetate was

used as a substrate for 3-HP production [53]. Another interesting strategy to improve the volumetric productivity in such slow-growing substrates is the use of the cells as whole-cell catalysts, i.e., splitting growth and bioproduction phase. Such approach has reported promising outcomes in *E. coli* [50,52].

The most relevant results reported in this section are summarized in Table 2.

From the results reported above and the derived discussion, it is deduced that the main advantages of the malonyl-CoA pathway compared to the glycerol pathway are: i) It does not require the addition of external cofactors (such as the vitamin B12); and ii) The presence of the intermediary metabolite MSA does not result in the production of large amounts of by-products, such as the PDO produced when the glycerol pathway is used (as a result of the reduction of 3-HPA).

Table 2. Reported results on the production of 3-HP through the malonyl-CoA pathway.

Microorganism	C-source	Culture conditions	Final titer ($g\ L^{-1}$)	Yield ($g\ g^{-1}$)	Productivity ($g\ L^{-1}\ h^{-1}$)	Reference
E. coli	Glucose	Fed-batch culture, IPTG induction.	48.4	0.53	-	[39]
E. coli	Glucose	Fed-batch culture, IPTG induction.	40.6	0.19	0.56	[42]
E. coli	Fatty acids (Palmitic acid)	Fed-batch culture, arabinose induction.	52	1.40*[1]	1.13*[1]	[43]
E. coli	Glucose + Acetate	Batch on glucose. Shift to fed-batch on acetate. IPTG induction.	6.5	0.39	0.10	[50]
E. coli	Acetate	Two-stage: 1) Shake-flask on rich medium. 2) Bioconversion of acetate to 3-HP. IPTG induction.	15.8	0.71*[2]	0.36*[2]	[52]
S. cerevisiae	Glycerol	Fed-batch culture.	9.8	0.13	0.10	[45]
S. pombe	Glucose	Fed-batch culture.	9.2	0.11	0.10	[35]
S. pombe	Cellobiose	Fed-batch culture.	11.2	0.12	0.14	[35]
C. glutamicum	Glucose + Acetate	Batch fermentation with glucose and acetate co-feeding.	3.8	0.19	0.08	[53]
M. extorquens	Methanol	Fed-batch culture.	0.09	0.02	<0.01	[38]
M. trichosporium	Methane + CO_2	Bioreactor sparged with Methane and CO_2.	0.06	0.02	<0.01	[37]

*[1]Calculated during the feeding phase (excluding previous batch phase on glucose to grow the cells). Equal to 0.75 Cmol $Cmol^{-1}$.
*[2]Calculated during the Bioconversion phase.

1.2.3. β-alanine pathway

The biosynthetic route producing 3-HP from β-alanine is a non-naturally occurring pathway. β-alanine is an intermediary precursor of vitamin B5, which is one of the components of the Coenzyme A (CoA). The β-alanine to 3-HP pathway consists of two steps (Figure 7). First, β-alanine can be converted into MSA by two different enzymes: the β-alanine-pyruvate aminotransferase (BAPAT) or the γ-aminobutyrate transaminase (GABT). Afterwards, MSA is converted to 3-HP in a reducing reaction consuming either NADH or NADPH [54–56].

The use of the malonyl-CoA and the β-alanine pathways were compared using a *S. cerevisiae* genome scale model, simulating different environmental conditions. The results showed that the use of the malonyl-CoA pathway to produce 3-HP resulted in higher oxygen dependency than the β-alanine pathway. This is explained by the net consumption of ATP when 3-HP is produced from glucose through the malonyl-CoA route, while there is net or null production of ATP when the β-alanine pathway is used [57].

Several genes were tested for each one of the two steps converting β-alanine into 3-HP in yeast. First, it was found that BAPAT from *Bacillus cereus* was the most appropriate enzyme to convert β-alanine into MSA. This finding was against expectations, as most of the patented sequences to catalyse this reaction were from *Pseudomonas* sp. [55]. Afterwards, it was concluded that *E. coli* NADPH dependant 3-hydroxy acid dehydrogenase (YDFG) was the best option for the second step of the pathway. The endogenous production of β-alanine is usually low. Actually, *S. cerevisiae* expressing the two aforementioned genes did not produce 3-HP. For this reason, overexpression of endogenous or heterologous pathways generating β-alanine was required. The only endogenous pathway producing β-alanine in yeast is linked to ornithine metabolism. Engineering this pathway to carry a high flux is challenging. For this reason, the bacterial gene *panD*, which encodes an aspartate-1-decarboxylase catalysing the conversion of L-aspartate into β-alanine, was expressed in the cytosol of *S. cerevisiae*. Aspartate is present in the yeast cytosol, and it is generated from cytosolic oxaloacetate. The resulting strain was able to produce 3-HP [57].

Further metabolic engineering of this strain to increase the delivery of L-aspartate was performed. The resulting strain produced 13.7 g L^{-1} of 3-HP from glucose in a fed-batch bioreactor [57]. This strain was characterized in multiple small chemostat

cultures to determine its optimal growth rate and the effect of C, N, or P-limitation on process parameters. The optimized fed-batch process was performed at a low growth rate (0.04 h^{-1}) and P-limiting conditions, resulting in, approximately, 27 g L^{-1} of 3-HP [58].

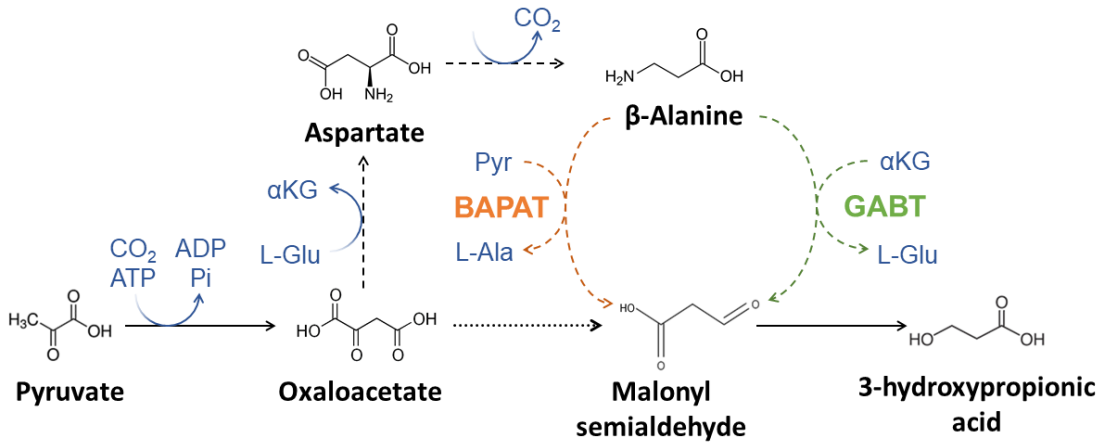

Figure 7. β-alanine to 3-HP (dashed arrows) and oxaloacetate to 3-HP (dotted arrows) pathways. Abbreviations: L-Glu: L-glutamic acid; αKG: α-ketoglutarate; Pyr: Pyruvate; L-Ala: L-alanine; BAPAT: β-alanine-pyruvate aminotransferase; and GABT: γ-aminobutyrate transaminase.

The β-alanine to 3-HP pathway has also been expressed in *E. coli*. A previously generated *E. coli* strain overproducing β-alanine was used as a chassis to express the β-alanine to 3-HP pathway. The BAPAT gene *PA0132* from *P. putida* and the *YdfG* from *E. coli* were expressed [59,60]. The resulting strain produced 31.1 g L^{-1} 3-HP in an optimized fed-batch culture using glucose as a substrate.

1.2.4. Non-natural routes

Computational tools can be used to find new non-naturally occurring pathways. These tools use all the available information from enzymatic and “omics” databases, such as Brenda (https://www.brenda-enzymes.org/), Metacyc (https://metacyc.org/) or KEGG (https://www.genome.jp/kegg/). The computational tools can be used to rank the new pathways based on various criteria, such as maximum product yield, pathway length, or thermodynamic feasibility.

Using the Biochemical Network Integrated Computational Explorer (BNICE), new pathways to produce 3-HP from pyruvate were found [61]. BNICE considers the existence of novel non-reported reactions which are deduced from a series of reaction rules. The new pathways were evaluated based on their thermodynamic feasibility

performing thermodynamic metabolic flux analysis (TMFA). Among the results, the β-alanine to 3-HP pathway was found as the most promising one, as it has a maximum theoretical yield of 2 $mol_{3\text{-}HP}$ $mol_{Glucose}^{-1}$, and it has a favourable ΔG. Several new pathways were found to also fulfil the maximum theoretical yield of 2 $mol_{3\text{-}HP}$ $mol_{Glucose}^{-1}$, but they involved some critical steps with an unfavourable ΔG. This is the case of the conversion of pyruvate into 3-HP via lactate, in a 2-steps route.

One of the new routes reported using BNICE was the oxaloacetate to 3-HP pathway, which was the shortest thermodynamically feasible pathway which was identified. This 3-steps pathway starts with the conversion of pyruvate into oxaloacetate, which is then converted into MSA by a hypothetic pyruvate carboxy-lyase. Finally, MSA is converted to 3-HP by an MSA reductase as reported for both the malonyl-CoA and the β-alanine pathway. The maximum theoretical yield for this pathway using glucose as substrate is 1.22 $mol_{3\text{-}HP}$ $mol_{Glucose}^{-1}$.

The use of the oxaloacetate to 3-HP pathway was recently reported in *S. cerevisiae*. The pyruvate carboxy-lyase reaction was catalysed by the benzoylformate decarboxylase from *P. putida* E23. The recombinant yeast strain produced 18.1 g L^{-1} of 3-HP at a volumetric productivity of 0.17 g L^{-1} h^{-1} in a fed-batch culture where glucose was used as a substrate [62].

1.4. Crude glycerol as a sustainable biomass-derived feedstock

The US Energy Department report on the most promising bulk-chemicals derived from biomass considers the revalorization of several biomass feedstocks, including starch, hemicellulose, cellulose, lignin, oil, and proteins [1]. Waste oils, like cooking oil or animal fat, are usually employed to produce biodiesel. Biodiesel consists of fatty-acid methyl esters (FAME), which are obtained from the transesterification of triglycerides with methanol. This reaction can be catalysed by an alkali catalyst (sodium or potassium hydroxide) or an enzyme (lipase). In both cases, glycerol is obtained as a side product [63]. The mixture of FAMEs and glycerol is separated. The recovered glycerol contains large amounts of methanol, moisture, free fatty acids, and ashes. This mixture, which may have a different composition depending on its source, is known as crude glycerol [64].

Worldwide production of crude glycerol has increased in parallel to the increasing biodiesel global production, which reached 40,000 million litres in 2020, and it is

forecasted it will reach 45,000 litres in 2027 [65]. The current glycerol global production largely exceeds its demand. The oversupply of glycerol, which leads to a drop in its market price, rises concerns on the actual sustainability of the biodiesel production, both from an environmental and an economic point of view. Therefore, conversion of the crude glycerol into other value-added products is required [64,65]. Many different applications have been already investigated, including both biological and chemical conversions [66].

For the biological conversion of crude glycerol into value-added products, a microorganism which can grow on such substrate is required. As crude glycerol contains methanol, which may accumulate into the bioreactor during a fed-batch culture, a microorganism which can consume and/or tolerate high methanol concentrations is required. For this reason, the use of the methylotrophic yeast *Pichia pastoris*, which is able to produce heterologous proteins from crude glycerol, has been extensively investigated [67–69]. Nevertheless, the use of *P. pastoris* to produce bulk chemicals of added value from glycerol has not been investigated, yet.

1.5. Microbial production of 3-HP from crude glycerol

Recently, an *E. coli* strain was engineered to produce 3-HP through the glycerol CoA-independent pathway. This strain was cultivated on a fed-batch culture using crude glycerol as a C-source, producing 61 g L^{-1} of 3-HP, with a product yield of 0.6 g g^{-1}, and a productivity of 2.28 g L^{-1} h^{-1} [20]. These results show the potential of the microbial conversion of crude glycerol into 3-HP.

However, *E. coli* cannot typically consume methanol, which may account for >20% of the weight in some crude glycerol variants [70]. In such case, if methanol is not consumed, methanol will accumulate into the reactor, leading to toxicity effects that would hamper cell growth [71]. Moreover, performing the cultivations at a pH below the pK_a of 3-HP (i.e., below pH 4.5) is desirable, as it can be coupled to the *in situ* purification of 3-HP from the fermentation broth using solvent extraction methods, avoiding the toxicity effects linked to high 3-HP concentrations [44,72,73]. Therefore, *P. pastoris* is a promising host to produce 3-HP from crude glycerol, as it can consume the methanol present in the crude glycerol and it can also grow at pH values as low as 3 [74,75].

1.6. *Pichia pastoris* as a host for metabolic engineering to produce bulk chemicals

Pichia pastoris is a methylotrophic Crabtree negative yeast. Several years ago, *P. pastoris* was classified within the genus of *Komagataella*, which contains six different species [76]. It was reported that, of all the *Komagataella* species, two different strains (*K. pastoris* and *K. phaffii*) had been previously refereed as *P. pastoris*. Today, the term *P. pastoris* is used to refer to all *Komagataella* strains used for biotechnological applications [77].

The yeast *P. pastoris* has been typically employed to produce heterologous proteins. There are two well stablished protein production systems derived from two strong promoters: i) the GAP promoter, which is constitutive (GAP) [78] and ii) the AOX1 promoter, which is induced by methanol [79]. The ability of *P. pastoris* to efficiently secrete heterologous proteins, the existence of the two aforementioned strong expression systems, and the capacity of *P. pastoris* to make mammalian-like post-translational modifications (PTM) to proteins have given *P. pastoris* a prominent role in today's biotechnological industry [80]. However, studies addressing the use of *Pichia pastoris* to produce bulk chemicals of interest is still scarce.

Production of xylitol was one of the first reports of metabolic engineering in *P. pastoris* for the production of a platform chemical. Xylitol can be used as a building block for multiple applications, such as the production of biopolymers. The researchers took advantage of the natural capacity of this yeast to produce D-arabitol under hypoxic and hyperosmotic conditions. Two heterologous genes were expressed, which allowed the conversion of D-arabitol into xylitol. The two genes were expressed constitutively using the strong and constitutive GAP promoter [81]. This strain produced 15.2 g L^{-1} of xylitol from 220 g L^{-1} of glucose.

Production of high-energy biofuels like isobutanol and isobutyl acetate from glucose was also achieved in *P. pastoris*. As isobutanol is produced from the L-valine precursor 2-ketoisovalerate, the pyruvate to 2-ketoisovalarate pathway was overexpressed. Two heterologous genes were also expressed to convert 2-ketoisovalerate into isobutanol. The expression of all these genes was under the control of the GAP promoter. The resulting strain produced 2.22 g L^{-1} of isobutanol or 51.2 mg L^{-1} isobutyl acetate from glucose [82].

The only bulk chemical which has been produced from glycerol in *P. pastoris* is lactic acid. The recombinant strain overexpressed a heterologous lactate dehydrogenase (LDH) from *Bos taurus* under the control of the GAP promoter and an endogenous lactate transporter under the control of the PGK promoter. This strain produced almost 30 g L^{-1} of lactic acid at a volumetric productivity of 0.673 g L^{-1} h^{-1} and an overall yield of 0.7 g g^{-1} when grown on an oxygen-limited fed-batch culture [83]. In another study, the simultaneous overexpression of LDH from *B. taurus* and the deletion of the pyruvate decarboxylase and the arabitol dehydrogenase allowed to maximize the yield to 0.855 g g^{-1}, while minimizing the production of by-products acetate and D-arabitol [84]. While pure glycerol was used as substrate, these results confirm the potential of *P. pastoris* to produce bulk chemicals to revalorize crude glycerol.

Other reports exist on the metabolic engineering of *P. pastoris* to produce high-value chemical compounds, such as 6-methylsalicylic acid [85], lycopene [86], β-carotene [87], or polyketides [88], among others. Production of such complex metabolites requires the expression of long pathways, involving the heterologous expression of multiple genes. Synthetic biology tools for *P. pastoris* have been developed in order to facilitate the simultaneous overexpression of multiple genes. Such tools are reviewed in the following section.

P. pastoris is also an attractive yeast to investigate the revalorization of methanol. Methanol is a promising substrate, as it can be sustainably obtained from the hydration of CO_2 [89,90]. The only example of methanol revalorization in the literature is the production of 2.79 g L^{-1} of malic acid using methanol as a sole carbon source [91].

P. pastoris has also been engineered to obtain an efficient xylose-consuming strain. Such capacity is crucial to obtain a *P. pastoris* strain which can be used to revalorize lignocellulosic feedstocks [92].

Finally, one of the most ambitious metabolic engineering projects in *P. pastoris* achieved a yeast strain which can grow on CO_2 as a C-source for biomass production, while it uses methanol as an energy source [93].

Most of the reported metabolic engineering projects described above took advantage on previous knowledge from the well stablished GAP and AOX1 heterologous protein production systems. However, new sets of promoters for synthetic biology applications in *P. pastoris* have been reported. In addition, systems biology research in

this yeast has provided relevant information for metabolic engineering applications. Some of these advances are reported in the following sections.

1.7. Synthetic biology tools for genetic engineering of *P. pastoris*

As described in the previous section, most metabolic engineering projects in *Pichia pastoris* relied on the use of the strong and well-stablished GAP and AOX1 promoters. However, use of multiple copies of such promoters may lead to a metabolic burden. In addition, the gene expression may be diluted when multiple copies of the same promoter are used [94]. Therefore, use of other promoters with lower expression might be interesting for the enzymes catalysing non-rate-limiting reactions. To this end, efforts have been made to expand the set of available promoters for *P. pastoris* [95–97].

In most cases, to obtain promising strains for the production of bulk chemicals, multiple genetic modifications are required. There are multiple strategies to facilitate the simultaneous addition of multiple expression cassettes, which allow to speed up the process of generating new strains. For example, strong bi-directional promoters have been described for *P. pastoris* [98,99]. The use of the self-cleaving 2A peptide also allows the simultaneous expression of multiple genes from a single polycistronic construct [100]. For higher throughput and versatility, modular cloning techniques allow the combinatorial assembly of gene expression cassettes, where multiple promoters, genes, and terminators may be tested. A kit for *Pichia pastoris* which uses Golden Gate cloning for the assembly of multiple modules is publicly available. This kit is named *GoldenPiCS* and it allows the simultaneous assembly of up to eight expression units in a single vector. The kit contains 20 promoters and 10 terminators. The plasmids are designed for the integration at 4 different loci, and they may be combined with 4 yeast selectable markers (geneticin, zeocin, hygromycin, and nourseothricin resistance) [101]. The versatility and modularity of this kit allowed to expand the applications of *P. pastoris* in the metabolic engineering and synthetic biology fields.

Use of selectable markers set a limit to the number of genetic modifications that can be applied to a strain. To foster further genetic modifications, marker-less genetic engineering protocols were required. First protocols used the Cre/*loxP* system, where the Cre recombinase catalyses the recombination between two *loxP* sites resulting in the excision of the selectable marker sequence [102]. The recombination of the two *loxP* sequences catalysed by Cre leaves a *loxP* scar in the genome. The system was improved by using mutated *loxP* sequences (*lox71* and *lox66*). Recombination of these

two sequences leaves a *lox72* scar sequence, which has reduced affinity towards the Cre recombinase [103]. This fact facilitates the integration of multiple expression cassettes in the genome of *Pichia pastoris*. Otherwise, as multiple *loxP* scars would be present in the genome, the Cre recombinase could recombine them removing large DNA fragments from the yeast's genome. However, use of this system for the integration of multiple genes requires multiple transformations and marker recycling steps, which are very time consuming.

More recently, a CRISPR/Cas9 (Clustered Regularly Interspaced Short Palindromic Repeats/CRISPR Associated protein 9) method was described for *P. pastoris* [104]. Use of CRISPR/Cas9 allows accurate and marker-free genetic engineering of *P. pastoris*. While the simultaneous integration and/or deletion of multiple genes has been described in *S. cerevisiae* [105], multiplex engineering of *P. pastoris* is still limited due to its high Non-Homologous End Joining (NHEJ) activity. Disruption of NHEJ related gene *Ku70* [106] or overexpression of the Homologous Recombination related genes from *S. cerevisiae* in *P. pastoris* [107] has allowed the efficient simultaneous integration of multiple genes at different loci.

Alternatively to the simultaneous multiplex genome integrations using CRISPR/Cas9, multiple expression cassettes can be integrated into a single locus. To this end, the Golden PiCS kit was expanded with CRISPR/Cas9 tools, resulting in the CrisPi kit [108]. This kit contains plasmids for Cas9 and sgRNA simultaneous expression. Moreover, it contains plasmids for the assembly of one or multiple expression cassettes with the homologous complementary regions to the targeted genomic locus.

The reported synthetic biology tools have made genetic engineering of *P. pastoris* easier and faster, which was required to cope with the synthetic biology trend: implementing long complex pathways and generating an increasing number of strains within the same project. As a result, these tools have fostered the use of *P. pastoris* for metabolic engineering applications.

1.8. Systems biology tools for metabolic engineering in *P. pastoris*

To modify the metabolism of an organism, it is first crucial to understand its natural metabolism. The use of -omics tools, including genomics, transcriptomics, proteomics, metabolomics, and fluxomics, together with years of basic research, have

enabled the identification of many of the individual components of metabolism (genes, proteins, and metabolites).

In the case of *P. pastoris,* the sequence of the genome of the strain GS115 was first published in 2009 [109]. Transcriptomics [110], proteomics [111], metabolomics [112,113], and fluxomics [114] studies have also been reported, describing the systems-level organization of *P. pastoris* under multiple conditions, such as: i) growth on methanol [115]; ii) growth on glucose under hypoxic conditions [116]; or iii) growth on glucose or glucose plus methanol mixtures [117,118].

Biological systems are highly complex. Computational tools are continuously being developed to enhance the understanding of such biological systems. Specific Genome Scale Metabolic Models (GSMM) of a microorganism can be constructed from the genomic data, as the genome contains the information of all the putative reactions which may take place in an organism [119]. In particular, several GSMM for *P. pastoris* have been published [120–122]. The GSMM can be further refined using transcriptomics or proteomics data, that will tell which among all the available reactions are active under certain conditions.

In metabolic engineering, determination of the metabolic flux distribution can provide meaningful information to anticipate the result of a genetic modification. Transcriptomics, proteomics, and metabolomics analyses can be used to describe the metabolic state of a cell, but fluxomics analyses (i.e., the quantification of the metabolic reaction rates or fluxes) provide the most complete picture of the metabolic phenotype [123]. To some extent, fluxomics are the result of the combination of the other -omics: genomics, transcriptomics, proteomics, and metabolomics. In other words, fluxomics are the result of the combined effect at the genomic, transcriptomic, proteomic, and the metabolomic/thermodynamic levels.

^{13}C-based Metabolic Flux Analysis (^{13}C-MFA) is the most extensively used technique to quantify the fluxes [124]. It uses a ^{13}C-labelled substrate as tracer to infer the metabolic reaction rates. ^{13}C-MFA can be divided into stationary and instationary approaches [125]. In stationary ^{13}C-MFA the samples are collected when the cultures are at a metabolic and isotopic steady-state, while the instationary approach uses cells which are at a metabolic steady-state, but the labelling pattern of the metabolites is still in a transient state towards the steady state (Figure 8).

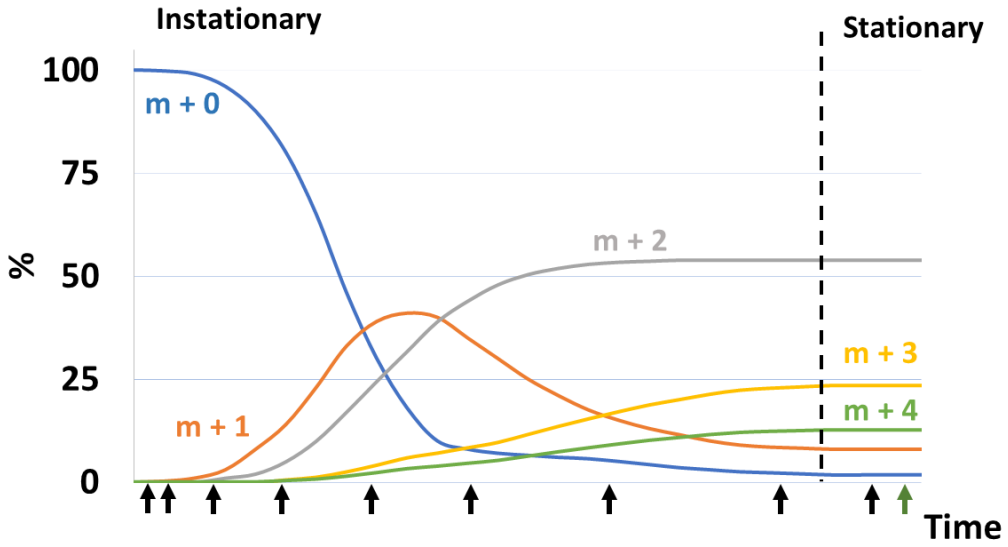

Figure 8. Stationary versus instationary ^{13}C-MFA. The graph shows the abundance of each isotopologue of a metabolite (m) over time. The legend shows the number of labelled C atoms in such metabolites (e.g., if two carbon atoms of metabolite 'm' are labelled with ^{13}C: 'm + 2'). In instationary ^{13}C-MFA, multiple samples are analysed (dark arrows). A single sample from the stationary phase is analysed in stationary ^{13}C-MFA (green arrow).

Both stationary and instationary ^{13}C-MFA studies have been performed in *P. pastoris* [114,117]. ^{13}C-MFA uses a stoichiometric model that also accounts for the C-transitions for each reaction. As only the central carbon metabolism is required, the models are typically obtained combining literature data, specific biomass composition, and assuming similarity with *Saccharomyces cerevisiae* when no data is available [114,116,126]. More recently, the use of a compression protocol to obtain a core model from the *P. pastoris* GSMM *iMT1026v3* was reported [127]. This protocol allows to obtain a core model directly derived from the GSMM, accounting for the substrate-specific biomass composition reactions.

Integration of the -omics derived data is valuable in many metabolic engineering applications. In particular, there are multiple examples of targeted genetic modifications derived from ^{13}C-MFA information [128,129]. Availability of all these tools grant the use of *P. pastoris* as a metabolic engineering chassis for multiple applications.

References

1. Werpy, T., and Petersen, G. (2004) Top value added chemicals from biomass. Volume I - Results of screening for potential candidates from sugars and synthesis gas. *U.S. Department of Energy*.
2. Bozell, J.J., and Petersen, G.R. (2010) Technology development for the production of biobased products from biorefinery carbohydrates - the US Department of Energy's "Top 10" revisited. *Green Chemistry*, 12 (4), 539–554.
3. Matsakas, L., Topakas, E., and Christakopoulos, P. (2014) New trends in microbial production of 3-hydroxypropionic acid. *Current Biochemical Engineering*, 1 (2), 141–154.
4. de Fouchécour, F., Sánchez-Castañeda, A.K., Saulou-Bérion, C., and Spinnler, H.É. (2018) Process engineering for microbial production of 3-hydroxypropionic acid. *Biotechnology Advances*, 36 (4), 1207–1222.
5. Jers, C., Kalantari, A., Garg, A., and Mijakovic, I. (2019) Production of 3-Hydroxypropanoic Acid From Glycerol by Metabolically Engineered Bacteria. *Frontiers in Bioengineering and Biotechnology*, 7, 124.
6. Matsakas, L., Hrůzová, K., Rova, U., and Christakopoulos, P. (2018) Biological production of 3-hydroxypropionic acid: An update on the current status. *Fermentation*, 4, 13.
7. Ji, R.Y., Ding, Y., Shi, T.Q., Lin, L., Huang, H., Gao, Z., and Ji, X.J. (2018) Metabolic engineering of yeast for the production of 3-hydroxypropionic acid. *Frontiers in Microbiology*, 9, 2185.
8. Kumar, V., Ashok, S., and Park, S. (2013) Recent advances in biological production of 3-hydroxypropionic acid. *Biotechnology Advances*, 31 (6), 945–961.
9. Garai-Ibabe, G., Ibarburu, I., Berregi, I., Claisse, O., Lonvaud-Funel, A., Irastorza, A., and Dueñas, M.T. (2008) Glycerol metabolism and bitterness producing lactic acid bacteria in cidermaking. *International Journal of Food Microbiology*, 121 (3), 253–261.
10. Luo, L.H., Seo, J.W., Baek, J.O., Oh, B.R., Heo, S.Y., Hong, W.K., Kim, D.H., and Kim, C.H. (2011) Identification and characterization of the propanediol utilization protein PduP of *Lactobacillus reuteri* for 3-hydroxypropionic acid production from glycerol. *Applied Microbiology and Biotechnology*, 89 (3), 697–703.
11. Dishisha, T., Pyo, S.H., and Hatti-Kaul, R. (2015) Bio-based 3-hydroxypropionic- and acrylic acid production from biodiesel glycerol via integrated microbial and chemical catalysis. *Microbial Cell Factories*, 14, 200.
12. Ashok, S., Raj, S.M., Rathnasingh, C., and Park, S. (2011) Development of recombinant *Klebsiella pneumoniae ΔdhaT* strain for the co-production of 3-hydroxypropionic acid and 1,3-propanediol from glycerol. *Applied Microbiology and Biotechnology*, 90 (4), 1253–1265.
13. Raj, S.M., Rathnasingh, C., Jung, W.C., Selvakumar, E., and Park, S. (2010) A novel NAD^+-dependent aldehyde dehydrogenase encoded by the *puuC* gene of *Klebsiella pneumoniae* DSM 2026 that utilizes 3- hydroxypropionaldehyde as a substrate. *Biotechnology and Bioprocess Engineering*, 15, 131–138.
14. Zhu, J.G., Ji, X.J., Huang, H., du, J., Li, S., and Ding, Y.Y. (2009) Production of 3-hydroxypropionic acid by recombinant *Klebsiella pneumoniae* based on aeration and ORP controlled strategy. *Korean Journal of Chemical Engineering*, 26 (6), 1679–1685.
15. Ashok, S., Sankaranarayanan, M., Ko, Y., Jae, K.E., Ainala, S.K., Kumar, V., and Park, S. (2013) Production of 3-hydroxypropionic acid from glycerol by recombinant *Klebsiella pneumoniae ΔdhaTΔyqhD* which can produce vitamin B12 naturally. *Biotechnology and Bioengineering*, 110 (2), 511–524.
16. Zhao, P., Ma, C., Xu, L., and Tian, P. (2019) Exploiting tandem repetitive promoters for high-level production of 3-hydroxypropionic acid. *Applied Microbiology and Biotechnology*, 103, 4017–4031.
17. Li, Y., Wang, X., Ge, X., and Tian, P. (2016) High production of 3-hydroxypropionic acid in *Klebsiella pneumoniae* by systematic optimization of glycerol metabolism. *Scientific Reports*, 6, 26932.
18. Raj, S.M., Rathnasingh, C., Jo, J.E., and Park, S. (2008) Production of 3-hydroxypropionic acid from glycerol by a novel recombinant *Escherichia coli* BL21 strain. *Process Biochemistry*, 43 (12), 1440–1446.
19. Mohan Raj, S., Rathnasingh, C., Jung, W.C., and Park, S. (2009) Effect of process parameters on 3-hydroxypropionic acid production from glycerol using a recombinant *Escherichia coli*. *Applied Microbiology and Biotechnology*, 84 (4), 649–657.
20. Kim, J.W., Ko, Y.S., Chae, T.U., and Lee, S.Y. (2020) High-level production of 3-

hydroxypropionic acid from glycerol as a sole carbon source using metabolically engineered *Escherichia coli*. *Biotechnology and Bioengineering*, 117 (7), 2139–2152.

21. Honjo, H., Tsuruno, K., Tatsuke, T., Sato, M., and Hanai, T. (2015) Dual synthetic pathway for 3-hydroxypropionic acid production in engineered *Escherichia coli*. *Journal of Bioscience and Bioengineering*, 120 (2), 199–204.
22. Sabet-Azad, R., Sardari, R.R.R., Linares-Pastén, J.A., and Hatti-Kaul, R. (2015) Production of 3-hydroxypropionic acid from 3-hydroxypropionaldehyde by recombinant *Escherichia coli* co-expressing *Lactobacillus reuteri* propanediol utilization enzymes. *Bioresource Technology*, 180, 214–221.
23. Noh, M.H., Lim, H.G., Moon, D., Park, S., and Jung, G.Y. (2020) Auxotrophic selection strategy for improved production of Coenzyme B12 in *Escherichia coli*. *iScience*, 23 (3), 100890.
24. Zhou, S., Catherine, C., Rathnasingh, C., Somasundar, A., and Park, S. (2013) Production of 3-hydroxypropionic acid from glycerol by recombinant *Pseudomonas denitrificans*. *Biotechnology and Bioengineering*, 110 (12), 3177–3187.
25. Thi Nguyen, T., Lama, S., Kumar Ainala, S., Sankaranarayanan, M., Singh Chauhan, A., Rae Kim, J., and Park, S. (2021) Development of *Pseudomonas asiatica* as a host for the production of 3-hydroxypropionic acid from glycerol. *Bioresource Technology*, 329, 124867.
26. Raynaud, C., Sarçabal, P., Meynial-Salles, I., Croux, C., and Soucaille, P. (2003) Molecular characterization of the 1,3-propanediol (1,3-PD) operon of *Clostridium butyricum*. *Proceedings of the Natural Academy of Sciences*, 100 (9), 5010–5015.
27. Lee, T.Y., Min, W.K., Kim, H.J., and Seo, J.H. (2020) Improved production of 3-hydroxypropionic acid in engineered *Escherichia coli* by rebalancing heterologous and endogenous synthetic pathways. *Bioresource Technology*, 299, 122600.
28. Chen, Z., Huang, J., Wu, Y., Wu, W., Zhang, Y., and Liu, D. (2017) Metabolic engineering of *Corynebacterium glutamicum* for the production of 3-hydroxypropionic acid from glucose and xylose. *Metabolic Engineering*, 39, 151–158.
29. Eisenreich, W., Strauss, G., Werz, U., Fuchs, G., and Bacher, A. (1993) Retrobiosynthetic analysis of carbon fixation in the phototrophic eubacterium *Chloroflexus aurantiacus*. *European Journal of Biochemistry*, 215 (3), 619–632.
30. Berg, I.A., Kockelkorn, D., Buckel, W., and Fuchs, G. (2007) A 3-hydroxypropionate/4-hydroxybutyrate autotrophic carbon dioxide assimilation pathway in archaea. *Science*, 318 (5857), 1782–1786.
31. Zarzycki, J., Brecht, V., Müller, M., and Fuchs, G. (2009) Identifying the missing steps of the autotrophic 3-hydroxypropionate CO_2 fixation cycle in *Chloroflexus aurantiacus*. *Proceedings of the Natural Academy of Sciences*, 106 (50), 21317–21322.
32. Crafts-Brandner, S.J., and Salvucci, M.E. (2000) Rubisco activase constrains the photosynthetic potential of leaves at high temperature and CO_2. *Proceedings of the Natural Academy of Sciences*, 97 (24), 13430–13435.
33. Hügler, M., Menendez, C., Schägger, H., and Fuchs, G. (2002) Malonyl-coenzyme A reductase from *Chloroflexus aurantiacus*, a key enzyme of the 3-hydroxypropionate cycle for autotrophic CO_2 fixation. *Journal of Bacteriology*, 184 (9), 2404–2410.
34. Rathnasingh, C., Raj, S.M., Lee, Y., Catherine, C., Ashok, S., and Park, S. (2012) Production of 3-hydroxypropionic acid via malonyl-CoA pathway using recombinant *Escherichia coli* strains. *Journal of Biotechnology*, 157 (4), 633–640.
35. Takayama, S., Ozaki, A., Konishi, R., Otomo, C., Kishida, M., Hirata, Y., Matsumoto, T., Tanaka, T., and Kondo, A. (2018) Enhancing 3-hydroxypropionic acid production in combination with sugar supply engineering by cell surface-display and metabolic engineering of *Schizosaccharomyces pombe*. *Microbial Cell Factories*, 17, 176.
36. Chang, Z., Dai, W., Mao, Y., Cui, Z., Wang, Z., and Chen, T. (2020) Engineering *Corynebacterium glutamicum* for the efficient production of 3-hydroxypropionic acid from a mixture of glucose and acetate via the malonyl-CoA pathway. *Catalysts*, 10 (2), 203.
37. Nguyen, D.T.N., Lee, O.K., Lim, C., Lee, J., Na, J.G., and Lee, E.Y. (2020) Metabolic engineering of type II methanotroph, *Methylosinus trichosporium* OB3b, for production of 3-hydroxypropionic acid from methane via a malonyl-CoA reductase-dependent pathway. *Metabolic Engineering*, 59, 142–150.
38. Yang, Y.M., Chen, W.J., Yang, J., Zhou, Y.M., Hu, B., Zhang, M., Zhu, L.P., Wang, G.Y., and Yang, S. (2017) Production of 3-hydroxypropionic acid in engineered *Methylobacterium extorquens* AM1 and its reassimilation through a reductive route. *Microbial Cell Factories*, 16, 179.
39. Lynch, M.D., Gill, R.T., and Warnecke-Lipscomb, T. (2011) Method for producing 3-hydroxypropionic acid and other products. WO 2011/038364 A1, issued 2011.

40. Liu, C., Wang, Q., Xian, M., Ding, Y., and Zhao, G. (2013) Dissection of malonyl-coenzyme A reductase of *Chloroflexus aurantiacus* results in enzyme activity improvement. *PLoS ONE*, 8 (9), e75554.
41. Son, H.F., Kim, S., Seo, H., Hong, J., Lee, D., Jin, K.S., Park, S., and Kim, K.J. (2020) Structural insight into bi-functional malonyl-CoA reductase. *Environmental Microbiology*, 22 (2), 752–765.
42. Liu, C., Ding, Y., Zhang, R., Liu, H., Xian, M., and Zhao, G. (2016) Functional balance between enzymes in malonyl-CoA pathway for 3-hydroxypropionate biosynthesis. *Metabolic Engineering*, 34, 104–111.
43. Liu, B., Xiang, S., Zhao, G., Wang, B., Ma, Y., Liu, W., and Tao, Y. (2019) Efficient production of 3-hydroxypropionate from fatty acids feedstock in *Escherichia coli*. *Metabolic Engineering*, 51, 121–130.
44. Chen, Y., Bao, J., Kim, I.K., Siewers, V., and Nielsen, J. (2014) Coupled incremental precursor and co-factor supply improves 3-hydroxypropionic acid production in *Saccharomyces cerevisiae*. *Metabolic Engineering*, 22, 104–109.
45. Kildegaard, K.R., Jensen, N.B., Schneider, K., Czarnotta, E., Özdemir, E., Klein, T., Maury, J., Ebert, B.E., Christensen, H.B., Chen, Y., Kim, I.K., Herrgård, M.J., Blank, L.M., Forster, J., Nielsen, J., and Borodina, I. (2016) Engineering and systems-level analysis of *Saccharomyces cerevisiae* for production of 3-hydroxypropionic acid via malonyl-CoA reductase-dependent pathway. *Microbial Cell Factories*, 15, 53.
46. Shiba, Y., Paradise, E.M., Kirby, J., Ro, D.K., and Keasling, J.D. (2007) Engineering of the pyruvate dehydrogenase bypass in *Saccharomyces cerevisiae* for high-level production of isoprenoids. *Metabolic Engineering*, 9 (2), 160–168.
47. Hellgren, J., Godina, A., Nielsen, J., and Siewers, V. (2020) Promiscuous phosphoketolase and metabolic rewiring enables novel non-oxidative glycolysis in yeast for high-yield production of acetyl-CoA derived products. *Metabolic Engineering*, 62, 150–160.
48. Zhang, Q., Zeng, W., Xu, S., and Zhou, J. (2021) Metabolism and strategies for enhanced supply of acetyl-CoA in *Saccharomyces cerevisiae*. *Bioresource Technology*, 342, 125978.
49. van Rossum, H.M., Kozak, B.U., Pronk, J.T., and van Maris, A.J.A. (2016) Engineering cytosolic acetyl-Coenzyme A supply in *Saccharomyces cerevisiae*: Pathway stoichiometry, free-energy conservation and redox-cofactor balancing. *Metabolic Engineering*, 36, 99–115.
50. Lama, S., Kim, Y., Nguyen, D.T., Im, C.H., Sankaranarayanan, M., and Park, S. (2021) Production of 3-hydroxypropionic acid from acetate using metabolically-engineered and glucose-grown *Escherichia coli*. *Bioresource Technology*, 320, 124362.
51. Lee, J.H., Cha, S., Kang, C.W., Lee, G.M., Lim, H.G., and Jung, G.Y. (2018) Efficient conversion of acetate to 3-hydroxypropionic acid by engineered *Escherichia coli*. *Catalysts*, 8 (11), 525.
52. Lai, N., Luo, Y., Fei, P., Hu, P., and Wu, H. (2021) One stone two birds: Biosynthesis of 3-hydroxypropionic acid from CO_2 and syngas-derived acetic acid in *Escherichia coli*. *Synthetic and Systems Biotechnology*, 6 (3), 144–152.
53. Chang, Z., Dai, W., Mao, Y., Cui, Z., Wang, Z., and Chen, T. (2020) Engineering *Corynebacterium glutamicum* for the efficient production of 3-hydroxypropionic acid from a mixture of glucose and acetate via the malonyl-CoA pathway. *Catalysts*, 10, 203.
54. Jessen, H.J., Liao, H.H., Gort, S.J., and Selifonova, O.V. (2008) Beta-alanine/ alpha-ketoglutarate aminotransferase for 3-hydroxypropionic acid production. WO 2008/027742 A1, issued 2008.
55. Liao, H.H., Gokaran, R.R., Gort, S.J., Jessen, H.J., and Selifonova, O.V. (2005) Production of 3-hydroxypropionic acid using beta-alanine/pyruvate aminotransferase. WO 2005/118719 A2, issued 2005.
56. Jessen, H., Rush, B., Hurtya, J., Mastel, B., Berry, A., Yaver, D., Catlett, M., and Bernhardt, M. (2012) Compositions and methods for 3-hydroxypropionic acid production. WO 2012/074818 A2, issued 2012.
57. Borodina, I., Kildegaard, K.R., Jensen, N.B., Blicher, T.H., Maury, J., Sherstyk, S., Schneider, K., Lamosa, P., Herrgård, M.J., Rosenstand, I., Öberg, F., Forster, J., and Nielsen, J. (2015) Establishing a synthetic pathway for high-level production of 3-hydroxypropionic acid in *Saccharomyces cerevisiae* via β-alanine. *Metabolic Engineering*, 27, 57–64.
58. Lis, A. v., Schneider, K., Weber, J., Keasling, J.D., Jensen, M.K., and Klein, T. (2019) Exploring small-scale chemostats to scale up microbial processes: 3-hydroxypropionic acid production in *S. cerevisiae*. *Microbial Cell Factories*, 18, 50.
59. Song, C.W., Kim, J.W., Cho, I.J., and Lee, S.Y. (2016) Metabolic Engineering of *Escherichia coli* for the Production of 3-Hydroxypropionic Acid and Malonic Acid through β-Alanine Route. *ACS Synthetic Biology*, 5 (11), 1256–1263.
60. Song, C.W., Lee, J., Ko, Y.S., and Lee, S.Y. (2015) Metabolic engineering of *Escherichia*

coli for the production of 3-aminopropionic acid. *Metabolic Engineering*, 30, 121–129.

61. Henry, C.S., Broadbelt, L.J., and Hatzimanikatis, V. (2010) Discovery and analysis of novel metabolic pathways for the biosynthesis of industrial chemicals: 3-hydroxypropanoate. *Biotechnology and Bioengineering*, 106 (3), 462–473.
62. Tong, T., Tao, Z., Chen, S., Gao, C., Liu, H., Wang, W., Liu, G.-Q., and Liu, L. (2021) A biosynthesis pathway for 3-hydroxypropionic acid production in genetically engineered *Saccharomyces cerevisiae*. *Green Chemistry*, 23, 4502.
63. Ma, F., and Hanna, M.A. (1999) Biodiesel production: a review. *Bioresource Technology*, 70, 1–15.
64. Ayoub, M., and Abdullah, A.Z. (2012) Critical review on the current scenario and significance of crude glycerol resulting from biodiesel industry towards more sustainable renewable energy industry. *Renewable and Sustainable Energy Reviews*, 16 (5), 2671–2686.
65. D'Angelo, S.C., Dall'Ara, A., Mondelli, C., Pérez-Ramírez, J., and Papadokonstantakis, S. (2018) Techno-economic analysis of a glycerol biorefinery. *ACS Sustainable Chemistry and Engineering*, 6 (12), 16563–16572.
66. Kaur, J., Sarma, A.K., Jha, M.K., and Gera, P. (2020) Valorisation of crude glycerol to value-added products: Perspectives of process technology, economics and environmental issues. *Biotechnology Reports*, 27, e00487.
67. Eda Çelik, S., Ozbay, N., Oktar, N., and Çalik, P. (2008) Use of biodiesel byproduct crude glycerol as the carbon source for fermentation processes by recombinant *Pichia pastoris*. *Industrial and Engineering Chemistry Research*, 47 (9), 2985–2990.
68. Tang, S., Boehme, L., Lam, H., and Zhang, Z. (2009) *Pichia pastoris* fermentation for phytase production using crude glycerol from biodiesel production as the sole carbon source. *Biochemical Engineering Journal*, 43 (2), 157–162.
69. Robert, J.M., Lattari, F.S., Machado, A.C., de Castro, A.M., Almeida, R.V., Torres, F.A.G., Valero, F., and Freire, D.M.G. (2017) Production of recombinant lipase B from *Candida antarctica* in *Pichia pastoris* under control of the promoter PGK using crude glycerol from biodiesel production as carbon source. *Biochemical Engineering Journal*, 118, 123–131.
70. Kumar, L.R., Yellapu, S.K., Tyagi, R.D., and Zhang, X. (2019) A review on variation in crude glycerol composition, bio-valorization of crude and purified glycerol as carbon source for lipid production. *Bioresource Technology*, 293, 122155.
71. Bennett, R.K., Gregory, G.J., Gonzalez, J.E., Har, J.R.G., Antoniewicz, M.R., and Papoutsakis, E.T. (2021) Improving the methanol tolerance of an *Escherichia coli* methylotroph via adaptive laboratory evolution enhances synthetic methanol utilization. *Frontiers in Microbiology*, 12, 638426.
72. Burgé, G., Moussa, M., Saulou-Bérion, C., Chemarin, F., Kniest, M., Allais, F., Spinnler, H.E., and Athès, V. (2017) Towards an extractive bioconversion of 3-hydroxypropionic acid: study of inhibition phenomena. *Journal of Chemical Technology and Biotechnology*, 92 (9), 2425–2432.
73. van Maris, A.J.A., Konings, W.N., van Dijken, J.P., and Pronk, J.T. (2004) Microbial export of lactic and 3-hydroxypropanoic acid: Implications for industrial fermentation processes. *Metabolic Engineering*, 6 (4), 245–255.
74. Damasceno, L.M., Pla, I., Chang, H.J., Cohen, L., Ritter, G., Old, L.J., and Batt, C.A. (2004) An optimized fermentation process for high-level production of a single-chain Fv antibody fragment in *Pichia pastoris*. *Protein Expression and Purification*, 37, 18–26.
75. Koganesawa, N., Aizawa, T., Shimojo, H., Miura, K., Ohnishi, A., Demura, M., Hayakawa, Y., Nitta, K., and Kawano, K. (2002) Expression and purification of a small cytokine growth-blocking peptide from armyworm *Pseudaletia separata* by an optimized fermentation method using the methylotrophic yeast *Pichia pastoris*. *Protein Expression and Purification*, 25 (3), 416–425.
76. Kurtzman, C.P. (2005) Description of *Komagataella phaffii* sp. nov. and the transfer of *Pichia pseudopastoris* to the methylotrophic yeast genus *Komagataella*. *International Journal of Systematic and Evolutionary Microbiology*, 55 (2), 973–976.
77. Peña, D.A., Gasser, B., Zanghellini, J., Steiger, M.G., and Mattanovich, D. (2018) Metabolic engineering of *Pichia pastoris*. *Metabolic Engineering*, 50, 2–15.
78. Waterham, H.R., Digan, M.E., Koutz, P.J., Lair, S. v., and Cregg, J.M. (1997) Isolation of the *Pichia pastoris* glyceraldehyde-3-phosphate dehydrogenase gene and regulation and use of its promoter. *Gene*, 186, 37–44.
79. Cregg, J.M., Madden, K.R., Barringer, K.J., Thill, G.P., and Stillman, C.A. (1989) Functional characterization of the two alcohol oxidase genes from the yeast *Pichia pastoris*. *Molecular and Cellular Biology*, 9 (3), 1316–1323.

80. Barrero Peña, J.J. (2020) Overcoming the secretory limitations in *Pichia pastoris* for recombinant protein production. (PhD thesis). Available at http://ddd.uab.cat. ISBN 978844909481.
81. Cheng, H., Lv, J., Wang, H., Wang, B., Li, Z., and Deng, Z. (2014) Genetically engineered *Pichia pastoris* yeast for conversion of glucose to xylitol by a single-fermentation process. *Applied Microbiology and Biotechnology*, 98 (8), 3539–3552.
82. Siripong, W., Wolf, P., Kusumoputri, T.P., Downes, J.J., Kocharin, K., Tanapongpipat, S., and Runguphan, W. (2018) Metabolic engineering of *Pichia pastoris* for production of isobutanol and isobutyl acetate. *Biotechnology for Biofuels*, 11, 1.
83. Lima, P.B.A., Mulder, K.C.L., Melo, N.T.M., Carvalho, L.S., Menino, G.S., Mulinari, E., Castro, V.H., Reis, T.F., Goldman, G.H., Magalhães, B.S., and Parachin, N.S. (2016) Novel homologous lactate transporter improves L-lactic acid production from glycerol in recombinant strains of *Pichia pastoris*. *Microbial Cell Factories*, 15, 158.
84. Melo, N.T.M., Pontes, G.C., Procópio, D.P., Cunha, G.C. de G., Eliodório, K.P., Paes, H.C., Basso, T.O., and Parachin, N.S. (2020) Evaluation of product distribution in chemostat and batch fermentation in lactic acid-producing *Komagataella phaffii* strains utilizing glycerol as substrate. *Microorganisms*, 8, 781.
85. Liu, Y., Bai, C., Liu, Q., Xu, Q., Qian, Z., Peng, Q., Yu, J., Xu, M., Zhou, X., Zhang, Y., and Cai, M. (2019) Engineered ethanol-driven biosynthetic system for improving production of acetyl-CoA derived drugs in Crabtree-negative yeast. *Metabolic Engineering*, 54, 275–284.
86. Bhataya, A., Schmidt-Dannert, C., and Lee, P.C. (2009) Metabolic engineering of *Pichia pastoris* X-33 for lycopene production. *Process Biochemistry*, 44 (10), 1095–1102.
87. Araya-Garay, J.M., Feijoo-Siota, L., Rosa-Dos-Santos, F., Veiga-Crespo, P., and Villa, T.G. (2012) Construction of new *Pichia pastoris* X-33 strains for production of lycopene and β-carotene. *Applied Microbiology and Biotechnology*, 93 (6), 2483–2492.
88. Gao, J., Jiang, L., and Lian, J. (2021) Development of synthetic biology tools to engineer *Pichia pastoris* as a chassis for the production of natural products. *Synthetic and Systems Biotechnology*, 6 (2), 110–119.
89. Du, X.L., Jiang, Z., Su, D.S., and Wang, J.Q. (2016) Research progress on the indirect hydrogenation of carbon dioxide to methanol. *ChemSusChem*, 9 (4), 322–332.
90. Albo, J., Alvarez-Guerra, M., Castaño, P., and Irabien, A. (2015) Towards the electrochemical conversion of carbon dioxide into methanol. *Green Chemistry*, 17, 2304–2324.
91. Guo, F., Dai, Z., Peng, W., Zhang, S., Zhou, J., Ma, J., Dong, W., Xin, F., Zhang, W., and Jiang, M. (2021) Metabolic engineering of *Pichia pastoris* for malic acid production from methanol. *Biotechnology and Bioengineering*, 118, 357–371.
92. Li, P., Sun, H., Chen, Z., Li, Y., and Zhu, T. (2015) Construction of efficient xylose utilizing *Pichia pastoris* for industrial enzyme production. *Microbial Cell Factories*, 14, 22.
93. Gassler, T., Sauer, M., Gasser, B., Egermeier, M., Troyer, C., Causon, T., Hann, S., Mattanovich, D., and Steiger, M.G. (2020) The industrial yeast *Pichia pastoris* is converted from a heterotroph into an autotroph capable of growth on CO_2. *Nature Biotechnology*, 38 (2), 210–216.
94. Aw, R., and Polizzi, K.M. (2013) Can too many copies spoil the broth? *Microbial Cell Factories*, 12, 128.
95. Vogl, T., and Glieder, A. (2013) Regulation of *Pichia pastoris* promoters and its consequences for protein production. *New Biotechnology*, 30 (4), 385–404.
96. Prielhofer, R., Maurer, M., Klein, J., Wenger, J., Kiziak, C., Gasser, B., and Mattanovich, D. (2013) Induction without methanol: Novel regulated promoters enable high-level expression in *Pichia pastoris*. *Microbial Cell Factories*, 12, 5.
97. Özçelik, A.T., Yilmaz, S., and Inan, M. (2015) *Pichia pastoris* promoters. *Methods in Molecular Biology*, 1923, 97–112.
98. Vogl, T., Kickenweiz, T., Pitzer, J., Sturmberger, L., Weninger, A., Biggs, B.W., Köhler, E.M., Baumschlager, A., Fischer, J.E., Hyden, P., Wagner, M., Baumann, M., Borth, N., Geier, M., Ajikumar, P.K., and Glieder, A. (2018) Engineered bidirectional promoters enable rapid multi-gene co-expression optimization. *Nature Communications*, 9, 3589.
99. Rajamanickam, V., Metzger, K., Schmid, C., and Spadiut, O. (2017) A novel bi-directional promoter system allows tunable recombinant protein production in *Pichia pastoris*. *Microbial Cell Factories*, 16, 152.
100. Geier, M., Fauland, P., Vogl, T., and Glieder, A. (2015) Compact multi-enzyme pathways in *P. pastoris*. *Chemical Communications*, 51 (9), 1643–1646.
101. Prielhofer, R., Barrero, J.J., Steuer, S., Gassler, T., Zahrl, R., Baumann, K., Sauer, M., Mattanovich, D., Gasser, B., and Marx, H. (2017) GoldenPiCS: A Golden Gate-derived modular cloning system for applied

synthetic biology in the yeast *Pichia pastoris*. *BMC Systems Biology*, 11, 123.

102. Marx, H., Mattanovich, D., and Sauer, M. (2008) Overexpression of the riboflavin biosynthetic pathway in *Pichia pastoris*. *Microbial Cell Factories*, 7, 23.

103. Pan, R., Zhang, J., Shen, W.L., Tao, Z.Q., Li, S.P., and Yan, X. (2011) Sequential deletion of *Pichia pastoris* genes by a self-excisable cassette. *FEMS Yeast Research*, 11 (3), 292–298.

104. Weninger, A., Hatzl, A.M., Schmid, C., Vogl, T., and Glieder, A. (2016) Combinatorial optimization of CRISPR/Cas9 expression enables precision genome engineering in the methylotrophic yeast *Pichia pastoris*. *Journal of Biotechnology*, 235, 139–149.

105. Mans, R., van Rossum, H.M., Wijsman, M., Backx, A., Kuijpers, N.G.A., van den Broek, M., Daran-Lapujade, P., Pronk, J.T., van Maris, A.J.A., and Daran, J.M.G. (2015) CRISPR/Cas9: A molecular Swiss army knife for simultaneous introduction of multiple genetic modifications in *Saccharomyces cerevisiae*. *FEMS Yeast Research*, 15 (2), fov004.

106. Liu, Q., Shi, X., Song, L., Liu, H., Zhou, X., Wang, Q., Zhang, Y., and Cai, M. (2019) CRISPR-Cas9-mediated genomic multiloci integration in *Pichia pastoris*. *Microbial Cell Factories*, 18, 144.

107. Gao, J., Ye, C., Cheng, J., Jiang, L., Yuan, X., and Lian, J. (2022) Enhancing homologous recombination efficiency in *Pichia pastoris* for multiplex genome integration using short homology arms. *ACS Synthetic Biology*, 11 (2), 547–553.

108. Gassler, T., Heistinger, L., Mattanovich, D., Gasser, B., and Prielhofer, R. (2019) CRISPR/Cas9-mediated homology-directed genome editing in *Pichia pastoris*. *Methods in Molecular Biology*, 1923, 211–225.

109. de Schutter, K., Lin, Y.C., Tiels, P., van Hecke, A., Glinka, S., Weber-Lehmann, J., Rouzé, P., van de Peer, Y., and Callewaert, N. (2009) Genome sequence of the recombinant protein production host *Pichia pastoris*. *Nature Biotechnology*, 27 (6), 561–566.

110. Zhu, T., Guo, M., Zhuang, Y., Chu, J., and Zhang, S. (2011) Understanding the effect of foreign gene dosage on the physiology of *Pichia pastoris* by transcriptional analysis of key genes. *Applied Microbiology and Biotechnology*, 89 (4), 1127–1135.

111. Huang, C.J., Damasceno, L.M., Anderson, K.A., Zhang, S., Old, L.J., and Batt, C.A. (2011) A proteomic analysis of the *Pichia pastoris* secretome in methanol-induced cultures. *Applied Microbiology and Biotechnology*, 90, 235–247.

112. Carnicer, M., Canelas, A.B., ten Pierick, A., Zeng, Z., van Dam, J., Albiol, J., Ferrer, P., Heijnen, J.J., and van Gulik, W. (2012) Development of quantitative metabolomics for *Pichia pastoris*. *Metabolomics*, 8 (2), 284–298.

113. Russmayer, H., Troyer, C., Neubauer, S., Steiger, M.G., Gasser, B., Hann, S., Koellensperger, G., Sauer, M., and Mattanovich, D. (2015) Metabolomics sampling of *Pichia pastoris* revisited: Rapid filtration prevents metabolite loss during quenching. *FEMS Yeast Research*, 15 (6), fov049.

114. Solà, A., Maaheimo, H., Ylönen, K., Ferrer, P., and Szyperski, T. (2004) Amino acid biosynthesis and metabolic flux profiling of *Pichia pastoris*. *European Journal of Biochemistry*, 271 (12), 2462–2470.

115. Rußmayer, H., Buchetics, M., Gruber, C., Valli, M., Grillitsch, K., Modarres, G., Guerrasio, R., Klavins, K., Neubauer, S., Drexler, H., Steiger, M., Troyer, C., al Chalabi, A., Krebiehl, G., Sonntag, D., Zellnig, G., Daum, G., Graf, A.B., Altmann, F., Koellensperger, G., Hann, S., Sauer, M., Mattanovich, D., and Gasser, B. (2015) Systems-level organization of yeast methylotrophic lifestyle. *BMC Biology*, 13, 80.

116. Baumann, K., Carnicer, M., Dragosits, M., Graf, A.B., Stadlmann, J., Jouhten, P., Maaheimo, H., Gasser, B., Albiol, J., Mattanovich, D., and Ferrer, P. (2010) A multi-level study of recombinant *Pichia pastoris* in different oxygen conditions. *BMC Systems Biology*, 4, 141.

117. Jordà, J., Suarez, C., Carnicer, M., ten Pierick, A., Heijnen, J.J., van Gulik, W., Ferrer, P., Albiol, J., and Wahl, A. (2013) Glucose-methanol co-utilization in *Pichia pastoris* studied by metabolomics and instationary ^{13}C flux analysis. *BMC Systems Biology*, 7, 17.

118. Solà, A., Jouhten, P., Maaheimo, H., Sánchez-Ferrando, F., Szyperski, T., and Ferrer, P. (2007) Metabolic flux profiling of *Pichia pastoris* grown on glycerol/methanol mixtures in chemostat cultures at low and high dilution rates. *Microbiology*, 153, 281–290.

119. Liu, L., Agren, R., Bordel, S., and Nielsen, J. (2010) Use of genome-scale metabolic models for understanding microbial physiology. *FEBS Letters*, 584 (12), 2556–2564.

120. Ye, R., Huang, M., Lu, H., Qian, J., Lin, W., Chu, J., Zhuang, Y., and Zhang, S. (2017) Comprehensive reconstruction and evaluation of *Pichia pastoris* genome-scale

metabolic model that accounts for 1243 ORFs. *Bioresources and Bioprocessing*, 4, 22.

121. Caspeta, L., Shoaie, S., Agren, R., Nookaew, I., and Nielsen, J. (2012) Genome-scale metabolic reconstructions of *Pichia stipitis* and *Pichia pastoris* and in silico evaluation of their potentials. *BMC Systems Biology*, 6 (24).

122. Tomàs-Gamisans, M., Ferrer, P., and Albiol, J. (2016) Integration and validation of the genome-scale metabolic models of *Pichia pastoris*: A comprehensive update of protein glycosylation pathways, lipid and energy metabolism. *PLoS ONE*, 11, e0148031.

123. Wittmann, C., and Portais, J.C. (2013) Metabolic Flux Analysis, in *Metabolomics in Practice*, Wiley-VCH Verlag GmbH & Co. KGaA, pp. 285–312.

124. Wiechert, W., Möllney, M., Petersen, S., and de Graaf, A.A. (2001) A universal framework for ^{13}C metabolic flux analysis. *Metabolic Engineering*, 3 (3), 265–283.

125. Wiechert, W., and Nöh, K. (2005) From stationary to instationary metabolic flux analysis. *Advances in Biochemical Engineering/Biotechnology*, 92, 145–172.

126. Jordà, J., Rojas, H., Carnicer, M., Wahl, A., Ferrer, P., and Albiol, J. (2014) Quantitative metabolomics and instationary ^{13}C-metabolic flux analysis reveals impact of recombinant protein production on trehalose and energy metabolism in *Pichia pastoris*. *Metabolites*, 4 (2), 281–299.

127. Tomàs-Gamisans, M., Ødum, A.S.R., Workman, M., Ferrer, P., and Albiol, J. (2019) Glycerol metabolism of *Pichia pastoris* (*Komagataella* spp.) characterised by ^{13}C-based metabolic flux analysis. *New Biotechnology*, 50, 52–59.

128. Caspeta, L., and Nielsen, J. (2013) Toward systems metabolic engineering of *Aspergillus* and *Pichia* species for the production of chemicals and biofuels. *Biotechnology Journal*, 8 (5), 534–544.

129. Nocon, J., Steiger, M.G., Pfeffer, M., Sohn, S.B., Kim, T.Y., Maurer, M., Rußmayer, H., Pflügl, S., Ask, M., Haberhauer-Troyer, C., Ortmayr, K., Hann, S., Koellensperger, G., Gasser, B., Lee, S.Y., and Mattanovich, D. (2014) Model based engineering of *Pichia pastoris* central metabolism enhances recombinant protein production. *Metabolic Engineering*, 24, 129–138.

2

BACKGROUND, OBJECTIVES, AND OUTLINE

Table of contents

2.1. Background

This research project has been carried out at the Systems Biology Laboratory of the Bioprocess Engineering and Applied Biocatalysis Group of the Chemical, Biological, and Environmental Engineering Department of the Universitat Autònoma de Barcelona.

Our research group has a long-standing and renowned experience in the use of *Pichia pastoris* for industrial biotechnology applications. So far, the main research focuses of the group have been: i) Production of enzymes, particularly lipases, in the yeast *Pichia pastoris,* focusing on bioprocess and strain optimization; and ii) Optimization of the enzymatic production of biodiesel.

This thesis has been carried within the framework of two projects founded by the Spanish Ministry of Science: CTQ2016-74959-R and PID2019-104666GB-I00. Both projects aimed at developing strategies towards the obtention of an integrated biodiesel biorefinery. To this end, the projects have three main goals: i) Optimization of the biodiesel biocatalytic process; ii) Optimization of the production of industrial lipases (or other heterologous proteins of industrial interest) in *P. pastoris* at a bioprocess and strain engineering level; and iii) Revalorization of the crude glycerol derived from the catalytic production of biodiesel.

The current thesis is within the framework of the 3rd objective of these projects. *P. pastoris* is metabolically engineered to produce high value-added products for the revalorization of crude glycerol. In particular, this thesis focuses on the production of 3-hydroxypropionic acid (3-HP).

2.2. Objectives

The main objective of this thesis was to obtain a *P. pastoris* recombinant strain producing 3-HP for the re-valorization of glycerol. To this end, the most updated available technologies for *P. pastoris* strain optimization were used.

The major objective can be narrowed down to the following bullet points:

- To obtain a *P. pastoris* chassis strain that produces 3-HP.
- To establish an accurate and sensitive 3-HP detection method.
- To optimize the performance of the 3-HP-producing *P. pastoris* strains using genetic and bioprocess engineering strategies.
- To use systems biology tools for the characterization of the 3-HP-producing *P. pastoris* strains.
- To use the information derived from the systems biology tools to further engineer the strains to improve the 3-HP yield and productivity.

2.3. Outline

In Chapter 3 (Results I), the motivation to choose the malonyl-CoA to 3-HP pathway for 3-HP production from glycerol in *P. pastoris* was described. Afterwards, the selected pathway was heterologously expressed, yielding the first 3-HP producing strains. Further genetic engineering strategies were used to increase the availability of the precursors of the pathway: NADPH and malonyl-CoA. Finally, the performance of the best strain was characterized in a fed-batch culture.

In Chapter 4 (Results II), the strains obtained in the previous chapter were further engineered. A second copy of the C-terminal domain of the malonyl-CoA reductase resulted in an increase of the product yield. However, unexpected results were obtained when the cytosolic acetyl-CoA production pathway was overexpressed, as the product yield decreased. To better understand such results, the strains were characterized using three independent methods: i) Classical screening conditions, where single end-point samples were withdrawn from deep-well plates cultures); ii) Single end-point sample from cultures under carbon-limited conditions using FeedBeads®, which simulate the conditions of a fed-batch culture; and iii) Multiple samples in the mid-exponential phase of batch mini-bioreactor cultures.

The three screening conditions resulted in different strain classifications. The two most promising strains were further characterized in a fed-batch culture. The best strain produced the highest 3-HP titer and productivity reported so far in yeast.

In Chapter 5, the most relevant strains from those generated in the previous two chapters were characterized using ^{13}C-Metabolic Flux Analysis (^{13}C-MFA). To do so, a High Throughput platform for fluxomics experiments was used for the first time in *P. pastoris*. Results clearly point to an acetyl-CoA and ATP competition for growth and 3-HP production which can be explained by the tight regulation of the glycolytic flux. Thus, it was concluded that, to further boost the 3-HP yield and productivity, the glycolytic flux needs to be increased. Moreover, the fluxome of *P. pastoris* strains at an acidic pH (pH 3.5) was characterized for the first time, showing the adaptation of *P. pastoris* to a low pH at a fluxome level. Altogether, the results point to the potential of *P. pastoris* to produce 3-HP at a low pH.

Finally, a protocol was written that describes the simultaneous High Throughput stationary ^{13}C-MFA of multiple *P. pastoris* strains (Annex I). The protocol describes all

the steps from experimental design to calculation of the fluxes: i) Generation of the core context-specific model; ii) Translation of the model into the appropriate (Flux TaBuLar; FTBL) format; iii) Optimization of the labelling pattern of the C-source; iv) Utilization of the fluxomics High Throughput mini-bioreactor platform; v) Sampling methodology and sample processing; vi) Analytical methods; vii) Data processing; and viii) Flux calculations.

To conclude, Chapter 6 provides the general conclusions derived from this work and explores some of the future targets to further optimize 3-HP production in *P. pastoris* from glycerol.

3

RESULTS I

Benchmarking recombinant *Pichia pastoris* for 3-hydroxypropionic acid production from glycerol

Chapter published as a research article in *Microbial Biotechnology*:

Fina A., Brêda, G. C. G. C., Pérez-Trujillo, M., Freire, D. M. G. D. M. G., Almeida, R. V. R. V., Albiol, J., and Ferrer, P. (2021). Benchmarking recombinant *Pichia pastoris* for 3-hydroxypropionic acid production from glycerol. *Microbial Biotechnology* 14(4), 1671–1682. doi:10.1111/1751-7915.13833.

Table of contents

Abstract

The use of the methylotrophic yeast *Pichia pastoris* (*Komagataella phaffi*) to produce heterologous proteins has been largely reported. However, investigations addressing the potential of this yeast to produce bulk chemicals are still scarce. In this study, we have studied the use of *P. pastoris* as a cell factory to produce the commodity chemical 3-hydroxypropionic acid (3-HP) from glycerol. 3-HP is a chemical platform which can be converted into acrylic acid, and to other alternatives to petroleum-based products. To this end, the *mcr* gene from *Chloroflexus aurantiacus* was introduced into *P. pastoris*. This single modification allowed the production of 3-HP from glycerol through the Malonyl-CoA pathway. Further enzyme and metabolic engineering modifications aimed at increasing cofactor and metabolic precursors availability allowed a 14-fold increase in the production of 3-HP compared to the initial strain. The best strain (PpHP6) was tested in a fed-batch culture, achieving a final concentration of 3-HP of 24.75 g L^{-1}, a product yield of 0.13 g g^{-1}, and a volumetric productivity of 0.54 g L^{-1} h^{-1}, which, to our knowledge, is the highest volumetric productivity reported in yeast. These results benchmark *P. pastoris* as a promising platform to produce bulk chemicals for the revalorization of crude glycerol and, in particular, to produce 3-HP.

3.1. Introduction

In 2004, the US Department of Energy (DOE) published the list of the top value-added bio-based chemicals to be produced from biomass [1]. The production of such bio-based products in a biorefinery is necessary to complement biofuel production, which is a low value-added product with a high price volatility. Co-producing biofuels and chemicals in an integrated biorefinery would allow the design of an economically robust and sustainable process, making it an attractive investment option. The DOE report ranked 3-hydroxypropionic acid (3-HP) among one of these top value-added chemicals to be produced in a biorefinery. The largest application of 3-HP is its conversion into acrylic acid and other products typically derived from petroleum [2,3]. The global market size of acrylic acid is estimated to reach 22,550 M$ in 2022 [4]. Due to such promising market forecast, Novozymes and Cargill announced a joint agreement to develop a platform to produce acrylic acid from biologically produced 3-HP in 2008 [5]. Nevertheless, up to date, the process has not been implemented at a large scale, as further development is still required.

While the revalorization of lignocellulosic products consisting of glucose and xylose has been largely investigated, there are other waste products that can be used as substrates to produce bulk chemicals. This is the case of crude glycerol, a side-product obtained during the enzymatic production of biodiesel. It is a mixture made of 60-80% glycerol, 10-20% methanol and 10-20% of soap or other undefined organic matter compounds [6]. The use of this mixture as substrate is limited by the fact that methanol is toxic to many microorganisms. The methylotrophic yeast *Pichia pastoris* is a promising microorganism for the revalorization of crude glycerol as it can efficiently grow using both glycerol and methanol as carbon sources. Moreover, *P. pastoris* can grow at a low pH, and it is reported that the cost of the downstream process is reduced if the fermentation is performed at a pH below the pK_a value of the acidic product [7]. For all these reasons, in this study we investigate the production of 3-HP from glycerol in the yeast *P. pastoris*.

P. pastoris is widely used in industrial biotechnology as an efficient host for recombinant protein production, and it has received increasing interest as a platform to produce fine and bulk chemicals [8,9]. Moreover, the efforts of the *P. pastoris* community have allowed the implementation of the necessary tools allowing its use in metabolic engineering research, including up-to-date genetic engineering tools like the

GoldenMOCS [10] and CRISPR-Cas9 [11], metabolic Genome Scale Models (GSM) [12], metabolomics and fluxomics protocols [13,14], and a wide knowledge of its behaviour at the bioreactor scale [15,16]. Another interesting trait of *P. pastoris* is that it is a Crabtree negative yeast. This is an interesting feature in metabolic engineering because overflow metabolism to undesired by-products, such as ethanol or glycerol, can be minimized. The full oxidation of the carbon source leads to a higher energetic yield than in Crabtree positive yeasts, like *Saccharomyces cerevisiae*, thus leading to potentially higher product yields [9,17]. Moreover, the extracellular concentration of some intermediate metabolites of the TCA cycle (i.e. malate or citrate) is lower in *P. pastoris* than in *S. cerevisiae* under similar conditions [13]. This trait simplifies the downstream processing of the products of interest.

The biological production of 3-HP has been largely investigated [18]. Several pathways have been tested in a number of microorganisms, including the industrial workhorses *Escherichia coli* and *S. cerevisiae*. Each pathway to produce 3-HP is named according to its precursor. The route that has obtained the highest yields and productivities is the coenzyme B12-dependant glycerol pathway [19,20]. However, the implementation of this route in *P. pastoris* is currently unfeasible at an industrial scale due to the high production costs caused by the requirement of coenzyme B12 addition, which is an expensive compound [21]. The 3-HP route through β-alanine has been investigated in *S. cerevisiae* [22] and *E. coli* [23] and the route which uses Malonyl-CoA as a precursor has been implemented in several microorganisms, including *E. coli* [24–26], *S. cerevisiae* [21,27] and *Shizosaccharomyces pombe* [28].

Using glucose as substrate, the maximum theoretical yield of the β-alanine to 3-HP pathway is higher than the route starting from Malonyl-CoA, as more ATP is required for the latter. However, when glycerol is used as a substrate, the maximum theoretical yield for both pathways equals 1, as there is net ATP production in both cases (see Annex II; Section 1.1). While the β-alanine pathway would require the expression of 3 heterologous genes [22] to achieve 3-HP production in *P. pastoris*, it is reported that the single expression of the bifunctional enzyme Malonyl-CoA Reductase from *Chloroflexus aurantiacus* (MCR_{Ca}) triggers 3-HP production in yeast through the Malonyl-CoA route [21]. This enzyme performs two NADPH-consuming consecutive reactions sequentially converting Malonyl-CoA to Malonate semialdehyde (MSA), and then MSA is converted to 3-HP (Figure 9).

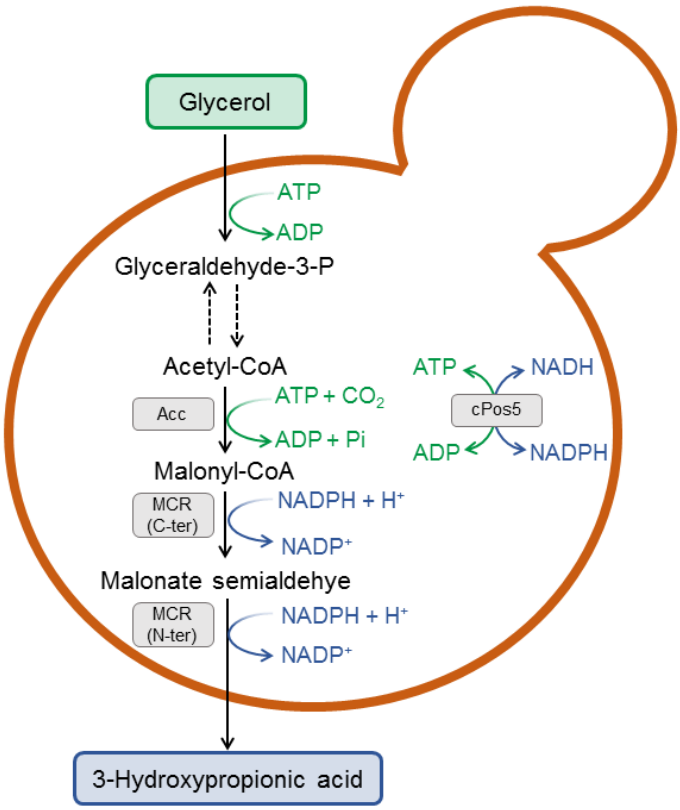

Figure 9. Simplified representation of the conversion of glycerol to 3-HP through the Malonyl-CoA route. The metabolic engineering targets to increase the availability of the precursors of the Malonyl-CoA to 3-HP pathway are included. Acc: Acetyl-CoA Carboxylase; MCR (C-ter): C-terminal domain of Malonyl-CoA Reductase; MCR (N-ter): N-terminal domain of Malonyl-CoA Reductase; cPos5: cytosolic NADH kinase.

In this study, the production of 3-HP using glycerol as substrate has been implemented in *P. pastoris* through the Malonyl-CoA pathway. The expression of mcr_{Ca} leads to 3-HP production in *P. pastoris*. This base strain has been further modified using two different strategies: protein engineering and metabolic engineering. The independent expression of the two subunits of the Malonyl-CoA reductase, has shown higher 3-HP production in other microorganisms [25]. This strategy has been further tested in *P. pastoris,* yielding a substantial improvement compared to the initial strain. Further modifications have been implemented to increase the fluxes producing the substrates of the Malonyl-CoA pathway to 3-HP (NADPH and Malonyl-CoA). The strain producing the highest 3-HP titre has been characterized in a fed-batch culture using glycerol as a substrate. Overall, the potential of *P. pastoris* as a promising host for 3-HP production from this renewable feedstock was demonstrated for the first time.

3.2. Results and discussion

3.2.1. Expression of *mcr*$_{Ca}$ in *P. pastoris* leads to 3-HP production

In the present work, we expressed *mcr*$_{Ca}$ gene in *P. pastoris* under the control of the constitutive and strong GAP promoter. Comparison of the resulting strain, PpHP1, to the reference strain (X-33) in triplicate shake flasks on Buffered Minimal Glycerol (BMG) medium showed that the sole expression of *mcr*$_{Ca}$ resulted in 3-HP production, while it did not affect cell growth (the μ_{max} of the control and PpHP1 strains was the same within the precision range, 0.24 ± 0.01 h^{-1} and 0.24 ± 0.01 h^{-1}, respectively). Moreover, no by-products were detected in any of the two strains (Annex II; Section 1.4; Supplementary Figure S3).

Notably, the PpHP1 strain produced 0.19 ± 0.03 g L^{-1} of 3-HP after 24 h of cultivation. Such 3-HP titter is considerably higher than those achieved in *S. pombe* [29] and *S. cerevisiae* [21] harbouring a similar genetic construction, and using glucose as a substrate (0.016 g L^{-1} and 0.093 g L^{-1}, respectively). Furthermore, the C-yield (Cmol of 3-HP per Cmol of substrate, i.e. glycerol or glucose) for the PpHP1 strain (0.015 ± 0.002 Cmol $Cmol^{-1}$) was remarkably higher than the one observed in other yeasts (0.0003 Cmol $Cmol^{-1}$ in *S. pombe,* and 0.0048 Cmol $Cmol^{-1}$ in *S. cerevisiae*). Remarkably, the specific activity of MCR in PpHP1 was 0.30 ± 0.06 U mg^{-1} of protein, which is remarkably higher than the specific activity reported in *S. cerevisiae* (0.008 U mg^{-1}; [21]). The combined effect of the strength of the *P. pastoris* GAP promoter and the fact that glycerol is more reduced than glucose, which leads to net production of ATP from the substrate, instead of net ATP consumption (Annex II; Section 1.1), points at *P. pastoris* as a promising cell factory for the bioproduction of 3-HP from glycerol.

3.2.2. Setting up the screening conditions for 3-HP producing *P. pastoris* clones

We established two independent analytical methods based on NMR and HPLC-MS for 3-HP quantification, which were cross-validated. The results using the HPLC-MS method diverge from those obtained using NMR when glycerol is still present in the medium (Annex II; Section 1.4; Supplementary Figure S4). This is explained by the matrix effect caused by the glycerol co-eluting with 3-HP from the column, which affects the ionization efficiency at the ionization source (ESI). However, once the glycerol is fully consumed, the HPLC-MS and the NMR methods yielded statistically identical results

when measuring the final 3-HP concentrations in the PpHP1 shake flask cultures described in Section 3.1 (i.e. 3-HP final concentrations of 0.18 ± 0.02 g L^{-1} of 3-HP and 0.19 ± 0.02 g L^{-1} of 3-HP, respectively).

Consumption of 3-HP has been reported in several microorganisms [30]. In order to evaluate whether the PpHP1 strain was able to assimilate this compound, this strain was grown in triplicate shake flasks using BMG, BMG medium supplemented with 2.5 g L^{-1} of 3-HP (BMG3HP) or Buffered Minimal medium supplemented with 2.5 g L^{-1} of 3-HP as a sole carbon source (BM3HP). Samples were collected after 24, 48 and 72 h. The 3-HP concentration remained constant throughout the 72 h in the cultures grown on BM3HP (no growth was observed). After 24 h, glycerol was exhausted from the BMG and BMG3HP, while the concentration of 3-HP remained unaltered between the 24 and the 72 h (data not shown), thereby indicating that *P. pastoris* does not assimilate 3-HP as C-source within the experimental time frame tested.

Considering these results, screening of the 3-HP producing strains was performed taking end-point samples after 48 h of incubation to ensure full consumption of glycerol, followed by 3-HP quantification using the HPLC-MS method.

3.2.3. Improvement of 3-HP production by MCR enzyme engineering

Recent studies have shown the positive effect of dissecting the MCR enzyme in the two subunits catalysing each of the two reactions converting Malonyl-CoA into 3-HP [25]. The presence of three point-mutations causing three aminoacidic changes (N940V, K1106R and S1114R) had an additional positive impact on 3-HP production in *E. coli* [26]. The same outcome has been demonstrated in *S. pombe*, where the expression of the N-terminal and the improved version of the C-terminal domain of MCR using two independent expression cassettes led to a 30-fold improvement in the final 3-HP titters, compared to the starting strain expressing the original sequence of MCR_{Ca} [29]. Therefore, we introduced two expression cassettes into *P. pastoris* allowing the independent expression of the coding DNA sequences for the N-terminal and the C-terminal domains of MCR (including the wild-type and the mutated version of the latter) under the control of the GAP promoter.

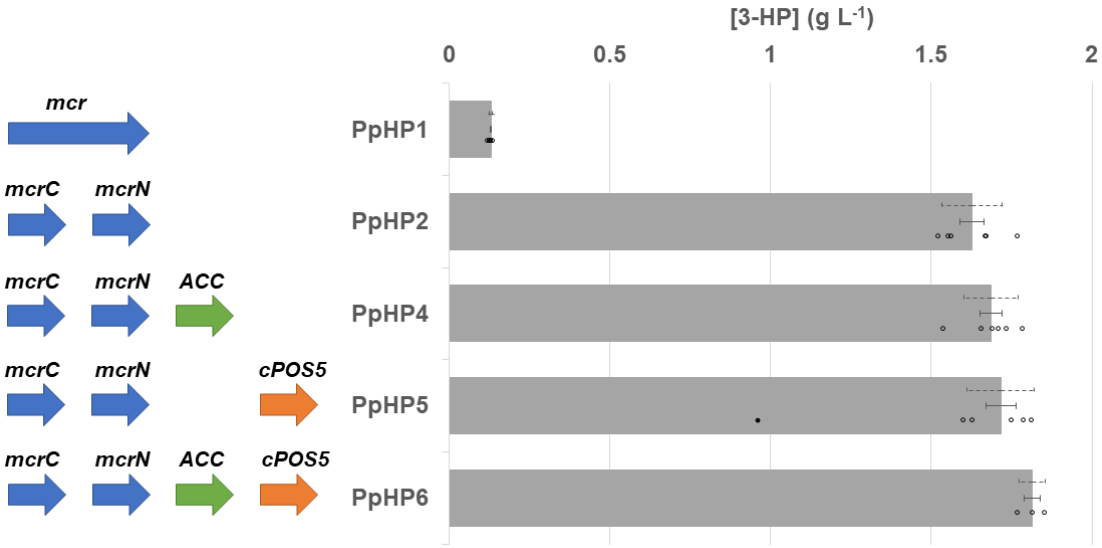

Figure 10. Production of 3-HP for each strain in the screening experiments. The genes heterologously expressed in each strain are depicted in the left side of the graph. The grey bars show the average 3-HP concentration at the end of the culture, the discontinuous line shows the standard deviation, the solid line indicates the SE and the circles show the average result for each clone. The solid circle of a PpHP5 clone shows the result of a clone which was discarded for the calculations, as it had a different behaviour from the rest of the clones of that strain. For PpHP6, only 3 clones could be screened. Despite that more than 50 transformants of PpHP6 were screened from 2 independent transformations using colony PCR, only 3 clones resulted positive.

As shown in Figure 10, the dissection of MCR (strain PpHP2) had a positive impact on 3-HP production, triggering a 12.5-fold increase in 3-HP production (1.63 ± 0.09 g L^{-1} 3-HP). Nevertheless, the introduction of the 3 point mutations in the C-terminal domain (strain PpHP3) resulted in a non-producing strain. Similarly, the introduction of these 3 point mutations to a non-dissected version of MCR resulted in a non-producing *P. pastoris* strain (data not shown). These point mutations are far from the reactive site and the NADPH binding site of the enzyme. It remains poorly understood how distant mutations may affect catalytic properties. Moreover, as the structure of the C-terminal domain of MCR from *C. aruantiacus* is not available, the exact effect of the point mutations on the protein conformational stability/quality is hard to predict, particularly when the protein is synthetized at high rates (i.e. using a strong promoter). Notably, the 12.5 fold-improvement obtained by dissecting MCR is in the same range as those reported in *S. pombe* and *E. coli*.

3.2.4. Metabolic engineering of *P. pastoris* to improve 3-HP production

Metabolic engineering for 3-HP production through the Malonyl-CoA pathway was aimed at increasing the availability of the two precursors of this route, namely

NADPH and Malonyl-CoA. To do so, the ACC_{Yl} and $cPOS5_{Sc}$ genes have been heterologously expressed in the PpHP2 strain. The reactions catalysed by the enzymes encoded by these two genes are depicted in Figure 9. Acc produces Malonyl-CoA from Acetyl-CoA, which is the precursor of the central carbon metabolism for 3-HP production. The overexpression of such enzyme has already been performed in *E. coli* [24], *S. cerevisiae* [21,27] and *S. pombe* [29] to increase the production of 3-HP. The enzyme cPos5 produces NADPH by means of NADH and ATP consumption, and the overexpression of its gene leads to an increase in the $NADPH/NADP^+$ ratio [31].

As shown in the Figure 10, the overexpression of Acc or cPos5 in the strain PpHP2 - resulting in the strains PpHP4 and PpHP5, respectively - led to a small increase in 3-HP production. Still, such increases were not statistically significant compared to the parental strain PpHP2 (*p*-values of 0.27 and 0.15, respectively). However, when both genes were overexpressed at the same time (PpHP6), a significant increase in the final 3-HP concentration was observed ($p = 0.015$).

The PpHP6 strain produced 1.81 ± 0.04 g L^{-1} of 3-HP, which represents a 14-fold increase compared to the starting strain (PpHP1), and a 12% increase compared to PpHP2. The C-yield for PpHP6 was 0.146 ± 0.003 Cmol $Cmol^{-1}$.

Similar strategies in other microorganisms resulted in similar outcomes. For example, in *E. coli*, the overexpression of either ACC or PntAB (a transhydrogenase encoding gene) led to a 2-fold increase, while the co-expression of both genes led to a 3-fold increase [24]. It is also worth noticing that in *S. pombe,* enzyme engineering and expression level adjustment of MCR led to a 30-fold increase in 3-HP titters, while increasing the availability of Acetyl-CoA and CoA in this strain resulted in a 2-fold increase. Altogether, these results point at the flux from Malonyl-CoA to 3-HP as the main limiting factor for 3-HP production. Further metabolic studies should corroborate this hypothesis. Indeed, the increase of the number of copies of the *mcr* gene has already been demonstrated to have a positive effect in 3-HP production in both *S. cerevisiae* [27] and *S. pombe* [29].

Overall, the product yield obtained by the strain PpHP6 during the screening phase (0.146 ± 0.003 Cmol $Cmol^{-1}$) is significantly higher (around 1.8-fold) to the highest yield observed in yeast under comparable conditions (deep-well plate culture using defined medium), i.e. using the *S. cerevisiae* strain 3HP-M11 producing 3-HP through

the Malonyl-CoA pathway, with a yield on glucose of 0.080 ± 0.008 Cmol Cmol^{-1} (calculated from data given by [27]).

3.2.5. Production of 3-HP in a fed-batch culture

The strain PpHP6 was further cultivated in a controlled fed-batch culture. First, a batch experiment was performed in order to determine the μ_{max} of PpHP6, and also the initial biomass concentration (X_0) and the biomass to substrate yield ($Y_{X/S}$), which are the parameters required to set the exponential feeding rate (see Section 3.4.5). The μ_{max} was 0.19 ± 0.1 h^{-1}, the X_0 was 18.6 ± 0.2 g L^{-1}, and the $Y_{X/S}$ 0.47 ± 0.01 g g^{-1}.

After the initial batch phase (22 h), the exponential feeding rate was set to maintain a growth rate equal to 0.1 h^{-1} (approximately 50% of the μ_{max}) (Figure 11A). After 44 h of cultivation (22 h of feeding phase), glycerol accumulation was observed, and the feeding pump was stopped. Thereafter, the fermentation was terminated after 45.5 h of cultivation, when the pO_2 increased, indicating that all the glycerol had been consumed. Overall, 195 g L^{-1} of glycerol were added into the reactor, and 24.75 ± 0.54 g L^{-1} of 3-HP were produced. The only by-product detected by NMR was arabitol in the late stages of the batch and the fed-batch phases.

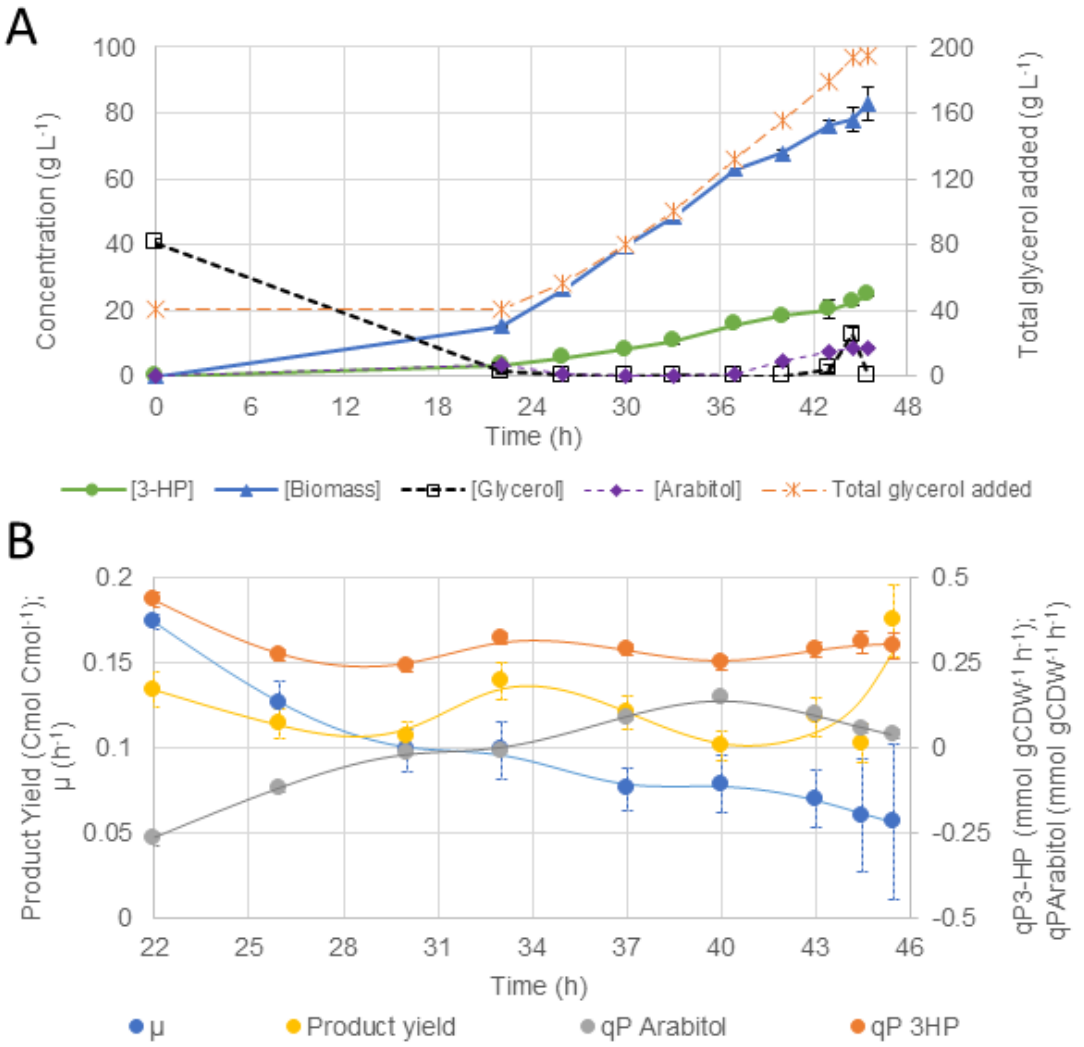

Figure 11. Fed-batch culture of PpHP6. **(A)** Biomass and metabolites concentration during cultivation, as well as total glycerol added (per liter) into the reactor are shown. It was calculated considering the volume of feeding added to the reactor and the actual culture volume. Error bars denote SE. **(B)** Growth rate (μ), product yield ($Yield_{3\text{-}HP/Glyc}$), q-rate of 3-HP (qP 3-HP), and q-rate of arabitol (qP Arabitol) of the strain PpHP6 throughout the feeding phase of the fed-batch culture at a pre-set μ of 0.1 h^{-1}. Error bars show the SE.

As already inferred from the evolution of physiological growth parameters over time, growth rate was not maintained during the whole feeding phase. Furthermore, the decrease in the growth rate was accompanied with the accumulation of glycerol and the production of arabitol towards the end of the cultivation. These results differ from previous observations of *P. pastoris* producing heterologous proteins in fed-batch cultures operated under analogous conditions (i. e. using a pre-programmed exponential substrate feeding strategy for controlled specific growth rate at 0.1 h^{-1}), where the μ remained constant throughout the feeding phase and no arabitol accumulation was detected, achieving up to 100 g L^{-1} of dry cell biomass [32]. The spline curves fitted to

the evolution of the growth rate (μ), product yield ($Y_{P/S}$), $qP_{3\text{-}HP}$, and $qP_{Arabitol}$ throughout the cultivation further reveal that the decrease in the growth rate coincides with the onset of glycerol accumulation and arabitol by-product excretion (Figure 11B). Conversely, product yield and $qP_{3\text{-}HP}$ followed the opposite trend, i.e. the $Y_{P/S}$ is reduced from 0.134 ± 0.010 Cmol $Cmol^{-1}$ at the first part of the feeding phase to yields close to 0.1 Cmol $Cmol^{-1}$ coinciding with the highest $qP_{Arabitol}$ values. These results show how during the beginning of the feeding phase the C-yield was close to the one obtained in the screening phase (0.146 ± 0.003 Cmol $Cmol^{-1}$), even though the average yield of the overall fed-batch culture was lower (0.130 ± 0.003 Cmol $Cmol^{-1}$ and 0.127 ± 0.003 g g^{-1}).

A possible explanation for the observed trends is the increase in the 3-HP concentration. Accumulation of 3-HP in the fermentation broth has been reported to be toxic for other microorganisms like *E. coli* and *S. cerevisiae*. Such toxicity may be triggered by the conversion of 3-HP into 3-hydroxypropanaldehyde (reuterin), which causes oxidative stress to the cells through its interaction with reduced glutathione [33,34]. The sequestration of glutathione leads to a decrease in the maximal growth rate of *S. cerevisiae* at high 3-HP concentrations [34].

Another plausible explanation of the decrease in the μ at the final stage of the culture may be the increase in the ATP expenditure for maintenance at high extracellular concentrations of weak organic acid, i.e. 3-HP. Protonated acid molecules may enter the cytoplasm by diffusion and later on dissociate, leading to an ATP cost for the re-secretion of the organic acid and the restoration of the intracellular pH. The expression of a 3-HP exporter in *E. coli* has proven to be beneficial, as it reduces stress caused by the intracellular dissociation of 3-HP [35]. Moreover, higher extracellular concentrations of 3-HP have a direct impact on the thermodynamics of its secretion, leading to an increase in ATP expenses for 3-HP export [7]. All these phenomena would ultimately impact on the $Y_{X/S}$ in *P. pastoris*, explaining the decrease in the growth rate and the accumulation of glycerol at the later stage of the fed-batch culture.

Moreover, we observe the production of arabitol at the end of the batch and the fed-batch phases (Figure 11A). Arabitol production in *P. pastoris* has been related to stress conditions caused by the Unfolded Protein Response (UPR) [36], high osmolarity [37], or hypoxic conditions, where arabitol production has been proposed to be used as a redox sink [38]. Additionally, arabitol by-product formation has been observed in lactic

acid-producing recombinant *P. pastoris* growing in batch cultures using glycerol as carbon source [39]. Therefore, the presence of arabitol points to a redox imbalance, either caused by 3-HP-derived toxicity effects, or by overexpression of cPos5. Further metabolomic and fluoxmic studies will help elucidating the cause.

Altogether, these results suggest that the pre-established bioreactor fed-batch cultivation protocols for heterologous protein production in *P. pastoris* are not necessarily optimal for the production of weak acids such as 3-HP, as its accumulation in the extracellular space and/or the toxic effect at high concentrations may lead to physiological changes negatively impacting on the bioprocess parameters such as the μ_{max} or $Y_{X/S}$. Moreover, the current cultivation protocol led to the production of arabitol as a side-product at the end of the fed-batch process, which caused a significant decrease in the product yield. Deletion of the Arabitol dehydrogenase (ArDH) gene in a lactic acid producing strain reduced arabitol production, resulting in a 20% increase in product titers [39].

The tolerance to 3-HP should also be addressed in order to increase further the product yield. To this end, both adaptive laboratory evolution (ALE) experiments and rational engineering strategies have proven successful to increase 3-HP tolerance in other yeast and could be therefore transferred to *P. pastoris.* Specifically, ALE experiments led to the conclusion that overexpression of the S-(hydroxymethyl)glutathione dehydrogenase gene (*SFA1*) in *S. cerevisiae* restored growth at 50 g L^{-1} of 3-HP [34]. Expression of two mutated versions of *SFA1* under the control of the native SFA1 promoter were also able to restore cell growth at 50 g L^{-1} of 3-HP. The *SFA1* residues which were mutated in *S. cerevisiae* are conserved in the homologous *P. pastoris* gene (PAS_chr3_1028). Therefore, a similar approach to avoid 3-HP toxicity could be tested in *P. pastoris*.

The overall productivity of the fed-batch culture was 0.54 ± 0.01 g L^{-1} h^{-1}. To our knowledge, this is the highest 3-HP productivity reported in yeast [40,41], and it is almost identical to the highest productivity reported using the Malonyl-CoA pathway, which was 0.56 g L^{-1} h^{-1} and it was reported in *E. coli* [26]. Such promising results can be attributed to the combination of three main factors: 1) The high specific MCR activity due to the strength of pGAP, extensively proven for heterologous protein production in *P. pastoris*; 2) The use of glycerol as a substrate, which delivers more ATP than glucose under aerobic conditions, leading to higher biomass and product yields compared to the use of

glucose; and 3) The use of glycerol as substrate allows for higher growth rates during the feeding phase compared to typical fed-batch cultivations of Crabtree-positive yeasts growing on glucose as substrate, thereby supporting higher volumetric productivities, while minimizing by-product formation.

3.3. Conclusions

In this study, we successfully introduced the Malonyl-CoA to 3-HP pathway in *P. pastoris* for 3-HP production. The use of pGAP, a strong constitutive promoter, to drive expression of the biosynthetic *mcr* gene, combined with the use of glycerol as carbon source, proved to be key to obtain higher specific activities than in other yeasts. The subsequent combination of protein and metabolic engineering strategies performed in this study have led to a 14-fold increase in the 3-HP yield. Moreover, a controlled fed-batch strategy has shown the ability of *P. pastoris* to produce up to 24.75 g L^{-1} of 3-HP in 45.5 h, achieving an overall yield of 0.13 Cmol $Cmol^{-1}$, and a productivity of 0.54 g L^{-1} h^{-1}. Overall, we benchmarked *P. pastoris* for 3-HP production, demonstrating the potential of this cell factory for platform chemicals bioproduction. In addition, this study serves as a basis for further optimisation of this platform through integrated systems metabolic engineering and bioprocess engineering strategies, which are paramount to reach economically attractive metrics for 3-HP production from crude glycerol in *P. pastoris*.

3.4. Experimental Procedures

3.4.1. Strain construction

A series of strains derived from the parental strain *P. pastoris* X-33 (Invitrogen-Thermo Fisher Scientific, MA, USA) was generated. Plasmids and strains used during this study are listed in Table 3. Three heterologous genes were expressed in *P. pastoris*, encoding for: a bi-functional Malonyl-CoA Reductase from *Chloroflexus aurantiacus* (mcr_{Ca}, Uniprot: Q6QQP7_CHLAU), an Acetyl-CoA Carboxylase from *Yarrowia lipolytica* (ACC_{Yl}, Uniprot: YALI0_C11407) and a cytosolic NADH kinase from *S. cerevisiae* ($cPOS_{Sc}$) [31]. The expression of all the heterologous genes was controlled by the strong and constitutive GAP promoter. A detailed description of the molecular cloning protocols used to generate the plasmids for this study is available in the Supplementary Materials of this chapter (Annex II; Section 1.2).

Table 3. List of plasmids and P. pastoris strains used during this study.

Plasmid name	Expression cassettes in the plasmid	Source
pBIZi_pGAP		Bioingenium SL
pBIZi_pGAP_MCR	P_{GAP} - *mcr*$_{Ca}$ - AOX1tt	This study
pBIZi_pGAP_MCR_N	P_{GAP}-*mcr*$_{Ca}$(N-ter)-AOX1tt	This study
pBIZi_pGAP_MCR_C	P_{GAP}-*mcr*$_{Ca}$(C-ter)-AOX1tt	This study
pBIZi_pGAP_MCR_E	P_{GAP}-*mcr*$_{Ca}$(Cter$_{N940V/K1106W/S1114R}$)-AOX1tt	This study
pBIZi_pGAP_MCR_NC	P_{GAP}-*mcr*$_{Ca}$(N-ter)-AOX1tt P_{GAP}-*mcr*$_{Ca}$(C-ter)-AOX1tt	This study
pBIZi_pGAP_MCR_NE	P_{GAP}-*mcr*$_{Ca}$(N-ter)-AOX1tt P_{GAP}-*mcr*$_{Ca}$(C-ter$_{N940V/K1106W/S1114R}$)-AOX1tt	This study
BB1_23		[10]
BB1_12_pGAP		[10]
BB1_34_ScCYC1tt		[10]
BB1_34_RPS3tt		[10]
BB2_AB		[10]
BB2_BC		[10]
BB3eH_14		[10]
BB3eH_AC		[10]
BB3eH_ACC	P_{GAP}-*ACC*$_{Yl}$(Δ*Bbs*I)-ScCYC1tt	This study
BB3eH_cPOS5	P_{GAP}-*cPOS5*$_{Sc}$-ScCYC1tt	This study
BB3eH_ACC_cPOS5	P_{GAP}-*ACC*$_{Yl}$(Δ*Bbs*I)-ScCYC1tt P_{GAP}- *cPOS5*$_{Sc}$-ScCYC1tt	This study

Strain name	Plasmid integration	Source
X-33		Invitrogen-Thermo Fisher Scientific
PpHP1	pBIZi_pGAP_MCR	This study
PpHP2	pBIZi_pGAP_MCR_NC	This study
PpHP3	pBIZi_pGAP_MCR_NE	This study
PpHP4	pBIZi_pGAP_MCR_NC BB3eH_ACC	This study
PpHP5	pBIZi_pGAP_MCR_NC BB3eH_cPOS5	This study
PpHP6	pBIZi_pGAP_MCR_NC BB3eH_ACC_cPOS5	This study

Electrocompetent *P. pastoris* cells were prepared as described elsewhere [42]. Plasmids derived from pBIZi_pGAP (Bioingenium SL, Spain) were linearized using AvrII

(New England Biolabs, MA, USA), while the ones derived from BB3eH were linearized using PmeI (New England Biolabs). Transformation was performed using 100 ng of purified linear DNA according to a previously described protocol [42].

Recombinant *P. pastoris* strains were selected on YPD agar plates (1% yeast extract, 2% peptone, 2% dextrose, 15 g L^{-1} agar) supplemented with the appropriate antibiotic (100 µg mL^{-1} zeocine or hygromycin 200 µg mL^{-1}) (InvivoGen, CA, USA). When the plates contained both zeocine and hygromycin, the concentration of each antibiotic was reduced by half (50 µg mL^{-1} zeocine and hygromycin 100 µg mL^{-1}).

3.4.2. Shake flask cultures

Cultures were first grown overnight on 5 mL of YPG medium (1% yeast extract, 2% peptone and 1% v/v glycerol) supplemented with the appropriate antibiotic in 50 mL Falcon tubes, at 30ºC, and 180 rpm. The overnight cultures were then diluted to an optical density at 600 nm (OD_{600}) of 0.5 on 5 mL of YPG and grown for 8 h at the same cultivation conditions. Afterwards, these cultures were used to inoculate a 500 mL baffled shake flask containing 50 mL of Buffered Minimal Glycerol medium (BMG) (100 mM potassium phosphate buffer pH 6, 1.34% Yeast Nitrogen Base (YNB), 0.4 mg L^{-1} biotin and 1% v/v glycerol) at a starting OD_{600} of 0.05. The shake flask cultures were grown at 30ºC and 180 rpm in an incubator shaker Multitron Standard (Infors HT, Bottmingen, Switzerland) with a 2.5 cm orbit.

3.4.3. Screening in deep-well plates

P. pastoris strains were inoculated from cryo-vials into 24 deep-well plates containing YPG medium supplemented with the appropriate antibiotic. Cultures were placed on a platform with a slope of 20º in an incubator shaker Multitron Standard with 25 mm orbit and grown overnight at 28ºC and 220 rpm. Afterwards, 50 µL of overnight cultures were used to inoculate a 24 deep-well plate containing 2 mL of BMG medium. If not stated otherwise, six clones of each strain were tested in triplicates. The cultures were grown for 48 h at the same conditions.

3.4.4. Enzymatic assay

P. pastoris X-33 and *P. pastoris* PpHP1 cells were grown overnight on YPG medium supplemented with zeocine when appropriate. The grown cultures were used to

inoculate a 100 mL shake flask containing 25 mL of fresh BMG medium at an initial OD600 of 0.1. When the cells reached an OD_{600} of about 2, 5 mL of each culture were centrifuged at 6,000 g. The pellets were washed twice with ice-cold PBS buffer and resuspended in 1 mL of breaking buffer (50 mM HEPES, 150 mM KCl, 1 mM DTT, 1 mM EDTA, pH 7.5, Halt Protease inhibitor Cocktail (Thermo Fisher Scientific)). Resuspended cells were then lysed using glass beads applying 5 cycles of 1 minute of vortexing followed by 2 minutes of incubation on ice. Cell lysates were centrifuged at 16,000 g and 4ºC for 20 min. The supernatant (soluble fraction) was transferred to a new tube and the amount of protein in the cell extract was quantified using the Bradford method (Pierce™ Coomassie Plus, Thermo Fisher Scientific). The MCR specific activity was quantified as previously reported (Chen *et al*., 2014). As MCR is a bifunctional enzyme consuming 2 NAPDH molecules to convert Malonyl-CoA into 3-HP, one unit of enzyme activity was defined as 2 µmol NADPH consumed per minute.

3.4.5. Bioreactor cultivation

For the bioreactor cultivations, the batch medium consisted of 40 g L^{-1} glycerol, 1.8 g L^{-1} citric acid, 0.02 g L^{-1} $CaCl_2 \cdot 2\ H_2O$, 12.6 g L^{-1} $(NH_4)_2HPO_4$, 0.5 g L^{-1} $MgSO_4 \cdot 7\ H_2O$, 0.9 g L^{-1} KCl, 50 µL antifoam Glanapon 2000 kz (Bussetti and Co GmbH, Vienna, Austria), 0.4 mg L^{-1} biotin, and 4.6 mL L^{-1} of PTM1 trace salts [43]. The pH of the medium was set to 5 using 5 M HCl. The feeding medium composition was 400 g L^{-1} glycerol, 10 g L^{-1} KCl, 6.45 g L^{-1} $MgSO_4 \cdot 7\ H_2O$, 0.35 g L^{-1} $CaCl_2 \cdot 2\ H_2O$, 0.2 mL L^{-1} antifoam Glanapon 2000 kz, 0.3 mg L^{-1} biotin, and 15 mL L^{-1} PTM1 trace salts. For the batch and the feeding media, all components except the biotin and the trace salts were mixed and autoclaved. Biotin and trace salts were filter-sterilized and added to the mixture once the medium had cooled down.

Fed-batch cultures were performed in duplicate in a 5-L Biostat B Bioreactor (Sartorius Stedim, Goettingen, Germany). The pH was maintained at 5 using Ammonia 15% (v/v). The temperature was set to 28ºC and air was added into the reactor at an aeration rate of 1 vvm (2 L min^{-1}). The agitation was gradually increased from 600 to 1,200 rpm to maintain a pO_2 above 25%. When increasing the agitation was insufficient to maintain the pO_2 above the set point, the agitation was set to 1,200 rpm and pure oxygen was mixed with air at the air inlet of the bioreactor to maintain a pO_2 above 25%, while maintaining an aeration rate of 2 L min^{-1}.

The batch phase was performed with a starting volume equal to 2 L, and the reactor was inoculated at a starting OD_{600} equal to 1. The feeding phase started after a sudden increase in the pO_2 indicating that all the glycerol from the batch phase had been consumed. A pre-set exponential feeding rate was used when adding the feeding medium into the reactor. Such exponential feeding rate was calculated according to previous literature [44], and it aimed to maintain pseudo-steady state conditions at a constant growth rate of 0.1 h^{-1} at C-limiting conditions. The working volume of the reactor was calculated as described elsewhere [32]. To calculate the exponential feeding rate the biomass concentration at the end of the batch phase (X_0) and the biomass to substrate yield ($Y_{X/S}$) were used.

3.4.6. Analytical methods and data processing

The analytical and biological replicates were averaged and the standard error (SE) for each measurement was calculated considering the number of biological replicates (number of independent samples).

The splines fitting the μ, the q-rates, and the product yield during the feeding phase of the fed-batch culture were performed using Matlab 2019 (Mathworks, MA, USA). The *fit* function was used together with the additional options: *'smoothingspline'* and *'SmoothingParam'=0.5*.

The OD_{600} measurements of the shake flask and the bioreactor cultures were performed using a Lange DR 3900 spectrophotometer (Hach, CO, USA).

To quantify the metabolites, the culture samples were first centrifuged at 12,000 g and 4ºC and then filtered using a 0.45 μm syringe filter of type HAWP (Millipore CA, USA). Glycerol and arabitol were quantified using an HPLC Dionex Ultimate3000 (Dionex - Thermo Fisher Scientific) coupled to a UV detector at 210 nm and an RI detector (Dionex - Thermo Fisher Scientific). The compounds were separated with an ionic exchange column ICSep ICE-COREGEL 87H3 (Transgenomic Inc., NE, USA) using 6 mM sulfuric acid as mobile phase at a flow rate of 0.6 mL min^{-1}. As 3-HP and glycerol elute the column at the same time, the 3-HP was quantified using two different methods: HPLC-MS and Nuclear Magnetic Resonance (NMR) spectroscopy. Standard samples for calibration were prepared using 3-hydroxypropionic acid sodium salt from Santa Cruz Biotechnology Inc. (CA, USA).

For the HPLC-MS method, we used a Prominence HPLC (Shimadzu, Kyoto, Japan) coupled to a single quadrupole Shimadzu-2010A mass spectrometry detector using electro spray ionization (ESI). The metabolites of the supernatant were separated using an ICSep 87H USP L17 column (Transgenomic Inc., NE, USA) and 16 mM formic acid as mobile phase at a flow-rate of 0.15 mL min^{-1}. 2 µL samples were injected into the column and the MS analyser was set to 89 m/z for negatively charged molecules, which corresponds to the m/z ratio for unprotonated 3-HP. The detector settings were: Curved Desolvation Line (CDL) temperature at 200°C, heat block temperature at 200°C, voltage of the detector at 1.5 kV, nebulizing gas (nitrogen) flow at 1.5 L min^{-1}, and drying gas (nitrogen) flow at 10 L min^{-1}. Each sample was analysed in duplicate.

For the NMR method, a Bruker AVANCE 600 spectrometer (600.13 MHz frequency for ^{1}H) equipped with a 5 mm TBI probehead and an autosampler (Bruker BioSpin, Rheinstetten, Germany) was utilized. The probe temperature was maintained at 300.0 K for all experiments. Once centrifuged and filtered, 300 µL of each culture aliquot were mixed with 300 µL of a D_2O stock solution containing an internal standard (3-(trimethylsilyl)-[2,2,3,3-$^{2}H_4$]-propionic acid sodium salt (TSP), 11.1 mM) and transferred to the NMR tube. All samples were analysed conducting standard quantitative 1D ^{1}H NMR experiments with presaturation of the residual water signal. Data were collected into 32k data points during an acquisition time of 1.7 s using a recycle delay of 15 s. Spectra were recorded in the time domain as interferograms (FID) across a spectral width of 9,615 Hz and as the sum of 128 transients. FIDs were automatically Fourier transformed (FT) and the spectra were phased, and baseline corrected. TSP was used as internal reference ($\delta(^{1}H)$ and $\delta(^{13}C)$ at 0.00 ppm)

The glycerol concentration obtained from the IR spectra of the HPLC analysis was corrected accounting for the 3-HP interference. The area at the IR detector corresponding to the amount of 3-HP quantified using the HPLC-MS or the NMR analyses was calculated and subtracted from the total IR area.

References

1. Werpy, T., and Petersen, G. (2004) Top value added chemicals from biomass. Volume I - Results of screening for potential candidates from sugars and synthesis gas. *U.S. Department of Energy*.
2. Kumar, V., Ashok, S., and Park, S. (2013) Recent advances in biological production of 3-hydroxypropionic acid. *Biotechnology Advances*, 31 (6), 945–961.
3. della Pina, C., Falletta, E., and Rossi, M. (2011) A green approach to chemical building blocks. The case of 3-hydroxypropanoic acid. *Green Chemistry*, 13 (7), 1624–1632.
4. Grand View Research (2016) Acrylic Acid Market Size Worth $22.55 Billion By 2022.
   [WWW document].
   URL https://www.grandviewresearch.com/press-release/globalacrylic-acid-market
5. Novozymes (2008) Cargill and Novozymes to enable production of acrylic acid via 3HPA from renewable raw materials.
   [Press release].
   URL https://www.novozymes.com/en/news/news-archive/2008/01/44469
6. Luo, X., Ge, X., Cui, S., and Li, Y. (2016) Value-added processing of crude glycerol into chemicals and polymers. *Bioresource Technology*, 215, 144–154.
7. van Maris, A.J.A., Konings, W.N., van Dijken, J.P., and Pronk, J.T. (2004) Microbial export of lactic and 3-hydroxypropanoic acid: Implications for industrial fermentation processes. *Metabolic Engineering*, 6 (4), 245–255.
8. Schwarzhans, J.P., Luttermann, T., Geier, M., Kalinowski, J., and Friehs, K. (2017) Towards systems metabolic engineering in *Pichia pastoris*. *Biotechnology Advances*, 35 (6), 681–710.
9. Peña, D.A., Gasser, B., Zanghellini, J., Steiger, M.G., and Mattanovich, D. (2018) Metabolic engineering of *Pichia pastoris*. *Metabolic Engineering*, 50, 2–15.
10. Prielhofer, R., Barrero, J.J., Steuer, S., Gassler, T., Zahrl, R., Baumann, K., Sauer, M., Mattanovich, D., Gasser, B., and Marx, H. (2017) GoldenPiCS: A Golden Gate-derived modular cloning system for applied synthetic biology in the yeast *Pichia pastoris*. *BMC Systems Biology*, 11, 123.
11. Weninger, A., Hatzl, A.M., Schmid, C., Vogl, T., and Glieder, A. (2016) Combinatorial optimization of CRISPR/Cas9 expression enables precision genome engineering in the methylotrophic yeast *Pichia pastoris*. *Journal of Biotechnology*, 235, 139–149.
12. Tomàs-Gamisans, M., Ferrer, P., and Albiol, J. (2016) Integration and validation of the genome-scale metabolic models of *Pichia pastoris*: A comprehensive update of protein glycosylation pathways, lipid and energy metabolism. *PLoS ONE*, 11, e0148031.
13. Carnicer, M., Canelas, A.B., ten Pierick, A., Zeng, Z., van Dam, J., Albiol, J., Ferrer, P., Heijnen, J.J., and van Gulik, W. (2012) Development of quantitative metabolomics for *Pichia pastoris*. *Metabolomics*, 8 (2), 284–298.
14. Ferrer, P., and Albiol, J. (2014) ^{13}C-Based Metabolic Flux Analysis of Recombinant *Pichia pastoris*. *Methods in Molecular Biology*, 1191, 291–313.
15. Looser, V., Bruhlmann, B., Bumbak, F., Stenger, C., Costa, M., Camattari, A., Fotiadis, D., and Kovar, K. (2014) Cultivation strategies to enhance productivity of *Pichia pastoris*: A review. *Biotechnology Advances*, 33 (6), 1177–1193.
16. Yang, Z., and Zhang, Z. (2018) Engineering strategies for enhanced production of protein and bio-products in *Pichia pastoris*: A review. *Biotechnology Advances*, 36, 182–195.
17. Dai, Z., Huang, M., Chen, Y., Siewers, V., and Nielsen, J. (2018) Global rewiring of cellular metabolism *renders Saccharomyces cerevisiae* Crabtree negative. *Nature Communications*, 9, 3059.
18. de Fouchécour, F., Sánchez-Castañeda, A.K., Saulou-Bérion, C., and Spinnler, H.É. (2018) Process engineering for microbial production of 3-hydroxypropionic acid. *Biotechnology Advances*, 36 (4), 1207–1222.
19. Raj, S.M., Rathnasingh, C., Jo, J.E., and Park, S. (2008) Production of 3-hydroxypropionic acid from glycerol by a novel recombinant *Escherichia coli* BL21 strain. *Process Biochemistry*, 43 (12), 1440–1446.
20. Rathnasingh, C., Raj, S.M., Jo, J.E., and Park, S. (2009) Development and evaluation of efficient recombinant *Escherichia coli* strains for the production of 3-hydroxypropionic acid from glycerol. *Biotechnology and Bioengineering*, 104 (4), 729–739.
21. Chen, Y., Bao, J., Kim, I.K., Siewers, V., and Nielsen, J. (2014) Coupled incremental precursor and co-factor supply improves 3-hydroxypropionic acid production in *Saccharomyces cerevisiae*. *Metabolic Engineering*, 22, 104–109.
22. Borodina, I., Kildegaard, K.R., Jensen, N.B., Blicher, T.H., Maury, J., Sherstyk, S.,

Schneider, K., Lamosa, P., Herrgård, M.J., Rosenstand, I., Öberg, F., Forster, J., and Nielsen, J. (2015) Establishing a synthetic pathway for high-level production of 3-hydroxypropionic acid in Saccharomyces cerevisiae via β-alanine. *Metabolic Engineering*, 27, 57–64.

23. Song, C.W., Kim, J.W., Cho, I.J., and Lee, S.Y. (2016) Metabolic Engineering of *Escherichia coli* for the Production of 3-Hydroxypropionic Acid and Malonic Acid through β-Alanine Route. *ACS Synthetic Biology*, 5 (11), 1256–1263.
24. Rathnasingh, C., Raj, S.M., Lee, Y., Catherine, C., Ashok, S., and Park, S. (2012) Production of 3-hydroxypropionic acid via malonyl-CoA pathway using recombinant *Escherichia coli* strains. *Journal of Biotechnology*, 157 (4), 633–640.
25. Liu, C., Wang, Q., Xian, M., Ding, Y., and Zhao, G. (2013) Dissection of malonyl-coenzyme A reductase of *Chloroflexus aurantiacus* results in enzyme activity improvement. *PLoS ONE*, 8 (9), e75554.
26. Liu, C., Ding, Y., Zhang, R., Liu, H., Xian, M., and Zhao, G. (2016) Functional balance between enzymes in malonyl-CoA pathway for 3-hydroxypropionate biosynthesis. *Metabolic Engineering*, 34, 104–111.
27. Kildegaard, K.R., Jensen, N.B., Schneider, K., Czarnotta, E., Özdemir, E., Klein, T., Maury, J., Ebert, B.E., Christensen, H.B., Chen, Y., Kim, I.K., Herrgård, M.J., Blank, L.M., Forster, J., Nielsen, J., and Borodina, I. (2016) Engineering and systems-level analysis of *Saccharomyces cerevisiae* for production of 3-hydroxypropionic acid via malonyl-CoA reductase-dependent pathway. *Microbial Cell Factories*, 15, 53.
28. Suyama, A., Higuchi, Y., Urushihara, M., Maeda, Y., and Takegawa, K. (2017) Production of 3-hydroxypropionic acid via the malonyl-CoA pathway using recombinant fission yeast strains. *Journal of Bioscience and Bioengineering*, 124 (4), 392–399.
29. Takayama, S., Ozaki, A., Konishi, R., Otomo, C., Kishida, M., Hirata, Y., Matsumoto, T., Tanaka, T., and Kondo, A. (2018) Enhancing 3-hydroxypropionic acid production in combination with sugar supply engineering by cell surface-display and metabolic engineering of *Schizosaccharomyces pombe*. *Microbial Cell Factories*, 17, 176.
30. Yang, Y.M., Chen, W.J., Yang, J., Zhou, Y.M., Hu, B., Zhang, M., Zhu, L.P., Wang, G.Y., and Yang, S. (2017) Production of 3-hydroxypropionic acid in engineered *Methylobacterium extorquens* AM1 and its reassimilation through a reductive route. *Microbial Cell Factories*, 16, 179.
31. Tomàs-Gamisans, M., Andrade, C.C.P., Maresca, F., Monforte, S., Ferrer, P., and Albiol, J. (2020) Redox engineering by ectopic overexpression of NADH kinase in recombinant *Pichia pastoris* (*Komagataella phaffii*): Impact on cell physiology and recombinant production of secreted proteins. *Applied and Environmental Microbiology*, 86, e02038-19.
32. Garcia-Ortega, X., Ferrer, P., Montesinos, J.L., and Valero, F. (2013) Fed-batch operational strategies for recombinant Fab production with *Pichia pastoris* using the constitutive GAP promoter. *Biochemical Engineering Journal*, 79, 172–181.
33. Schaefer, L., Auchtung, T.A., Hermans, K.E., Whitehead, D., Borhan, B., and Britton, R.A. (2010) The antimicrobial compound reuterin (3-hydroxypropionaldehyde) induces oxidative stress via interaction with thiol groups. *Microbiology*, 156 (6), 1589–1599.
34. Kildegaard, K.R., Hallström, B.M., Blicher, T.H., Sonnenschein, N., Jensen, N.B., Sherstyk, S., Harrison, S.J., Maury, J., Herrgård, M.J., Juncker, A.S., Forster, J., Nielsen, J., and Borodina, I. (2014) Evolution reveals a glutathione-dependent mechanism of 3-hydroxypropionic acid tolerance. *Metabolic Engineering*, 26, 57–66.
35. Nguyen-Vo, T.P., Ko, S., Ryu, H., Kim, J.R., Kim, D., and Park, S. (2020) Systems evaluation reveals novel transporter *YohJK* renders 3 - hydroxypropionate tolerance in *Escherichia coli*. *Scientific Reports*, 10, 1906.
36. Tredwell, G.D., Aw, R., Edwards-Jones, B., Leak, D.J., and Bundy, J.G. (2017) Rapid screening of cellular stress responses in recombinant *Pichia pastoris* strains using metabolite profiling. *Journal of Industrial Microbiology and Biotechnology*, 44 (3), 413–417.
37. Dragosits, M., Stadlmann, J., Graf, A., Gasser, B., Maurer, M., Sauer, M., Kreil, D.P., Altmann, F., and Mattanovich, D. (2010) The response to unfolded protein is involved in osmotolerance of *Pichia pastoris*. *BMC Genomics*, 11, 207.
38. Baumann, K., Carnicer, M., Dragosits, M., Graf, A.B., Stadlmann, J., Jouhten, P., Maaheimo, H., Gasser, B., Albiol, J., Mattanovich, D., and Ferrer, P. (2010) A multi-level study of recombinant *Pichia pastoris* in different oxygen conditions. *BMC Systems Biology*, 4, 141.
39. Melo, N.T.M., Pontes, G.C., Procópio, D.P., Cunha, G.C. de G., Eliodório, K.P., Paes, H.C., Basso, T.O., and Parachin, N.S. (2020) Evaluation of product distribution in chemostat and batch fermentation in lactic acid-producing *Komagataella phaffii* strains utilizing glycerol as substrate. *Microorganisms*, 8, 781.
40. de Fouchécour, F., Sánchez-Castañeda, A.K., Saulou-Bérion, C., and Spinnler, H.É.

(2018) Process engineering for microbial production of 3-hydroxypropionic acid. *Biotechnology Advances*, 36 (4), 1207–1222.

41. Lis, A. v., Schneider, K., Weber, J., Keasling, J.D., Jensen, M.K., and Klein, T. (2019) Exploring small-scale chemostats to scale up microbial processes: 3-hydroxypropionic acid production in *S. cerevisiae*. *Microbial Cell Factories*, 18, 50.
42. Sears, I.B., O'Connor, J., Rossanese, O.W., and Glick, B.S. (1998) A versatile set of vectors for constitutive and regulated gene expression in *Pichia pastoris*. *Yeast*, 14 (8), 783–790.
43. Maurer, M., Kühleitner, M., Gasser, B., and Mattanovich, D. (2006) Versatile modeling and optimization of fed batch processes for the production of secreted heterologous proteins with *Pichia pastoris. Microbial Cell Factories, 5, 37.*
44. Cos, O., Resina, D., Ferrer, P., Montesinos, J.L., and Valero, F. (2005) Heterologous production of *Rhizopus oryzae* lipase in *Pichia pastoris* using the alcohol oxidase and formaldehyde dehydrogenase promoters in batch and fed-batch cultures. *Biochemical Engineering Journal*, 26 (2–3), 86–94.

4

RESULTS II

Combining metabolic engineering and multiplexed screening methods for 3-hydroxypropionic acid production in *Pichia pastoris*

Chapter published as a research article in *Frontiers in Bioengineering and Biotechnology*:

Fina A., Heux, S., Albiol, J., and Ferrer, P. (2021). Combining metabolic engineering and multiplexed screening methods for 3-hydroxypropionic acid production in *Pichia pastoris*. *Frontiers in Bioengineering and Biotechnology,* 10, 942304. doi: 10.3389/fbioe.2022.942304

Table of contents

Abstract

Production of 3-hydroxypropionic acid (3-HP) in *Pichia pastoris* (*syn. Komagataella phaffii*) *via* the malonyl-CoA pathway has been recently demonstrated using glycerol as a carbon source, but the reported metrics were not commercially relevant. The flux through the heterologous pathway from malonyl-CoA to 3-HP was hypothesized as the main bottleneck. In the present study, different metabolic engineering approaches have been combined to improve the productivity of the original 3-HP producing strains. To do so, an additional copy of the gene encoding for the potential rate-limiting step of the pathway, i.e. the C-terminal domain of the malonyl-CoA reductase, was introduced. In addition, a variant of the endogenous acetyl-CoA carboxylase (*ACC1*^{S1132A}) was overexpressed with the aim to increase the delivery of malonyl-CoA. Furthermore, the genes encoding for the pyruvate decarboxylase, aldehyde dehydrogenase and acetyl-CoA synthase, respectively, were overexpressed to enhance conversion of pyruvate into cytosolic acetyl-CoA, and the main gene responsible for the production of the by-product D-arabitol was deleted. Three different screening conditions were used to classify the performance of the different strains: 24-deep-well plates batch cultures, small-scale cultures in falcon tubes using FeedBeads® (i.e., slow release of glycerol over time), and mini bioreactor batch cultures. The best two strains from the FeedBeads® screening, PpHP8 and PpHP18, were tested in bioreactor fed-batch cultures using a pre-fixed exponentially increasing feeding rate. The strain PpHP18 produced up to 37.05 g L^{-1} of 3-HP at 0.712 g L^{-1} h^{-1} with a final product yield on glycerol of 0.194 Cmol·Cmol^{-1} in fed-batch cultures. Remarkably, PpHP18 did not rank among the 2-top producer strains in small scale batch cultivations in deep-well plates and mini bioreactors, highlighting the importance of multiplexed screening conditions for adequate assessment of metabolic engineering strategies. These results represent a 50% increase in the product yield and final concentration, as well as over 30% increase in volumetric productivity compared to the previously obtained metrics for *P. pastoris*. Overall, the combination of glycerol as carbon source and a metabolically engineered *P. pastoris* strain resulted in the highest 3-HP concentration and productivity reported so far in yeast.

4.1. Introduction

Microbial production of platform chemicals is an increasingly attractive alternative to petrochemical-derived products. One such chemical, 3-hydroxypropionic acid (3-HP), is an organic acid that can be chemically converted to acrylic acid, 1,3-propanediol, and malonic acid, among others [1], offering a great potential for bioproduction of a wide range of polymers. In fact, 3-HP has been included in the list of the top platform chemicals that can be obtained from biomass (Werpy et al ., 2004).

3-HP can be naturally produced by several bacteria through different biosynthetic routes. Among them, the glycerol-dependant pathway, and the pathways via malonyl-CoA and β-alanine intermediates have been the most extensively investigated [2,3]. Multiple microorganisms have been engineered to produce 3-HP, including bacteria [4] and yeast [5]. The highest 3-HP concentrations and productivities achieved so far have been obtained in *Escherichia coli* (76.2 $g \cdot L^{-1}$ of 3-HP and 1.89 $g \cdot L^{-1} \cdot h^{-1}$, respectively [6]) and *Klebsiella pneumoniae* [7]. Both bacterial species were engineered to produce 3-HP through the glycerol-dependent pathway. This facilitated the use of glycerol as a carbon source and, ultimately, of crude glycerol, which is an abundant, inexpensive and renewable feedstock produced as a main by-product of the conventional biodiesel production process. Moreover, glycerol is very attractive for production of organic acids such as 3-HP due to its higher degree of reduction compared to glucose.

Production of 3-HP in yeast has been mainly pursued by introducing the malonyl-CoA or β-alanine pathways, e.g. reaching a titer of about 13.7 $g \cdot L^{-1}$ and with a 0.14 C-mol C-mol^{-1} yield on glucose in *Saccharomyces cerevisiae* fed-batch cultures [8]. The methylotrophic yeast *Pichia pastoris* (syn*. Komagataella phaffii*) is able to grow efficiently on glycerol. Furthermore, crude glycerol may contain from 1% to 25% w/w methanol [9], making this feedstock ideal for a methylotrophic microorganism such as *P. pastoris*. In addition, this yeast can grow at a pH as low as 3 [10,11], which allows performing the fermentation process at a pH below the pKa of 3-HP (4.51). This would enable the use of *in situ* product recovery systems, thereby avoiding 3-HP accumulation to toxic levels and facilitating 3-HP export from cells [12,13]. The 3-HP extraction yield using a membrane-assisted *in situ* product recovery system was increased from 5% to 74% when the pH of the medium was decreased from 5 to 3.2 [13].

In a recent study, we addressed the use of *P. pastoris* to produce 3-HP from glycerol [14]. This yeast was metabolically engineered to express the malonyl-CoA

reductase pathway, which consists of two consecutive steps reducing malonyl-CoA into 3-HP, while consuming two NADPH molecules (Figure 12). Specifically, we expressed the gene encoding for the bi-functional enzyme malonyl-CoA reductase (MCR) from *Chloroflexus aurantiacus.* This pathway provides the simplest way to produce 3-HP from glycerol in *P. pastoris*, as the glycerol-dependant pathway is coenzyme B12-dependant. Since *P. pastoris* does not naturally produce coenzyme B-12, the introduction of the glycerol-dependant pathway for 3-HP biosynthesis pathway in this cell factory would require either the addition of such expensive cofactor to the fermentation medium or the co-expression of the multistep B-12 biosynthetic pathway [15].

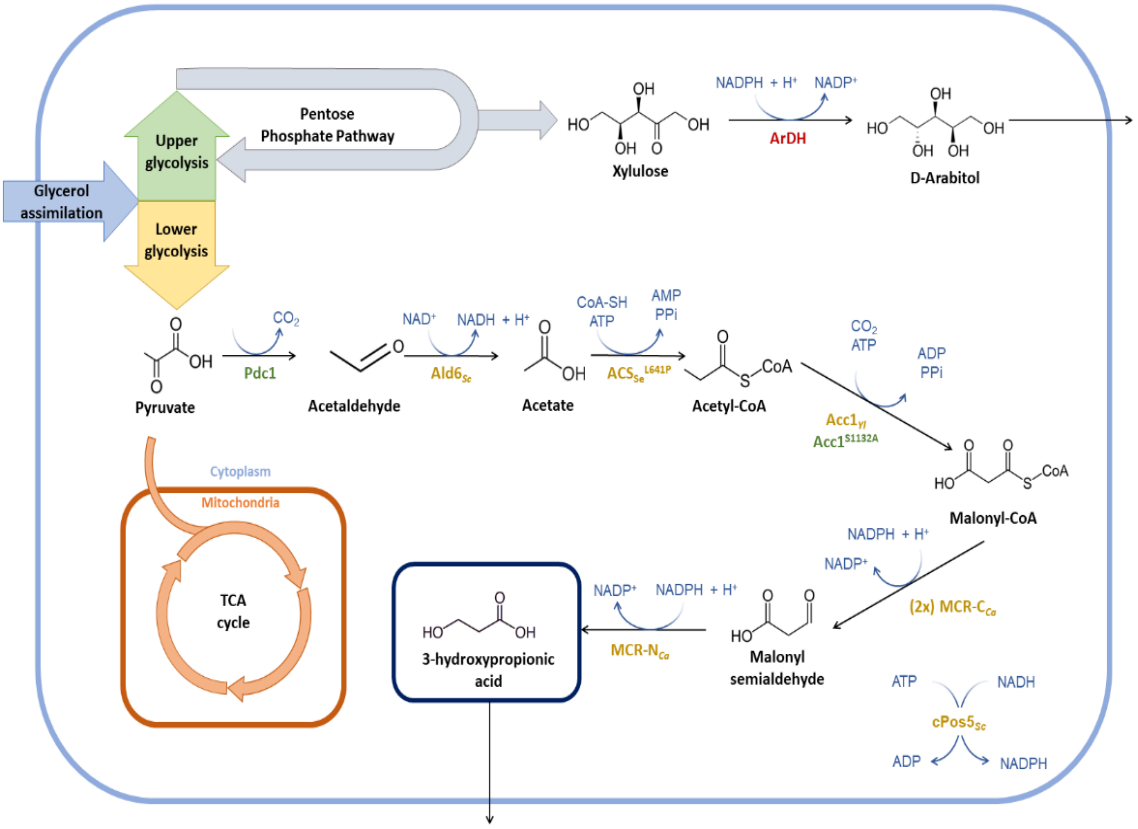

Figure 12. Summary of metabolic engineering strategies for the optimisation of 3-HP production in *P. pastoris*. Strain engineering started from the 3-HP producing strain PpHP6 containing the malonyl-CoA to 3-HP pathway[14]. Heterologous enzymes are depicted in yellow, endogenous enzymes being overexpressed are shown in green, and the enzymes catalysing the reactions of genes being deleted are shown in red. The (2x) indicates that a second copy of the MCR-C_{Ca} gene was introduced. Enzyme abbreviations: Pdc1, pyruvate decarboxylase; $Ald6_{Sc}$, aldehyde dehydrogenase from *S. cerevisiae*; ACS_{Se}^{L641P}, acetyl-CoA synthase from *S. enterica* with the mutation L641P; $Acc1_{Yl}$, acetyl-CoA carboxylase from *Y. lipolytica*; $Acc1^{S1132A}$, acetyl-CoA carboxylase from *P. pastoris* with the mutation S1132A; MCR-C_{Ca}, C-terminal domain of the malonyl-CoA reductase from *C. aurantiacus*; MCR-N_{Ca}, N-terminal domain of the malonyl-CoA reductase from *C. aurantiacus*; $cPos5_{Sc}$, NADH kinase from *S. cerevisiae* relocated into the cytoplasm; ArDH, D-arabitol dehydrogenase.

In addition, several improvements were made to the original strain. First, the independent expression of the two MCR subunits was implemented, leading to a 12.5-fold increase in 3-HP production. Second, the resulting strain was further engineered to increase the availability of NADPH and malonyl-CoA, which are the two substrates of this route. To this end, the acetyl-CoA carboxylase gene from *Yarrowia lipolytica* (*ACC1*$_{Yl}$) and a NADH kinase from *Saccharomyces cerevisiae* (*cPOS5*$_{Sc}$) were expressed in the cytosol. However, this strategy resulted in rather modest improvements in terms of product yield, pointing to the delivery of malonyl-CoA as a major bottleneck to further improve 3-HP production. Notably, this strain produced up to 24.75 g L^{-1} of 3-HP in 45.5 h in a fed-batch culture using glycerol as a carbon source, which is, to our knowledge, the highest productivity reported so far in yeast (0.54 g L^{-1} h^{-1}) [14].

Despite providing the first demonstration of the potential of *P. pastoris* for 3-HP production from glycerol, 3-HP production metrics from our previous study are still far from being industrially-relevant, as a minimum productivity of 2.5 g L^{-1} h^{-1}, 50~100 g·L^{-1} and >0.5 g/g yield are generally required to achieve an economically feasible bioprocess for carboxylic acid production [16,17].

Here, further metabolic engineering of the previously developed 3-HP-producing strains [14] was performed to increase the production metrics. In particular, we aimed at improving both the biosynthetic pathway for 3-HP from its metabolic precursor (acetyl-CoA), as well as improving the metabolic flux towards acetyl-CoA synthesis and reducing by-product (arabitol) formation. Notably, we used three different small-scale cultivation systems for better characterisation of the impact of genetic modifications on cell growth and product yields and subsequent transfer to bioreactor-scale cultivations.

4.2. Materials and Methods

4.2.1. Molecular biology and strains

All the strains used in this study are listed in Table 4. A detailed description of the molecular biology workflow to generate each strain can be found in the Supplementary Materials of this chapter (Annex II; Section 2). The modular cloning vectors GoldenPics ([18]; Addgene Kit #1000000133) and the vectors for CRISPR-Cas9 of the CrisPi kit [19]; Addgene Kit #1000000136) were used.

For the new strains generated by CRISPR-Cas9, the integration cassette was amplified from *P. pastoris* genome using a high-fidelity Q5 polymerase (New England Biolabs, MA, USA) and the recommended protocol [19]. The integration loci are also indicated in the Supplementary Materials of this chapter (Annex II; Section 2). The integrity of the inserted cassette was verified by Sanger sequencing at the Genomics and Bioinformatics Service of the Universitat Autònoma de Barcelona.

The strains generated using the GoldenPics plasmids were generated by integration of the heterologous DNA at the loci described in the Supplementary Materials of this chapter (Annex II; Section 2).

Table 4. Strain list.

Strain name	Parental strain	Additional expression cassettes or deleted genes compared to parental strain	Source
X-33			Invitrogen-Thermo Fisher Scientific (MA, USA)
PpHP2	X-33	pGAP_*mcr-N*$_{Ca}$_AOX1tt pGAP_*mcr-C*$_{Ca}$_AOX1tt	[14]
PpHP6	PpHP2	pGAP_*ACC1*$_{Yl}$_ScCYC1tt pGAP_*cPOS5*$_{Sc}$_RPS3tt	[14]
PpHP7	PpHP2	pGAP_ *mcr-C*$_{Ca}$_TDH3tt	This study
PpHP9	PpHP7	pGAP_ACC1^{S1132A}_AOX1tt	This study Plasmid source [20]; Addgene #126740
PpHP11	PpHP7	pTEF1_*acs*$_{Se}^{L641P}$_RPS3tt	This study
PpHP12	PpHP7	pTEF1_*acs*$_{Se}^{L641P}$_RPS3tt pMDH3_*ALD6*$_{Sc}$_TDH3tt	This study
PpHP8	PpHP6	pGAPeN_ *mcr-C*$_{Ca}$_TDH3tt	This study
PpHP13	PpHP8	pTEF1_*acs*$_{Se}^{L641P}$_RPS3tt	This study
PpHP14	PpHP8	pTEF1_*acs*$_{Se}^{L641P}$_RPS3tt pMDH3_*ALD6*$_{Sc}$_TDH3tt	This study
PpHP15	PpHP8	Δ*ArDH*	This study
PpHP16	PpHP8	Δ*ArDH* pPDC1_*PDC1*_PDC1tt	This study
PpHP17	PpHP13	Δ*ArDH*	This study
PpHP18	PpHP13	Δ*ArDH* pPDC1_*PDC1*_PDC1tt	This study

4.2.2. Copy Number Determination by droplet digital PCR (ddPCR)

The number of copies of the gene *mcr-C$_{Ca}$* of the highest producing clones of the strains PpHP7 and PpHP8 was tested with droplet digital PCR (ddPCR) following a previously reported method [21], except that the QX200™ ddPCR™ EvaGreen Supermix (Biorad, CA, USA) was used instead of Taqman probes. First, the genomic DNA of the highest producing clones was purified using the Wizard® Genomic DNA Purification Kit from Promega (WI, USA). Afterwards, 0.5 µg of genomic DNA were restricted using the restriction enzymes BamHI-FD and EcoRI-FD from Thermo Fisher Scientific (MA, USA). Subsequently, the genomic DNA was diluted to a concentration of 1 ng µL^{-1}.

Second, a master mix of 22.5 µL was prepared with the forward primer at 0.4 µM, the reverse primer at 0.2 µM, and the restricted genomic DNA at 0.08 ng µL^{-1}. Afterwards, the master mix was mixed with 22.5 µL of EvaGreen 2X master solution and was thoroughly mixed by vortexing. Following droplet generation using a Droplet generator (Biorad, CA, USA), the droplets were transferred to a 96-tubes rack and subsequently sealed with a PCR Plate Heat Seal. The PCR was carried using a C1000 Touch Thermal Cycler (Biorad, CA, USA). The annealing temperature was set to 60ºC. Finally, the ddPCR results were analysed using a QX200 Droplet Digital PCR system (Biorad, CA, USA).

The primers used for ddPCR are listed in Table 5. The primer pairs ddPCR_mcrCCa_FW and ddPCR_mcrCCa_RV were used to amplify the *mcr-C$_{Ca}$* gene. Primers ddPCR_act_FW and ddPCR_act_RV were used to amplify the β-actin (*ACT1)* endogenous gene, which was used as reference of a single-copy gene.

Table 5. Oligonucleotides used for gene copy number determination analysis with ddPCR.

Primer name	Primer sequence
ddPCR_mcrCCa_FW	CCTAACGATGTTGCTGCTTTGGAG
ddPCR_mcrCCa_RV	GGATCAGGTGGATTAGGCAAGTTAGC
ddPCR_act_FW	TCCGGTGGTACTACTATGTTCC
ddPCR_act_RV	GATAGAACCACCGATCCATACG

4.2.3. 24-Deep-well plates screening

P. pastoris strains were inoculated into 50 mL falcon tubes containing 5 mL of YPG (1% yeast extract, 2% peptone and 1% v/v glycerol) supplemented with 100 µg mL^{-1} zeocin (InvivoGen, CA, USA). The cells were grown overnight at 30ºC and 200 rpm in an incubator shaker Multitron Standard (Infors HT, Bottmingen, Switzerland) with a 2.5 cm orbit. 50 µL of overnight-grown cultures were used to inoculate each well of a 24 deep-well plate containing 2 mL of Buffered Minimal Glycerol (BMG) medium, containing 100 mM potassium phosphate buffer pH 6, 1.34% yeast nitrogen base (YNB), 1% v/v glycerol, and 0.4 mg L^{-1} biotin. The cultures were incubated at 28ºC and 220 rpm in the same incubator shaker using a platform with a slope of 20° to improve the aeration. The cultures were grown for 48 h to ensure the full consumption of the substrate. Thereafter, culture samples were centrifuged at 12,000 g for 5 min and filtered through a 0.20 µm pore size syringe filter (SLLGX13NK, Merck Millipore, CA, USA). The 3-HP was quantified using HPLC.

The parental clones PpHP2 and PpHP6 were screened in triplicates. Six to eight clones were screened in triplicates for the strains generated by single-homology integration (PpHP7, PpHP8, and PpHP9). One single clone was screened in triplicates for the strains generated using CRISPR-Cas9.

4.2.4. Small-scale screening in falcon tubes using FeedBeads®

The inoculum was prepared following the same protocol described for the deep-well plates screenings. Afterwards, 50-mL falcon tubes were filled with 5 mL of Buffer Minimal medium (BM; 100 mM potassium phosphate buffer pH 6, 1.34% YNB and 0.4 mg L^{-1} biotin), supplemented with one Glycerol FeedBeads® (SMFB12001, Kuhner Shaker GmbH, Germany). Each FeedBead® releases 40 mg of glycerol in 48 h. The cultures were inoculated with 50 µL of the overnight saturated cultures. The falcon tubes were incubated in an incubator shaker at 200 rpm and 30ºC for 48 h. Each clone was tested in triplicate. A triplicate control was performed by adding one FeedBead® to a falcon with 5 mL of BM medium. These controls were used to determine the actual release of glycerol under the tested conditions.

Culture samples were centrifuged at 12,000 g for 5 min and filtered through a 0.20 µm pore size syringe filter (SLLGX13NK, Merck Millipore). The 3-HP was quantified using HPLC as described below.

4.2.5. Mini bioreactors screening

The automated cultivation and sampling platform described elsewhere was used [22].

The bioreactor medium contained 2.5 g L^{-1} glycerol, 1.8 g L^{-1} citric acid, 0.02 g L^{-1} $CaCl_2 \cdot 2\ H_2O$, 12.6 g L^{-1} $(NH_4)_2HPO_4$, 0.5 g L^{-1} $MgSO_4 \cdot 7\ H_2O$, 0.9 g L^{-1} KCl, 50 µL antifoam Glanapon 2000 kz (Bussetti and Co GmbH, Vienna, Austria), 0.4 mg L^{-1} biotin and 4.6 ml L^{-1} of PTM1 trace salts [23]. The pH was set to 5 using 1 M HCl. The medium was autoclaved without the trace salts and the biotin, which were filter sterilized and added to the medium under sterile conditions. Each mini bioreactor was filled with 15 mL of medium. The pre-inoculum was prepared as described for the other two screening methods (deep-well plates and falcon tubes with FeedBeads®). The overnight-saturated cultures were used to inoculate 250 mL shake flasks with 25 mL of YPG at a starting OD_{600} of 0.5-1.5. The cells were grown for 8 h at 28ºC and 160 rpm in a shaker incubator to ensure the cells were at the exponential phase. Each bioreactor was inoculated at a starting OD_{600} of 0.025. Each strain was tested in triplicate.

The temperature of the bioreactors was set to 28ºC. The dissolved oxygen (DO) and the pH were monitored throughout the cell culture. Samples were automatically withdrawn from the bioreactors every 2 h for the first 16 h of culture to monitor the OD_{600}. After 16 h, samples were withdrawn hourly during 8 h for both OD_{600} monitoring and supernatant analysis. The 250 µL samples for culture supernatant analysis were automatically placed on 96-well plates with a 0.45 µm pore size filter bottom. The samples were filtered by applying vacuum. Glycerol, 3-HP, and D-arabitol were quantified using NMR as described below.

The growth rate (μ_{max}), the specific substrate consumption rate (qS_{Glyc}), and the specific 3-HP and D-arabitol production rates (qP_{3HP} and qP_{Abt}) were calculated during the exponential growth phase using the R program PhysioFit [24].

4.2.6. Fed-batch cultures in bioreactors

The cultures were carried out using a DASGIP Parallel Bioreactor System (Eppendorf, Germany). The starting volume of each 1.3 L reactor vessel was 400 mL. The Batch Medium described for the mini bioreactors with 40 g L^{-1} of glycerol was used. All the medium components except the biotin and the trace salts were mixed, placed into

the reactor, and autoclaved. Biotin and trace salts were added through the septum port after autoclaving the reactor. The pH was controlled at 5 using 15% ammonia (only base addition was used). Aeration was set to 1 vvm (0.4 $L \cdot min^{-1}$). The DO was set to 30%, and it was automatically controlled using the following cascade: i) Increasing the stirring rate from 400 to 1200 rpm; ii) Compressed air was mixed with pure oxygen to increase the percentage of oxygen of the inlet gas. The reactors were inoculated at a starting OD_{600} of 1. The inocula were prepared as described elsewhere [25].

The feeding medium composition was 400 g L^{-1} glycerol, 10 g L^{-1} KCl, 6.45 g L^{-1} $MgSO_4 \cdot 7\ H_2O$, 0.35 g L^{-1} $CaCl_2 \cdot 2\ H_2O$, 0.2 ml L^{-1} antifoam Glanapon 2000 kz, 1.2 mg L^{-1} biotin and 15 ml L^{-1} PTM1 trace salts. All the feeding medium components except the biotin and the trace salts were mixed and autoclaved. Biotin and trace salts were filter-sterilized and added to the feeding medium under sterile conditions. Feeding medium was added to the bioreactor using the exponentially increasing feed-rate described by Equation 1, where F(t) is the feeding rate at every time, t_0 is the time where the feeding starts (end of the batch phase), $X(t_0)$ is the biomass concentration at the end of the batch phase, $V(t_0)$ is the starting volume of the reactor (the volume for the batch phase), $Y_{X/S}$ is the biomass to substrate yield, and S_0 is the concentration of substrate in the feeding medium. Equation 1 was simplified by assuming $Y_{X/S}$ would not vary significantly between the batch and the fed-batch phase (Equation 2). In Equation 2, S_{batch} is the concentration of substrate for the batch medium (40 g L^{-1}).

$$F(t) = \frac{\mu[X(t_0)V(t_0)]}{Y_{X/S}S_0} e^{[\mu(t-t_0)]} \qquad \text{(Equation 1)}$$

$$X(t_0) = Y_{X/S}S_{batch} \qquad \text{(Equation 2)}$$

Therefore, the flow rate of the feeding medium was set using Equation 3.

$$F(t) = \frac{\mu S_{batch}V(t_0)}{S_0} e^{[\mu(t-t_0)]} \qquad \text{(Equation 3)}$$

The feeding started once the DO increased above 60%, indicating that all the substrate of the batch phase had been consumed. Samples were collected for biomass cell dry weight (CDW) determination and supernatant analysis. The CDW was quantified in triplicates. From 0.5 to 2 mL of culture were filtered through pre-weighted glass microfiber filters (APFF04700, Merck Millipore). The filters were then washed with 10 mL of distilled water with 9 g L^{-1} NaCl and dried overnight at 105ºC. The filters containing the dry biomass were weighted to calculate the CDW.

Culture samples were centrifuged 5 min at 12,000 g and the supernatant was filtered with a 0.2 µm pore size syringe filter (SLLGX13NK, Merck Millipore). The filtered supernatant was analysed with HPLC for glycerol, 3-HP, and D-arabitol quantification.

4.2.7. HPLC analysis

HPLC was used to quantify the glycerol, the D-arabitol, and the 3-HP from the supernatant of the deep-well plates, the FeedBeads® screening, and the fed-batch bioreactor samples. A previously described HPLC protocol was used [14]. The 3-HP was quantified from the UV spectrum. Glycerol and D-arabitol were quantified from the Refractive Index (RI) spectrum. As 3-HP and glycerol have the same retention time and 3-HP is also detected on the RI detector, the area corresponding to the 3-HP (previously quantified from the UV signal) was subtracted to latter calculate the actual glycerol concentration.

4.2.8. NMR analysis

Glycerol, D-arabitol, and 3-HP were quantified from the culture supernatants of the mini bioreactor cultures using 1D-1H Nuclear Magnetic Resonance (NMR) on a Bruker Advance III 800MHz spectrometer (Bruker BioSpin, Germany). Prior to the analyses, 180 µL of filtered culture supernatant samples were mixed with 20 µL of 10 mM TSP (3-(trimethylsilyl)-[2,2,3,3-$^{2}H_4$]-propionic acid sodium salt), which was used as an internal standard. The NMR spectrometer was coupled to a 5 mm CQPI cryoprobe, which was set to 280 K. A 30º presaturation pulse was recorded, followed by a relaxation delay of 7 s. The software TopSpin 3.6.4 (Bruker BioSpin, Germany) was used for the integration of the peaks.

4.3. Results and Discussion

4.3.1. Increasing *mcr*-C_{Ca} copy number leads to higher 3-HP production

Previous results showed that the co-overexpression of *ACC1* and *cPOS5* in the initial 3-HP-producing strain PpHP2 (Table 4) led to a small but significant increase in the 3-HP yield on glycerol in strain PpHP6 (from 0.131 Cmol Cmol^{-1} to 0.146 Cmol Cmol^{-1}) [14]. However, the overexpression of either *ACC* or *cPOS5* did not result into any further significant impact on 3-HP production, highlighting the

malonyl-CoA reductase step as a major bottleneck for 3-HP production, rather than the supply of malonyl-CoA and NADPH availability.

Thereby, a second copy of the C-terminal domain of the malonyl-CoA reductase gene (*mcr-C_{Ca}*) under the control of the strong and constitutive GAP promoter was added to the PpHP2 and PpHP6 strains, generating strains PpHP7 and PpHP8, respectively. For each strain, six independently isolated clones were tested in triplicate using deep-well plates and BMG medium. The highest producer clone for strains PpHP7 and PpHP8 produced 1.81 ± 0.02 g L^{-1} and 2.29 ± 0.01 g L^{-1} of 3-HP (i.e., 0.143 ± 0.001 and 0.180 ± 0.001 Cmol $Cmol^{-1}$ yield on glycerol, respectively). The gene copy analysis showed that both clones contained 2 copies of *mcr-C_{Ca}*. The 3-HP yield achieved by the strains PpHP2 and PpHP6 was 0.130 ± 0.005 and 0.146 ± 0.004 Cmol $Cmol^{-1}$, respectively. Therefore, the addition of a second copy of *mcr-C_{Ca}* to PpHP2 and PpHP6 led to a 1.38 and 1.23-fold improvement, respectively (*P-values* of 0.01 and 0.0001), as shown in Figure 13.

These results are consistent with previous studies with other yeasts such as *S. cerevisiae* or *Schyzosaccharomyces pombe*. The use of a multicopy integrative vector containing the *mcr_{Ca}* and the *ACC1* gene from *S. cerevisiae* led to a 3-fold increase in 3-HP production in *S. cerevisiae* [26]. In *S. pombe,* the addition of a second copy of *mcr-C_{Ca}* led to an almost 3-fold improvement in the 3-HP yield. Addition of a third copy of *mcr-C_{Ca}* led to a further 2-fold improvement in 3-HP production, while the addition of a fourth copy of the same gene, or the addition of a second copy *mcr-N_{Ca}* did not have an impact on the final 3-HP titre [27].

Nevertheless, the increase in 3-HP production achieved in *P. pastoris* when additional copies of the *mcr-C_{Ca}* gene were introduced was significantly lower than the one achieved in other yeasts. Notably, the MCR specific activity of cell extracts of *P. pastoris* expressing *mcr_{Ca}* under the control of pGAP was more than one order of magnitude higher than the same gene expressed under the control of pTEF1 in *S. cerevisiae* [14,28]. Additional bottleneck(s) upstream of the malonyl-CoA reductase reaction steps are probably limiting the 3-HP production, so no further copies of *mcr-C_{Ca}* were introduced.

4.3.2. Expression of the de-regulated *ACC1*^{S1132A} mutant does not improve 3-HP production

The acetyl-CoA carboxylase (Acc) catalyses the conversion of acetyl-CoA into malonyl-CoA. The enzyme Acc1^{S1132A} from *P. pastoris* contains a site mutation (S1132A) that prevents the post-translational inactivation of the enzyme by phosphorylation when glucose is depleted [29]. Expression of this endogenous *ACC1* variant under the control of the GAP promoter showed a positive impact on the production of acetyl-CoA derived drugs in *P. pastoris* [20]. The same approach was used in PpHP7, but the new strain (PpHP9) produced less 3-HP than the parental strain (0.138 ± 0.001 Cmol Cmol^{-1}, Figure 13).

Acc1 is organized as a homodimer. The phosphorylation of one of the two monomers inactivates the enzymatic complex [30]. Therefore, it is plausible that the co-existence of the heterologous mutated version of Acc1 and the endogenous non-mutated versions leads to the formation of inactive heterodimers, hindering the effect of Acc1^{S1132A} overexpression. This hypothesis is supported by previous studies showing that replacement of the endogenous *ACC1* sequence with *ACC1*^{S1132A} was required to ensure that Acc1 activity would only be controlled by Acc1^{S1132A} expression levels [31]. Deletion of the endogenous *ACC1* gene in strains PpHP9 may thus had a positive effect on 3-HP production. Moreover, it is well reported that Acc1 is a highly regulated enzyme [30,32]. In addition to its post-translational regulation, this enzyme is also regulated by allosteric inhibition [33,34]. Differences in the kinetic parameters between the two Acc1 variants might also explain the differences in the final 3-HP yield.

In contrast, the overexpression of *ACC1* from *Y. lipolytica* in *P. pastoris* led to a small increase in 3-HP production [14]. The yield in PpHP8 (harboring Acc1$_{Yl}$) was around 1.25-fold higher than in PpHP7. These results are consistent with recent studies where the heterologous expression of *ACC1* from *Y. lipolytica* yielded a higher accumulation of malonyl-CoA than the overexpression of the endogenous *S. cerevisiae ACC1* [35].

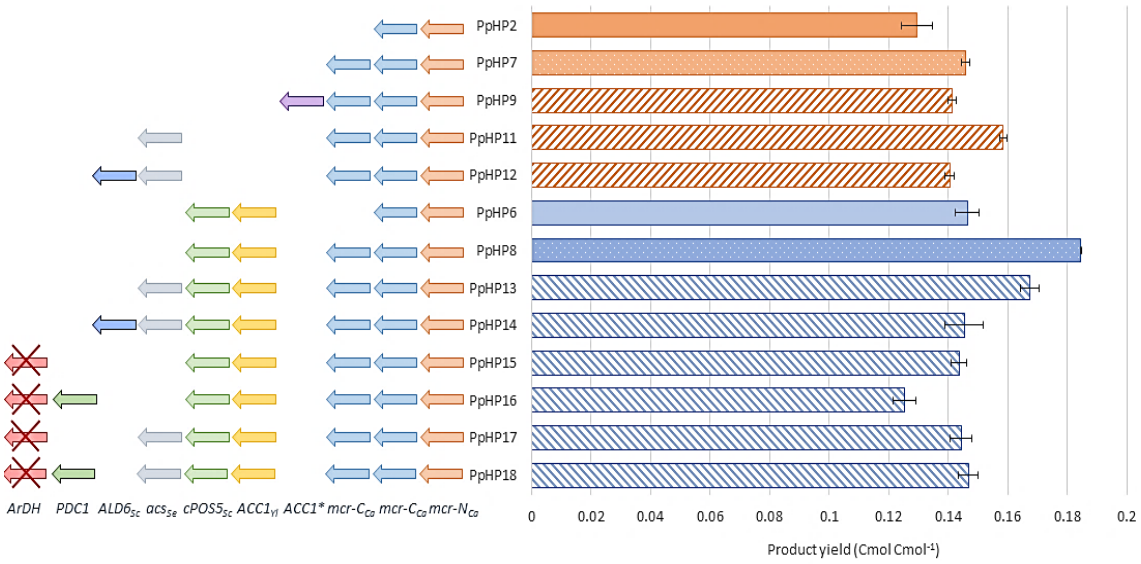

Figure 13. 3-HP production yield of the recombinant *P. pastoris* strains tested in deep-well plates. The genetic modifications performed to each strain are shown at the left side of the graph. The product yield in Cmol Cmol^{-1} is shown at the right side of the graph.

4.3.3. Metabolic engineering for increased acetyl-CoA supply and minimization of by-product formation

The endogenous cytosolic acetyl-CoA biosynthesis pathway was overexpressed to pull the conversion of pyruvate into acetyl-CoA. To this end, a modified Acetyl-CoA synthase from *Salmonella enterica* was used (acs_{Se}^{L641P}). The gene harbours a mutation (L641P) to suppress the post-translational inhibition of the enzyme by acetylation [36]. Expression of acs_{Se}^{L641P} was tested with or without the co-expression of the aldehyde dehydrogenase gene *ALD6* from *S. cerevisiae*. The two genes were expressed under the control of the TEF1 and MDH3 promoters, respectively, which are two mid-to-high expression constitutive promoters [18]. Use of pGAP was dismissed to avoid the dilution of the expression of the other genes, as there are already 5 heterologous genes under the control of pGAP [37,38].

Expression of acs_{Se} in strains PpHP7 and PpHP8, generating strains PpHP11 and PpHP13, led to opposite effects. While PpHP11 produced significantly more 3-HP (0.153 ± 0.002 Cmol Cmol^{-1} yield) than PpHP7 (*P-value* of 0.0003), its expression in PpHP13 led to a reduction of the yield (*P-value* 0.0006), as shown in Figure 13.

The expression of the aldehyde dehydrogenase *ALD6* in both PpHP11 and PpHP13 (PpHP12 and PpHP14, respectively) led to a decrease in the 3-HP yield for both

strains (Figure 13). Interestingly, the deletion of *ALD6* in *S. cerevisiae* led to a reduced susceptibility to 3-HP, as Ald6 might catalyse the conversion of 3-HP into the toxic compound 3-hydroxypropanaldehyde (3-HPA) [39]. Thus, it is plausible that *ALD6* overexpression in 3-HP producing *P. pastoris* strains leads to an increased accumulation of 3-HPA.

Finally, the overexpression of endogenous pyruvate decarboxylase (*PDC1*) was tested. To this end, an additional copy of *PDC1* under the control of its endogenous promoter was added to the genomes of the strains PpHP8 and PpHP13. Addition of a second copy of *PDC1* was coupled to the deletion of the *ArDH* gene, which is reported as the main responsible of the D-arabitol production in *P. pastoris* [40]. To distinguish the effect of the deletion of *ArDH* from the overexpression of *PDC1*, strains PpHP15 and PpHP17 were generated by deleting *ArDH* from strains PpHP8 and PpHP13, respectively (without an additional copy of *PDC1*). The strains PpHP16 and PpHP18 were also obtained from PpHP8 and PpHP13, and they harbour both the deletion of *ArDH* and a second copy of the endogenous *PDC1*. None of the new strains produced more 3-HP than their parental strains (Figure 13).

4.3.4. Screening under substrate-limiting conditions yields different ranking of strains compared to conventional substrate-excess screening strategies

Previous results obtained in deep-well plates showed that the overexpression of the cytosolic acetyl-CoA production pathway did not result in a significant increase in the final 3-HP production. Moreover, accumulation of D-arabitol was not observed in none of the strains, as was the case for PpHP6 strain in fed-batch cultivations [14]. Thus, the effect of *ArDH* deletion could not be properly assessed at small scale. Therefore, a representative subset of the strains constructed in this study were further cultured in two additional systems: i) Mini bioreactors, favouring fully aerobic conditions and easy withdrawal of multiple samples. ii) Falcon tubes containing FeedBeads®, which release glycerol at a low and constant rate (40 mg in 48 h), thereby permitting cell growth at a low rate, i.e. under substrate-limiting conditions resembling a fed-batch process.

The mini bioreactors were sampled during the exponential phase, which allowed to accurately determine the μ_{max} and the q-rates of the consumption of glycerol and the production of 3-HP and D-arabitol of the different strains, whereas endpoint samples (at 48 h) were taken from cultivations in falcon tubes containing FeedBeads®.

Notably, comparison of the results from these alternative screening conditions with the deep-well plate cultivations (Figure 14) reveals that the ranking of the strains based on their product yield varies depending on the screening condition. PpHP8 exhibited the highest product yield for the three screening conditions. However, the combined effect of ACS and Pdc1 overexpression and *ArDH* deletion (strain PpHP18) was clearly growth condition dependent. Indeed, the 3-HP production of the two strains, PpHP8 and PpHP18, was very similar at a low growth rate (i.e. using FeedBeads®), but differed significantly at μ_{max} (i.e., in the mini bioreactor experiment). Interestingly, 3-HP yields were generally higher in deep-well plates and falcon tubes, where oxygen transfer is usually considered as rate-limiting during cultivation, than in fully aerobic mini bioreactor cultures. This is consistent with the fact that the pGAP promoter is upregulated in *P. pastoris* cells growing on glucose under hypoxic conditions [41].

Moreover, strains PpHP13, PpHP15, PpHP17, and PpHP18 showed a much lower 3-HP product yield than PpHP8 when the cells were grown in mini bioreactors. Conversely, the μ_{max} of strain PpHP8 was the lowest of this subset of stains. An inverse correlation between μ_{max} and 3-HP product yield was observed. Despite lower growth rates would be generally expected for the strains with a larger number of heterologously overexpressed genes, overexpression of ACS and Pdc1 and the deletion of *ArDH* led to a higher μ_{max}. Acc1 overexpression has been reported to cause growth impairment in yeast [26,42]. This reduction in the growth rate was attributed to a metabolic burden. The fact the cell growth improves when the cytosolic acetyl-CoA pathway is overexpressed suggests that the lower growth rate of PpHP8 might be caused by a limitation in acetyl-CoA supply for the biosynthetic reactions. Such hypothesis is supported by the fact that the product yield of strains PpHP8 and PpHP18 are almost identical when the cells are grown at a low growth rate (i.e. using FeedBeads®). This is also reinforced by the differential D-arabitol production of strains PpHP8 and PpHP13. The presence of arabitol denotes a redox imbalance (Fina et al., 2021). When the delivery of acetyl-CoA is improved by overexpressing ACS (PpHP13), the D-arabitol production decreases.

Notably, the mini bioreactors data reveals that the deletion of *ArDH* from strain PpHP8 (strain PpHP15) resulted in a decrease in the D-arabitol yield and an improvement of the μ_{max}. Production of D-arabitol from glycerol results in net ATP consumption. Thus, the reduction in the D-arabitol production leads to higher energetic yield from the substrate, as well as a better carbon conservation (as less by-product D-arabitol is produced), thereby potentially increasing acetyl-CoA supply and supporting

higher growth rates. However, this might result in reduced Acetyl-CoA availability for 3-HP production.

Altogether, the observed results indicate the supply of cytosolic acetyl-CoA as a major limiting factor to further increase the 3-HP yield.

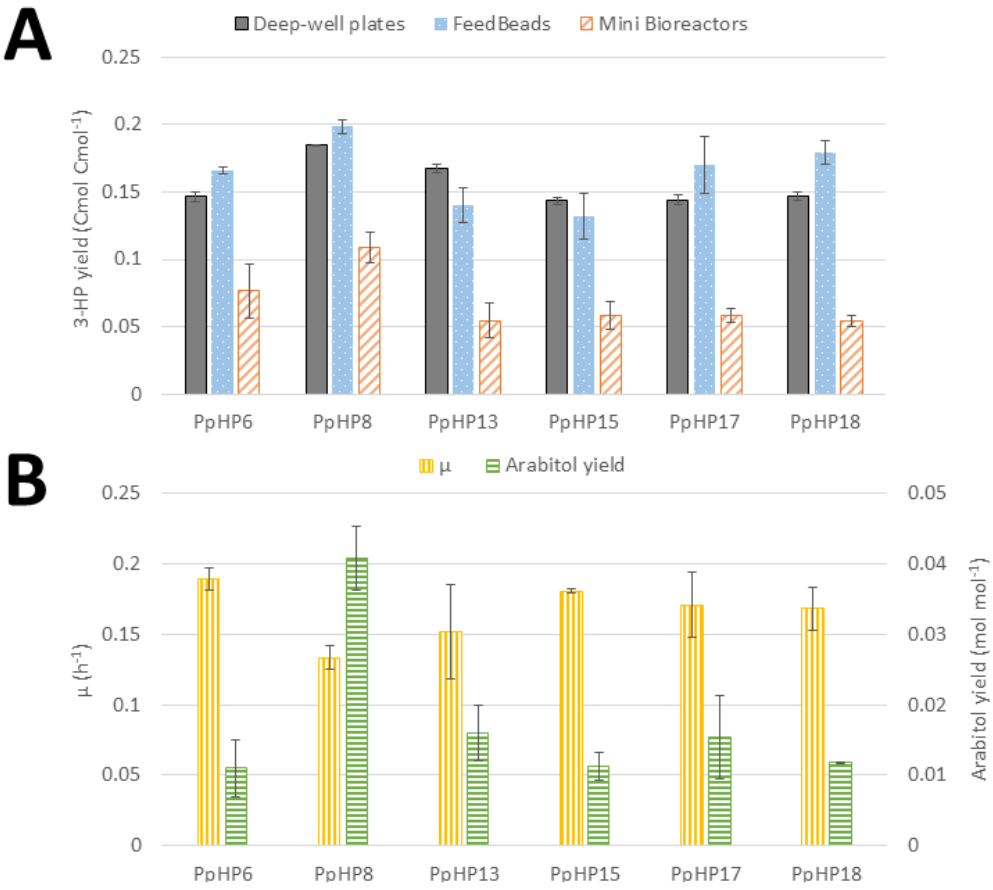

Figure 14. Comparison of the most relevant 3-HP producing *P. pastoris* strains under three different screening conditions. **(A)** 3-HP production yield in deep-well plates (grey solid bars), FeedBeads® (blue dotted bars), and mini bioreactors (orange striped bars). **(B)** Growth rate (yellow vertically striped bars) and arabitol production yield (green horizontally striped bars) for each strain grown in mini bioreactors.

4.3.5. Fed-batch cultures

The use of FeedBeads® mimics the conditions at a fed-batch culture, where cells grow under substrate-limiting conditions, i.e., at growth rates below the μ_{max}. The strains PpHP8 and PpHP18, which showed the highest 3-HP yields in FeedBeads® cultures, were thus further tested in a fed-batch bioreactor culture using a pre-programmed exponential glycerol feeding strategy to maintain the growth rate at 0.075 h^{-1}, which is approximately half the value of the μ_{max} of the two strains (0.133 h^{-1} and 0.165 h^{-1}, respectively). The feeding phase finished when the equivalent to 195 g L^{-1} of glycerol

were added to the reactor, to compare the results with our previous experiments where the same overall amount of substrate was used [14]. Thereafter, the cultivation was finalised when the DO signal increased, indicating the depletion of any residual glycerol that might have been accumulated during the late phase of the fed-batch culture. The cultivation profiles for both strains are shown in Figure 15.

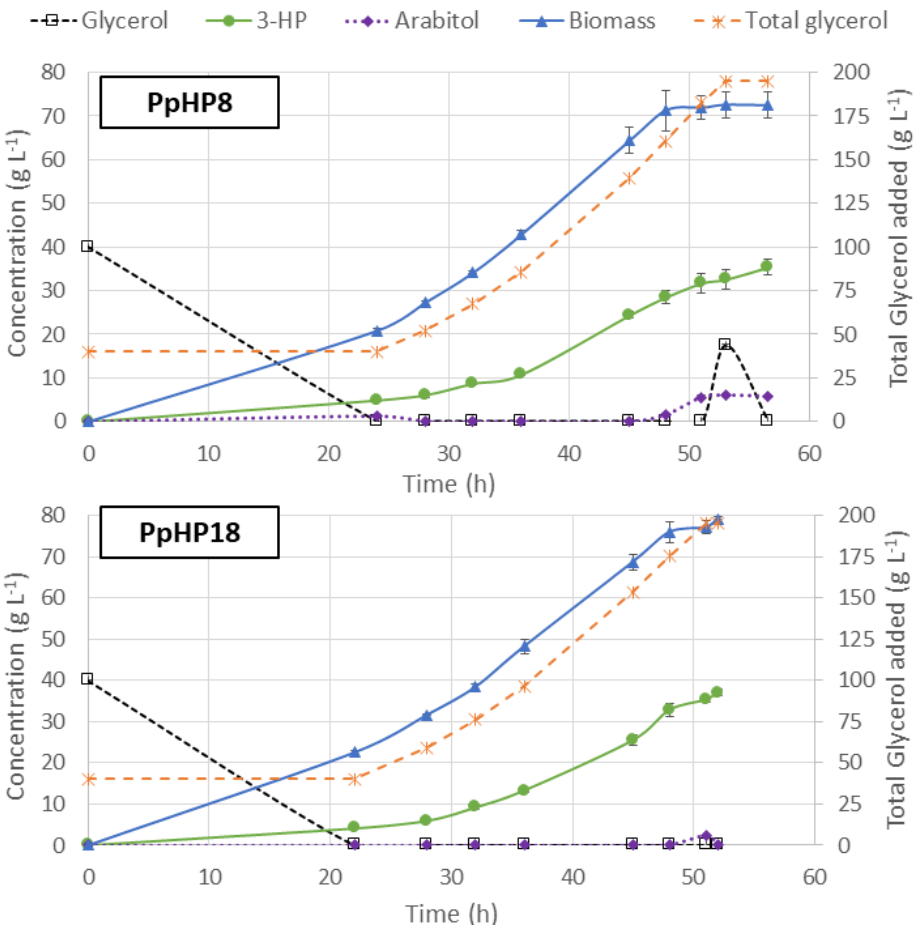

Figure 15. Profiles of fed-batch cultivations of the PpHP8 (top) and PpHP18 (bottom) strains. Concentration of glycerol, biomass, 3-HP, and D-arabitol are represented using the left-side y-axis. The total amount of glycerol added to the reactor, normalized by the actual volume of the reactor at every time is represented using the y-axis at the right side. The average result of two independent cultivations is shown. The error bars correspond to the standard deviation for the duplicate.

At the end of the batch phase, PpHP8 produced 4.92 ± 0.17 g L^{-1} 3-HP, while the strain PpHP18 produced 4.11 ± 0.17 g L^{-1} 3-HP. These results agree with the observations from the mini bioreactors, where the yield of PpHP8 was higher than the yield of PpHP18. However, 3-HP concentration at the end of the fed-batch culture of PpHP18 reached 37.05 ± 0.73 g L^{-1}, while the PpHP8 strain reached 35.40 ± 1.85 g L^{-1}. Thus, the yield during the feeding phase was higher for PpHP18 than PpHP8. Moreover,

the fact PpHP18 μ_{max} is higher than the one of PpHP8 resulted in a shorter batch phase (22 h compared to 24 h). Previous studies revealed that *P. pastoris* cannot sustain the growth rate in fed-batch cultivations at a pre-set μ of 0.10 h^{-1} when 3-HP concentrations reached concentrations above 15 g L^{-1}, leading to the accumulation of glycerol and D-arabitol in the reactor medium [14]. This phenomenon is still observed in PpHP8 strain growing at 0.075 h^{-1}, where 17.41 g L^{-1} of glycerol and 6.01 g L^{-1} of D-arabitol accumulated into the reactor, while no glycerol nor D-arabitol accumulation were observed for PpHP18. For this reason, the PpHP18 cultivation was finalised just after stopping the addition of the feeding. Overall, the fed-batch for PpHP18 lasted 52 h, while the fed-batch of PpHP8 lasted 56.5 h. Thus, the volumetric productivity of PpHP18 was significantly higher than the volumetric productivity of PpHP8 (0.712 ± 0.010 g L^{-1} h^{-1} compared to 0.627 ± 0.033 g L^{-1} h^{-1}). The overall product yield on glycerol was 0.194 ± 0.004 Cmol $Cmol^{-1}$ for PpHP18 and 0.186± 0.010 Cmol $Cmol^{-1}$ for PpHP8.

The productivity obtained for the strain PpHP18 is the highest productivity reported in yeast, and, to our knowledge, it is also the highest productivity reported using the malonyl-CoA pathway to produce 3-HP in any microorganism. Furthermore, 37.05 g L^{-1} is the highest 3-HP concentration reported in yeast, highlighting the potential of the combined use of the *P. pastoris* cell factory and glycerol as feedstock for 3-HP production. Notably, the metabolically engineered PpHP18 strain showed a 50% increase in the final 3-HP titre and yield, and a 31.9% increase in volumetric productivity compared to the initial strain (PpHP6).

4.4. Conclusions

Production of 3-HP in *P. pastoris* through the malonyl-CoA reductase has been previously reported. The aim of this work was to improve its production by several metabolic engineering strategies. Improvement of the 3-HP yield was obtained by adding a second copy of *mcr-*C_{Ca}*.* However, (i) increasing the availability of malonyl-CoA by overexpressing a post-translationally unregulated Acc1 from *P. pastoris;* (ii) overexpressing endogenous acetyl-CoA pathway (ACS, Ald6, and Pdc1) or (iii) limiting the production of arabitol by deleting *ArDH* did not improve 3-HP production in small-scale cultures.

The work of this study demonstrates clearly that the system and the mode of cultivation clearly affected the phenotype of the strains. For instance, the strain PpHP18 showed the highest production of 3-HP in fed-batch cultivation mode but not in deep-well

plates and mini bioreactors operated in batch. This provides clear evidence on the importance to implement robust and reliable small-scale cultivation methods allowing for the mid/high throughput characterisation of strain performance under bioprocess-like conditions. However, the results obtained with the FeedBeads® were similar to the ones obtained in fed-bath cultures, thereby validating this methodology as a reliable method for strain screening/ranking and fast translation to bioreactor-scale.

Overall, our study showed that the multiplexed screening methodologies allowed to improve the information content, thereby supporting the formulation of hypotheses of previously unidentified metabolic bottlenecks such as that the supply of cytosolic acetyl-CoA may be limiting 3-HP production. Nonetheless, further studies, e.g. using ^{13}C-based metabolic flux analysis and metabolomics are needed to design novel metabolic engineering strategies.

References

1. della Pina, C., Falletta, E., and Rossi, M. (2011) A green approach to chemical building blocks. the case of 3-hydroxypropanoic acid. *Green Chemistry*, 13 (7), 1624–1632.
2. Kumar, V., Ashok, S., and Park, S. (2013) Recent advances in biological production of 3-hydroxypropionic acid. *Biotechnology Advances*, 31 (6), 945–961.
3. de Fouchécour, F., Sánchez-Castañeda, A.K., Saulou-Bérion, C., and Spinnler, H.É. (2018) Process engineering for microbial production of 3-hydroxypropionic acid. *Biotechnology Advances*, 36 (4), 1207–1222.
4. Jers, C., Kalantari, A., Garg, A., and Mijakovic, I. (2019) Production of 3-Hydroxypropanoic Acid From Glycerol by Metabolically Engineered Bacteria. *Frontiers in Bioengineering and Biotechnology*, 7, 124.
5. Ji, R.Y., Ding, Y., Shi, T.Q., Lin, L., Huang, H., Gao, Z., and Ji, X.J. (2018) Metabolic engineering of yeast for the production of 3-hydroxypropionic acid. *Frontiers in Microbiology*, 9, 2185.
6. Kim, J.W., Ko, Y.S., Chae, T.U., and Lee, S.Y. (2020) High-level production of 3-hydroxypropionic acid from glycerol as a sole carbon source using metabolically engineered *Escherichia coli*. *Biotechnology and Bioengineering*, 117 (7), 2139–2152.
7. Zhao, P., Ma, C., Xu, L., and Tian, P. (2019) Exploiting tandem repetitive promoters for high-level production of 3-hydroxypropionic acid. *Applied Microbiology and Biotechnology*, 103, 4017–4031.
8. Borodina, I., Kildegaard, K.R., Jensen, N.B., Blicher, T.H., Maury, J., Sherstyk, S., Schneider, K., Lamosa, P., Herrgård, M.J., Rosenstand, I., Öberg, F., Forster, J., and Nielsen, J. (2015) Establishing a synthetic pathway for high-level production of 3-hydroxypropionic acid in *Saccharomyces cerevisiae* via β-alanine. *Metabolic Engineering*, 27, 57–64.
9. Luo, X., Ge, X., Cui, S., and Li, Y. (2016) Value-added processing of crude glycerol into chemicals and polymers. *Bioresource Technology*, 215, 144–154.
10. Werten, M.W.T., van den Bosch, T.J., Wind, R.D., Mooibroek, H., and de Wolf, F.A. (1999) High-yield secretion of recombinant gelatins by *Pichia pastoris*. *Yeast*, 15 (11), 1087–1096.
11. Cregg, J.M., Vedvick, T.S., and Raschke, W.C. (1993) Recent advances in the expression of foreign genes in *Pichia pastoris*. *Nature Biotechnology*, 11 (8), 905–910.
12. van Maris, A.J.A., Konings, W.N., van Dijken, J.P., and Pronk, J.T. (2004) Microbial export of lactic and 3-hydroxypropanoic acid: Implications for industrial fermentation processes. *Metabolic Engineering*, 6 (4), 245–255.
13. Chemarin, F., Athès, V., Bedu, M., Loty, T., Allais, F., Trelea, I.C., and Moussa, M. (2019) Towards an *in situ* product recovery of bio-based 3-hydroxypropionic acid: influence of bioconversion broth components on membrane-assisted reactive extraction. *Journal of Chemical Technology and Biotechnology*, 94 (3), 964–972.
14. Fina, A., Brêda, G.C.G.C., Pérez-Trujillo, M., Freire, D.M.G.D.M.G., Almeida, R.V.R.V., Albiol, J., and Ferrer, P. (2021) Benchmarking recombinant *Pichia pastoris* for 3-hydroxypropionic acid production from glycerol. *Microbial Biotechnology*, 14 (4), 1671–1682.
15. Ma, F., and Hanna, M.A. (1999) Biodiesel production: a review. *Bioresource Technology*, 70, 1–15.
16. Werpy, T., and Petersen, G. (2004) Top Value Added Chemicals from Biomass Volume I - Results of Screening for Potential Candidates from Sugars and Synthesis Gas. *U.S. Department of Energy*.
17. Mazzoli, R. (2021) Current progress in production of building-block organic acids by consolidated bioprocessing of lignocellulose. *Fermentation*, 7, 248.
18. Prielhofer, R., Barrero, J.J., Steuer, S., Gassler, T., Zahrl, R., Baumann, K., Sauer, M., Mattanovich, D., Gasser, B., and Marx, H. (2017) GoldenPiCS: A Golden Gate-derived modular cloning system for applied synthetic biology in the yeast *Pichia pastoris*. *BMC Systems Biology*, 11, 123.
19. Gassler, T., Heistinger, L., Mattanovich, D., Gasser, B., and Prielhofer, R. (2019) CRISPR/Cas9-mediated homology-directed genome editing in *Pichia pastoris*. *Methods in Molecular Biology*, 1923, 211–225.
20. Liu, Y., Bai, C., Liu, Q., Xu, Q., Qian, Z., Peng, Q., Yu, J., Xu, M., Zhou, X., Zhang, Y., and Cai, M. (2019) Engineered ethanol-driven biosynthetic system for improving production of acetyl-CoA derived drugs in Crabtree-negative yeast. *Metabolic Engineering*, 54, 275–284.
21. Cámara, E., Albiol, J., and Ferrer, P. (2016) Droplet digital PCR-aided screening and characterization of *Pichia pastoris* multiple

gene copy strains. *Biotechnology and Bioengineering*, 113 (7), 1542–1551.

22. Heux, S., Juliette, P., Stéphane, M., Serguei, S., and Jean-Charles, P. (2014) A novel platform for automated high-throughput fluxome profiling of metabolic variants. *Metabolic Engineering*, 25, 8–19.
23. Maurer, M., Kühleitner, M., Gasser, B., and Mattanovich, D. (2006) Versatile modeling and optimization of fed batch processes for the production of secreted heterologous proteins with *Pichia pastoris*. *Microbial Cell Factories*, 5, 37.
24. Peiro, C., Millard, P., de Simone, A., Cahoreau, E., Peyriga, L., Enjalbert, B., and Heux, S. (2019) Chemical and metabolic controls on dihydroxyacetone metabolism lead to suboptimal growth of *Escherichia coli*. *Applied and Environmental Microbiology*, 85 (15), e00768-19.
25. Garcia-Ortega, X., Ferrer, P., Montesinos, J.L., and Valero, F. (2013) Fed-batch operational strategies for recombinant Fab production with *Pichia pastoris* using the constitutive GAP promoter. *Biochemical Engineering Journal*, 79, 172–181.
26. Kildegaard, K.R., Jensen, N.B., Schneider, K., Czarnotta, E., Özdemir, E., Klein, T., Maury, J., Ebert, B.E., Christensen, H.B., Chen, Y., Kim, I.K., Herrgård, M.J., Blank, L.M., Forster, J., Nielsen, J., and Borodina, I. (2016) Engineering and systems-level analysis of *Saccharomyces cerevisiae* for production of 3-hydroxypropionic acid via malonyl-CoA reductase-dependent pathway. *Microbial Cell Factories*, 15, 53.
27. Takayama, S., Ozaki, A., Konishi, R., Otomo, C., Kishida, M., Hirata, Y., Matsumoto, T., Tanaka, T., and Kondo, A. (2018) Enhancing 3-hydroxypropionic acid production in combination with sugar supply engineering by cell surface-display and metabolic engineering of *Schizosaccharomyces pombe*. *Microbial Cell Factories*, 17, 176.
28. Chen, Y., Bao, J., Kim, I.K., Siewers, V., and Nielsen, J. (2014) Coupled incremental precursor and co-factor supply improves 3-hydroxypropionic acid production in *Saccharomyces cerevisiae*. *Metabolic Engineering*, 22, 104–109.
29. Choi, J.W., and da Silva, N.A. (2014) Improving polyketide and fatty acid synthesis by engineering of the yeast acetyl-CoA carboxylase. *Journal of Biotechnology*, 187, 56–59.
30. Hunkeler, M., Stuttfeld, E., Hagmann, A., Imseng, S., and Maier, T. (2016) The dynamic organization of fungal acetyl-CoA carboxylase. *Nature Communications*, 7, 11196.
31. Wen, J., Tian, L., Xu, M., Zhou, X., Zhang, Y., and Cai, M. (2020) A synthetic malonyl-coa metabolic oscillator in *Komagataella phaffii*. *ACS Synthetic Biology*, 9 (5), 1059–1068.
32. Chen, X., Yang, X., Shen, Y., Hou, J., and Bao, X. (2018) Screening phosphorylation site mutations in yeast acetyl-CoA carboxylase using malonyl-CoA sensor to improve malonyl-CoA-derived product. *Frontiers in Microbiology*, 9, 47.
33. Goodridge, A.G. (1972) Regulation of the activity of acetyl coenzyme A carboxylase by palmitoyl coenzyme A and citrate. *Journal of Biological Chemistry*, 247 (21), 6946–6952.
34. Qiao, K., Imam Abidi, S.H., Liu, H., Zhang, H., Chakraborty, S., Watson, N., Kumaran Ajikumar, P., and Stephanopoulos, G. (2015) Engineering lipid overproduction in the oleaginous yeast *Yarrowia lipolytica*. *Metabolic Engineering*, 29, 56–65.
35. Pereira, H., Azevedo, F., Domingues, L., and Johansson, B. (2022) Expression of *Yarrowia lipolytica* acetyl-CoA carboxylase in *Saccharomyces cerevisiae* and its effect on in-vivo accumulation of Malonyl-CoA. *Computational and Structural Biotechnology Journal*, 20, 779–787.
36. Shiba, Y., Paradise, E.M., Kirby, J., Ro, D.K., and Keasling, J.D. (2007) Engineering of the pyruvate dehydrogenase bypass in *Saccharomyces cerevisiae* for high-level production of isoprenoids. *Metabolic Engineering*, 9 (2), 160–168.
37. Marx, H., Mecklenbräuker, A., Gasser, B., Sauer, M., and Mattanovich, D. (2009) Directed gene copy number amplification in *Pichia pastoris* by vector integration into the ribosomal DNA locus. *FEMS Yeast Research*, 9 (8), 1260–1270.
38. Aw, R., and Polizzi, K.M. (2013) Can too many copies spoil the broth? *Microbial Cell Factories*, 12, 128.
39. Kildegaard, K.R., Hallström, B.M., Blicher, T.H., Sonnenschein, N., Jensen, N.B., Sherstyk, S., Harrison, S.J., Maury, J., Herrgård, M.J., Juncker, A.S., Forster, J., Nielsen, J., and Borodina, I. (2014) Evolution reveals a glutathione-dependent mechanism of 3-hydroxypropionic acid tolerance. *Metabolic Engineering*, 26, 57–66.
40. Melo, N.T.M., Pontes, G.C., Procópio, D.P., Cunha, G.C. de G., Eliodório, K.P., Paes, H.C., Basso, T.O., and Parachin, N.S. (2020) Evaluation of product distribution in chemostat and batch fermentation in lactic acid-producing *Komagataella phaffii* strains utilizing glycerol as substrate. *Microorganisms*, 8 (5), 781.
41. Baumann, K., Dato, L., Graf, A.B., Frascotti, G., Dragosits, M., Porro, D., Mattanovich, D., Ferrer, P., and Branduardi, P. (2011) The impact of oxygen on the transcriptome of recombinant *S. cerevisiae* and *P. pastoris* - a

comparative analysis. *BMC Genomics*, 12, 218.

42. Shi, S., Chen, Y., Siewers, V., and Nielsen, J. (2014) Improving production of malonyl coenzyme A-derived metabolites by abolishing Snf1-dependent regulation of Acc1. *mBio*, 5 (3), e01130-14.

5

RESULTS III

High throughput ^{13}C-based Metabolic Flux Analysis of 3-hydroxypropionic acid producing *Pichia pastoris* reveals limited availability of acetyl-CoA and ATP due to tight control of the glycolytic flux

Manuscript in preparation.

Authors: Albert Fina[1], Pierre Millard[2], Stéphanie Heux[2], Joan Albiol[1], and Pau Ferrer[1]

Affiliation: [1]Department of Chemical, Biological and Environmental Engineering, Universitat Autònoma de Barcelona, Bellaterra, Spain; [2] TBI, Université de Toulouse, CNRS, INRAE, INSA, Toulouse, France

Supplementary Materials of this chapter were submitted to the Dipòsit Digital de Documents of the Universitat Autònoma de Barcelona. They can be accessed online using the following link: https://doi.org/10.5565/ddd.uab.cat/264385

Table of contents

Abstract

Production of 3-hydroxypropionic acid (3-HP) through the malonyl-CoA pathway has yielded promising results in *Pichia pastoris* (*Komagataella phaffii*), demonstrating the potential of this cell factory to produce this platform chemical and other acetyl-CoA-derived products using glycerol as a carbon source. However, further metabolic engineering of the original *P. pastoris* 3-HP-producing strains resulted in unexpected outcomes, e.g. significantly lower product yield and/or growth rate. In order to gain understanding on the metabolic constraints underlying these observations, the fluxome of ten *P. pastoris* 3-HP-producing strains has been characterized using a high throughput ^{13}C-based metabolic flux analysis platform. The results described herein indicate that the tight control of the glycolytic flux hampers cell growth due to the depletion of cytosolic acetyl-CoA. When the cytosolic acetyl-CoA synthesis pathway is overexpressed, the cell growth increases, but the product yield decreases due to the higher growth-associated ATP costs. In addition, the six most relevant strains were also cultured at pH 3.5, providing valuable insights into the adaptation of *P. pastoris* to an acidic pH for the first time, which is of high interest for the bioprocess integration of carboxylic acid production.

5.1. Introduction

The methylotrophic yeast *Pichia pastoris* (syn. *Komagataella phaffii*) has gained a lot of attention in the recent years due to its promising results in metabolic engineering applications [1–3]. Recent studies have showed the great potential of *P. pastoris* to produce 3-HP [4,5]. 3-HP is a bulk chemical with a large interest due to its multiple applications. It was listed among the top-value added products to be obtained from biomass by the Department of Energy of the United States [6]. 3-HP can be converted to acrylic acid, which is used to produce superabsorbent plastics, as well as to other chemicals of interest, such as malonic acid or 1,3-propanediol [6,7].

3-HP production in *P. pastoris* has recently been achieved by heterologously expressing the bi-functional enzyme malonyl-CoA reductase (MCR) from *Chloroflexus aurantiacus* [4]. Further strain optimization based on rational strain engineering resulted in somewhat limited improvement (ca. 50% increase) of product yield [5]. So far, the highest 3-HP production reported in *P. pastoris* is 37 g/L of 3-HP at a volumetric productivity of 0.712 g L^{-1} h^{-1} in a fed-batch culture using glycerol as a carbon source [5].

One of the advantages of using *P. pastoris* to produce 3-HP is its ability to grow at a low pH. Performing the cultures at an acidic pH allows the organic acids extraction from the fermentation media using non-toxic solvents. This process is simpler, and it generates less waste products than classical downstream processes [8,9]. Moreover, *in situ* product recovery systems can be implemented, avoiding reaching toxic levels of 3-HP [10]. However, while the cultivation of *P. pastoris* at pH as low as 3 has been widely studied as a strategy to minimise the activity of some endogenous proteases [11,12], there are no previous studies on the impact of low pH on the fluxome of *P. pastoris*.

Recent advances in the field of synthetic biology allow the generation of a high number of recombinant microbial strains in a short amount of time within a single metabolic engineering project. Typically, the strains are tested in small scale cultivation systems such as microtiter plates or shake flasks, and the best performing ones are further characterized at a bioreactor scale. However, with the development of high throughput (HT) bioreactor platforms, it is now possible to characterize a whole set of genotypic variants at the fluxomic level providing the most complete and systematic description of the metabolic state of a cell [13,14]. A strain's fluxome is a result derived from the combination of it's genome, transcriptome, proteome, and metabolome, and the

regulatory interactions between these components. Thus, fluxomics can be used to identify regulatory mechanisms that may be hampering a strain's performance [15,16].

^{13}C-based Metabolic Flux Analysis (^{13}C-MFA) is the most wide-spread technique for the quantification of the fluxes [17]. It consists in using a ^{13}C-labelled substrate as tracer to latter infer the metabolic reaction rates. HT analysis of multiple strains has focused on stationary ^{13}C-MFA (i.e., cells are collected at a metabolic and isotopic steady-state) because the sampling protocol is easier to automatize compared to instatioanary ^{13}C-MFA, as there is a remarkably lower number of samples to process and analyse [13].

The use of ^{13}C-MFA for the characterization of *P. pastoris* fluxes has been largely reported using glucose, glycerol, or combinations of thereof with methanol [18–20]. Nonetheless, the exploitation of HT ^{13}C-MFA tools and methodologies for the characterisation of *P. pastoris* metabolism remains largely unexplored.

The aim of this study was to thus characterize the impact of different genetic modifications into the fluxome of a set of *P. pastoris* strains that produce 3-HP using glycerol as a sole carbon source. To this end, a genome-scale reduced metabolic model was obtained using a previously described Genome Scale Metabolic (GSM) model compression protocol for *P. pastoris* [19,21]. The fluxomics analyses were expected to provide meaningful insights of the bottlenecks of this yeast's metabolism towards 3-HP production. Moreover, the fluxome of the 3-HP producing strains growing at pH 3.5 was also characterized.

5.2. Materials and methods

5.2.1. Strains

The *P. pastoris* strains used in this study are listed in Table 6. These were all derived from the parental strain X-33 (Invitrogen-Thermo Fisher Scientific, MA, USA), which was used as a reference strain for this study. The construction of all strains has been previously described elsewhere [4,5]. The stoichiometry of the engineered reactions and corresponding enzymes in the 3-HP-producing *P. pastoris* strains are depicted in Figure 16.

Table 6. Strains used in this study. The genotype indicates the overexpressed genes and corresponding promoter, and the deleted genes.

Strain name	Genotype	Reference
X-33		Invitrogen-Thermo Fisher Scientific
PpHP1	pGAP_*mcr*$_{Ca}$	[4]
PpHP2	pGAP_*mcr-N*$_{Ca}$ pGAP_*mcr-C*$_{Ca}$	[4]
PpHP5	pGAP_*mcr-N*$_{Ca}$ pGAP_*mcr-C*$_{Ca}$ pGAP_*cPOS5*$_{Sc}$	[4]
PpHP6	pGAP_*mcr-N*$_{Ca}$ pGAP_*mcr-C*$_{Ca}$ pGAP_*ACC1*$_{Yl}$ pGAP_*cPOS5*$_{Sc}$	[4]
PpHP8	pGAP_*mcr-N*$_{Ca}$ pGAP_*mcr-C*$_{Ca}$ pGAP_*mcr-C*$_{Ca}$ pGAP_*ACC1*$_{Yl}$ pGAP_*cPOS5*$_{Sc}$	[5]
PpHP13	pGAP_*mcr-N*$_{Ca}$ pGAP_*mcr-C*$_{Ca}$ pGAP_*mcr-C*$_{Ca}$ pGAP_*ACC1*$_{Yl}$ pGAP_*cPOS5*$_{Sc}$ pTEF1_*acs*$_{Se}^{L641P}$	[5]
PpHP15	pGAP_*mcr-N*$_{Ca}$ pGAP_*mcr-C*$_{Ca}$ pGAP_*mcr-C*$_{Ca}$ pGAP_*ACC1*$_{Yl}$ pGAP_*cPOS5*$_{Sc}$ Δ*ArDH*	[5]
PpHP17	pGAP_*mcr-N*$_{Ca}$ pGAP_*mcr-C*$_{Ca}$ pGAP_*mcr-C*$_{Ca}$ pGAP_*ACC1*$_{Yl}$ pGAP_*cPOS5*$_{Sc}$ pTEF1_*acs*$_{Se}^{L641P}$ Δ*ArDH*	[5]
PpHP18	pGAP_*mcr-N*$_{Ca}$ pGAP_*mcr-C*$_{Ca}$ pGAP_*mcr-C*$_{Ca}$ pGAP_*ACC1*$_{Yl}$ pGAP_*cPOS5*$_{Sc}$ pTEF1_*acs*$_{Se}^{L641P}$ Δ*ArDH* pPDC1_*PDC1*	[5]

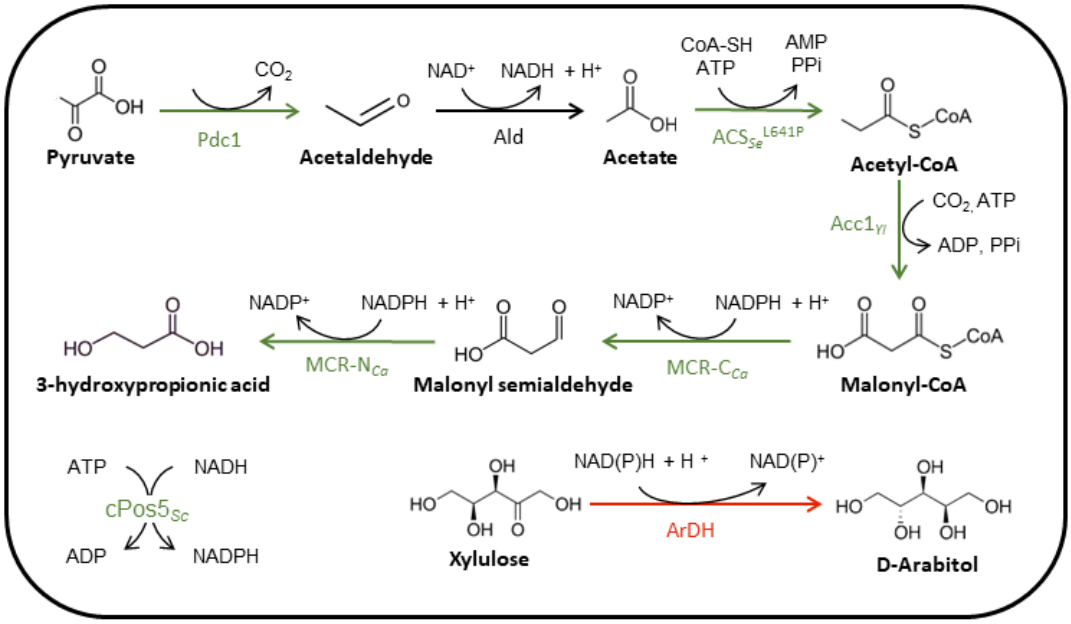

Figure 16. Metabolic pathway from pyruvate to 3-HP through cytosolic acetyl-CoA and malonyl-CoA in *P. pastoris*. The reactions catalysed by all the enzymes linked to overexpressed or deleted genes are displayed. Enzyme abbreviations: Pdc1: Pyruvate decarboxylase 1; Ald: Endogenous cytosolic aldehyde dehydrogenase; ACS_{Se}^{L641P}: Acetyl-CoA synthase from *Salmonella enterica* harbouring the point mutation L641P to avoid post-translational inhibition of the enzyme by acetylation; $Acc1_{Yl}$: Acetyl-CoA carboxylase from *Y. lipolytica*; MCR-C_{Ca}: C-terminal domain of the malonyl-CoA reductase from *C. aurantiacus*; MCR-N_{Ca}: N-terminal domain of the malonyl-CoA reductase from *C. aurantiacus*; $cPos5_{Sc}$: NADH kinase from *S. cerevisiae* located on the cytosol; ArDH: Arabitol dehydrogenase. Green and red arrows and enzyme abbreviations indicate whether the corresponding genes were overexpressed or deleted, respectively.

5.2.2. Model generation

The genome scale model *iMT1026v3* [21,22] was compressed using *CellNetAnalyzer* [23] in Matlab (Matlab inc., Mathworks, MA, USA). A contextualized core model was generated protecting the reactions, metabolites, and phenotypes that had been previously described for *P. pastoris* grown on glycerol as sole carbon source [19]. Additionally, D-arabitol secretion was protected, as it has been previously reported that theses strains produce D-arabitol as by-product in both batch and fed-batch cultures [4]. Cytosolic acetate production was also kept during model compression, as cytosolic acetate is used as substrate for 3-HP production. The models and scripts to compress *iMT1026v3* model into a core model can be found in the Supplementary File S1.

The newly generated core model was manually curated taking into account relevant literature-based knowledge. First, production of isoleucine consumes mitochondrial pyruvate instead of 2-(α-hydroxyethyl)thiamine diphosphate. The production of lysine uses mitochondrial acetyl-CoA and α-ketoglutarate from the cytosol,

instead of vice versa. Finally, alanine production is derived from mitochondrial pyruvate, instead of cytosolic pyruvate [24–26]. In addition, as biosynthesis of glutamate, glutamine, aspartate, and asparagine may take place in both the cytoplasm and the mitochondria, both pathways were included. The 3-HP production pathway from cytosolic acetate was also included. The new model was named *PpaCore_3HP.mat*. All the necessary files to generate the new core model (*PpaCore_3HP.mat*) from the GSM model can be found in the Supplementary File S2.

Some of the amino acid biosynthetic reactions were manually lumped to reduce the number of overall reactions and metabolites. Some of the intermediary metabolites of the lumped reactions were present in the biomass production reactions. The stoichiometry of the biomass formation equation was corrected to remove these metabolites. These modifications can be found in the Supplementary File S3.

The final core model was latter manually translated into the FTBL (Flux TaBuLar) format [17,27] , and the reactions producing 3-HP from cytosolic acetate (the closest intermediary metabolite to malonyl-CoA in the core model) were introduced. The final FTBL core model for the *P. pastoris* 3-HP producing strains can be found in the Supplementary File S4 *(PpaCore_3HP.ftbl).*

5.2.3. *In silico* design of ^{13}C-labelling experiments

The context-specific core model of *P. pastoris* metabolism including the 3-HP formation reactions (*PpaCore_3HP.ftbl*) was used to calculate the optimal isotopic composition of the substrate using *IsoDesign* [28]. *IsoDesign* uses *influx_s* [29] to calculate the precision of the fluxes at each given labelling input. Therefore, *influx_s* was previously used to set the fitting mode for each reaction flux as free (F), determined (D), or constrained (C).

For the evaluation of the *IsoDesign* results, the substrate combinations yielding the highest number of fluxes with a SD<1 was calculated. The substrate combinations were ranked based on the sum of SDs of the reactions with a SD<1. Afterwards, the substrates providing the highest precision of the fluxes of the upper glycolysis (UG) and the pentose phosphate pathway (PPP) were ranked. The IsoDesign results indicated that the best substrate combination consisted of 20% 1-^{13}C-glycerol and 80% 2-^{13}C-glycerol (Supplementary File S11).

5.2.4. Media, cultivation conditions, and automated sampling

Seed cultures for the mini-bioreactor cultivations were prepared as follows: 50 mL falcon tubes containing 5 mL YPG (1% w/v yeast extract, 2% w/v peptone, and 1% v/v glycerol) medium were inoculated from cryostock and incubated overnight at 30ºC and 200 rpm. The overnight cultures were transferred to a 250 mL shake flask containing 25 mL YPG at a starting OD_{600} of 1 and subsequently grown for 8 h at 30ºC and 200 rpm. The cultures were harvested at the exponential phase and used to inoculate the mini-bioreactor cultures.

A HT fluxomics platform consisting of 48 mini-bioreactors was used for the cultivation and the sampling [30]. The batch medium contained 1.8 g L^{-1} citric acid, 0.02 g L^{-1} $CaCl_2 \cdot 2\ H_2O$, 12.6 g L^{-1} $(NH_4)_2HPO_4$, 0.5 g L^{-1} $MgSO_4 \cdot 7\ H_2O$, 0.9 g L^{-1} KCl, 0.4 mg L^{-1} biotin, and 4.6 ml L^{-1} of PTM1 trace salts [31]. The pH of the medium was adjusted to 5 or 3.5 using HCl. The batch medium was supplemented with 0.5 g L^{-1} glycerol labelled at position 1 and 2 g L^{-1} glycerol labelled at position 2 (20% 1-^{13}C-glycerol and 80% 2-^{13}C-glycerol). Labelled substrates were obtained from Innovachem SAS (France). All the components of the medium except for the trace salts, the biotin, and the labelled glycerol were mixed and autoclaved. The other components were filter-sterilized and introduced into the batch medium under sterile conditions. Each bioreactor was filled with 15 mL of medium.

All the strains listed in Table 6 were tested in triplicate in bioreactor cultures at pH 5. The cultures were inoculated at a starting OD_{600} of 0.025. The strains X-33, PpHP1, PpHP6, PpHP8, PpHP15, and PpHP18 were tested in triplicate at pH 3.5. The cultures were inoculated at a starting OD_{600} of 0.05.

The bioreactors were aerated using compressed air and the temperature was set to 28ºC.

Automated sampling was programmed to measure the OD_{600} off-line every two hours for the first 16 h of cultivation. After 16 h of cultivation, sampling of the OD_{600} was performed every hour (during the exponential phase of the cultures). From the 16 to the 24 h of cultivation, 250 µL samples were withdrawn hourly from each culture for supernatant analysis. The samples were placed on 96-well plates with a 0.45 µm filter bottom and vacuum filtered immediately. A final supernatant sample was withdrawn after 27 h cultivation. After 27 h cultivation, OD_{600} samples were withdrawn every 2.5 h for

10 h. Sampling and OD_{600} data from the mini-bioreactor cultures can be found on Supplementary File S5.

When each culture reached an OD_{600} above 1, a 500 µL sample was withdrawn from the culture. The samples were quenched on 3.5 mL quenching solution (40% v/v acetonitrile, 40% v/v methanol, 20 % water and 0.1 M formic acid) at -20ºC. Samples were stored at -20ºC between 1 and 3 h until further processing.

5.2.5. Analyses

5.2.5.1. Supernatant analysis with NMR

Glycerol, 3-HP, and D-arabitol were quantified from the filtered supernatant samples using Nuclear Magnetic Resonance (NMR). 180 µL sample and 20 µL of 10 mM TSP (3-(trimethylsilyl)-[2,2,3,3-$^{2}H_4$]-propionic acid sodium salt) were mixed. TSP was used as an internal standard. 1D-^{1}H NMR was used on a Bruker Advance III 800 MHz spectrometer (Bruker BioSpin, Germany) coupled to a 5 mm CQPI cryoprobe, which was set to 280 K. The NMR data was recorded after a 30º presaturation pulse (zgpr30) and a relaxation delay of 7 s. TopSpin 3.6.4 (Bruker BioSpin, Germany) was used for the analysis of the NMR spectra. Commercial succinate at 1 g L^{-1} (43057, Sigma Aldrich, MO, USA) was used for the re-quantification of TSP. All data was corrected based on the quantification of succinate. The peak integration data from the NMR analyses can be found in Supplementary File S6.

5.2.5.2. Sample processing and analysis of the proteinogenic amino acids using LC/MS

Quenched samples were vortexed for 30 s and centrifuged at 5,000 g for 5 min in a swing-rotor centrifuge. Pellets were freeze-dried using a Rotavapor (Büchi, Switzerland). The biomass was treated with 150 µL 6N HCl at 110ºC for 16 h. The acid was evaporated in the rotavapor. Each sample was washed using 100 µL milliQ water and subsequently dried in the rotavapor. This step was repeated twice to eliminate all the acid traces. Finally, the pellets were resuspended on 200 µL milliQ water. The samples were centrifuged at 10,000 g for 5 min to eliminate the biomass debris. 40 µL of supernatant (containing the amino acids) were diluted onto 460 µL milliQ water.

The diluted amino acids were analyzed using a previously described HPLC-MS method [32]. The UHPLC Vanquis was coupled to a mass spectrometry (MS) detector Orbitrap W Exactive Plus with a heated electrospray ionization source (Thermo Fisher Scientific, MA, USA). HPLC-MS was used with a precolumn Discovery HS F5 Supelguard Cartridge of 20 x 2.1 mm with particle size 5 µm (Supelco Bellefonte, PEN, USA) and a column Discovery HS F5 HPLC column of 150 x 2.1 mm with particle size 5 µm (Supelco Bellefonte). Solvent A consisted of 0.1% v/v formic acid in ultrapure water and Solvent B of 0.1% v/v formic acid in acetonitrile. The flow rate of the eluent was set to 0.25 mL min^{-1}, and the temperature of the sampler and the column were set to 4ºC and 30ºC, respectively. Solvent B set points were varied as follows: 0 min: 2%; 2 min: 2%; 10 min: 5%; 16 min: 35%; 20 min: 100%; 24 min: 100%. Finally, the set points of the initial conditions (2% solvent B) were set for 6 min before the injection of the next sample. The injection volume was 5 µL.

The MS detector was set to detect the positive ions on FTMS mode. The resolution was set to 70'000, the capillary temperature to 320ºC, and the source heater temperature to 300ºC. Sheath gas and auxiliary gas flow rates were set to 40 and 10 arbitrary units, respectively. The S-lens RF level was set to 40% and the source voltage to 5 kV. The MS was set to measure the exact mass of all C isotopologues of all the amino acids (Supplementary File S7).

The isotopologue distribution of the amino acids was corrected considering the isotopologue labelling of the inoculum and the natural abundance of all isotopes using IsoCor [33]. Raw and processed data can be found in Supplementary file S8.

5.2.6. Bioprocess parameters

The OD_{600} and the NMR supernatant analyses results were used to calculate the growth rate (µ) and the specific production or consumption rates (q-rates) for glycerol, 3-HP, and D-arabitol. To this end, Physiofit was used [34]. The absorbance at OD_{600} was correlated to the biomass concentration using the conversion factor 0.563 g_{CDW}/OD_{600}, the rationale being that all the strains used in this study shared the same conversion factor in the culture conditions used. This value was derived from calculating the µ (which is independent from the conversion factor) of the triplicate cultures of the reference strain (X-33) at pH 5. Afterwards, the genome scale model *iMT1026v3* was used to calculate the uptake rate of glycerol at such growth rate (0.21 h^{-1}) considering a non-growth associated ATP consumption of 2.51 mmol g_{CDW}^{-1} h^{-1} [21], which resulted 3.4 $mmol_{Glyc}$

g_{CDW}^{-1} h^{-1}. This calculation was done in Matlab using the Cobra Toolbox [35]. Finally, the conversion factor that correlates the experimental data and the computational results was calculated. The biomass yield for X-33 using the calculated conversion factor resulted in 0.73 g_{CDW} g_{Glyc}^{-1}, which falls within the reported experimental values [21].

The biomass concentration data can be found together with the OD_{600} data Supplementary File S4.

The bioprocess parameters results calculated using Physiofit can be found in the Supplementary File S9.

5.2.7. ^{13}C-Metabolic Flux Analysis

Flux calculations were performed using *influx_s* [29] and the previously obtained FTBL format model. The bioprocess parameters and the corrected data of the isotopologue distribution of the amino acids were used as input data. As some regions of the flux map were poorly determined, the function *sln* was used to apply the method of minimization of the sum of all fluxes [36].

All fluxes were normalized to the rate of the substrate uptake rate. A sensitivity analysis was performed using the Monte-Carlo method with 100 independent simulations. Statistical analyses (chi-square test) was used to determine sufficient goodness of the fit ($p<0.05$) for each experiment. The average flux and the standard deviation of the mean were calculated from the biological replicates with sufficient goodness of the fit.

Flux map figures were performed using Omix2.0.7 (Omix Gmbh, Germany) [37]. The figures show the average absolute/relative flux and the standard deviation of the triplicates.

5.2.8. Flux Balance Analysis

Flux Balance Analysis (FBA) [38] using the CobraToolbox in Matlab and the previously described *PpaCore_3HP.mat* model was performed. The experimental confidence intervals obtained from the Monte Carlo analyses were used as an upper and lower boundary for each flux. Afterwards, FBA was performed using the maximization of the flux of the ATP of maintenance reaction (ATPM) as objective function. This is the objective function resulting in the best description of the intracellular fluxes of a cell

culture growing on a batch culture with excess of substrate [39]. FBA results were also used to calculate the ATP produced and consumed at each pathway by each strain. The Matlab script, the input file with the Monte Carlo results, and the FBA results file can be found in the Supplementary File S10.

5.3. Results and discussion

5.3.1. HT cultivation bioprocess parameters

The series of previously available 3-HP-producing *P. pastoris* strains [4,5] were grown in glycerol batch cultures at pH 5 using the HT cultivation platform. Quantification of the exometabolites and the biomass concentration allowed calculating the bioprocess parameters (specific substrate consumption and (by)products production rates (q-rates) and μ_{max}) for each strain (Figure 17), which is a prerequisite for metabolic flux calculations. Results were consistent with previously reported cultivation data [4,5]. In a nutshell, comparison between strains PpHP1 and PpHP2 reveals that dissection of MCR from *C. aurantiacus* into each of its two subunits led to a 10-fold increase in the 3-HP yield, whereas the overexpression of the genes encoding for an acetyl-CoA carboxylase from *Yarrowia lipolytica* (*ACC1*) and a cytosolic version of the mitochondrial NADH kinase from *Saccharomyces cerevisiae* (*cPOS5*) in strain PpHP6 led to a further increase in product yield. In addition, the expression of a second copy of the gene encoding the C-terminal domain of MCR yielded the highest 3-HP-producing strain (PpHP8), which was also the slowest growing strain and the strain producing the largest amount of D-arabitol in batch cultures. As previously reported, the overexpression of the genes encoding for the cytosolic acetyl-CoA synthesis pathway (i.e. acs_{Se}^{L641P} and *PDC1*, Figures 16) in the strain PpHP8 (yielding strain PpHP18) restored the growth rate, but the 3-HP yield dropped drastically [5]. These results pointed at a limitation of resources in PpHP8 when growing at a maximal growth rate [5], thereby resulting in an opposite trend between biomass and product yields. Strikingly, the biomass yield for PpHP8-derived strains overexpressing acs_{Se}^{L641P} (PpHP13, ppHP17), and *PDC1* plus acs_{Se}^{L641P} (PpHP18) were lower than the biomass yield of strain PpHP8.

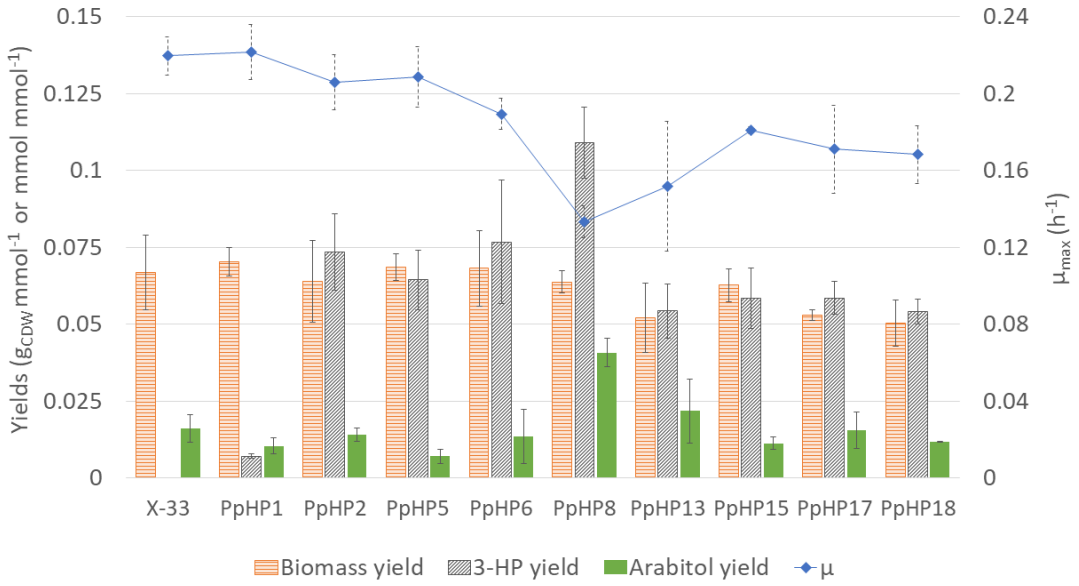

Figure 17. Biomass, product, and by-product yields and μ_{max} of the parental *P. pastoris* strain and nine 3-HP-producing strains cultivated in batch mini bioreactor cultures at pH 5. Orange bars show the biomass yield, grey bars show the 3-HP yield, green bars show the arabitol yield, and the blue diamonds depict the μ_{max}. Standard deviation of the replicates is depicted.

5.3.2. Fluxome of *P. pastoris* 3-HP-producing strains at pH 5

The bioprocess parameters of the series of strains obtained from batch cultivations and the amino acids isotopologue distributions derived from the corresponding labelling experiments were used to calculate the intracellular fluxes using *influx_s*. The metabolic flux data sets for each strain can be found in the Supplementary File S12. A summary of the results (value of each flux, chi-square test result, and cost) can be found in Supplementary File S13.

The metabolic flux profile of the reference strain (X-33) obtained using the HT robotic platform is comparable to the previously reported results for the same strain growing in glycerol chemostats on a similar medium [19]. Noticeably, the fluxes of the upper glycolysis (UG) and pentose phosphate pathway (PPP) in our batch experiments (i.e. at μ_{max}) were higher than the ones observed in chemostat cultures at lower growth rates (0.05, 0.10 and 0.16 h^{-1}), coherent with the positive correlation between growth rate and the UG and PPP fluxes previously observed in glycerol chemostats. Similarly, fluxes of the lower glycolysis (LG) and the tricarboxylic acid (TCA) cycle reactions were lower than the ones observed in chemostat cultures at lower growth rates, also coherent with the reported inverse correlation between growth rate and LG and TCA cycle fluxes.

To facilitate comparison of metabolic flux distributions amongst strains, a heat map illustrating the fold-change comparison between the intracellular relative fluxes (i.e. normalised to the specific glycerol uptake rate) of each recombinant strain compared to the relative fluxes of the reference strain cultivated at pH 5 is shown in Figure 18. The most drastic changes were observed in the relative fluxes through the UG and PPP reactions. First, when the MCR activity was increased by expressing separately the two MCR domains (i.e. PpHP2 compared to PpHP1), the fluxes of the UG and PPP increased noticeably (10-50%). Such trend can be explained by an increase in the NADPH requirements, as NADPH is used as the electron donor for the two consecutive reactions catalysed by MCR. When the gene encoding the heterologous cytosolic NADH kinase (*cPOS5*$_{Sc}$) was overexpressed (PpHP5), the observed fluxes of the UG and PPP reactions were 15-50% lower compared to PpHP2. It is well known that the NADPH/NADP$^+$ ratio controls the fluxes towards the oxidative branch of the PPP [40]. Overexpression of *cPOS5* in *P. pastoris* provides the cell with an additional source of NADPH, leading to a higher NADPH/NADP$^+$ ratio [41]. Therefore, decrease of UG and PPP fluxes in PpHP5 compared to PpHP2 was consistent with an increased NADPH/NADP$^+$ ratio.

No major changes were observed when *ACC1*$_{Yl}$ was overexpressed (i.e. in strain PpHP6, compared to strain PpHP5). For the strain PpHP8, which harboured an additional copy of the gene encoding for MCR-C$_{Ca}$, the highest fluxes towards 3-HP production were observed, while the UG and PPP fluxes were the lowest among all strains. Such observation agrees with the results for the strain PpHP5, as the increase in the NADPH requirements due to production of 3-HP followed independent trends with the fluxes of the oxidative branch of the PPP.

Heterologous expression of *acs*$_{Se}^{L641P}$ in strain PpHP8 (i.e. generating strain PpHP13) led to a drastic switch in the strain's fluxome. The relative fluxes through the UG and PPP increased remarkably in PpHP13, while showing a lower relative flux towards 3-HP production compared to PpHP8 or PpHP6 strains. Moreover, the biomass yield of PpHP13 was lower. Therefore, considering the NADPH requirements for biomass and 3-HP production, increased production of NADPH through the PPP seems unfounded. Deletion of the gene encoding for the NADPH-dependent arabitol dehydrogenase enzyme (*ArDH*) in strains PpHP8 and PpHP13 (i.e. obtaining strains PpHP15 and PpHP17, respectively) led to small changes in the strains' fluxomes under the tested growth conditions. Finally, overexpression of *PDC1* in PpHP17 (resulting in

PpHP18) led to the highest relative flux through the UG and PPP. However, neither the biomass yield nor the 3-HP yield were affected (Figure 17).

Changes in the fluxes through LG and the TCA cycle reactions followed the opposite trend to the UG and the PPP. Small differences in the fluxes through the glyoxylate cycle were also observed. However, as the absolute values of these fluxes are low (below 0.025 mmol $mmol^{-1}$ h^{-1}), absolute changes of these fluxes do not have an impact on the strain's biomass and product yields.

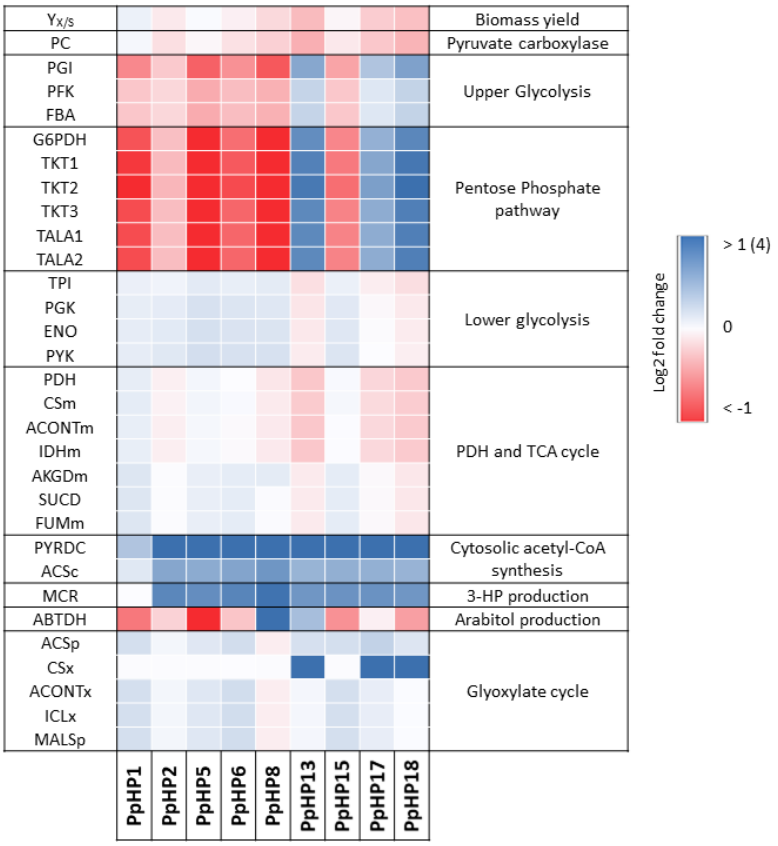

Figure 18. Reaction flux fold-change between each one of the ten 3-HP-producing recombinant strains compared to the reference strain (X-33). All colours are referred to the -1 to +1 colour scale, except the reactions 'MCR', where the upper boundary of the colour scale is set to +4. Moreover, in the case of 'MCR' the fluxes fold-change is referred to the flux of strain PpHP1. $Y_{X/S}$ is the biomass to substrate yield. The reaction corresponding to each reaction abbreviation can be found in the Supplementary File S3/S4.

Further comparison of the absolute flux distributions (i.e. non-normalised to the glycerol specific uptake rate) in the reference and the 3-HP-producing strains PpHP8 and PpHP18 (Figure 19) provided further insights.

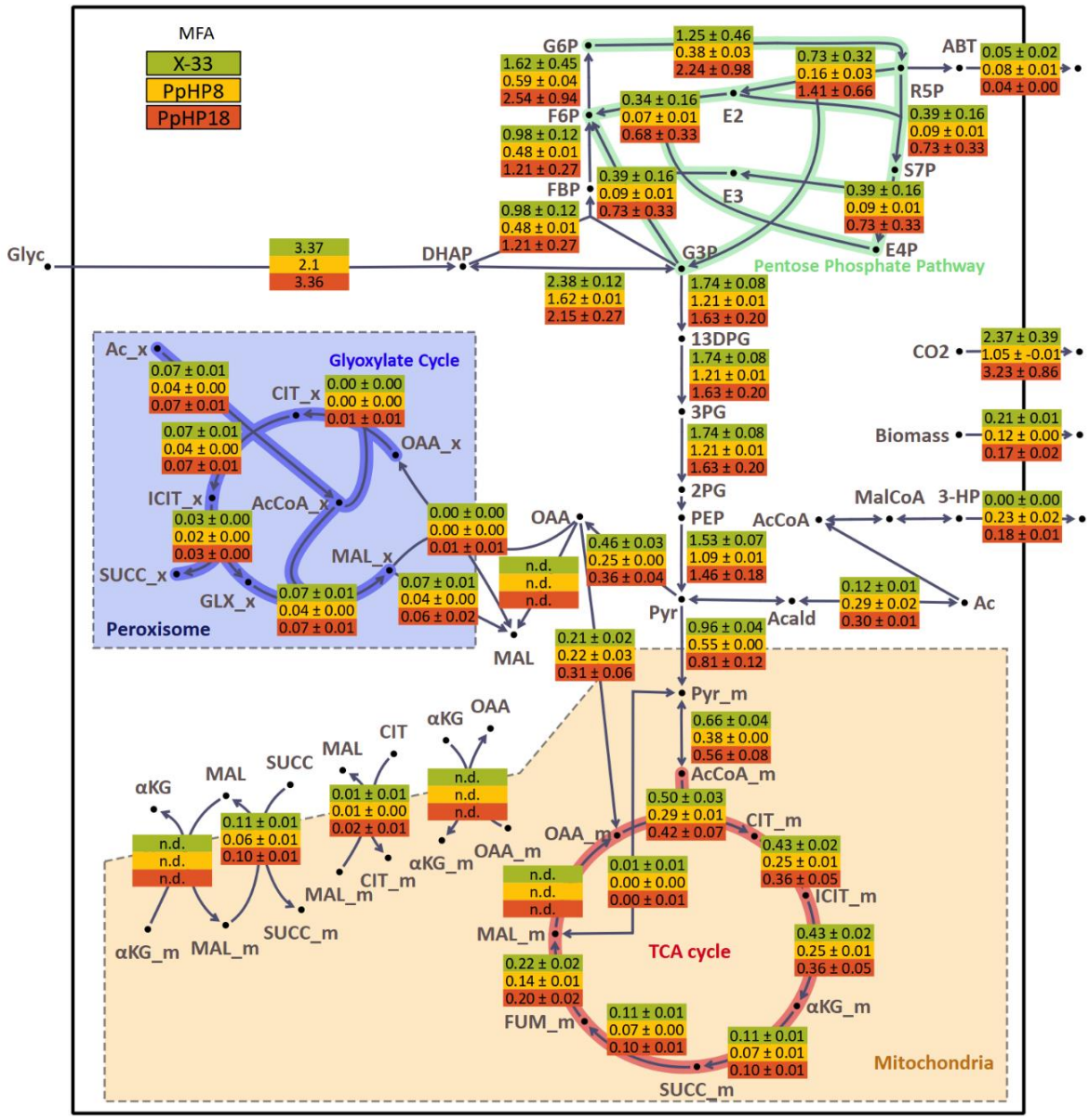

Figure 19. Flux map for the reference (X-33), PpHP8, and PpHP18 strains growing in glycerol batch cultures at pH 5. The average and the standard deviation of the absolute fluxes for each triplicate experiment are displayed. Fluxes are given in mmol $gCDW^{-1}$ h^{-1}. Abbreviations: G6P: Glucose-6-phosphate; F6P: Fructose-6-phosphate; FBP: Fructose bisphosphate; Glyc: Glycerol; DHAP: Dihydroxyacetone phosphate; G3P: Glyceraldehyde-3-phosphate; R5P: Ribose-5-phosphate; S7P: Sedoheptulose-7-phosphate; E4P: Erythrose-4-phosphate; ABT: D-Arabitol; E2: glycolaldehyde moiety of the non-oxidative PPP reactions; E3: dihydroxyacetone moiety of the non-oxidative PPP reactions; 13DPG: 1,3-Bisphosphoglycerate; 3PG: 3-phosphoglycerate; 2PG: 2-phosphoglycerate; PEP: Phosphoenolpyruvate; Pyr: Pyruvate; Acald: Acetaldehyde: Ac: Acetate; AcCoA: Acetyl-CoA; MalCoA: Malonyl-CoA; 3-HP: 3-Hydroxypropionic acid; CIT: Citrate; ICIT: Isocitrate; αKG: α-ketoglutarate; SUCC: Succinate; FUM: Fumarate; MAL: Malate; OAA: Oxaloacetate; GLX: Glyoxylate.

First, overexpression of the 3-HP production pathway led to a higher pyruvate decarboxylase flux at the pyruvate node in PpHP8 compared to the reference strain (0.29 mmol g_{CDW}^{-1} h^{-1} and 0.12 mmol g_{CDW}^{-1} h^{-1}, respectively). The overexpression of

ACS_{Se}^{L641P} and Pdc1 in strain PpHP8 did not result in a higher flux towards cytosolic acetyl-CoA in strain PpHP18, as the absolute flux values for the two strains were almost identical (0.29 and 0.30 mmol g_{CDW}^{-1} h^{-1}, respectively). Compared to the reference strain, the LG fluxes in strain PpHP18 did not increase due to the overexpression of the cytosolic acetyl-CoA production pathway. All these findings agree with previous results in *S. cerevisiae*, where the overexpression of *PDC1* led to a higher flux towards this pathway, while it did not pull a higher glycolytic flux [42]. It is well described that the glycolytic flux is tightly controlled in yeast *S. cerevisiae*, and the glycolytic flux cannot be increased by overexpression of individual enzymes [43]. In the case of *P. pastoris*, increased glycolytic fluxes have only been described under low oxygen availability [44,45] or when a transcription factor controlling the expression of all the glycolytic genes is overexpressed [46]. Therefore, as pyruvate is pulled into the production of 3-HP but the glycolytic flux and the uptake of glycerol do not increase, the overall ATP yield of the 3-HP-producing strains decreases.

The PpHP18 has remarkably higher UG and PPP fluxes than strain PpHP8 (Figure 19). The UG and PPP have a low carbon and energy yield. Therefore, while *PDC1* is being overexpressed, the energy requirements in strain PpHP18 sink the pyruvate into the TCA cycle for ATP generation, hampering the flux towards cytosolic acetyl-CoA and, ultimately, reducing the 3-HP yield. On the contrary, as PpHP8 grows at a lower rate, the energy requirements of the strain are reduced, leaving more substrate available to produce 3-HP.

Overall, comparison of absolute flux distributions suggests that, in order to further increase the 3-HP yield in strain PpHP8, the glycolytic fluxes would need to be significantly increased. Moreover, it is also concluded that the high ATP requirements of strain PpHP18 cause the observed differences between these two strains.

5.3.3. Calculation of ATP and NADPH producing and consuming fluxes in *P. pastoris* 3-HP-producing strains reveals distinct NADPH availability and ATP maintenance requirements amongst strains

The results from the previous section show that the fluxes through the PPP decrease when the cytosolic NADH kinase was heterologously expressed. Coherently, calculated NADPH regeneration rates derived from the ^{13}C-MFA (Figure 20A) indicate that the NADPH produced by the glucose-6-phosphate dehydrogenase (G6PDH)

reaction was lower than the actual NADPH requirements in some of the strains overexpressing the *cPOS5* gene (i.e. strains PpHP5, PpHP6, andPpHP8), indirectly supporting that the NADH kinase reaction contributed to cover the cell's NADPH requirements.

It is also observed that strains PpHP13, PpHP17, and PpHP18, which overexpress the cytosolic acetyl-CoA production pathway (i.e. Pdc1 and ACS_{Se}^{L641P}), produced more NADPH through the oxidative branch of the PPP than the actual cell requirements. The substantial increase in the fluxes through UG and PPP for such strains coincided with an increase in the specific glycerol uptake rate and the growth rate (Figure 20A and Figure 17), but the biomass yield decreased (Figure 17). Despite the standard deviation of the fluxes for the UG and PPP fluxes of strains PpHP13, PpHP17, and PpHP18 are large, it can be concluded that these strains did not benefit from the heterologous expression of cPos5, while PpHP5, PpHP6, and PpHP8 do. NADPH production by NADH kinase is more efficient in terms of both carbon and ATP conservation than the use of the UG and PPP, which would explain the reduction in the biomass and 3-HP yield in the strains PpHP13, PpHP17, and PpHP18.

To verify the consistency of the observed metabolic fluxes, FBA was used to verify the redox and energy conservation of the ^{13}C-MFA results. FBA results confirmed that both redox and energy balances could be conserved at the given experimental fluxes. The FBA results were also used to calculate the ATP produced and sinked at each pathway by each strain.

A higher ATP of maintenance for strains PpHP13, PpHP17, and PpHP18 was observed, as depicted in Figure 20B, being PpHP18 the strain with the highest ATP requirements among all strains. Conversely, the calculated ATP requirement for strain PpHP8 was the lowest, particularly due to the lowest growth associated maintenance energy (GAME) requirements, as it is the slowest growing strain.

Figure 20B shows there is a direct correlation between the overall ATP requirements of the strain and the amount of pyruvate that was directed into the TCA cycle for ATP production. While 54.1% of the pyruvate was channelled into the mitochondria in the reference strain, 45.7% was directed through the same pathway in strain PpHP8. The use of pyruvate raised to 52.0% and 52.7% when the cytosolic acetyl-CoA pathway was expressed (strains PpHP13 and PpHP18, respectively) to compensate for the higher ATP requirements.

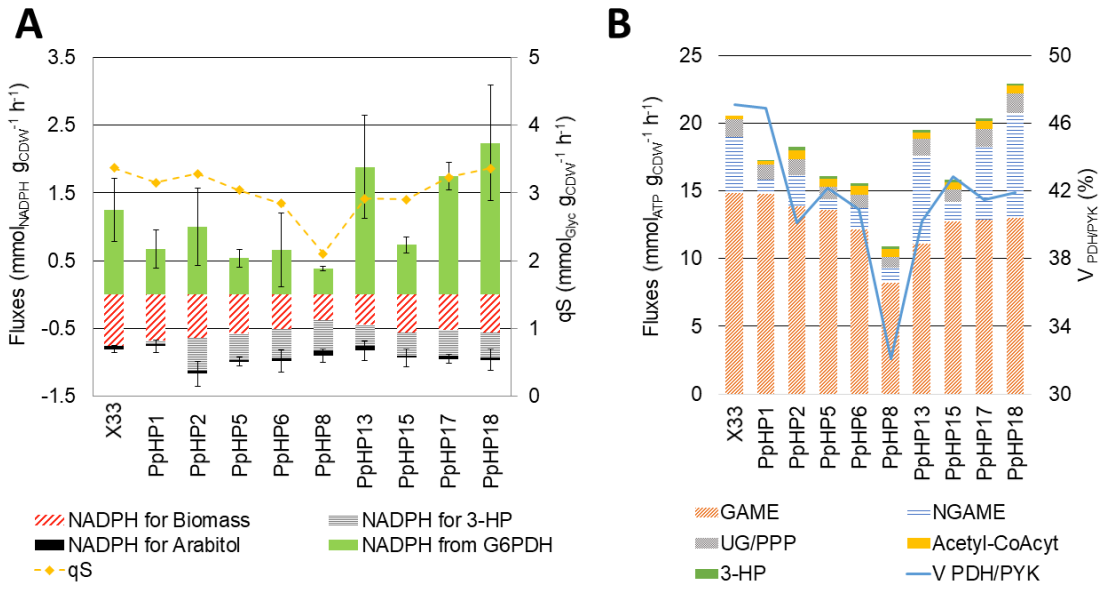

Figure 20. A) Production and consumption rates of NADPH (estimated from the ^{13}C-MFA results) and specific glycerol uptake rates for each strain. **B)** FBA results. The y-axis on the left side shows the sum of the fluxes for the main ATP-consuming reactions. The y-axis on the right side shows the percentage of pyruvate entering the mitochondria and the TCA cycle. To do so, the ratio of the fluxes of PYK (the main cytosolic pyruvate producing reaction) and PDH was calculated. Abbreviations: G6PDH, glucose-6-phosphate dehydrogenase; GAME, growth associated maintenance energy; NGAME, non-growth associated maintenance energy; UG/PPP: upper glycolysis and pentose phosphate pathway; Acetyl-CoAcyt: Cytosolic acetyl-CoA production pathway; $V_{PDH/PYK}$: Ratio between the fluxes of the pyruvate dehydrogenase (PDH) and the pyruvate kinase (PYK) reactions.

Results in Figure 20 also shows that not only the growth rate of strain PpHP8 was remarkably lower than the growth rate of the reference strain (0.13 h^{-1} and 0.22 h^{-1}, respectively), but also the substrate uptake rate for PpHP8 was lower than the uptake rate of strain X-33 (2.10 and 3.37 mmol $gCDW^{-1}$ h^{-1}). Noticeably, the glycerol uptake rate for all the recombinant strains grown at pH 5 fell within the same range (2.90 to 3.37 $mmol_{Glyc}$ $gCDW^{-1}$ h^{-1}, Figure 20), except for strain PpHP8, which was remarkably lower (2.10 $mmol_{Glyc}$ $gCDW^{-1}$ h^{-1}). A high activity of the malonyl-CoA to 3-HP pathway probably led to a reduced availability of acetyl-CoA for this strain. Acetyl-CoA plays a central role on the biosynthesis of precursors, and it plays a key role in physiological regulation processes, such as the acylation of histones [47]. Growth defects have also been reported in *S. cerevisiae* strains harbouring a high acetyl-CoA carboxylase activity, where depletion of acetyl-CoA was described as the most likely cause of hampered growth [48]. Moreover, the observed increase in the growth rate and the uptake rate when acs_{Se}^{L641P} was overexpressed support this hypothesis.

Altogether, these results point to acetyl-CoA depletion in strain PpHP8, hampering growth rate. When the cytosolic acetyl-CoA pathway was overexpressed (strains PpHP13, PpHP17, and PpHP18), growth rate increased. Increase in the growth rate increased ATP requirements, which increased channelling of pyruvate into the TCA cycle, hampering the 3-HP product yield.

5.3.4. The fluxome of *P. pastoris* at pH 3.5 reveals higher ATP maintenance requirements and higher D-arabitol production at lower pH

It has been reported that a pH of 3.5 (i.e., 1 unit below the pK_a of 3-HP) was optimal for the further downstream processing of 3-HP by solvent extraction [10]. Therefore, some 3-HP producing strains (i.e. PpHP1, PpHP6, PpHP8, PpHP15, and PpHP18) were further tested at pH 3.5.

Figure 21A describes the flux map for the reference strain at pH 5 and 3.5. No remarkable differences in the fluxome at such two conditions were observed for this strain. In contrast, higher UG and PPP fluxes were observed at pH 3.5 than at pH 5 in strains PpHP1, PpHP6, PpHP8, PpHP15, and PpHP18 (see Supplementary Figure S6 (Annex II; Section 3) for the comparison of the fluxes at pH 5 and 3.5 for strain PpHP8; see Supplementary File S13 for the other strains). A higher production of D-arabitol was also observed in most strains when growing at low pH (Figure 17 and Supplementary Figure S7 (Annex II; Section 3)).

The fold-change of the relative fluxes of each recombinant strains grown at pH 3.5 are shown in Figure 6B. The fold-changes were calculated using the relative fluxes of the reference strain grown at pH 3.5. The results show that the impact of each genetic modification in the flux of each strain followed a similar trend at pH 5 and pH 3.5 (Figure 18 and Figure 21B, respectively). 3-HP was produced at pH 3.5, but the yield was slightly lower than the one achieved at pH 5 for all the tested strains. For instance, the highest 3-HP producing strain at both pH values was PpHP8, which produced 3-HP at a yield of 0.084 ± 0.007 Cmol $Cmol^{-1}$ at pH 3.5 (0.081 ± 0.006 g g^{-1}), which is 23% lower than the product yield of the same strain at pH 5.

Figure 21 (next page). A. Flux map with the relative fluxes for the parental strain grown at pH 5 and pH 3.5. Metabolite abbreviation can be found in the figure caption of Figure 19 (page 118). **B.** Fold-change of the relative fluxes at a culture pH of 3.5 of the strains PpHP1, PpHP6, PpHP8, PpHP15, and PpHP18 compared to the parental strain. The colour scale describes the fold-change at a -1 to 1 range. MCR flux fold-change is compared to PpHP1. The upper bound of the colour scale of MCR is set to 4. **C.** NADPH sink fluxes and G6PDH flux of strains grown at pH 3.5. The qS for each strain is depicted using the y-axis.

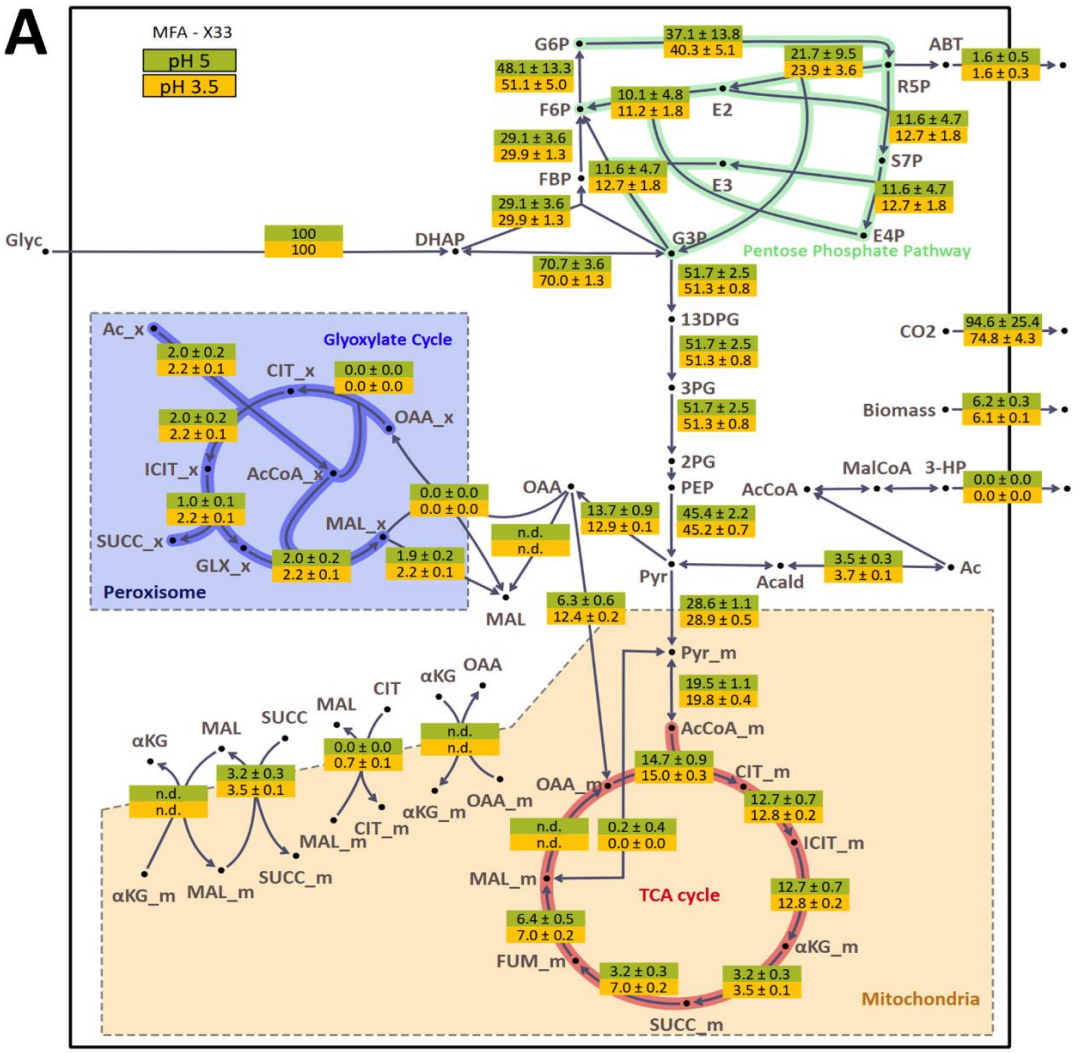
A
MFA - X33
pH 5
pH 3.5
Glyc
DHAP
G6P
F6P
FBP
G3P
E2
E3
E4P
R5P
S7P
ABT
Pentose Phosphate Pathway
13DPG
3PG
2PG
PEP
Pyr
AcCoA
Acald
Ac
CO2
Biomass
MalCoA
3-HP
OAA
MAL
Glyoxylate Cycle
Peroxisome
Ac_x
CIT_x
OAA_x
ICIT_x
AcCoA_x
MAL_x
SUCC_x
GLX_x
Mitochondria
Pyr_m
AcCoA_m
CIT_m
ICIT_m
αKG_m
SUCC_m
FUM_m
MAL_m
OAA_m
TCA cycle
B
Biomass yield
Pyruvate
Upper Glycolysis
Pentose Phosphate pathway
Lower glycolysis
PDH and TCA cycle
Cytosolic acetyl-CoA synthesis
3-HP production
Arabitol
Glyoxylate cycle
PpHP1
PpHP6
PpHP8
PpHP15
PpHP18
Log2 fold change
> 1 (4)
0
< -1
C
X-33
PpHP1
PpHP6
PpHP8
PpHP15
PpHP18
NADPH from G6PDH
NADPH for Biomass
NADPH for 3-HP
NADPH for Arabitol
qS

Regarding the NADPH production and consumption fluxes for each strain, the same trends were also observed at pH 3.5 (Figure 21C), that is, NADPH requirements in strain PpHP8 exceeded NADPH production from the PPP, meaning the flux through the cytosolic NADH kinase reaction compensated for that difference. In contrast, the NADPH production through the PPP in strain PpHP18 greatly exceeded the requirements.

Figure 21C also shows that substrate uptake rate also followed the same trend at both pH 5 and pH 3.5.

Altogether, these results contribute to the understanding of the adaptation of this yeast to a low pH at a fluxome level. Production of D-arabitol at acidic pH was increased for all the 3-HP-producing strains (from 2 to 20-fold). *P. pastoris* produces D-arabitol under several stress conditions, such as under hypoxia or osmotic stress [49,50]. Thus, higher D-arabitol production at a lower pH is probably due to a stress response. Moreover, the biomass yield at pH 3.5 was lower for most strains (Figure 17 and Supplementary Figure S7 (Annex II; Section 3)), indicating a higher ATP requirement for maintenance. Such results have already been described in other yeasts grown at lower pH, such as *S. cerevisiae*, where the decrease in the biomass yield was also attributed to an increase in the ATP of maintenance [51]. Moreover, the 3-HP yield was lower than the one of the same strains at pH 5, coherent with previous studies describing 3-HP production in *S. cerevisiae* grown at pH 3.5 [52]. The observed decrease in the product yield when the ATP usage increases confirms that ATP is a limiting factor towards increasing the 3-HP yield. Similarly, increased D-arabitol production, which is a NADPH sink, can also explain the decrease in the 3-HP yield.

Still, as metabolic flux profiles at pH 3.5 remained mostly unchanged compared to those at pH 5, it is plausible that strain engineering strategies at both pH will have the same outcome.

5.4. Conclusions

This study describes the simultaneous characterization of a set of 3-HP-producing *P. pastoris* recombinant strains at two relevant process conditions (pH 5 and pH 3.5) using a HT approach that has allowed to save time and resources compared to conventional strain-by-strain sequential approach. It provides meaningful insights regarding the impact of each genetic perturbation on the metabolic flux distribution of the

3-HP producing strain, pointing at competition for energy and carbon resources for either cell growth or 3-HP production as the major cause of the observed phenotypes, regardless the pH of the culture. Thus, it is concluded that both acetyl-CoA and ATP limitations are the main bottlenecks hampering 3-HP production in *P. pastoris*. To overcome such bottlenecks, a strategy to increase the glycolytic fluxes (e.g. rewiring the regulatory mechanisms of this pathway and/or selecting cultivation conditions that favour higher glycolytic fluxes) should be addressed. Overall, this study will contribute towards the improvement of *P. pastoris* strains and bioprocess engineering strategies to produce 3-HP and other acetyl-CoA-derived products.

Supplementary materials

The supplementary materials of this section have been submitted to the Dipòsit Digital de Documents (DDD) of the Universitat Autònoma de Barcelona. They can be downloaded from the following link: 10.5565/ddd.uab.cat/264385

List of Supplementary Files and description:

1. **Supplementary Files S1**: **Model compression**
   Short description: Genome Scale Metabolic model for *Pichia pastoris* metabolism. Matlab format compatible with scripts of *CobraToolbox* and *CellNetAnalyzer*. It includes the genome scale model in *CobraToolbox* and *CellNetAnalyzer* formats, the Matlab scripts for model compression, and the resulting pruned and core models.

2. **Supplementary Files S2: Model manual modifications**
   Short description: It includes the Matlab model to convert the *PpaCore* model into *PpaCore_3HP*, which includes some manual corrections of the reactions and the inclusion of the malonyl-CoA to 3-HP reactions.

3. **Supplementary Files S3: FTBL model generation and corrections**
   Short description: File containing the translation of the Matlab format Core model into a FTBL format model. It also includes the information for the simplification of the biomass stoichiometry reaction.

4. **Supplementary Files S4 - PpaCore_3HP**
   Short description: Core model of the metabolism of 3-HP-producing *Pichia pastoris* in FTBL format.

5. **Supplementary Files S5 - Pipetting OD600 and biomass concentration data from the mini bioreactor cultures**
   Short description: Raw data from the mini-bioreactor cultures. Including: pipetting data (time and subtracted volume), OD_{600}, and calculation of the biomass concentration from the OD_{600}.

6. **Supplementary Files S6: NMR results**

   Short description: Quantification of metabolites in the supernatant samples. NMR results. Peak integration data and processed data (concentration of each metabolite in g L^{-1}).

7. **Supplementary Files S7: MS mz ratios for the analysis of the AA**

   Short description: m/z setpoints for the analysis of all the ^{13}C-isotopologues of the amino acids using LC-MS.

8. **Supplementary Files S8 - Raw MS data and inoculum and IsoCor correction**

   Short description: Raw MS data (peak integration results) and processing: isotopologue relative abundance, correction of the ratios using the volume of inoculum, anc correction of the isotopologue distribution based on the abundance of the natural isotopes using *IsoCor*.

9. **Supplementary Files S9: Bioprocess parameters results**

   Short description: Bioprocess parameters results for each experiment and calculation of the average values for each strain at each pH.

10. **Supplementary Files S10: FBA input files scripts and results**

    Short description: Summary of the Monte Carlo results from the ^{13}C-MFA. The Monte Carlo results are used as input file for the Matlab script to perform Flux Balance Analysis for each strain. The FBA results are also included.

11. **Supplementary Files S11: *IsoDesign* results**

    Short description: Results obtained from *IsoDesign* using the PpaCore_3HP.ftbl model. *IsoDesign* is used for the optimization of the C-source for ^{13}C-MFA.

12. **Supplementary Files S12: ^{13}C-MFA raw results**

    Short description: Raw results from ^{13}C-MFA. It includes the input FTBL file for each experiment, and the *kvh* result file for each experiment generated using *influx_s*.

13. Supplementary Files S13: Flux results

Short description: Summary of all the results from the ^{13}C-MFA. It includes the flux results for all the expriments (average, SD, and Monte Carlo analysis results). It also includes the average and SDs of the fluxes for each triplicate experiment.

References

1. Peña, D.A., Gasser, B., Zanghellini, J., Steiger, M.G., and Mattanovich, D. (2018) Metabolic engineering of *Pichia pastoris*. *Metabolic Engineering*, 50, 2–15.
2. Schwarzhans, J.P., Luttermann, T., Geier, M., Kalinowski, J., and Friehs, K. (2017) Towards systems metabolic engineering in *Pichia pastoris*. *Biotechnology Advances*, 35 (6), 681–710.
3. De, S., Mattanovich, D., Ferrer, P., and Gasser, B. (2021) Established tools and emerging trends for the production of recombinant proteins and metabolites in *Pichia pastoris*. *Essays in Biochemistry*, 65 (2), 293–307.
4. Fina, A., Brêda, G.C.G.C., Pérez-Trujillo, M., Freire, D.M.G.D.M.G., Almeida, R.V.R.V., Albiol, J., and Ferrer, P. (2021) Benchmarking recombinant *Pichia pastoris* for 3-hydroxypropionic acid production from glycerol. *Microbial Biotechnology*, 14 (4), 1671–1682.
5. Fina, A., Heux, S., Albiol, J., and Ferrer, P. (2022) Combining Metabolic Engineering and Multiplexed Screening Methods for 3-Hydroxypropionic Acid Production in *Pichia pastoris*. 10, 942304.
6. Werpy, T., and Petersen, G. (2004) Top Value Added Chemicals from Biomass Volume I - Results of Screening for Potential Candidates from Sugars and Synthesis Gas. *U.S. Department of Energy*.
7. della Pina, C., Falletta, E., and Rossi, M. (2011) A green approach to chemical building blocks. the case of 3-hydroxypropanoic acid. *Green Chemistry*, 13 (7), 1624–1632.
8. van Maris, A.J.A., Konings, W.N., van Dijken, J.P., and Pronk, J.T. (2004) Microbial export of lactic and 3-hydroxypropanoic acid: Implications for industrial fermentation processes. *Metabolic Engineering*, 6 (4), 245–255.
9. López-Garzón, C.S., and Straathof, A.J.J. (2014) Recovery of carboxylic acids produced by fermentation. *Biotechnology Advances*, 32 (5), 873–904.
10. Chemarin, F., Athès, V., Bedu, M., Loty, T., Allais, F., Trelea, I.C., and Moussa, M. (2019) Towards an *in situ* product recovery of bio-based 3-hydroxypropionic acid: influence of bioconversion broth components on membrane-assisted reactive extraction. *Journal of Chemical Technology and Biotechnology*, 94 (3), 964–972.
11. Koganesawa, N., Aizawa, T., Shimojo, H., Miura, K., Ohnishi, A., Demura, M., Hayakawa, Y., Nitta, K., and Kawano, K. (2002) Expression and purification of a small cytokine growth-blocking peptide from armyworm *Pseudaletia separata* by an optimized fermentation method using the methylotrophic yeast *Pichia pastoris*. *Protein Expression and Purification*, 25 (3), 416–425.
12. Damasceno, L.M., Pla, I., Chang, H.J., Cohen, L., Ritter, G., Old, L.J., and Batt, C.A. (2004) An optimized fermentation process for high-level production of a single-chain Fv antibody fragment in *Pichia pastoris*. *Protein Expression and Purification*, 37, 18–26.
13. Heux, S., Bergès, C., Millard, P., Portais, J.C., and Létisse, F. (2017) Recent advances in high-throughput ^{13}C-fluxomics. *Current Opinion in Biotechnology*, 43 (3), 104–109.
14. Heux, S., Meynial-Salles, I., O'Donohue, M.J., and Dumon, C. (2015) White biotechnology: State of the art strategies for the development of biocatalysts for biorefining. *Biotechnology Advances*, 33 (8), 1653–1670.
15. Wasylenko, T.M., and Stephanopoulos, G. (2015) Metabolomic and ^{13}C-metabolic flux analysis of a xylose-consuming *Saccharomyces cerevisiae* strain expressing xylose isomerase. *Biotechnology and Bioengineering*, 112 (3), 470–483.
16. Kohlstedt, M., Becker, J., and Wittmann, C. (2010) Metabolic fluxes and beyond-systems biology understanding and engineering of microbial metabolism. *Applied Microbiology and Biotechnology*, 88, 1065–1075.
17. Wiechert, W., Möllney, M., Petersen, S., and de Graaf, A.A. (2001) A universal framework for ^{13}C metabolic flux analysis. *Metabolic Engineering*, 3 (3), 265–283.
18. Ferrer, P., and Albiol, J. (2014) ^{13}C-Based Metabolic Flux Analysis of Recombinant *Pichia pastoris*. *Methods in Molecular Biology*, 1191, 291–313.
19. Tomàs-Gamisans, M., Ødum, A.S.R., Workman, M., Ferrer, P., and Albiol, J. (2019) Glycerol metabolism of *Pichia pastoris* (*Komagataella* spp.) characterised by ^{13}C-based metabolic flux analysis. *New Biotechnology*, 50, 52–59.
20. Rußmayer, H., Buchetics, M., Gruber, C., Valli, M., Grillitsch, K., Modarres, G., Guerrasio, R., Klavins, K., Neubauer, S., Drexler, H., Steiger, M., Troyer, C., al Chalabi, A., Krebiehl, G., Sonntag, D., Zellnig, G., Daum, G., Graf, A.B., Altmann, F., Koellensperger, G., Hann, S., Sauer, M., Mattanovich, D., and Gasser, B. (2015) Systems-level organization of yeast methylotrophic lifestyle. *BMC Biology*, 13, 80.

21. Tomàs-Gamisans, M., Ferrer, P., and Albiol, J. (2018) Fine-tuning the *P. pastoris* iMT1026 genome-scale metabolic model for improved prediction of growth on methanol or glycerol as sole carbon sources. *Microbial Biotechnology*, 11 (1), 224–237.
22. Tomàs-Gamisans, M., Ferrer, P., and Albiol, J. (2016) Integration and validation of the genome-scale metabolic models of *Pichia pastoris*: A comprehensive update of protein glycosylation pathways, lipid and energy metabolism. *PLoS ONE*, 11, e0148031.
23. Klamt, S., Saez-Rodriguez, J., and Gilles, E.D. (2007) Structural and functional analysis of cellular networks with CellNetAnalyzer. *BMC Systems Biology*, 1 (2), 2.
24. Lehnen, M., Ebert, B.E., and Blank, L.M. (2017) A comprehensive evaluation of constraining amino acid biosynthesis in compartmented models for metabolic flux analysis. *Metabolic Engineering Communications*, 5, 34–44.
25. Solà, A., Maaheimo, H., Ylönen, K., Ferrer, P., and Szyperski, T. (2004) Amino acid biosynthesis and metabolic flux profiling of *Pichia pastoris*. *European Journal of Biochemistry*, 271 (12), 2462–2470.
26. Gombert, A.K., dos Santos, M.M., Christensen, B., and Nielsen, J. (2001) Network identification and flux quantification in the central metabolism of *Saccharomyces cerevisiae* under different conditions of glucose repression. *Journal of Bacteriology*, 183 (4), 1441–1451.
27. Wiechert, W., and de Graaf, A.A. (1997) Bidirectional reaction steps in metabolic networks. *Biotechnology and Bioengineering*, 55 (1), 101–135.
28. Millard, P., Sokol, S., Letisse, F., and Portais, J.-C. (2014) IsoDesign: A software for optimizing the design of ^{13}C-metabolic flux analysis experiments. *Biotechnology and Bioengineering*, 111 (1), 202–208.
29. Sokol, S., Millard, P., and Portais, J.C. (2012) Influx_s: Increasing numerical stability and precision for metabolic flux analysis in isotope labelling experiments. *Bioinformatics*, 28 (5), 687–693.
30. Heux, S., Juliette, P., Stéphane, M., Serguei, S., and Jean-Charles, P. (2014) A novel platform for automated high-throughput fluxome profiling of metabolic variants. *Metabolic Engineering*, 25, 8–19.
31. Maurer, M., Kühleitner, M., Gasser, B., and Mattanovich, D. (2006) Versatile modeling and optimization of fed batch processes for the production of secreted heterologous proteins with *Pichia pastoris*. *Microbial Cell Factories*, 5, 37.
32. Heuillet, M., Bellvert, F., Cahoreau, E., Letisse, F., Millard, P., and Portais, J.C. (2018) Methodology for the Validation of Isotopic Analyses by Mass Spectrometry in Stable-Isotope Labeling Experiments. *Analytical Chemistry*, 90 (3), 1852–1860.
33. Millard, P., Delépine, B., Guionnet, M., Heuillet, M., Bellvert, F., and Létisse, F. (2019) IsoCor: Isotope correction for high-resolution MS labeling experiments. *Bioinformatics*, 35 (21), 4484–4487.
34. Peiro, C., Millard, P., de Simone, A., Cahoreau, E., Peyriga, L., Enjalbert, B., and Heux, S. (2019) Chemical and metabolic controls on dihydroxyacetone metabolism lead to suboptimal growth of *Escherichia coli*. *Applied and Environmental Microbiology*, 85 (15), e00768-19.
35. Schellenberger, J., Que, R., Fleming, R., Thiele, I., Orth, J., Feist, A., Zielinski, D., Bordbar, A., Lewis, N., Rahmanian, S., Kang, J., Hyduke, D., and Palsson, B. (2011) Quantitative prediction of cellular metabolism with constraint-based models: the COBRA Toolbox v2.0. *Nature Protocols*, 6 (9), 1290–1307.
36. Holzhütter, H.G. (2004) The principle of flux minimization and its application to estimate stationary fluxes in metabolic networks. *European Journal of Biochemistry*, 271 (14), 2905–2922.
37. Droste, P., Miebach, S., Niedenführ, S., Wiechert, W., and Nöh, K. (2011) Visualizing multi-omics data in metabolic networks with the software Omix - A case study. *BioSystems*, 105 (2), 154–161.
38. Orth, J.D., Thiele, I., and Palsson, B.Ø.O. (2010) What is flux balance analysis? *Nature Biotechnology*, 28 (3), 245–248.
39. Schuetz, R., Kuepfer, L., and Sauer, U. (2007) Systematic evaluation of objective functions for predicting intracellular fluxes in *Escherichia coli*. *Molecular Systems Biology*, 3, 119.
40. Christodoulou, D., Link, H., Fuhrer, T., Kochanowski, K., Gerosa, L., and Sauer, U. (2018) Reserve Flux Capacity in the Pentose Phosphate Pathway Enables Escherichia coli's Rapid Response to Oxidative Stress. *Cell Systems*, 6 (5), 569-578.e7.
41. Tomàs-Gamisans, M., Andrade, C.C.P., Maresca, F., Monforte, S., Ferrer, P., and Albiol, J. (2020) Redox engineering by ectopic overexpression of NADH kinase in recombinant *Pichia pastoris* (*Komagataella phaffii*): Impact on cell physiology and recombinant production of secreted proteins. *Applied and Environmental Microbiology*, 86, e02038-19.
42. van Hoek, P., Flikweert, M.T., van der Aart, Q.J.M., Steensma, H.Y., van Dijken, J.P., and Pronk, J.T. (1998) Effects of pyruvate

decarboxylase overproduction on flux distribution at the pyruvate branch point in *Saccharomyces cerevisiae*. *Applied and Environmental Microbiology*, 64 (6), 2133–2140.

43. Schaaff, I., Heinisch, J., and Zimmerman, F. (1989) Overexpression of glycolytic enzymes in yeast. *Yeast*, 5 (4), 285–290.
44. Baumann, K., Carnicer, M., Dragosits, M., Graf, A.B., Stadlmann, J., Jouhten, P., Maaheimo, H., Gasser, B., Albiol, J., Mattanovich, D., and Ferrer, P. (2010) A multi-level study of recombinant *Pichia pastoris* in different oxygen conditions. *BMC Systems Biology*, 4, 141.
45. Baumann, K., Dato, L., Graf, A.B., Frascotti, G., Dragosits, M., Porro, D., Mattanovich, D., Ferrer, P., and Branduardi, P. (2011) The impact of oxygen on the transcriptome of recombinant *S. cerevisiae* and *P. pastoris* - a comparative analysis. *BMC Genomics*, 12, 218.
46. Ata, Ö., Rebnegger, C., Tatto, N.E., Valli, M., Mairinger, T., Hann, S., Steiger, M.G., Çalık, P., and Mattanovich, D. (2018) A single Gal4-like transcription factor activates the Crabtree effect in *Komagataella phaffii*. *Nature Communications*, 9 (1), 1–10.
47. Shi, L., and Tu, B.P. (2015) Acetyl-CoA and the regulation of metabolism: Mechanisms and consequences. *Current Opinion in Cell Biology*, 33, 125–131.
48. Pereira, H., Azevedo, F., Domingues, L., and Johansson, B. (2022) Expression of *Yarrowia lipolytica* acetyl-CoA carboxylase in *Saccharomyces cerevisiae* and its effect on in-vivo accumulation of Malonyl-CoA. *Computational and Structural Biotechnology Journal*, 20, 779–787.
49. Dragosits, M., Stadlmann, J., Graf, A., Gasser, B., Maurer, M., Sauer, M., Kreil, D.P., Altmann, F., and Mattanovich, D. (2010) The response to unfolded protein is involved in osmotolerance of *Pichia pastoris*. *BMC Genomics*, 11 (1), 207.
50. Baumann, K., Carnicer, M., Dragosits, M., Graf, A.B., Stadlmann, J., Jouhten, P., Maaheimo, H., Gasser, B., Albiol, J., Mattanovich, D., and Ferrer, P. (2010) A multi-level study of recombinant *Pichia pastoris* in different oxygen conditions. *BMC Systems Biology*, 4, 141.
51. Hakkaart, X., Liu, Y., Hulst, M., el Masoudi, A., Peuscher, E., Pronk, J., van Gulik, W., and Daran-Lapujade, P. (2020) Physiological responses of *Saccharomyces cerevisiae* to industrially relevant conditions: Slow growth, low pH, and high CO_2 levels. *Biotechnology and Bioengineering*, 117 (3), 721–735.
52. Borodina, I., Kildegaard, K.R., Jensen, N.B., Blicher, T.H., Maury, J., Sherstyk, S., Schneider, K., Lamosa, P., Herrgård, M.J., Rosenstand, I., Öberg, F., Forster, J., and Nielsen, J. (2015) Establishing a synthetic pathway for high-level production of 3-hydroxypropionic acid in *Saccharomyces cerevisiae* via β-alanine. *Metabolic Engineering*, 27, 57–64.

6

GENERAL CONCLUSIONS AND FUTURE OUTLOOK

Pichia pastoris has been extensively studied to produce heterologous proteins. However, its potential as cell factory for the production of metabolites remains largely unexplored. *A priori*, there are features that make *P. pastoris* an attractive chassis to produce fine and bulk chemical products of industrial interest from renewable feedstocks. Firstly, it can grow on defined medium reaching high cell densities. Moreover, compared to the traditional industrial workhorses *Escherichia coli* and *Saccharomyces cerevisiae*, *P. pastoris* can grow on crude glycerol, a by-product from the biodiesel industry, or methanol, which can also be obtained from renewable sources, e.g. CO_2. Finally, it can grow at a low pH, which facilitates the downstream processing of certain classes of products such as carboxylic acids by solvent extraction. Such downstream methods can also be applied *in situ* to avoid reaching toxic carboxylic acid concentrations, leading to a higher product yield and productivity.

In this study, *P. pastoris* has been metabolically engineered to produce 3-hydroxypropionic acid (3-HP) through the malonyl-CoA pathway. 3-HP is a carboxylic acid that serves as a chemical platform to produce various chemicals of interest with numerous applications. The aim of the project was to develop *P. pastoris* strains producing 3-HP as an exemplary case to investigate its potential as a chassis organism to produce organic acids from crude glycerol. As this feedstock is a side-product from the biodiesel production industry, revalorization of such side stream would contribute towards the goal of building a circular bioeconomy.

Notably, heterologous expression of the malonyl-CoA reductase from *Chloroflexus aurantiacus* (mcr_{Ca}) under the control of pGAP resulted in a higher 3-HP yield in *P. pastoris* (strain PpHP1) than in other previously tested host organisms. Coherently, the MCR specific activity in this strain was an order of magnitude higher than the reported values in other microorganisms with similar genetic constructions. Therefore, the availability of a strong, constitutive, and well-characterized promoter such as pGAP appear as an important tool towards the successful development of *P. pastoris* metabolic engineering projects for metabolite production. In addition to the pGAP expression system, it is derived that the synthetic biology, systems biology, and bioprocess engineering tools developed in the last few decades for the optimization of *P. pastoris* strains and processes to produce heterologous proteins pave the way for the implementation of the same tools for the production of bulk chemicals in this yeast.

Afterwards, metabolic engineering strategies were focused on increasing the expression of the heterologous malonyl-CoA to 3-HP pathway and increasing the

availability of the precursors of such pathway (malonyl-CoA and NADPH). Metabolic engineering of the initial *P. pastoris* 3-HP producing strain (resulting in strain PpHP8) led to an 18-fold increase in the 3-HP product yield (from 0.01 Cmol $Cmol^{-1}$ to 0.18 Cmol $Cmol^{-1}$ of glycerol). Such results clearly benchmark *P. pastoris* as a promising candidate for the production of not only 3-HP, but also other acetyl-CoA or malonyl-CoA products, such as free fatty acids or polyketides.

Additional metabolic engineering cycles of strain PpHP8 were aimed at increasing acetyl-CoA availability and reducing production of by-product D-arabitol. Nevertheless, the resulting strain (PpHP18) showed a lower product yield. Multiplexed screening methods (cultures on deep-well plates, mini-bioreactors, and falcon tubes with FeedBeads®) contributed to further understand the impact of each genetic modification on strain performance parameters, i.e. product yield and growth rate.

3-HP production of strains PpHP8 and PpHP18 was very similar at low growth rates (i.e., using FeedBeads®), but different at μ_{max} (i.e., in the mini bioreactor and deep-well plates experiments). As the cultivation method based on FeedBeads® resembles fed-batch cultivation conditions, the two strains that ranked as top 3-HP producers in this screening system (PpHP8 and PpHP18) were selected for further tests at bioreactor scale. Remarkably, strain PpHP18 did not rank among the 2-top 3-HP-producers in deep-well and mini bioreactor batch cultures. The better results obtained for PpHP18 at a bioreactor scale proof that use of FeedBeads® during screening protocols provides valuable information for the characterization of the strains under bioprocess-relevant conditions. Characterization of the strains using several screening strategies proved to be beneficial towards further understanding the effect of each genetic modification on the yeast's performance. Getting the utmost amount of information from each strain during the screening phase contributes towards making assessed experimental designs for the following DBTL cycles.

The 3-HP concentration (37.05 g L^{-1}) and productivity (0.71 g L^{-1} h^{-1}) achieved in a fed-batch culture of the strain PpHP18 using glycerol as sole C-source were the highest metrics reported in yeast to date. Higher metrics have been achieved in bacterial hosts such as *E. coli* or *Klebsiella pneumoniae*. However, use of such bacterial strains for the commercial implementation of a 3-HP production process poses some disadvantages. First, they expressed the glycerol to 3-HP CoA-independent pathway, which is coenzyme-B12 dependent. To avoid the addition of such expensive cofactor, yeast extract is added to the medium. Moreover, these bacteria produce more by-products

than *P. pastoris* PpHP18 (which does not produce any major by-product). Presence of yeast extract and by-products in fermentation broth can make the downstream process more complex and costly.

Literature availability describing the regulatory mechanisms of the metabolism of *P. pastoris* is still scarce. Availability of High Throughput platforms for systems biology (e.g. fluxomcis) will contribute towards accelerating the knowledge on such matter. The High Throughput ^{13}C-Metabolic Flux Analysis (^{13}C-MFA) protocol reported in this PhD thesis has allowed to simultaneously characterize the fluxome of multiple strains at two bioprocess-relevant conditions (pH 5 and pH 3.5). Clearly, automatised platforms like the one utilised herein are necessary to match with the increasing number of strains that are lately generated within the same project due to the rapid advances in the synthetic biology field, thereby supporting the acceleration and debottlenecking of the design-build-test-learn (DBTL) cycle for strain engineering. Moreover, this study demonstrates that such platforms can be easily adapted to test different microorganisms and feedstocks.

Combined ^{13}C-MFA results showed that the observed phenotypes are a result of the crosstalk between: i) the availability of precursors for growth and, in particular, the availability of acetyl-CoA; and ii) the ATP availability to satisfy growth demands. This was clearly observed when comparing strains PpHP8 and PpHP18: While the growth rate of strain PpHP8 was remarkably reduced, once the acetyl-CoA production pathway was overexpressed (strain PpHP18), the growth rate increased. However, as growth-associated ATP and carbon precursor requirements also increased, production of 3-HP was negatively affected.

The ^{13}C-MFA results also point to a tight control of the glycolytic flux, as simultaneous overexpression of most genes of the pyruvate to 3-HP pathway (*PDC1*, acs_{Se}^{L641P}, $ACC1_{Yl}$, *mcr*-C_{Ca}, and *mcr*-N_{Ca}) in strain PpHP18 did not pull a higher glycolytic flux compared to the parental strain (X-33). Such tight control of the glycolytic flux has also been described in yeast *S. cerevisiae*. However, while *S. cerevisiae* is a Crabtree positive yeast, *P. pastoris* is Crabtree negative. Therefore, regulation of the glycolytic flux and, in particular, of the fluxes at the pyruvate node for these two yeasts might be remarkably different.

To further increase product yield, the malonyl-CoA to 3-HP production pathway could be further overexpressed. Similarly, the pyruvate to cytosolic acetyl-CoA and malonyl-CoA pathway could also be overexpressed. However, as observed in the

^{13}C-MFA experiments, none of these strategies resulted in higher glycolytic fluxes at maximal growth rate (μ_{max}). Therefore, while such strategies may increase the product yield, they may also result in a remarkable decrease in the strain's growth rate, which would negatively impact the productivity of the strain. Therefore, strategies aiming at increasing the glycolytic fluxes could positively impact both the product yield and the productivity.

Finally, 3-HP toxicity has been reported in other microorganisms. We also observed how high 3-HP concentrations at the late stages of the fed-batch processes hampered cell growth of *P. pastoris*. Therefore, strategies to avoid such toxicity effect in *P. pastoris* should also be addressed. Both targeted genetic engineering and adaptive laboratory evolution approaches have increased the 3-HP tolerance in other microorganisms. Similar approaches could be pursued in *P. pastoris*.

Annex I

High throughput stationary ^{13}C-based Metabolic Flux Analysis of *Pichia pastoris* strains

Chapter submitted for publication as a Book Chapter of the *Pichia protocols* series from *Methods in Molecular Biology*

Authors: Albert Fina[1], Pierre Millard[2], Cécilia Bérgès[2], Pau Ferrer[1], Joan Albiol[1], and Stéphanie Heux[2]

Affiliation: [1]Department of Chemical, Biological and Environmental Engineering, Universitat Autònoma de Barcelona, Bellaterra, Spain; [2] TBI, Université de Toulouse, CNRS, INRAE, INSA, Toulouse, France

Supplementary Materials of this chapter were submitted to the Dipòsit Digital de Documents of the Universitat Autònoma de Barcelona. They can be accessed online using the following link: https://doi.org/10.5565/ddd.uab.cat/263045

Table of contents

Abstract

^{13}C-based Metabolic Flux Analysis (^{13}C-MFA) is an experimental approach allowing the quantification of the intracellular reaction rates (fluxes) that has become a valuable tool in the field of metabolic systems engineering. Rapid advances in the area of synthetic biology are leading to the generation of large numbers of engineered strains for the same research project. Thereby, the use of high throughput cultivation and analytical platforms is required in order to test and characterise these sets of strains and extract meaningful information for further strain engineering cycles. Here, a detailed protocol for fluxome determination of a set of *Pichia pastoris* strains using a high throughput cultivation platform is described.

1. Introduction

Fluxomics can be defined as a set of methodologies for quantitative analysis of the distribution of metabolic fluxes (i.e. *in vivo* rates of metabolic reaction) in an organism, providing a tool for analysis of metabolic phenotypes. Determining the metabolic flux distribution of a microorganism can be used to assess the impact of a genetic modification or environmental perturbation at the metabolic level, as well as to identify genetic engineering targets for further strain improvements. However, besides the extracellular (input-output) exchange fluxes, it is generally not possible to directly measure intracellular metabolic fluxes in a metabolic network. Thus, several techniques combining experimental measurements with mathematical modelling approaches have been developed for their determination. The most well-established of those techniques rely on the use of isotopically labelled substrates, and on the measurement of label incorporation into metabolic intermediates and by-products. There exist multiple protocols for fluxomic analyses, which are usually grouped into two main sub-groups: Stationary and instationary (also known as isotopic non-stationary) fluxomics [1]. Stationary ^{13}C-based Metabolic Flux Analysis (^{13}C-MFA) relies on the evaluation of the metabolic fluxes under metabolic and isotopic steady-state conditions, that is, defined as constant metabolic fluxes, metabolites concentration, and labelling pattern of the metabolites over time. Therefore, samples are withdrawn from the culture once the isotopic and metabolic steady states have been reached (i.e., from a chemostat culture or a mid-exponential phase of a batch culture). Afterwards, isotope incorporation into metabolites can be determined using Mass Spectrometry (MS) coupled with Liquid Chromatography (LC) or Gas Chromatography (GC), which provide access to their isotopologue distribution, and/or Nuclear Magnetic Resonance (NMR), which provides positional labelling information [2]. In the case of instationary fluxomics, a switch from non-labelled to partially or fully labelled substrate (or vice versa) is performed in a culture under steady state conditions. Afterwards, multiple samples are withdrawn while labelling progresses towards its steady state. Again, the fluxes can be determined from the isotopologue distribution or the positional labelling of the metabolites. In this case, the metabolic fluxes and the concentration of the metabolites remain constant, but the labelling of the metabolites changes over time. Both stationary and instationary fluxomics of *P. pastoris* strains have been described [3–5]. Compared to the instationary approach, stationary ^{13}C-MFA requires less samples, resulting in a less experimentally and computationally demanding task. In contrast, instationary approach enhances the

precision of flux measurements, improves the coverage of metabolic network (e.g. to measure fluxes through parallel reactions), and allows measuring fluxes in microorganisms that metabolize C1 compounds such as CO_2 or methanol [6] (see Note 8).

To perform a fluxomics experiment, a model of the pathways of interest, typically central carbon metabolism, is required. Models of *P. pastoris* core metabolism were obtained combining literature data, specific biomass composition, and assuming similarity with *Saccharomyces cerevisiae* when no data was available [5,7,8]). Recently, the use of a core model derived from the *P. pastoris* Genome Scale Model (GSM) *iMT1026v3* was reported [9]. The GSM *iMT1026v3* contains the biomass composition of *P. pastoris* for different C-sources (glucose, glycerol, methanol, and combinations of thereof), as well as the reactions for the synthesis of model heterologous proteins [10]. Moreover, not all enzymes are active in all culture condition. Therefore, the compression of this GSM into a context-specific substrate dependant core model is preferred [11,12].

Easiness of genetic engineering of *P. pastoris* due to multiple recent advances in the synthetic biology field has led to the rapid generation of multiple strains in a short time [13–15]. To study the effect of the genetic manipulations on the strain metabolism, it is convenient to be able to analyse a large battery of strains using fluxomics. Performing high throughput instationary fluxomics would require a significantly higher number of samples together with fast sampling and quenching procedures. As not all the steps of the process can be fully automatized (sample treatment, peak integration, etc.), high throughput instationary fluxomics are still beyond the current feasible automatization capabilities. Therefore, the current protocol will describe the workflow to perform high throughput stationary ^{13}C-MFA in batch cultures of *P. pastoris*. A simplified representation of the workflow described in this chapter can be found in Supplementary Figure S1.

A high throughput fluxomics approach for yeast has previously been described [16]. In that protocol, cells were cultivated on 96-deep well plates, where cell growth was manually monitored. A single sample was taken at the mid-exponential phase and the fluxes were derived from the analysis of this sample. The determination of the extracellular exchange fluxes was obtained by fitting an exponential equation to the first and last points of the exponential phase. In the present case, the high throughput stationary ^{13}C-MFA protocol will describe the use of a robotic platform with multiple mini

bioreactors, which allows a better control of the growth conditions (pH, O_2, etc.). Multiple samples can be collected to calculate the substrates and products exchange rates. Therefore, biases caused by a lag phase between strains can be avoided. Moreover, automatization of absorbance density measurements reduces the noise derived from withdrawing the plate from the incubator shaker to measure the biomass concentration. In this protocol, a custom-made platform that was designed specifically for high throughput fluxomics was used [17]. This platform contains 48 mini bioreactors and samples are withdrawn and treated (quenching, centrifugation, and/or filtration) automatically. However, other high throughput cultivation platforms could be adapted to the same use [18].

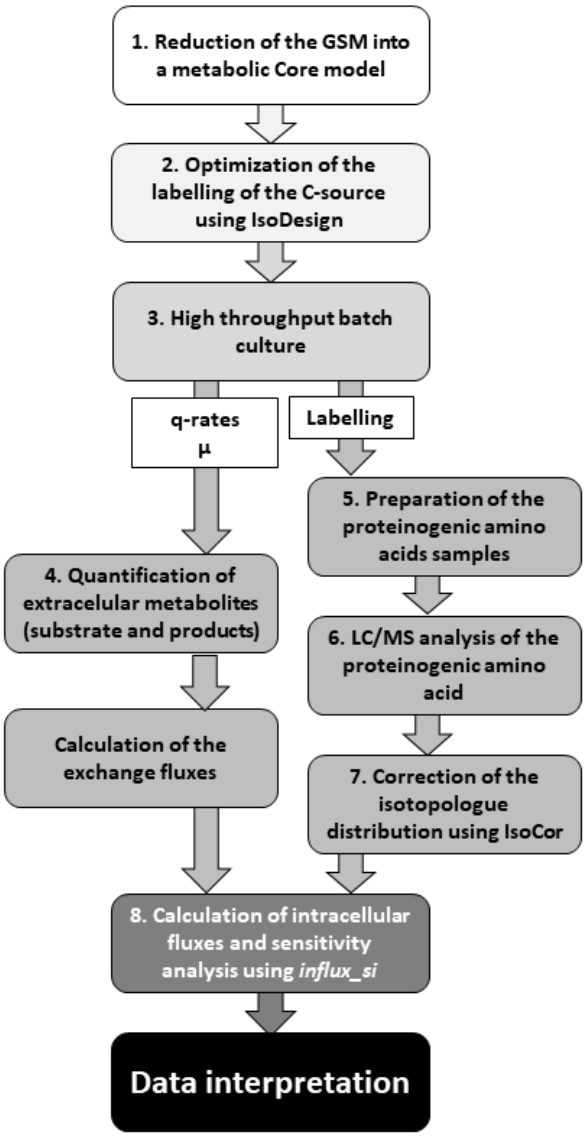

Supplementary figure S1. Workflow for the high throughput metabolic flux profiling of a set of *P. pastoris* strains.

In this work, the isotopic distribution of the proteinogenic amino acids was analysed using LC/MS. However, all the sections of the protocol besides section 3.6 would remain identical if the positional labelling of the proteinogenic amino acids was determined using NMR. Similarly, sections 3.1 and 3.2 of this protocol would remain without changes if the intracellular metabolite isotopologue distributions were measured. The protocols described elsewhere to quench the metabolism and analyse the intracellular metabolites from the cell culture could be used [5,19]. Additionally, sections 3.4, 3.7, and 3.8 would still apply, using the data obtained from the intracellular metabolites measurements, instead of the proteinogenic amino acids results.

2. Materials and Software requirements

2.1. Software required (see Note 1).

1. Matlab (Matlab inc., Mathworks, MA, USA).
2. *Cobra Toolbox* [20], which is a Matlab toolbox for the constrain-based analysis of metabolic networks.
3. *CellNetAnalyzer* toolbox for Matlab [21], which is a group of methods to analyse the structure and function of metabolic, signalling, and regulatory networks.
4. *influx_si* [22], which requires installation of *Anaconda* with *Python3*. A detailed guideline for the installation of *influx_si* can be found at https://metasys.insa-toulouse.fr/software/influx/doc/install.html. *Influx_si* is used to calculate the fluxes of metabolic reactions from a given model and the labelling data from fluxomics experiments.
5. *IsoDesign* [23], which can be downloaded from https://metasys.insa-toulouse.fr/software/isodes/. This software is used to optimize the labelling of the C-source for fluxomics applications.
6. *PhysioFit* [24], an R-based tool to calculate the cell growth and the production and consumption rates. It can be downloaded from https://github.com/MetaSys-LISBP/PhysioFit.
7. *IsoCor* [25], a *Python3*-based tool which is used to correct the MS labelling data for the presence of naturally-occurring isotopes (^{2}H, ^{13}C, ^{15}N, etc.). It can be downloaded from https://isocor.readthedocs.io/.

2.2. Starting Genome-Scale Metabolic model (GSM) model

1. The *iMT1026v3* (Tomàs-Gamisans et al., 2018; https://www.ebi.ac.uk/biomodels/MODEL1612130000) or any other *P. pastoris* GSM can be used.

2.3. High throughput mini bioreactor culture components

1. YPG medium: 10% w/v yeast extract, 20% w/v peptone, and 1% v/v glycerol.

2. High throughput culture platform: The use of a High Throughput Fluxomics robotic platform including an automated sampling, quenching, and processing of samples for fluxomic applications is recommended [17]. However, other multiple mini bioreactor systems including inline, online or atline OD_{600} measurements, such as the ones reviewed elsewhere [18], could be also used.

3. Batch medium: 2.5 g L^{-1} glycerol (conveniently partially ^{13}C-labelled), 1.8 g L^{-1} citric acid, 0.02 g L^{-1} $CaCl_2 \cdot 2\ H_2O$, 12.6 g L^{-1} $(NH_4)_2HPO_4$, 0.5 g L^{-1} $MgSO_4 \cdot 7\ H_2O$, 0.9 g L^{-1} KCl, 0.4 mg L^{-1} biotin, and 4.6 ml L^{-1} of PTM1 trace salts [27]. The pH adjusted to 5.0 using HCl. The ^{13}C-labelled glycerol could be replaced with other labelled C-sources, such as ^{13}C-labelled glucose, depending on the condition to investigate or question to address.

4. To sterilize the medium, mix all medium compounds except the biotin, the PTM1 salts and the labelled substrate. Autoclave the medium. Filter-sterilize the concentrated C-source, the biotin, and the PTM1 salts. Add the filter sterilized components to the autoclaved medium components in sterile conditions.

2.4. Equipment for sample preparation

1. Centrifuge.
2. HCl 6N.
3. Rotavapor (Büchi, Switzerland).

2.5. Materials and equipment for proteinogenic amino acids labelling analysis using LC/MS

1. Column: Discovery HS F5 HPLC column of 150 x 2.1 mm with particle size 5 µm (Supelco Bellefonte, PEN, USA).
2. Precolumn: Discovery HS F5 Supelguard Cartridge of 20 x 2.1 mm with particle size 5 µm (Supelco Bellefonte, PEN, USA).
3. Liquid Chromatography system, such as UHPLC Vanquish (Thermo Fisher Scientific, MA, USA).
4. High resolution mass spectrometry detector, such as Orbitrap Q Exactive Plus, with a heated electrospray ionization (HESI) source (Thermo Fisher Scientific, MA, USA).
5. Acetonitrile and formic acid. LC/MS grade.
6. Ultrapure water (milli Q).
7. Solvent A: 0.1% v/v formic acid in ultrapure water.
8. Solvent B: 0.1% v/v formic acid in acetonitrile.

3. Methods

3.1. Reduction of the GSM into a metabolic Core model

1. Install Matlab, COBRA toolbox and *CellNetAnalyzer* toolbox if not already done. Launch Matlab and the *CobraToolbox* on your computer. Load the GSM *iMT1026v3*, which is provided in the Supplementary Files (*iMT1026v3.mat*; Supplementary File S1). Check that the installations and the model are running by constraining the uptake rates for all C-sources using the function *changeRxnBounds* to set the lower boundaries to 0. Set the lower bound of glycerol to -1 mmol $\cdot$ g_{CDW}^{-1} $\cdot$ h^{-1} and change the upper boundaries of the biomass composition reactions for growth on glycerol (*LIPIDS_glyc, PROTEINS_glyc, STEROLS_glyc,* and *BIOMASS_glyc*) to 1000. The boundaries for the other biomass composition reactions, available for growth on alternative carbon sources,

should be set to 0. Set the value of the ATP of maintenance (*ATPM*) to 2.51 mmol · g_{CDW}^{-1} · h^{-1} [26]. Perform FBA using the maximization of the growth rate as the objective function. The maximal growth rate result should be 0.0587 h^{-1}.

2. The following model reduction steps are based on the *NetworkReducer* algorithm [28]. Once working installations of Matlab and the *CobraToolbox* are ready, launch *CellNetAnalyzer* by running the function *startcna.m*. Afterwards, upload the *PpaGS.mat* (Supplementary File S2), which corresponds to the *iMT1026v3* model in a format readable for *CellNetAnalyzer.* Alternativelly use the '*CNAcobra2cna*' function of the *CellNetAnalyzer* toolbox (also included in the COBRA toolbox) to convert a COBRA model to a *CellNetAnalyzer* readable format. See *CellNetAnalyzer* manual for additional details. Use the Matlab script *model_reduction.m* (Supplementary File S3) to obtain a reduced model from the *P. pastoris* GSM. Change the reactions and metabolites that you want to be protected in the final model using the vectors *protect_reac* and *protect_met*, respectively (see Note 2). Specific phenotypes can also be protected using the vector *protect_func*. In the *model_reduction.m* file, mentioned above, reactions coupled to the measurements of glycerol uptake rate and growth rate were protected [9,26]. As a result of this step, a Pruned Model is obtained from the GSM. The Pruned Model is also included in the Supplementary Files for completeness (*PpaPruned.mat*; Supplementary File S5).
3. Use the Matlab script *model_compression.m* (Supplementary File S4) to compress the Pruned Model into a Core Model. Again, protect the desired reactions and metabolites using the vectors *protect_reac_pr* and *protect_spec*. In the present case, the amino acids should be protected in the *protect_spec* vector, as it is required that the biomass formation equation contains the individual stoichiometry of each amino acid. As a result of this step, a Core Model is obtained from the Pruned Model. The resulting core model is included in the Supplementary Files (*PpaCore.mat*; Supplementary File S6).
4. Check the consistency of the reduced model by repeating the step 1 of this block using the Pruned and the Core models. Use the function *convertCNAModelToCbModel* of the *CellNetAnalyzer Toolbox* to convert

the model from *CellNetAnalyzer* into *COBRA toolbox* format. Make sure the predicted maximal growth rate is the same for the GSM, the Pruned, and the Core models.

5. Before writing the model in FTBL (Flux TaBuLar) format [29,30], the core model can be further manually curated. First, make sure the biosynthetic reactions use the precursors from the right cellular compartment considering the knowledge from previous literature. For example, in the assayed conditions, alanine is derived from mitochondrial pyruvate [7], while the *PpaCore.mat* model considers it is made from cytosolic pyruvate. Similarly, biosynthesis of lysine uses acetyl-CoA from the mitochondria and cytosolic α-ketoglutarate, which was also corrected in the *PpaCore.mat* model [31,32], as the P*paCore.mat* model described the synthesis of lysine from cytosolic acetyl-CoA and mitochondrial α-ketoglutarate. Moreover, the biosynthetic pathway towards isoleucine uses mitochondrial pyruvate instead of the intermediary metabolite 2-(α-hydroxyethyl)thiamine diphosphate [7]. Finally, the compartment where biosynthesis of glutamate, glutamine, aspartate, and asparagine occurs is not known. Therefore, the biosynthetic reactions of these amino acids in both the cytoplasm and the mitochondria needs to be considered. These corrections were applied to the model using the script *PpaCoreCorrection.m*, which generates the model *PpaCore2.mat*. Both documents can be found on the Supplementary Files (Supplementary File S8 and Supplementary File S9, respectively).
6. Lump the amino acid biosynthetic reactions of the *PpaCore2.mat* model that produce intermediary metabolites that only intervene in the synthesis of one amino acid. As some of these intermediary metabolites might also be present in the biomass formation equation, correct the biomass equation (see Note 3). To do so, you need to take the stoichiometric matrix, and multiply the column of the reaction producing the component that you want to remove by the stoichiometric value of the component in the biomass reaction, and then subtract the result from the biomass reaction column, keeping the resulting column as the new biomass equation. This can be easily done in a Spreadsheet (check the Supplementary File S7 (*Model_reactions.xlsx*; sheet *Biomass stoichiom. modification*). At the end, you will get a biomass stoichiometric equation

similar to the one obtained in the Supplementary File S7 (*Model_reactions.xlsx*; sheet *Biomass stoichiom. simplification*), where the stoichiometric coefficient for each amino acid is equal to its reported abundance in the biomass [26].

7. Write the model in FTBL. This format only accounts for the molecules involved in the C-transitions of the reactions (excluding the molecules involved in the redox, energy, or nitrogen exchange). You can find the correspondence of the reactions of the PpaCore model with the reactions of the FTBL model in the '*PpaCore to FTBL model*' sheet of the *Model_reactions.xlsx* (Supplementary File S7). You will also find the template FTBL format of the *P. pastoris* Core model in the Supplementary File S10 (*PpaCoreFTBL.ftbl*).
8. Influx contains the functions *influx_s* and *influx_i* for stationary and instationary ^{13}C-MFA, respectively. As we are focusing on the use of stationary ^{13}C-MFA, test the function *influx_s* with the *PpaCoreFTBL.ftbl* model. Make sure the model is running (you can check the error message in the *.err* file, or the results provided in the *.kvh* file). Setting each reaction as constrained (C), dependent (D), or free (F) is crucial for the model. Constrained reactions correspond to the reactions with fluxes that have a known flux. For instance, the backward flux of reactions assumed to be irreversible *in vivo* can be constrained to 0. The free reactions correspond to the reactions not directly determined by the resulting linear system, thus corresponding to the degrees of freedom of the system. Therefore, they will have to be identified. The free reactions are typically found at the crossing nodes, where the flux will be split into several branches. The model will fit the fluxes of the free reactions to fit the measured data. Finally, the dependent reactions are the rest of the reactions. The fluxes of the dependent reactions are determined from the free and constrained fluxes to ensure all metabolites of the network are balanced (consistently with the metabolic steady-state condition). You can take advantage of the additional arguments "*--ffguess --noopt"* in *influx_si*. This tool will help you on the classification of the fluxes into C, D, or F.

3.2. Optimization of the labelling of the C-source using IsoDesign

1. Once the FTBL model is running on *influx_s*, use *IsoDesign* to test the optimal C-source combination to obtain the highest resolution from the measured data. A template file for *IsoDeisgn* is provided (*PpaCoreFTBL_IsoDesign.ftbl*; Supplementary File S11). In that file, a combination of five alternative ^{13}C-labelled glycerol substrates is included (U-$^{12}C_3$-glycerol, 1-$^{13}C_1$-glycerol, 2-$^{13}C_1$-glycerol, 1,3-$^{13}C_2$-glycerol, and U-$^{13}C_3$-glycerol).
2. The output file obtained from *IsoDesign* contains the calculated standard deviation (SD) for each flux given each combination of labelled glycerol used as substrate. Using a spreadsheet or any other convenient computational tool (*Matlab, Python, R,* etc.), one can calculate the number of acceptably determined fluxes, given a certain criterion, such as *SD* below a given threshold value. The substrate combinations can also be ranked according to the maximal precision for a single flux or a set of fluxes. Therefore, the most appropriate substrate will primarily depend on the biological question addressed in the study.

3.3. High throughput batch culture

1. Inoculate the *P. pastoris* clones to be analyzed in 50 mL falcon tubes containing 5 mL YPG medium supplemented with the appropriate antibiotic (if needed). Cultivate the cells overnight in an incubator shaker at 30ºC and 200 rpm.
2. Use the saturated overnight cultures to inoculate a 250 mL shake flask culture containing 25 mL YPG medium at a starting OD_{600} of 1 (see Note 4). Cultivate the cells for 6-10 h in an incubator shaker at 30°C and 200 rpm. The fastest growing strains may be inoculated at a lower OD_{600}. The objective is to obtain cells at the exponential phase (OD_{600} in the range 5-10) in 6-10 h.
3. Add the batch sterile medium into each reactor of the high throughput culture platform. The volume may be adjusted depending on the cultivation set up.

4. Take the shake flasks from the incubator. Use the cultures from step 2 to inoculate each reactor at a starting OD_{600} of 0.025. The temperature of the reactors is set to 28ºC.
5. Using 2.5 g L^{-1} of glycerol, the exponential phase ends when the cells reach an OD_{600} around 2-2.5. Thus, 500 µL samples for proteinogenic amino acids analysis are withdrawn from the cultures when the OD_{600} reaches 1, to ensure the cultures are at a mid-exponential phase (metabolic pseudo-steady state). Ideally, the samples should be automatically withdrawn from the culture to minimize manual interventions (see Note 5 and Note 6).
6. Immediately centrifuge the samples at 4ºC and discard the supernatant. Store the cell pellet at -20ºC until further use.
7. Throughout the exponential growth of the cell culture, 250 µL samples need to be withdrawn for the analysis of the culture supernatant. Ten 250 µL samples can be withdrawn from all cultures, each sampled elapsed by 1h. The samples can be automatically withdrawn, placed on 96-well plates with a 0.45 µm filter bottom and vacuum filtered immediately. Afterwards, the supernatants are automatically placed into a new 96-well plate, which can be stored at -20°C. If an automated sampling and filtering system is not available, the process can be manually performed using syringe filters.

3.4. Quantification of extracellular metabolites (substrates and products) and calculation of exchange fluxes

1. Quantification of the concentration of ^{13}C-labelled substrate(s) and by-products in culture supernatants usingy 1D-^{1}H NMR on a Bruker Advance III 800MHz spectrometer (Bruker BioSpin, Germany) with a 5 mm CQPI cryoprobe is described, but any other relevant method (HPLC or LC/MS) may be used.
2. 180 µL supernatant samples were mixed with 20 µL of a D_2O stock solution containing 10 mM 3-(trimethylsilyl)-[2,2,3,3-$^{2}H_4$]-propionic acid sodium salt (TSP). TSP was used as an internal standard and for spectra calibration.

3. The probe temperature of the NMR spectrometer was set at 280 K, and the NMR data was recorded after a 30º presaturation pulse (zgpr30), followed by a relaxation delay of 7 s.
4. The NMR spectrum was analyzed using TopSpin 4.3.1 (Bruker BioSpin, Germany).
5. The growth rate and the specific production/consumption rates need to be calculated. To do so, take the OD_{600} data of the cultures and the supernatant concentration of the substrate and products from the NMR analysis. The OD_{600} data needs to be converted into Cell Dry Weight (CDW) concentration. Do the appropriate experiments to determine such parameter for the spectrophotometer, the *P. pastoris* strain, and the OD_{600} range you are using.
6. Using *PhysioFit* [24] or any other similar custom-made script or software, calculate the μ_{max} and the specific production/consumption rates. Use only the measurements of the exponential phase of the culture (OD_{600}<2.5 for the conditions described in this protocol).

3.5. Preparation of the proteinogenic amino acid samples

1. The frozen pellets were resuspended on 150 µL 6N HCl and incubated overnight (16 h) at 110 °C. Use a glass tube with an acid-resistant cap sealing, so HCl does not leak from the tube. The HCl will hydrolyze the cells and also the peptide bonds of the proteins.
2. Evaporate the HCl in the rotavapor. Make sure the rotavapor and the tubing connections can stand HCl, and connect the gas outlet to a condenser, so HCl gas is not released to the environment. Use the pressure gradient described in Supplementary Table S1.

Supplementary Table S1. Vacuum evaporator gradient protocol description.

Starting pressure (mbar)	Ending pressure (mbar)	Time (min)
800	500	10
500	500	1
500	300	10
300	200	10
200	200	5
200	100	15
100	100	10
100	75	10
75	75	5
75	0	15
0	0	∞

3. Resuspend the pellet in 100 µL ultrapure water and evaporate the water using the rotavapor. This step is performed to remove all the HCl.
4. Repeat the previous step.
5. Finally, resuspend the pellet on 200 µL ultrapure water. Centrifuge at 10,000 g for 5 min. The pellet contains the biomass debris, while the supernatant contains the free proteinogenic amino acids.
6. Take 40 µL of the supernatant and transfer to a tube with 460 µL of ultrapure water.

3.6. LC/MS analysis of the proteinogenic amino acid

1. A previously described protocol was used [33].
2. Liquid chromatography: The precolumn and column described in the materials section are used. Set the flow of the eluent at 0.25 mL.min^{-1}, the sampler temperature at 4°C, the column temperature at 30°C, and the volume of injection at 5 µL. Use the gradient described in Supplementary Table S2.

Supplementary Table S2. Gradient description for the solvents A and B of the Liquid Chromatography.

Time (min)	Solvent A (%)	Solvent B (%)
0	98	2
2	98	2
10	95	5
16	65	35
20	0	100
24	0	100
24,1	98	2
30	98	2

3. Mass Spectrometry: Use the parameters described in Supplementary Table S3. Set the equipment to measure all the *m/z* positive ratios described at the Supplementary Table S8 (Annex II, Section 4); see Note 7). The relative abundance of each isotopologue can be calculated from its relative area compared to the sum of the areas of all isotopologues for the same amino acid.

Supplementary Table S3. Mass spectrometry parameters.

Variable	Setpoint
Mode	Positive
Acquisition mode	FTMS mode
Resolution	70 000 *(400 m/z)*
Capillary temperature	320°C
Source heater temperature	300°C
Sheath gas flow rate	40 arbitrary units
Auxiliary gas flow rate	10 arbitrary units
S-Lens RF level	40%
Source voltage	5 kV
Duration	30 min

4. Place 100 µL of the samples containing the proteinogenic amino acids described in the step 3.5.6 into HPLC glass vials with inserts and run the protocol to perform the analyses.

3.7. Correction of the isotopologue distribution using IsoCor

1. The isotopologue distribution needs to be corrected for the presence of the isotopes at natural abundance. To do so, provide the isotopologue distribution obtained from the LC/MS analysis into *IsoCor* and select the appropriate correction options (isotopic purity of the tracer and natural abundance of the tracer element).
2. *IsoCor* generates a results file that can be used in *influx_si* to calculate the fluxes. A detailed protocol for the use of *IsoCor* can be found elsewhere (Millard et al., 2019; https://isocor.readthedocs.io/).

3.8. Calculation of intracellular fluxes and sensitivity analysis using *influx_si*

1. The measured μ_{max} and q-rates need to be normalized by the specific substrate uptake rate (qS), as the fluxes of all strains and cultures will be scaled to the qS for each strain. The quotient of the μ_{max} or q-rates with the qS is the equivalent to the biomass and the product yields. Add the yield results (and associated standard deviations) to the *MEASUREMENTS* section of the *PpaCoreFTBL.ftbl* file.
2. Add the corrected isotopologue distribution data obtained with *IsoCor* to the *MASS_SPECTROMETRY* section of the *PpaCoreFTBL.ftbl* file containing the measurements for that strain. Run *influx_s* to obtain the calculated fluxes.
3. The flux results can be found in the *linear stats* section of the results '*.kvh'* file. Moreover, at the end of the '*.kvh'* file, the statistical goodness of fit obtained from a chi-squared test is shown. The results clearly indicate if the measurements were accurately fitted (at a confidence level of 95%). If the fit is satisfactory, the calculated fluxes (and associated standard deviation) can be interpreted. An inconsistent fit may be due to i) errors in measurements and/or ii) errors in the model. For instance, it is possible that reactions which were not considered for the model carry a significant flux, and thereby need to be included in the model to fit the data satisfactorily. Therefore, some iterations between the raw data and the model may be required until an acceptable fit is achieved.

4. In case *influx_si* encounter an error in the calculation process, the cause of the error will be provided in a *.err* file. For instance, this situation may occur if the definition of some fluxes as Constrained (C), Free (F), or Dependent (D) is not consistent (see section 3.1.8 of this chapter).
5. Finally, you may use some additional features of *influx_s* to get the most information out from your data. For example, using the additional argument "*--sens mc=100*" you can perform a Monte Carlo sensitivity analysis with 100 simulations to assess the robustness of the results. You can also use the additional argument "*sln*" to minimize the sum of fluxes which are not identifiable from the available isotopic measurements, following the principle that cells would have a fitness advantage of using the least amount of enzyme [34]. Use of *"sln"* is therefore particularly interesting when some fluxes are poorly determined.

4. Notes

Note 1. All the software and computational tools used for this study contain tutorials and/or test functions. Doing the tutorials of all the tools before starting the experimental design is highly recommended.

Note 2. If the objective of the project is to characterize the fluxome of a *P. pastoris* strain producing a heterologous chemical compound, make sure to protect the reactions producing the precursors of this product. Later, add the heterologous pathway to both the Core and the FTBL Core models.

Note 3. Simplification of the model by lumping the reactions producing intermediary metabolites will greatly reduce the overall number of reactions. That will be useful, as this will reduce the number of reactions for the C-transitions model. If two reactions are lumped and an intermediary metabolite is removed, make sure that such intermediary metabolite is not involved in any other reactions. This can be easily done by checking the corresponding metabolite row in the stoichiometric matrix. In case it is involved in other reactions, make sure to correct the stoichiometry of the other reactions, too. Make also sure that the carbon positions from the substrate(s) are properly mapped to the product(s) of the lumped reaction.

Note 4. The OD_{600} measures always refer to the absorbance at 600 nm using 1 cm cuvette. If measured using a different system (i.e., microplate reader), the correlation between the two spectrophotometers should be tested.

Note 5. Smaller volumes may be withdrawn from the culture (i.e., 50 µL), but this should be considered at step 3.5.6. In case only 50 µL are withdrawn, the proteinogenic amino acids from step 3.5.4 (the supernatant after the centrifugation step) can be directly placed into an HPLC vial with insert for LC/MS analysis.

Note 6. If the biomass samples cannot be withdrawn and processed immediately, it is recommended to store the samples in quenching solution at -20°C for up to 2 h. The quenching solution consists of 40% v/v acetonitrile, 40% v/v methanol, 20 % water and 0.1 M formic acid. Use LC/MS-grade reagents. In that case, an additional step to evaporate all the quenching solution is required before the HCl is added to the cell pellet. The same rotavapor and the same protocol described in Supplementary Table S1 can be used.

Note 7. Methionine and Tryptophan cannot be measured using the reported method. Moreover, asparagine and glutamine are converted into aspartate and glutamate during the acidic hydrolysis of the biomass with HCl. Therefore, the method provides the isotopologue distribution of aspartate plus asparagine, and glutamate plus glutamine instead of the individual isotopologue distribution of each amino acid.

Note 8. The results from the ^{13}C-MFA can be used as measurements of the *PpaCore2.mat* stoichiometric model to perform Flux Balance Analysis (FBA) using the *CobraToolbox* [20].

Note 9. Using stationary or instationary ^{13}C-MFA, the fluxes are calculated from the changes in the labelling of the metabolites resulting from the flux, the stoichiometry, and the C-transitions of a reaction. Fluxomics of microorganisms growing on a one carbon sources (i.e., methanol or CO_2) can only be performed using isotopically non-stationary fluxomics, as incorporation of the labelled or un-labelled substrate would happen randomly due to the absence of C-bonds in the substrate. Recently, isotopically non-stationary fluxomics using methanol as a sole C-source was reported in *Bacillus methanolicus* [35], but a similar approach has not been used in *P. pastoris*, yet. Nevertheless, both stationary and isotopically non-stationary fluxomics in *Pichia pastoris* using glycerol/methanol or glucose/methanol mixtures have been reported [36,37].

IsoDesign can also be used to optimize the labelling of the substrates when two or more C-sources are co-consumed. However, the high throughput approach reported here might not apply, as the system is performed in batch cultures. Under such conditions where catabolite repression is active, as there is an excess of glucose or glycerol, the cells would not co-consume methanol.

Supplementary materials

The supplementary materials of this section have been submitted to the Dipòsit Digital de Documents (DDD) of the Universitat Autònoma de Barcelona. They can be downloaded from the following link: https://doi.org/10.5565/ddd.uab.cat/263045

List of Supplementary Files and description:

1. **Supplementary File S1: *iMT1026v3.mat***
   Short description: Genome Scale Metabolic model for Pichia pastoris metabolism. Matlab format compatible with scripts of CobraToolbox.

2. **Supplementary File S2: *PpaGS.mat***
   Short description: Genome Scale Metabolic model for Pichia pastoris metabolism. Matlab format compatible with scripts of CellNetAnalyzer.

3. **Supplementary File S3: *model_reduction.m***
   Short description: Matlab function using scripts from CellNetAnalyzer for the reduction of a Pichia pastoris Genome Scale Model into a Pruned model.

4. **Supplementary File S4: *model_compression.m***
   Short description: Matlab function using scripts from CellNetAnalyzer for the compression of a Pichia pastoris Pruned model into a Core model.

5. **Supplementary File S5: *PpaPruned.mat***
   Short description: Pruned model of Pichia pastoris metabolism in the CellNetAnalyzer format.

6. **Supplementary File S6*: PpaCore.mat***
   Short description: Core model of Pichia pastoris metabolism in CellNetAnalyzer format.

7. **Supplementary File S7: *Model_reactions.xlsx***
   Short description: Excel file describing the conversion of the Pichia pastoris Core model in CellNetAnalyzer format into the FTBL format. It also describes the compression of the Biomass formation reaction into a reaction which does not account for irrelevant intermediary metabolites.

8. **Supplementary File S8: *PpaCoreCorrection.m***
   Short description: Matlab script that takes the PpaCore.mat model and it translates it into CobraToolbox format.It also describes some literature-based corrections which are applied to the model. As a result, the PpaCore2.mat model is generated.

9. **Supplementary File S9: *PpaCore2.mat***
   Short description: Core model of Pichia pastoris metabolism in CobraToolbox format.

10. **Supplementary File S10: *PpaCoreFTBL.ftbl***
    Short description: Core model of Pichia pastoris metabolism in FTBL format, which is readable for influx_si.

11. **Supplementary File S11: *PpaCoreFTBL_IsoDesign.ftbl***
    Short description: Generated from the PpaCoreFTBL.ftbl model. It can be used as an input model for IsoDesign for the optimization of the C-source for 13C-Metabolix Flux Analysis.

References

1. Wiechert, W., and Nöh, K. (2005) From stationary to instationary metabolic flux analysis. *Advances in Biochemical Engineering/Biotechnology*, 92, 145–172.
2. Millard, P., Sokol, S., Kohlstedt, M., Wittmann, C., Létisse, F., Lippens, G., and Portais, J.C. (2021) IsoSolve: an integrative framework to improve isotopic coverage and consolidate isotopic measurements by mass spectrometry and/or nuclear magnetic resonance. *Analytical Chemistry*, 93 (27), 9428–9436.
3. Ferrer, P., and Albiol, J. (2014) ^{13}C-based metabolic flux analysis in yeast: The *Pichia pastoris case*. *Methods in Molecular Biology*, 1152, 209–232.
4. Ferrer, P., and Albiol, J. (2014) ^{13}C-based metabolic flux analysis of recombinant *Pichia pastoris*. *Methods in Molecular Biology*, 1191, 291–313.
5. Jordà, J., Rojas, H., Carnicer, M., Wahl, A., Ferrer, P., and Albiol, J. (2014) Quantitative metabolomics and instationary ^{13}C-metabolic flux analysis reveals impact of recombinant protein production on trehalose and energy metabolism in *Pichia pastoris*. *Metabolites*, 4 (2), 281–299.
6. Nöh, K., and Wiechert, W. (2011) The benefits of being transient: Isotope-based metabolic flux analysis at the short time scale. *Applied Microbiology and Biotechnology*, 91 (5), 1247–1265.
7. Solà, A., Maaheimo, H., Ylönen, K., Ferrer, P., and Szyperski, T. (2004) Amino acid biosynthesis and metabolic flux profiling of *Pichia pastoris*. *European Journal of Biochemistry*, 271 (12), 2462–2470.
8. Baumann, K., Carnicer, M., Dragosits, M., Graf, A.B., Stadlmann, J., Jouhten, P., Maaheimo, H., Gasser, B., Albiol, J., Mattanovich, D., and Ferrer, P. (2010) A multi-level study of recombinant *Pichia pastoris* in different oxygen conditions. *BMC Systems Biology*, 4, 141.
9. Tomàs-Gamisans, M., Ødum, A.S.R., Workman, M., Ferrer, P., and Albiol, J. (2019) Glycerol metabolism of *Pichia pastoris* (*Komagataella* spp.) characterised by ^{13}C-based metabolic flux analysis. *New Biotechnology*, 50, 52–59.
10. Tomàs-Gamisans, M., Ferrer, P., and Albiol, J. (2016) Integration and validation of the genome-scale metabolic models of *Pichia pastoris*: A comprehensive update of protein glycosylation pathways, lipid and energy metabolism. *PLoS ONE*, 11, e0148031.
11. Robaina Estévez, S., and Nikoloski, Z. (2014) Generalized framework for context-specific metabolic model extraction methods. *Frontiers in Plant Science*, 5, 491.
12. Richelle, A., Chiang, A.W.T., Kuo, C.C., and Lewis, N.E. (2019) Increasing consensus of context-specific metabolic models by integrating data-inferred cell functions. *PLoS Computational Biology*, 15 (4), e1006867.
13. De, S., Mattanovich, D., Ferrer, P., and Gasser, B. (2021) Established tools and emerging trends for the production of recombinant proteins and metabolites in *Pichia pastoris*. *Essays in Biochemistry*, 65 (2), 293–307.
14. Prielhofer, R., Barrero, J.J., Steuer, S., Gassler, T., Zahrl, R., Baumann, K., Sauer, M., Mattanovich, D., Gasser, B., and Marx, H. (2017) GoldenPiCS: A Golden Gate-derived modular cloning system for applied synthetic biology in the yeast *Pichia pastoris*. *BMC Systems Biology*, 11, 123.
15. Weninger, A., Hatzl, A.M., Schmid, C., Vogl, T., and Glieder, A. (2016) Combinatorial optimization of CRISPR/Cas9 expression enables precision genome engineering in the methylotrophic yeast *Pichia pastoris*. *Journal of Biotechnology*, 235, 139–149.
16. Ebert, B.E., and Blank, L.M. (2014) Successful downsizing for high-throughput ^{13}C-MFA applications. *Methods in Molecular Biology*, 1191, 127–142.
17. Heux, S., Juliette, P., Stéphane, M., Serguei, S., and Jean-Charles, P. (2014) A novel platform for automated high-throughput fluxome profiling of metabolic variants. *Metabolic Engineering*, 25, 8–19.
18. Bareither, R., and Pollard, D. (2011) A review of advanced small-scale parallel bioreactor technology for accelerated process development: Current state and future need. *Biotechnology Progress*, 27, 2–14.
19. Carnicer, M., Canelas, A.B., ten Pierick, A., Zeng, Z., van Dam, J., Albiol, J., Ferrer, P., Heijnen, J.J., and van Gulik, W. (2012) Development of quantitative metabolomics for *Pichia pastoris*. *Metabolomics*, 8 (2), 284–298.
20. Becker, S.A., Feist, A.M., Mo, M.L., Hannum, G., Palsson, B., and Herrgard, M.J. (2007) Quantitative prediction of cellular metabolism with constraint-based models: The COBRA Toolbox. *Nature Protocols*, 2 (3), 727–738.
21. Klamt, S., Saez-Rodriguez, J., and Gilles, E.D. (2007) Structural and functional analysis of cellular networks with CellNetAnalyzer. *BMC Systems Biology*, 1, 2.
22. Sokol, S., Millard, P., and Portais, J.C. (2012) Influx_s: Increasing numerical stability and precision for metabolic flux analysis in isotope

labelling experiments. *Bioinformatics*, 28 (5), 687–693.

23. Millard, P., Sokol, S., Letisse, F., and Portais, J.-C. (2014) IsoDesign: A software for optimizing the design of ^{13}C-metabolic flux analysis experiments. *Biotechnology and Bioengineering*, 111 (1), 202–208.
24. Peiro, C., Millard, P., de Simone, A., Cahoreau, E., Peyriga, L., Enjalbert, B., and Heux, S. (2019) Chemical and metabolic controls on dihydroxyacetone metabolism lead to suboptimal growth of *Escherichia coli*. *Applied and Environmental Microbiology*, 85, 15.
25. Millard, P., Delépine, B., Guionnet, M., Heuillet, M., Bellvert, F., and Létisse, F. (2019) IsoCor: Isotope correction for high-resolution MS labeling experiments. *Bioinformatics*, 35 (21), 4484–4487.
26. Tomàs-Gamisans, M., Ferrer, P., and Albiol, J. (2018) Fine-tuning the *P. pastoris* iMT1026 genome-scale metabolic model for improved prediction of growth on methanol or glycerol as sole carbon sources. *Microbial Biotechnology*, 11 (1), 224–237.
27. Maurer, M., Kühleitner, M., Gasser, B., and Mattanovich, D. (2006) Versatile modeling and optimization of fed batch processes for the production of secreted heterologous proteins with *Pichia pastoris*. *Microbial Cell Factories*, 5, 37.
28. Erdrich, P., Steuer, R., and Klamt, S. (2015) An algorithm for the reduction of genome-scale metabolic network models to meaningful core models. *BMC Systems Biology*, 9, 48.
29. Wiechert, W., and de Graaf, A.A. (1997) Bidirectional reaction steps in metabolic networks. *Biotechnology and Bioengineering*, 55 (1), 101–135.
30. Wiechert, W., Möllney, M., Petersen, S., and de Graaf, A.A. (2001) A universal framework for ^{13}C metabolic flux analysis. *Metabolic Engineering*, 3 (3), 265–283.
31. Gombert, A.K., dos Santos, M.M., Christensen, B., and Nielsen, J. (2001) Network identification and flux quantification in the central metabolism of *Saccharomyces cerevisiae* under different conditions of glucose repression. *Journal of Bacteriology*, 183 (4), 1441–1451.
32. Lehnen, M., Ebert, B.E., and Blank, L.M. (2017) A comprehensive evaluation of constraining amino acid biosynthesis in compartmented models for metabolic flux analysis. *Metabolic Engineering Communications*, 5, 34–44.
33. Heuillet, M., Bellvert, F., Cahoreau, E., Letisse, F., Millard, P., and Portais, J.C. (2018) Methodology for the validation of isotopic analyses by mass spectrometry in stable-isotope labeling experiments. *Analytical Chemistry*, 90 (3), 1852–1860.
34. Holzhütter, H.G. (2004) The principle of flux minimization and its application to estimate stationary fluxes in metabolic networks. *European Journal of Biochemistry*, 271 (14), 2905–2922.
35. Delépine, B., Gil López, M., Carnicer, M., Vicente, C.M., Wendisch, V.F., and Heux, S. (2020) Charting the Metabolic Landscape of the Facultative Methylotroph *Bacillus methanolicus*. *mSystems*, 5, e00745-20.
36. Solà, A., Jouhten, P., Maaheimo, H., Sánchez-Ferrando, F., Szyperski, T., and Ferrer, P. (2007) Metabolic flux profiling of *Pichia pastoris* grown on glycerol/methanol mixtures in chemostat cultures at low and high dilution rates. *Microbiology*, 153 (1), 281–290.
37. Jordà, J., Suarez, C., Carnicer, M., ten Pierick, A., Heijnen, J.J., van Gulik, W., Ferrer, P., Albiol, J., and Wahl, A. (2013) Glucose-methanol co-utilization in *Pichia pastoris* studied by metabolomics and instationary ^{13}C flux analysis. *BMC Systems Biology*, 7, 17.

Annex II

Supplementary materials

Table of contents

1. Supplementary materials Chapter 3. Results I

1.1. Maximum theoretical yield and metabolic routes to 3-HP

The stoichiometric analysis shown in the Supplementary Figure S2 shows how the maximum theoretical yield using glycerol as a substrate is equal for both pathways (the β-alanine and the Maloyl-CoA pathway), even though in the β-alanine route the net production of ATP is higher than in the Maloyl-CoA one. Regarding the use of glucose as a substrate, in the β-alanine pathway there is no net cost nor production of ATP, while the conversion of glucose to 3-HP through Malonyl-CoA has a net cost of ATP.

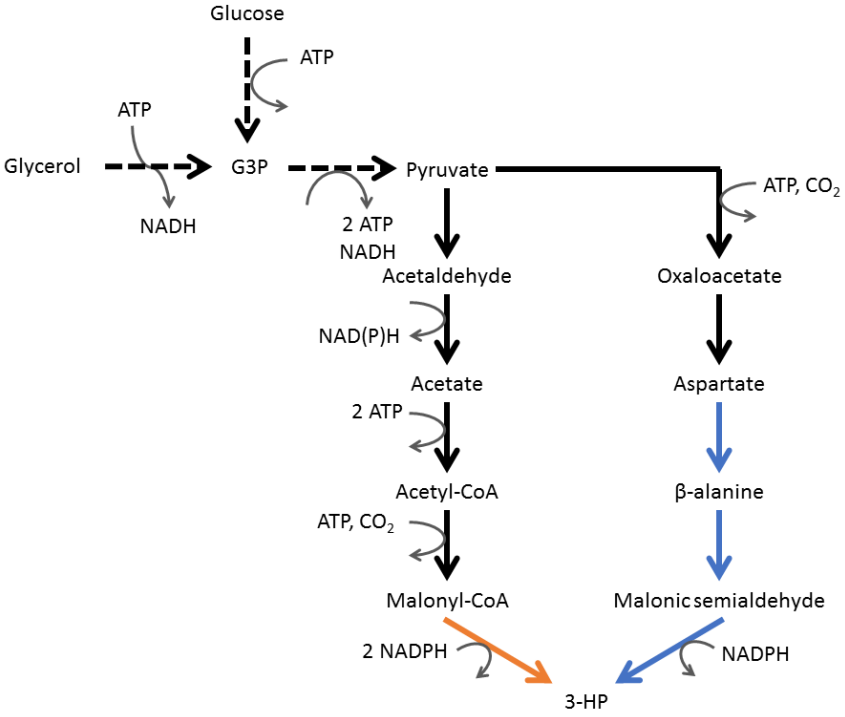

ATP Synthase: NADH + H⁺ → NAD⁺ + 2.5 ATP

Redox balancing mechanisms: NADPH → NADH

β-Alanine pathway	0.5 Glucose → 3-HP
Malonyl-CoA pathway	0.5 Glucose + 2 ATP → 3-HP
β-Alanine pathway	Glycerol → 3-HP + 2.5 ATP
Malonyl-CoA pathway	Glycerol → 3-HP + 0.5 ATP

Supplementary Figure S2. Metabolic pathways to 3-HP reported in yeast and calculations of the maximum theoretical yield using glycerol or glucose as substrate. The black arrows indicate endogenous reactions of *P. pastoris* metabolism, the orange arrows indicate the heterologous reactions of the Malonyl-CoA pathway, and the blue arrows show the heterologous reactions of the β-alanine pathway. The two sequential reactions of the Malonyl-CoA conversion to 3-HP are simplified in a single arrow, as they are performed by a bi-functional enzyme (Malonyl-CoA Reductase, MCR).

1.2. Cloning protocol details

The Malonyl-CoA Reductase gene of *Chloroflexus aurantiacus* (*mcr_{Ca}*, Uniprot: Q6QQP7_CHLAU) was synthesized, codon optimized for *P. pastoris* expression, and cloned into pBIZi_pGAP by GenScript (NJ, USA) to obtain the plasmid pBIZi_pGAP_MCR. The plasmid pBIZi_pGAP was provided by Bioingenium SL (Barcelona, Spain) and its features are shown in the Supplementary Figure S5.

A list of all the primers used for this study is available in the Supplementary table . All the primers were purchased to Integrated DNA Technologies (IA, USA).

The plasmids pBIZi_pGAP_MCR_N and pBIZi_pGAP_MCR_C were generated from pBIZi_pGAP_MCR. To generate pBIZi_pGAP_MCR_N, the plasmid pBIZi_pGAP_MCR was used as template for a PCR using the Phusion® High-Fidelity DNA Polymerase (New England Biolabs, MA, USA) and the primers pair N_ter_MCR_FW and N_ter_MCR_RV. The PCR product was purified from a 1% agarose gel, self-ligated using the T4-DNA ligase (New England Biolabs) and transformed into an aliquot of chemocompetent *Escherichia coli* DH5α. The same protocol was used to obtain the plasmid pBIZi_pGAP_MCR_C using the primers C_ter_MCR_FW and C_ter_MCR_RV.

To build the plasmid pBIZi_pGAP_MCR_E, two high-fidelity PCRs were performed using the pBIZi_pGAP_MCR_C as template. One using the primers pair MCR_evolv_1 and MCR_evolv_4 and the second one using the primers pair MCR_evolv_2 and MCR_evolv_3. The two PCR fragments were then joint to generate pBIZi_pGAP_MCR_E using the In-Fusion HD Cloning Kit (TaKaRa Bio, CA, USA).

For the plasmid pBIZi_pGAP_MCR_NC and pBIZi_pGAP_MCR_NE, not only the two expression cassettes for MCR(Nter) and MCR(Cter) (or MCR($Cter_{N940V/K1106W/S1114R}$) were cloned, but also one of the AvrII sequences present in the P_{GAP} was modified, because the restriction enzyme AvrII is used for plasmid linearization and transformation into *P. pastoris*.

To generate the plasmids pBIZi_pGAP_MCR_NC, three PCR products were generated using the following primer pairs and DNA templates: i) InFus_MCR_Nter_FW and pGAP_AvrII_mut_RV using pBIZi_pGAP_MCR_N as template; ii) pGAP_AvrII_mut_FW and InFus_MCR_Nter_RV using pBIZi_pGAP_MCR_N as

template; iii) InFus_MCR_Cter_FW and InFus_MCR_Cter_RV using pBIZi_pGAP_MCR_C as template. Afterwards, the three PCR products were ligated using the In-Fusion HD Cloning Kit. To obtain the plasmid pBIZi_pGAP_MCR_NE, the same protocol was used but for the PCR iii, the plasmid pBIZi_pGAP_MCR_E was used as template.

The gene encoding for the Acetyl-CoA Carboxylase from *Yarrowia lipolytica* (*ACC_{Yl}*, Uniprot: YALI0_C11407) was codon optimized for *P. pastoris* expression and cloned in pGAPZB by Epoch Life Science (TX, USA). The *ACC* sequence was modified to eliminate all the BbsI restriction sequences to allow its subcloning using the Golden PiCS kits and protocols [1]. To do so, a protocol was designed to perform the BbsI mutations and the cloning of *ACC* into the plasmid BB1_23 simultaneously. First, two PCR products were performed using pGAPZB-ACC as template: i) using the primers pair ACC_FW_GP_BsaI_2 and ACC_GG_1_RV_BsaI; ii) ACC_GG_2_FW_BsaI and ACC_RV_GP_Bsa3. A DNA gBlock was purchased to Integrated DNA Technologies (IA, USA), which consisted of a DNA fragment encoding the central part of *ACC* where seven point-mutations had been performed to eliminate the BbsI restriction sequences. For each point mutation, a high codon usage was maintained. Afterwards, the two PCR products and the gBlock were cloned in BB1_23 using the enzyme BsaI-HFv2 from New England Biolabs and the Golden Gate protocol recommended by the restriction enzyme provider.

The cytosolic NADH kinase gene *$cPOS5_{Sc}$* was amplified from pPUZZLE-cPOS5 [2] using the primers cPOS5_GP_FW_2 and cPOS5_GP_RV_3 and cloned in BB1_23 using the enzyme BsaI-HFv2.

Subsequent subcloning of *cPOS5* and *ACC*(ΔBbsI) was performed as described elsewhere [1] to generate the plasmids BB3eH_ACC, BB3eH_cPOS5 and BB3eH_ACC_cPOS5.

All the plasmids whose generation involved a PCR step were sequenced in the Genomics and Bioinformatics Service of the Universitat Autònoma de Barcelona (Bellaterra, Spain).

1.3. Supplementary tables

Supplementary table S4. Primers list.

Primer name	Primer sequence
N_ter_MCR_FW	/5Phos/TAAGAGCTCGAGACCACTAGTACGG*
N_ter_MCR_RV	GATGTTAGCTGGGATGTTCAAAGTGATTTC
C_ter_MCR_FW	TCTGCTACTACTGGTGCTAGATCTG
C_ter_MCR_RV	/5Phos/CATCGTTTCGAAATAGTTGTTCAATTGATTG*
MCR_evolv_1	CTATCAGCCAAATAGTAAACAGTAGCC
MCR_evolv_2	GGCTACTGTTTACTATTTGGCTGATAGAGTTGTTTCTGGA GAGACTTTTCACCCTTC
MCR_evolv_3	AGCACCATCAGACAAAGCAATCCATCTAGCAACTCTGAAG TGATGAGTCAAC
MCR_evolv_4	ATTGCTTTGTCTGATGGTGCTAGATTGGCTTTGGTTACTCC AGAAACTAC
InFus_MCR_Nter_FW	CATTTCCCCGAAAAGTGCCACA
InFus_MCR_Nter_RV	TGCGCGGAACCCCTATTTGTTTA
InFus_MCR_Cter_FW	ACAAATAGGGGTTCCGCGCAGATCTTTTTTGTAGAAATGT CTTGG
InFus_MCR_Cter_RV	TGGCACTTTTCGGGGAAATGCCATGGTACATTCTTCGCAG GC
pGAP_AvrII_mut_FW	CCACCGCCCGTTACCGTCCCAAGGAAATTTTACTCTGCTG GAGAG
pGAP_AvrII_mut_RV	TGGGACGGTAACGGGCGGTGGAAG
ACC_FW_GP_BsaI_2	GATGGTCTCACATGCGTTTACAACTTAGAACACTGACTAG GAG
ACC_GG_1_RV_BsaI	TCATGGTCTCtAGAGTAAAGATACTCTACAGTACCAGCACT AAC
ACC_GG_2_FW_BsaI	CAATGGTCTCcGTTCCCTTAGAAGAATTACATTCTCATTTG GAAACTC
ACC_RV_GP_BsaI_3	GCTTAGGTCTCAAAGCTTACAAACCTTTCAGCAGTTCTGC TC
cPOS5_FW_GP_BsaI_2	GATGGTCTCACATGATGTCCACTTTGGACTCCCATTCC
cPOS5_RV_GP_BsaI_3	GCTTAGGTCTCAAAGCTTAGTCGTTGTCAGTCTGTCTCTTA GTC

*/5Phos/ means the 5' end of the primer is phosphorylated.

1.4. Supplementary Figures

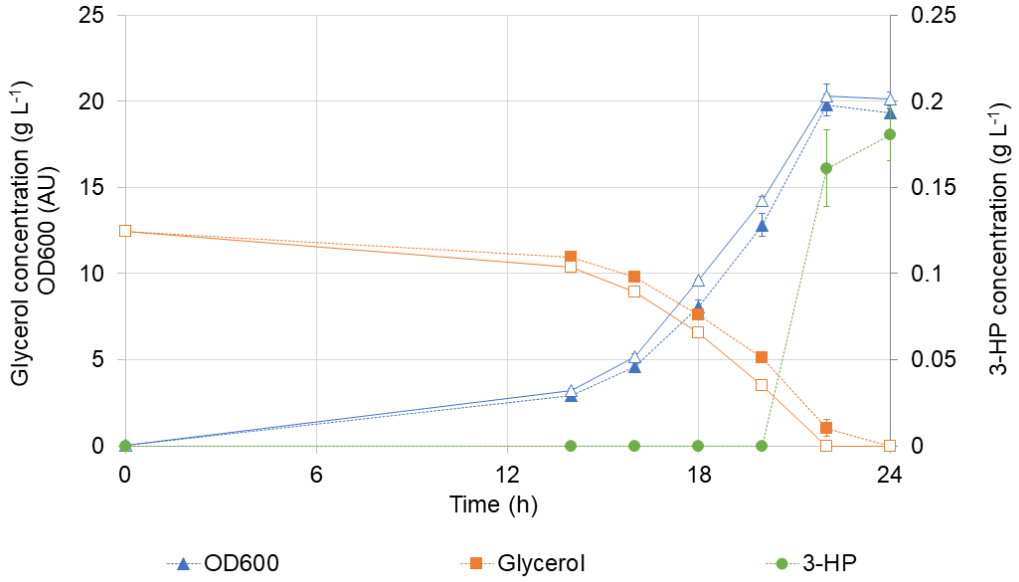

Supplementary Figure S3. Shake flask cultures of *P. pastoris* X-33 reference strain (solid lines and empty symbols) and a representative clone of the PpHP1 strain (dashed lines and filled symbols). Cultures were carried out in triplicate and error bars show the SE.

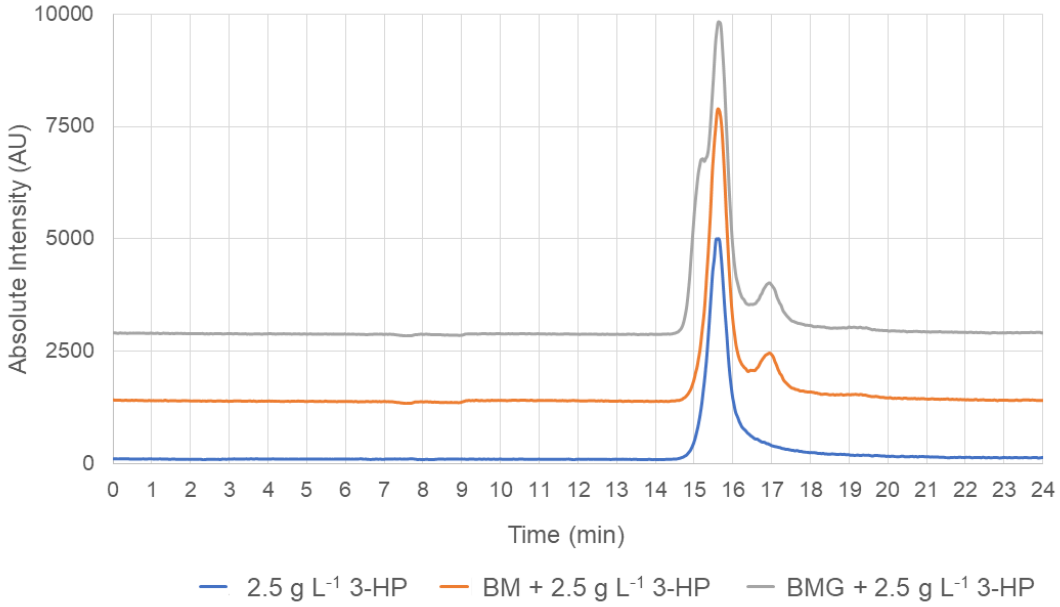

Supplementary Figure S4. MS chromatogram of the Absolute intensity detected at a m/z of -89 of three different samples analysed by LC-MS. The blue line shows the result of a standard sample of 2.5 g L^{-1} of 3-HP, the orange sample shows the result of Buffered Minimal (BM) medium supplemented with 2.5 g L^{-1} of 3-HP (BM + 2.5 g L^{-1} 3-HP), and the grey line corresponds to the analysis of Buffered Minimal medium supplemented with 1% v/v Glycerol and 2.5 g L^{-1} of 3-HP (BMG + 2.5 g L^{-1} 3-HP). The maximum peak intensity was observed at 16.2 min. The matrix effect caused by glycerol co-elution with 3-HP can be observed between times 14.5 and 15.5 min.

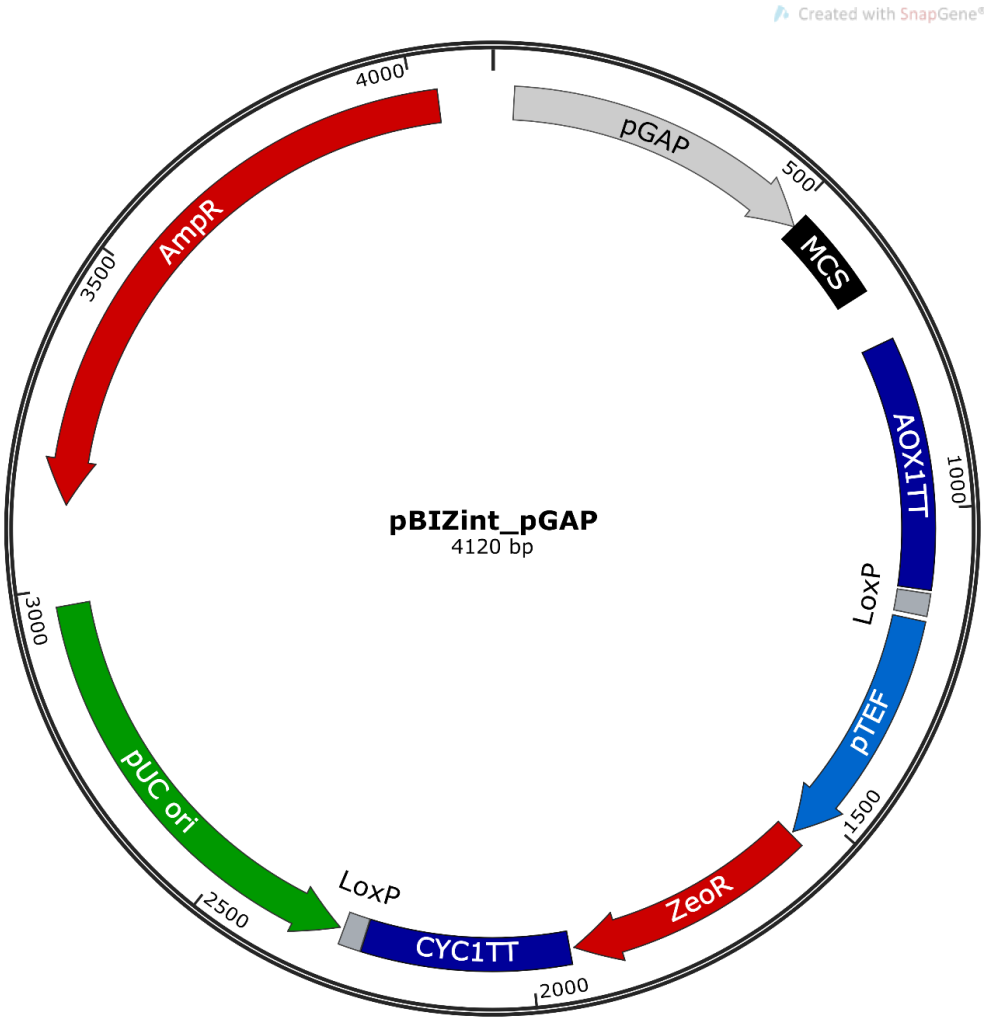

Supplementary Figure S5. pBIZi_pGAP features.

2. Supplementary materials Chapter 4. Results II

All restriction enzymes and Q5 high-fidelity polymerase were purchased to New England Biolabs (MA, USA).

The strains PpHP2 and PpHP6 had been previously generated in our lab. The list of plasmids used in this study are listed in the Supplementary Table S5.

When using the GoldenPiCS plasmids, its associated protocol for Golden Gate cloning was used [1]. The same name code is used to refer to the overhang sequences generated using the Golden Gate restriction enzymes BsaI and BbsI is used.

Supplementary Table S5. Plasmids list and description.

Plasmid name	Features / Use	Source
pBIZi_pGAP_MCR_C		[3]
BB3eN_14		[1]; Addgene #1000000133
BB1_pGAP_12	To generate BB3eN_pGAP_mcrC_TDH3tt	[1]; Addgene #1000000133
BB1_23		[1]; Addgene #1000000133
BB1_TDH3tt_34		[1]; Addgene #1000000133
BB1_23_MCR_C		This study
BB3eN_pGAP_mcrC_TDH3tt	Expression cassette pGAP_ *mcr-C*$_{Ca}$_TDH3tt. Integration at site *ENO1* intergenic region.	This study
pK_pGAP_ACC1*	Expression cassette pGAP_*ACC1**_AOX1tt	[4]; Addgene #126740
BB3cK_pGAP_23*_pLAT2_Cas9	Plasmid carrying a clonsing site for the sgRNA and the hCas9 expressed under the control of pLAT2.	[5]; Addgene #1000000136
BB3cK_pGAP_23*_pLAT2_Cas9_RGI2	Transcription of sgRNA targeting a double strand break at the *RGI2* locus. Expression of hCas9 under the control of pLAT2.	This study
BB3nK_AD		[5]; Addgene #1000000136
BB3nK_ACS1_at_RGI2	Expression cassette pTEF1_*acs*$_{Se}^{L641P}$_RPS3tt flanked with 1 kb homology sequences targeting at the *RGI2* locus.	This study
BB3nK_ACS1_ALD6_at_RGI2	Expression cassette pTEF1_*acs*$_{Se}^{L641P}$_RPS3tt and pMDH3_*ALD6*$_{Sc}$_TDH3tt flanked with 1 kb homology sequences targeting at the *RGI2* locus.	This study
BB3cK_pGAP_23*_pLAT2_Cas9_ArDH	Transcription of sgRNA targeting a double strand break at the ArDH locus. Expression of hCas9 under the control of pLAT2	This study

To obtain the plasmid pBIZi_pGAP_MCR_C, first, the coding sequence of *mcr-C*$_{Ca}$ was amplified using primers adding the BsaI recognition sequence and the overhangs described in the GoldenPiCS protocol. The PCR amplicon was cloned into BB1_23 using BsaI. As a result, the plasmid BB1_23_MCR_C was obtained. Sequence integrity was checked by Sanger sequencing. Finally, BB3eN_pGAP_mcrC_TDH3tt was obtained using BB3eN_14, BB1_pGAP_12, BB1_23_MCR_C, and BB1_TDH3tt_34 and the Golden Gate protocol reported above with the restriction enzyme BbsI. The targeted integration locus was the intergenic region upstream of *ENO1*. The plasmid BB3eN_pGAP_mcrC_TDH3tt was linearized using PmeI and transformed into *P. pastoris* strains PpHP2 and PpHP6 to generate the strains PpHP7 and PpHP8, respectively.

PpHP9 was generated from linearizing the plasmid pK_pGAP_ACC1* with AvrII and transforming into PpHP7. The targeted integration locus was pGAP. The plasmid pK_pGAP_ACC1* contains two selection markers (geneticin resistance and histidine prototrophy). As PpHP7 was derived from the parental X-33 strain from Invitrogen (Thermo Fisher Scientific, MA, USA), which is prototroph for histidine, geneticin was used for the selection of clones having incorporated the plasmid.

Supplementary Table S6. Gene name and locus targetted for the double strand break during CrisPR-Cas9-based genetic engineering. The sgRNA sequence is shown. The PAM sequence is underlined.

Locus	sgRNA sequence (PAM underlined)
RGI2 (PAS_chr1-1_0407)	TCTCAACGTATTTATATGGTCGG
ArDH (PAS_chr2-2_0019)	TGGATCACGCACAATCAAGATGG

To generate the plasmids and the donor DNA required for CrisPR-Cas9, a previously described protocol was used [5]. Two single guide RNA (sgRNA) were designed targeting an intergenic region upstream of gene RGI2 and the coding region of D-arabitol dehydrogenase (ArDH). The sequence of the complementary sgRNA targeting at each genomic locus are listed in Supplementary Table S6.

The plasmids BB3nK_ACS1_at_RGI2 and BB3nK_ACS1_ALD6_at_RGI2 were build to obtain the donor DNA to knock-in the expression cassettes of the modified Acetyl-CoA Synthase from *Salmonella enterica* harbouring a mutation L614P (*acs*$_{Se}$*) and the aldehyde dehydrogenase from *Saccharomyces cerevisiae* (*ALD6*$_{Sc}$*).* The sequence of the whole expression cassettes pTEF1_*acs*$_{Se}^{L641P}$_RPS3tt and

pMDH3_*ALD6*$_{Sc}$_TDH3tt were purchased to Integrated DNA Technologies (IA, USA) in a HiFi gBlock. The sequence of *acs*$_{Se}^{L641P}$ and *ALD6*$_{Sc}$ were codon optimized for *P. pastoris* expression using the codon optimization tool of Integrated DNA Technologies, avoiding the introduction of BsaI and BbsI recognition sites. The coding sequences were flanked with the promoter (pTEF1 or pMDH3) and terminator (RPS3tt and TDH3tt) sequences found in the GoldenPiCS kit. BsaI recognition sequences resulting in overhangs B and E were added to the gBlock pTEF1_*acs*$_{Se}^{L641P}$_RPS3tt, while BsaI recognition sequences resulting in overhangs E and C were added to the gBlock pMDH3_*ALD6*$_{Sc}$_TDH3tt. To build the plasmid BB3nK_ACS1_at_RGI2, high-fidelity PCR was performed using genomic DNA from *P. pastoris* X-33 and primer pairs RGI_5H_FW_A/RGI_5H_RV_B and RGI_3H_FW_E/RGI_5H_RV_D (see Supplementary Table S7). The first two primers generated a 763 bp amplicon with BsaI recognition sites at both ends generating overhangs A and B. The second pair or primers generated a 733 bp PCR product with BsaI recognition sites at both ends generating overhangs E and D. The two amplicons were mixed with BB3nK_AD and the gBlock pTEF1_*acs*$_{Se}^{L641P}$_RPS3tt. Using the Golden Gate protocol described for BsaI-HFv2, the plasmid BB3nK_ACS1_at_RGI2 was obtained.

To generate BB3nK_ACS1_ALD6_at_RGI2, the second primers pair was switched to RGI_3H_FW_C/ RGI_5H_RV_D to generate a PCR product of the same length, but having BsaI recognition sequences resulting in overhang sequences C and D. Performing Golden Gate using the two PCR products, the two described gBlocks, and BB3nK_AD, the plasmid BB3nK_ACS1_ALD6_at_RGI2 was obtained.

To obtain the strains PpHP11 and PpHP13, 1 µg of the circular plasmid BB3cK_pGAP_23*_pLAT2_Cas9_RGI2 was transformed into strains PpHP7 and PpHP8, respectively, together with 3 µg of the donor DNA containing the expression cassette pTEF1_*acs*$_{Se}^{L641P}$_RPS3tt flanked with RGI homology sequences at both ends. The donor DNA was obtained from excision from plasmid BB3nK_ACS1_at_RGI2 using BbsI.

Similarly, to obtain the strains PpHP12 and PpHP14, 1 µg of the circular plasmid BB3cK_pGAP_23*_pLAT2_Cas9_RGI2 was transformed into strains PpHP7 and PpHP8, respectively, together with 5 µg of the donor DNA containing the expression cassettes pTEF1_*acs*$_{Se}^{L641P}$_RPS3tt and pMDH3_*ALD6*$_{Sc}$_TDH3tt flanked with RGI

homology sequences at both ends. The donor DNA was obtained from excision from plasmid BB3nK_ACS1_ALD6_at_RGI2 using BbsI.

Supplementary Table S7. Primers list and sequence.

Primer name	Sequence
RGI_5H_FW_A	TTTTCGCGGTCTCCGATCGAGGTTTACAAGCTGTGATGTTCC
RGI_5H_RV_B	TCCGGTGGTCTCCCCGGTGATGAACTGCCCGTCAAATTG
RGI_3H_FW_C	TTTTCGCGGTCTCAAATTGAAGTGGCTTCATAATTTCAGAACTC
RGI_3H_FW_E	TTTTCGCGGTCTCAGGAGTTGAAGTGGCTTCATAATTTCAGAACTC
RGI_5H_RV_D	TCCGGTGGTCTCCAGCTCGTTCGCTATATTATCATAGCCCAG
PDC_FW	ACCAAGCAAATAAACGCAAAGAGCAAC
PDC_RV	CTTAGCATAGTACAGAGTGGAAGCGG
ArDH_5H_FW	CATGAGAGACATATAACATTTTACAGAGCGG
ArDH_5H_RV	CAGCAACCGTCTTTGCTTGC
ArDH_5H_PDC_RV	GCTCTTTGCGTTTATTTGCTTGGTCAGCAACCGTCTTTGCTTGC
ArDH_3H_PDC_FW	CGCTTCCACTCTGTACTATGCTAAGGATCCGGCTCGTCCTCATCA
ArDH_3H_FW	GCAAGCAAAGACGGTTGCTGTGATCCGGCTCGTCCTCATCA
ArDH_3H_RV	AGACAGGCCTTATGGAGAACA
ArDH_check_in_FW	CATAGTTCCAAGCTTCAGATTGG
ArDH_check_in_RV	GTATGCGACTTGAGGTTGTGG

To knock-out the main D-arabitol dehydrogenase encoding gene (*ArDH*), homology sequences upstream and downstream of the recognition site of the sgRNA were selected. The donor DNA results of the junction of the two aforementioned sequenced. Integration of such donor DNA would result in the excision of the whole *ArDH*

expression cassette. Two high-fidelity PCR were performed using the genomic DNA of *P. pastoris* X-33 as a template and primer pairs ArDH_5H_FW/ArDH_5H_RV and ArDH_3H_FW/ArDH_3H_RV. The two amplicons (805 bp and 904 bp, respectively) were joined using a standard Overlap Extension PCR protocol to generate the donor DNA. The strains PpHP15 and PpHP17 were obtained from transforming 1 µg of the circular plasmid BB3cK_pGAP_23*_pLAT2_Cas9_ArDH and 1 µg of the donor DNA into the strains PpHP8 and PpHP13, respectively.

Finally, to knock-in a second copy of the Pyruvate Decarboxylase encoding gene (*PDC1*) while knocking-out *ArDH*, the whole expression cassette of *PDC1* was amplified using the Q5 high-fidelity polymerase primers pair PDC_FW and PDC_RV and the genomic DNA from *P. pastoris* X-33 as a template. An amplicon of 3149 bp was obtained. Afterwards, the flanking homologous sequences to the *ArDH* targeting sgRNA were amplified from the genomic DNA of *P. pastoris* X-33 with primer pairs ArDH_5H_FW/ArDH_5H_PDC_RV and ArDH_3H_PDC_FW/ArDH_3H_RV. To obtain the donor DNA, the two amplicons (829 bp and 908 bp, respectively) were joined with ArDH using a standard Overlap Extension PCR protocol, resuting in a PCR fragment of 4835 bp. The strains PpHP16 and PpHP18 were obtained from transforming 1 µg of the circular plasmid BB3cK_pGAP_23*_pLAT2_Cas9_ArDH and 4 µg of the donor DNA into the strains PpHP8 and PpHP13, respectively.

The whole *PDC1* expression cassette was amplified from *P. pastoris* strains PpHP15, PpHP16, PpHP17, and PpHP18 using the colony PCR protocol with Q5 high-fidelity polymerase described elsewhere [5]. The PCR products were Sanger sequenced to confirm the integrity of the sequence.

To check that the endogenous *ArDH* expression cassette did not reintegrate in a different locus, a colony PCR with primer pairs ArDH_check_in_FW/ArDH_check_in_RV was performed to strains PpHP8, PpHP15, PpHP16, PpHP17, and PpHP18. These primers amplify a 526 bp PCR product within the coding region of *ArDH*. PpHP8 was used as a positive control. No PCR product was obtained for strains PpHP15, PpHP16, PpHP17, and PpHP18, confirming the correct excision of *ArDH* in these strains.

3. Supplementary materials Chapter 5. Results III

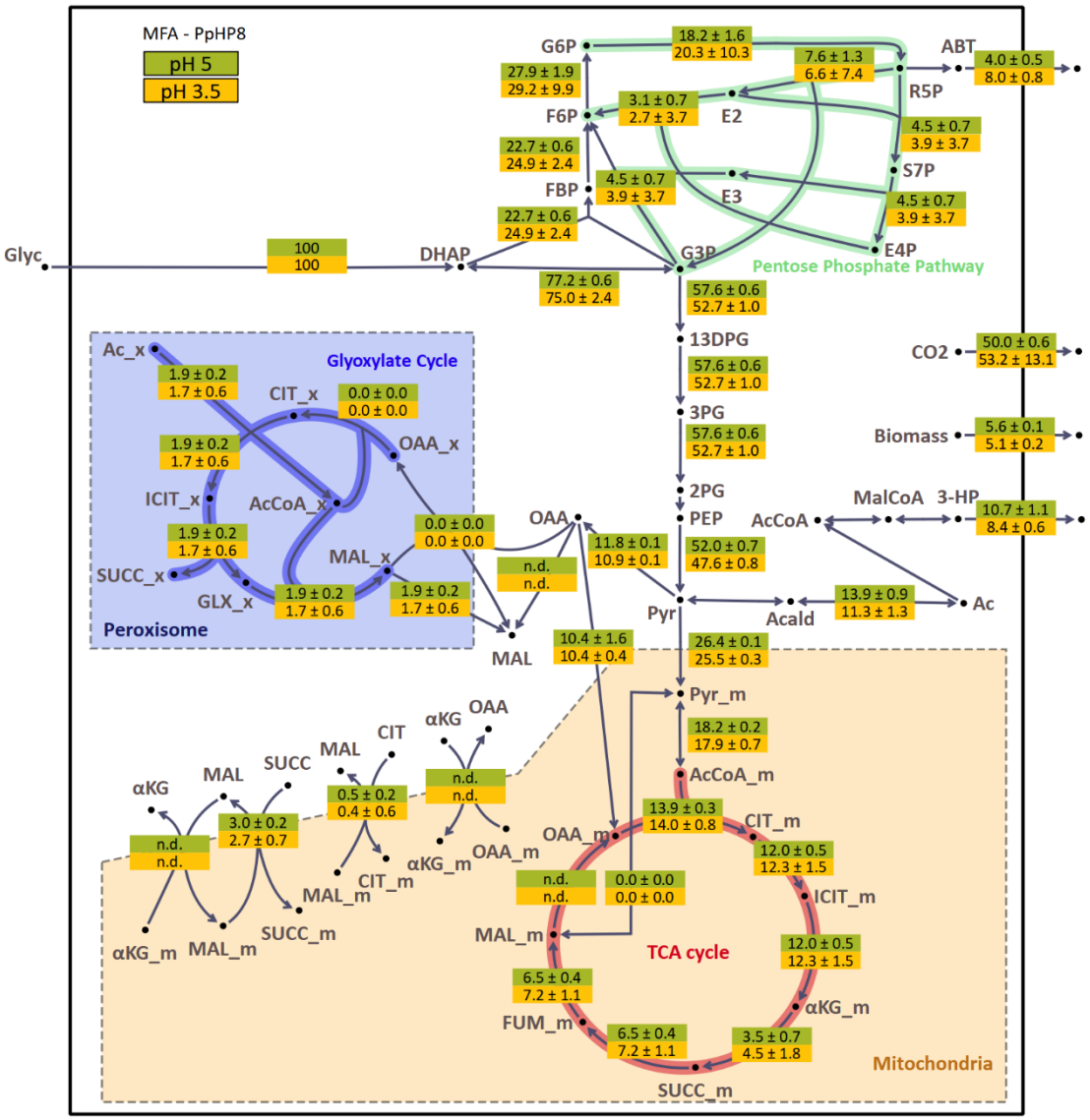

Supplementary Figure S6. Comparison of the relative fluxes at pH 5 and 3.5 for strain PpHP8. Metabolite abbreviation can be found in the figure caption of Figure 19 (page 118).

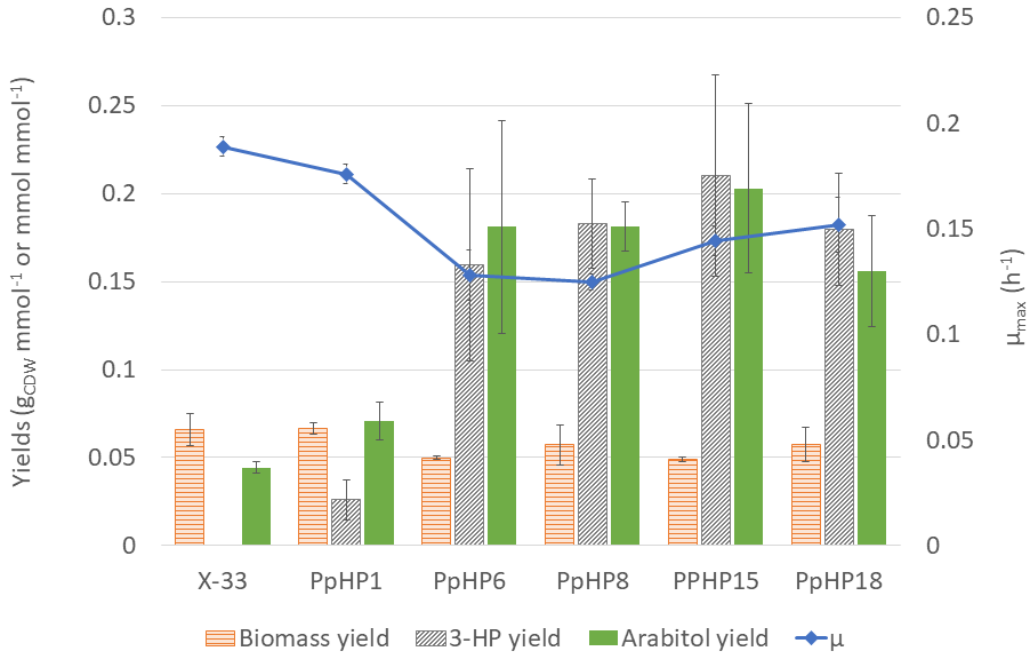

Supplementary Figure S7. Biomass, product, and by-product yields and μ_{max} of the parental *P. pastoris* strain and nine 3-HP-producing strains cultivated in batch mini bioreactor cultures at pH 3.5. Orange bars show the biomass yield, grey bars show the 3-HP yield, green bars show the arabitol yield, and the blue diamonds depict the μ_{max}. Standard deviation of the replicates is depicted.

4. Supplementary materials Annex I

Supplementary Table S8. List of amino acids with their formula, the possible isotopologues, their m/z after protonation ($[M + H]^+$), and the approximate retention time.

Metabolite	Formula	Isotopologue	$[M+H]^+$	Retention time (min)
Alanine	$C_3H_7NO_2$	M0	90.0548	2.46
		M1	91.0582	
		M2	92.0615	
		M3	93.0649	
Arginine	$C_6H_{14}N_4O_2$	M0	175.1187	3.69
		M1	176.1221	
		M2	177.1254	
		M3	178.1288	
		M4	179.1322	
		M5	180.1355	
		M6	181.1389	
Aspartate/ Asparagine	$C_4H_7NO_4$	M0	134.0446	2.15
		M1	135.0480	
		M2	136.0513	
		M3	137.0547	
		M4	138.0580	
Glutamate/ Glutamine	$C_5H_9NO_4$	M0	148.0603	2.42
		M1	149.0637	
		M2	150.0670	
		M3	151.0704	
		M4	152.0737	
		M5	153.0771	
Glycine	$C_2H_5NO_2$	M0	76.0393	2.23
		M1	77.0426	
		M2	78.0460	
Histidine	$C_6H_9N_3O_2$	M0	156.0766	3.25
		M1	157.0799	
		M2	158.0833	
		M3	159.0866	
		M4	160.0900	
		M5	161.0933	
		M6	162.0967	
Isoleucine	$C_6H_{13}NO_2$	M0	132.1018	9.40
		M1	133.1051	
		M2	134.1085	
		M3	135.1118	
		M4	136.1152	
		M5	137.1185	
		M6	138.1219	

Leucine	$C_6H_{13}NO_2$	M0	132.1018	10.70
		M1	133.1051	
		M2	134.1085	
		M3	135.1118	
		M4	136.1152	
		M5	137.1185	
		M6	138.1219	
Lysine	$C_6H_{14}N_2O_2$	M0	147.1127	3.23
		M1	148.1161	
		M2	149.1194	
		M3	150.1228	
		M4	151.1261	
		M5	152.1295	
		M6	153.1328	
Phenylalanine	$C_9H_{11}NO_2$	M0	166.0859	15.90
		M1	167.0893	
		M2	168.0926	
		M3	169.0960	
		M4	170.0993	
		M5	171.1027	
		M6	172.1061	
		M7	173.1094	
		M8	174.1128	
		M9	175.1161	
Proline	$C_5H_9NO_2$	M0	116.0703	2.45
		M1	117.0737	
		M2	118.0770	
		M3	119.0804	
		M4	120.0837	
		M5	121.0871	
Serine	$C_3H_7NO_3$	M0	106.0498	2.17
		M1	107.0532	
		M2	108.0565	
		M3	109.0599	
Threonine	$C_4H_9NO_3$	M0	120.0654	2.32
		M1	121.0688	
		M2	122.0721	
		M3	123.0755	
		M4	124.0788	

Tyrosine	$C_9H_{11}NO_3$	M0	182.0810	10.10
		M1	183.0844	
		M2	184.0877	
		M3	185.0911	
		M4	186.0944	
		M5	187.0978	
		M6	188.1011	
		M7	189.1045	
		M8	190.1079	
		M9	191.1112	
Valine	$C_5H_{11}NO_2$	M0	118.0862	4.45
		M1	119.0896	
		M2	120.0929	
		M3	121.0963	
		M4	122.0996	
		M5	123.1030	

References

1. Prielhofer, R., Barrero, J.J., Steuer, S., Gassler, T., Zahrl, R., Baumann, K., Sauer, M., Mattanovich, D., Gasser, B., and Marx, H. (2017) GoldenPiCS: A Golden Gate-derived modular cloning system for applied synthetic biology in the yeast *Pichia pastoris*. *BMC Systems Biology*, 11, 123.

2. Tomàs-Gamisans, M., Andrade, C.C.P., Maresca, F., Monforte, S., Ferrer, P., and Albiol, J. (2020) Redox engineering by ectopic overexpression of NADH kinase in recombinant *Pichia pastoris* (*Komagataella phaffii*): Impact on cell physiology and recombinant production of secreted proteins. *Applied and Environmental Microbiology*, 86, e02038-19.

3. Fina, A., Brêda, G.C., Pérez-Trujillo, M., Freire, D.M.G., Almeida, R.V., Albiol, J., and Ferrer, P. (2021) Benchmarking recombinant *Pichia pastoris* for 3-hydroxypropionic acid production from glycerol. *Microbial Biotechnology*, 14 (4), 1671–1682.

4. Liu, Y., Bai, C., Liu, Q., Xu, Q., Qian, Z., Peng, Q., Yu, J., Xu, M., Zhou, X., Zhang, Y., and Cai, M. (2019) Engineered ethanol-driven biosynthetic system for improving production of acetyl-CoA derived drugs in Crabtree-negative yeast. *Metabolic Engineering*, 54, 275–284.

5. Gassler, T., Heistinger, L., Mattanovich, D., Gasser, B., and Prielhofer, R. (2019) CRISPR/Cas9-mediated homology-directed genome editing in *Pichia pastoris*. *Methods in Molecular Biology*, 1923, 211–225.